ETHANOL PRODUCTION BY *Saccharomyces cerevisiae* IMMOBILIZED IN CALCIUM ALGINATE

Thesis by

Betty J. M. Hannoun

In Partial Fulfillment of the Requirements

for the Degree of

Doctor of Philosophy

California Institute of Technology

Pasadena, California

1988

(Submitted March 4, 1988)

To Mom and Dad

and

Imad and Deena

ACKNOWLEDGMENTS

I would like to thank my advisor, Professor Gregory Stephanopoulos, for the support he provided me while I was conducting this research. His kindness is appreciated.

Thanks also go to Professor James Bailey for allowing me to carry out experiments in his laboratory over an extended period of time and to his research group for numerous technical discussions. I greatly appreciate Ken Reardon for his assistance in the laboratory and Nancy DaSilva and Jackie Shanks, who helped in many ways. I would like to thank Professor Pau Chau for his assistance in conducting several final experiments at UCSD.

I thank my husband, Imad, for his unfailing encouragement, patience, and technical assistance.

ABSTRACT

Glucose and ethanol diffusion coefficients in calcium alginate were measured in a diffusion cell using the lag time method. The diffusion coefficients decreased as the alginate concentration increased. Glucose and ethanol concentrations had no effect on the diffusion coefficients. Also the presence of 20 % dead yeast cells had no effect on the diffusion coefficients.

Experiments were conducted under anaerobic conditions to determine the intrinsic, specific rates of growth, glucose uptake, and ethanol production for *Saccharomyces cerevisiae* immobilized in calcium alginate. The simultaneous processes of diffusion and reaction were analyzed in an alginate membrane to determine the intrinsic, specific growth and reaction rates from glucose and ethanol concentration measurements made outside the alginate phase. Under anaerobic conditions, the specific growth rate of immobilized *S. cerevisiae* decreased by 20 % compared to the growth rate for suspended cells. The specific glucose uptake rate and specific ethanol production rate increased by a factor of four (4) compared to suspended cells. The ethanol yield remained the same and the biomass yield decreased to one-fifth (1/5) the yield for suspended cells.

Further experiments were conducted under aerobic conditions to investigate the effects of dissolved oxygen concentration on the specific rates of growth, glucose uptake, and ethanol production of immobilized *S. cerevisiae*. Oxygen appears to affect immobilized cells similarly to the way it affects suspended cells.

A mathematical model was developed to quantify the effects of oxygen, glucose, and ethanol on the intrinsic, specific rates of growth, glucose uptake,

and ethanol production of immobilized cells. The model was tested using *S. cerevisiae* immobilized in calcium alginate beads in a well-mixed batch reactor. The mathematical model accurately predicts the bulk fluid glucose and ethanol concentrations.

The mathematical model for intrinsic, specific rates of growth, glucose uptake, and ethanol production was used to simulate the behavior of a continuous plug flow reactor and a continuous stirred tank reactor for ethanol production by *S. cerevisiae* immobilized in calcium alginate beads. Unsteady-state reactor operation was considered. The effects of bead size, feed glucose concentration, residence time, and dissolved oxygen concentration on reactor performance were investigated.

TABLE OF CONTENTS

LIST OF TABLES

LIST OF FIGURES

CHAPTER 1

INTRODUCTION

Biochemicals are compounds that are produced from living or once living organisms. Currently, the biochemical industry is in a state of rapid expansion. New products are being developed continuously because of advances in genetic engineering. As the number of biochemicals increases annually, the need for efficient production processes is growing as well. Technological improvements in biochemical production processes are required to make some biochemicals competitive economically with equivalent synthetic chemicals. For chemicals that cannot be produced synthetically, process improvements are still needed to reduce production costs. Reduced costs will allow the opening of new markets for biochemicals.

1.1 IMMOBILIZED CELLS

Immobilizing microorganisms on solid support matrices has significant potential for improving conventional biochemical production processes. Higher flow rates can be maintained in continuous immobilized cell reactors because the flow rate is not limited by the growth rate of the organism as it is in a chemostat. Since biomass is retained in an immobilized cell reactor, higher biomass concentrations are feasible when immobilized cells are employed. Furthermore, a relatively cell-free product stream from an immobilized cell reactor makes downstream processing easier. For nongrowth associated products, immobilized cells lead to improved product yields because less of the substrate

is required for biomass synthesis. Higher yields have also been reported for growth-associated products (1).

There are several disadvantages to using immobilized cells for biochemical production. Cell growth in the reactor can lead to break up of the support material. If cell growth is limited by removing essential nutrients such as nitrogen from the medium, the immobilized cells deactivate with time. Mass transfer limitations may also decrease the overall reaction rates of immobilized cells because substrates must diffuse to the cells and toxic products must diffuse away from the cells. Research in the field of immobilized cells can help in solving the problems associated with immobilized cell reactors.

There are four basic methods of cell immobilization. They include: 1) aggregation, 2) adsorption, 3) entrapment, and 4) membrane confinement. Both viable and nonviable cells are immobilized for biochemical production. Some examples of naturally occurring immobilized cells are bacteria attached to soil particles and slippery rocks in a stream bed.

1.1.1 Aggregation

Some species of bacteria form aggregates or flocs naturally. Flocculating agents can be used to induce other cells to aggregate. The strength of cell aggregates is influenced by medium characteristics such as pH, ionic strength, and nutrient concentrations (2). Flocculation has been used for ethanol production; however, cell flocs are relatively weak mechanically. Gas release alone can lead to break up of the flocs (3). Coupling agents can be used to crosslink and thus strengthen cell aggregates, but most crosslinking agents are toxic to the cells.

1.1.2 Surface Attachment

In many applications cells are attached to the surface of a solid support. Support materials used for cell attachment include ion exchange resins (4), wood chips (5), ceramic (6), magnetite particles (7), sawdust (8), and porous silica (9), among other things. Most organisms are negatively charged at a normal pH and therefore adsorb weakly to positively charged supports (4). The concentration of cells is limited by the available surface area of the support, so porous particles are more attractive than nonporous particles for surface immobilization. Messing and Oppermann demonstrated that the optimal pore size for biomass adsorption depends on the size of the organism and the method of cell division (10).

Because of the instability of adsorbed cells, their commercial potential is currently limited. Changes in medium composition or cell age can cause elution of adsorbed cells from support material (11). Shear forces from fluid flow remove adsorbed cells (5). Trickling filter wastewater treatment processes employ surface attached cells. In the 1820's the Schuetzenbach process was developed for converting ethanol to acetic acid via adsorbed cells (12).

Cell-solid bonds can be strengthened by covalently crosslinking adsorbed cells to support material with chemicals such as glutaraldehyde. As with cell aggregates, crosslinking agents can deactivate cells.

1.1.3 Entrapment

Recent interest in immobilized cells has focused on entrapment methods. Both synthetic and natural polymers are used to entrap cells. Cells are mixed thoroughly with a liquid polymer solution; then the solution is polymerized. The polymerization conditions must be controlled to avoid damaging the cells. Most entrapment methods allow cell growth to continue after polymerization.

Nutrients and products must diffuse through the polymeric matrix to or from the cells. In many cases the overall reaction rates of entrapped cells are limited by mass-transfer rates.

Polyacrylamide is a synthetic polymer used frequently for whole cell entrapment. The polymer is strong mechanically; however, the monomer unit and the polymerization conditions are toxic to most cells. Siess and Divies found that entrapment in polyacrylamide destroys between 40 and 80 % of *Saccharomyces cerevisiae* cells, depending on the physiological state of the cells (13). Freeman and Aharonowitz used prepolymerized polyacrlyamide hydrazide to entrap cells (14). Polyacrlyamide hydrazide retains the mechanical strength of polyacrylamide but causes less damage to the cells during gelation. Kuu and Polack used polyacrylamide to treat agar and carrageenan beads, thus strengthening the beads (15).

Various other synthetic polymers have been used for cell immobilization including polyurethane foam (16), methacrylates, and polyesters (17).

Increasingly, natural polymers are being being used for whole-cell entrapment. Alginate and carrageenan can be polymerized while maintaining 100 % cell viability. Kierstan and Bucke have detailed the experimental procedure for entrapping cells in calcium alginate (18). Conditions for the gelation of carrageenan were investigated by Tosa, et al. (19). Although weaker mechanically than synthetic polymers, alginate and carrageenan can be employed sucessfully in immobilized cell reactors (20, 21). The composition of the medium must be controlled for alginate gel because monovalent cations and chelating agents lead to deterioration of the gel. Agar has also been used to entrap cells in the laboratory, but appears unsuitable for larger operations due to its mechanical

instability (22).

The Tanabe Seiyaku Company of Japan produces l-malic and l-aspartic acids commercially by entrapping *Brevibacterium ammoniagenes* and *Escherichia coli*, respectively, in carrageenan. These two commercial processes utilize nonviable immobilized cells (23).

Alginate is a natural polymer. Monovalent alginate salts are water-soluble. Alginate is polymerized by displacing monovalent cations with divalent cations, which crosslink the alginate chains. Alginate gels are porous structures with bulk pore sizes on the order of 10 μm (24). In the presence of high concentrations of monovalent ions or in the presence of chelating agents, polymerized alginate is easily dissolved. Thus, viable cells can be removed from the alginate matrix for quantification or examination.

1.1.4 Membrane Confinement

Microorganisms can be physically confined in ultrafiltration membranes for biochemical production. Hollow fiber reactors have been used extensively on the laboratory scale. The fibers consist of tubular ultrafiltration membranes arranged in a dialysis unit. Cells are usually immobilized in the interior of the fibers, while nutrients and products diffuse through the fiber walls. Karel and Robertson measured rates of protein production and degradation for *Pseudomonas putida* immobilized in a hollow fiber reactor (25). They demonstrated that the growth of the organism in the hollow fibers was limited by the availability of oxygen. Thus, mass transfer can limit the productivity of hollow fiber reactors.

Liquid membrane encapsulation can be used to immobilize cells. Mohan and Li demonstrated the reduction of nitrate and nitrite ions by *Micrococcus den-*

itrificans encapsulated in a surfactant-liquid membrane (26). The liquid membrane protected the cells from toxic mercuric ions in the bulk fluid, yet allowed diffusion of sbstrates and products to and from the cells. They also observed a broader pH and temperature optimum for encapsulated cells compared to suspended cells.

1.2 METABOLIC EFFECTS OF IMMOBILIZATION

What makes immobilized cells interesting from a research perspective is that numerous reports have appeared in the literature about metabolic changes that are due to cell immobilization. However, a great deal of the literature is difficult to interpret because experimental complexities have prevented many researchers from measuring final biomass concentrations and solute concentrations close to the cell surface. Some of the more complete investigations with *Saccharomyces* are summarized in Table 1.1. In 1977, Navarro and Durand measured a 6 fold increase in the ethanol production rate of *S. carlbergenesis* adsorbed onto porous glass beads (1). They also found a slight increase in the ethanol yield. Similarly, in 1979, Marcipar, et al. reported that the oxygen uptake rate of *S. cerevisiae* increased 6.7 fold when the cells were adsorbed onto ceramic support (27). For *S. cerevisiae* entrapped in polyacrylamide hydrazide, researchers discovered higher concentrations of DNA, glycogen, and glucan and lower concentrations of trehalose (13). In another investigation, researchers observed enhanced ethanol tolerance when cells were entrapped in polyacrylamide hydrazide (28). A decreased rate of oxygen uptake and an increased growth rate have been reported for *S. cerevisiae* adsorbed on inert support (29). In 1987, Doran and Bailey observed a 2 fold increase in the glucose uptake rate of *S.*

Table 1.1

METABOLIC EFFECTS OF IMMOBILIZATION

METHOD	METABOLIC EFFECT(S)
Adsorption (1977)	6 x increase in specific ethanol production rate
Adsorption (1979)	7 x increase in specific oxygen utilization rate
Entrapment (1981)	Higher concentration of DNA, glycogen, and glucan
Entrapment (1982)	Enhanced ethanol tolerance
Adsorption (1982)	25 % decrease in specific oxygen uptake rate, 26 % increase in growth rate
Adsorption (1987)	2 x increase in specific glucose uptake rate, 50 % increase in ethanol production rate, 45 % decrease in growth rate

cerevisiae attached to crosslinked gelatin beads. They also reported a 45 % decrease in the growth rate (30).

Explanations of metabolic changes that are due to cell immobilization include increased membrane permeability (27), the development of a protective environment around the cells (27), a decrease in water activity (31), changes in intracellular pH (32), and the formation of polyploid cells(30). Few researchers have experimentally demonstrated the cause of the metabolic changes they observed. Using flow cytometry and cell component assays, Doran and Bailey produced evidence that cells attached to the surface of crosslinked gelatin continue to duplicate their DNA normally but fail to produce buds at the usual rate. Failure to produce buds leads to cells with a high concentration of DNA, or polyploidy, which affects the metabolic rates of the cells (30).

1.3 *Saccharomyces cerevisiae*

Saccharomyces cerevisiae is an industrially important organism. It has been used extensively in commercial brewing and baking processes. Additionally, *S. cerevisiae* has potential as a host organism for heterologous protein production because of its ability to glycosylate, fold, and secrete proteins (33). Because of its commercial significance, the culture requirements and metabolism of *S. cerevisiae* are well characterized.

In recent decades, interest has developed in the production of ethanol by *S. cerevisiae* and other microorganisms. Increases in the price of oil during the 1970's made alternative energy sources more attractive economically. Although oil prices have since declined, the threat of future oil price escalations encourages research and development in the area of biochemical fuels. Furthermore,

ethanol has a market of significant size in the chemical industry.

Process improvements in the biological production of ethanol may make fermentations more competitive with synthetic processes. Immobilization of *S. cerevisiae* for ethanol production has potential as an alternative to conventional suspended cell processes. Characterizing the effects of immobilization on the metabolism of *S. cerevisiae* will assist in the development of commercial immobilized cell processes. The available information on suspended *S. cerevisiae* can also be used in attempting to understand how immobilization affects the cell's metabolism.

The culture requirements and metabolism of *S. cerevisiae* are summarized below. Only the characteristics of the organism pertinent to this investigation are included. More detailed descriptions of *S. cerevisiae* have been written by Doran (3) and Grosz (34).

1.3.1 Culture Requirements

S. cerevisiae can utilize sugars, ethanol, and other substrates for growth. Sugars can be fermented anaerobically to carbon dioxide and ethanol or oxidized aerobically to carbon dioxide. Glucose concentrations above 1 g/l repress the oxidative pathway. *S. cerevisiae* undergoes diauxic growth in the presence of glucose. Glucose is first fermented to ethanol and carbon dioxide. Then a lag phase ensues during which the organism synthesizes enzymes required for growth on ethanol. Ethanol utilization by *S. cerevisiae* requires the presence of oxygen. The second growth phase on ethanol is characterized by a lower growth rate.

S. cerevisiae requires biotin, pantothenic acid, and nicotinic acid for growth.

Other vitamins in the medium may enhance growth but can usually be synthesized from the appropriate precursors (35).

Trace amounts of oxygen are required for continuous growth of *S. cerevisiae*. The need for oxygen can be eliminated by suppling sterols and fatty acids in the medium.

Ethanol, an end product of glucose fermentation, inhibits the growth and metabolism of *S. cerevisiae*. Under most conditions batch fermentations stop when the ethanol concentration reaches 100 g/l.

1.3.2 Metabolic Pathways

The major metabolic pathways of *S. cerevisiae* are outlined in Figure 1.1. Glucose is catabolized to pyruvate through the glycolytic pathway. If respiration occurs, pyruvate is converted to carbon dioxide and water via the tricarboxylic acid cycle and oxidative phosphorylation. Fermentation, on the other hand, converts pyruvate to ethanol and carbon dioxide. The stoichiometric equation for the conversion of glucose to carbon dioxide and water is:

$$C_6H_{12}O_6 + 6O_2 + 36P + 36ADP \longrightarrow 6CO_2 + 6H_2O + 36ATP.$$

Oxygen is the terminal electron acceptor for oxidative phosphorylation. The stoichiometric equation for the conversion of glucose to ethanol and carbon dioxide is:

$$C_6H_{12}O_6 + 2P + 2ADP \longrightarrow 2C_2H_5OH + 2CO_2 + 2ATP.$$

While oxidation leads to a net production of thirty-six molecules of ATP per molecule of glucose, fermentation produces only two molecules of ATP per molecule of glucose.

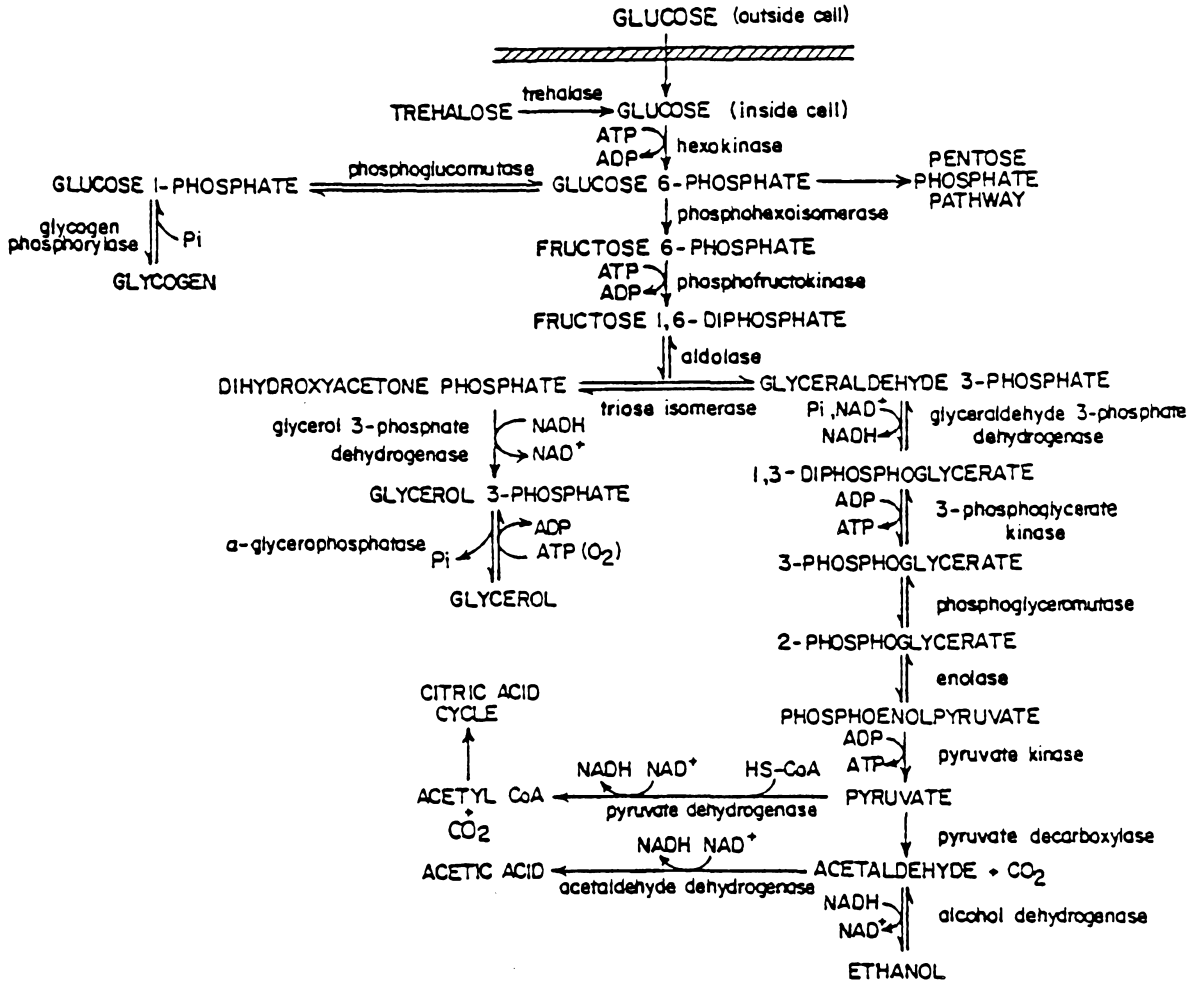

Figure 1.1 **Major Metabolic Pathways of *S. cerevisiae*** (3) Doran, 1985.

Under certain conditions glycerol and acetic acid are synthesized during glucose metabolism. Glycerol is derived from dihydroxyacetonephosphate, which is an intermediate in the glycolytic pathway. Acetic acid is produced under alkaline conditions from acetaldehyde. Neither glycerol nor acetic acid was produced in significant quantities in this investigation.

1.3.3 Glucose Uptake

Glucose appears to be transported into the cell by facilitated diffusion. A concentration gradient is the driving force for facilitated diffusion, and no energy is spent in the transport process. Facilitated diffusion requires a carrier protein in the cell membrane to translate the solute molecule from the outside of the cell to the inside of the cell membrane. Several investigators have observed that the rate of glucose transport becomes saturated, indicating that a carrier protein exists (36,37). Since glucose transport continues when cell metabolism is inhibited, energy is not required for glucose transport (38). Furthermore, glucose cannot be concentrated inside the cell membrane (39). Thus, glucose transport is by facilitated diffusion.

1.3.4 Effects of Oxygen and Glucose

The roles of glucose and oxygen in the metabolism of *S. cerevisiae* are quite complicated. At low glucose concentrations, the dissolved oxygen concentration determines whether growth proceeds by oxidative phosphorylation or by fermentation. For glucose derepressed cells Rogers and Stewart determined K_m to be 6.4 x 10^{-3} mg/l for mitochondrial respiratory enzymes (40), where K_m is defined as the dissolved oxygen concentration required for half-maximal

activity. Mitochondrial respiratory enzymes participate in oxidative phosphorylation. Glucose is known to repress the activity of respiratory enzymes. The degree of repression, however, has not been completely elucidated. Chapman and Bartley found that oxygen partially alleviates glucose repression of respiratory enzymes (41). Other researchers have found that cytochrome synthesis can be completely blocked by a lack of oxygen but not by high glucose concentrations alone (42).

The glyoxylate cycle is an anabolic pathway in yeast for synthesis of tricarboxylic acid cycle intermediates. The development of a functional glyoxylate cycle occurs at significantly higher dissolved oxygen concentrations than respiratory enzyme synthesis. The K_m for glyoxylate cycle enzymes in glucose derepressed cells is 3.8×10^{-2} mg/l (40). The synthesis of glyoxylate cycle enzymes appears to be closely related to the dissolved oxygen concentration at which the biomass synthesis rate increases and the ethanol production rate decreases. Polakis and Bartley (43) demonstrated that two key enzymes of the glyoxylate cycle are repressed by glucose. Further evidence exists that glyoxylate cycle enzymes may be entirely absent as long as glucose is present (44).

Oxygen has a significant effect on the plasma-membrane composition of *S. cerevisiae*. When cultivated under anaerobic conditions, the cells become depleted of fatty acids and sterols unless lipid supplements are supplied in the medium. Aeration of the medium leads to synthesis of essential membrane lipids. For cells grown in continuous culture at dissolved oxygen concentrations from 0.0 to 0.09 mg/l, the total fatty acid content of the cells increased from 35 to 125 mg/g of yeast as the oxygen concentration rose. The percent

of total fatty acids that were unsaturated and the sterol content also increased significantly (40). The plasma-membrane lipid composition of *S. cerevisiae* has been directly related to the ethanol tolerance of the cells (45).

1.4 INTRINSIC REACTION RATES

While a few researchers have measured the intrinsic reaction rates of surface-attached cells, not one has measured the intrinsic rates of growing entrapped cells. Cell growth and substrate and product diffusion in the solid phase make intrinsic rates extremely difficult to measure. Commercially, there is a great deal of interest in cells immobilized in alginate and carrageenan. In designing an immobilized cell system it is important to know the specific reaction rates of immobilized cells. Furthermore, entrapment may affect cells differently than surface attachment methods, because in entrapment procedures the entire cell membrane is surrounded by the polymeric matrix. Therefore, the results of experiments with surface- attached cells cannot be extrapolated to entrapped cells. Since cell growth during immobilization affects the properties of the cells, experiments should be conducted under growth conditions.

1.5 RESEARCH OBJECTIVES

The objectives of this investigation were first to develop a method for accurately measuring intrinsic reaction rates of exponentially growing cells. The next step was to utilize the method to measure the intrinsic reaction rates of *S. cerevisiae* immobilized in calcium alginate under various aeration conditions and to compare the results to suspended cell reaction rates. The third step was to use the experimental data to develop a model for the growth and reaction of

immobilized *S. cerevisiae*. After testing the model in a batch reactor, the model was used to design and optimize a plug flow reactor and a continuous stirred tank reactor for ethanol production.

REFERENCES

(1) Navarro, J. M., and G. Durand, "Modification of Yeast Metabolism by Immobilization onto Porous Glass," *Eur. J. Appl. Microbiol. Biotechnol.*, *4*, 243–254 (1977).

(2) Abbott, B. J., "Immobilized Cells," in *Annual Reports on Fermentation Processes*, *2*, Academic Press, London, 1978, pp. 91–123.

(3) Doran, Pauline M., *Effects of Immobilization on the Metabolism of Yeast*, Ph. D. Thesis, California Institute of Technology, 1985.

(4) Daugulis, A. J., N. M. Brown, W. R. Cluett, and D. B. Dunlop, "Production of Ethanol by Adsorbed Yeast Cells," *Biotechnol. Lett.*, *3*, 651–656 (1981).

(5) Moo-Young, M., J. Lamptey, and C. W. Robinson, "Immobilization of Yeast Cells on Various Supports for Ethanol Production," *Biotechnol. Lett.*, *2*, 541–548 (1980).

(6) Ghommidh, C., J. M. Navarro, and R. A. Messing, "A Study of Acetic Acid Production by Immobilized Acetobacter Cells: Product Inhibition Effects," *Biotechnol. Bioeng.*, *24*, 1991–1999 (1982).

(7) Horisberger, M., "Immobilization of Protein and Polysaccharides on Magnetite Particles: Selective Binding of Microorganisms by Concanavalin A-Magnetite," *Biotechnol. Bioeng.*, *18*, 1647–1651 (1976).

(8) Thonart, Ph., M. Custinne, and M. Paquot, "Zeta Potential of Yeast Cells: Applications in Cell Immobilization," *Enzyme Microb. Technol.*, *4*, 191–194 (1982).

(9) Dias, S. M. M., J. M. Novais, and J. M. S. Cabral, "Immobilization of

Yeasts on Titanium Activated Inorganic Supports," *Biotechnol. Lett.*, *4*, 203–208 (1982).

(10) Messing, R. A., and R. A. Oppermann, "Pore Dimensions for Accumulating Biomass. I. Microbes that Reproduce by Fission or by Budding," *Biotechnol. Bioeng.*, *21*, 49–58 (1979).

(11) Rotman, B., "Uses of Ion Exchange Resins in Microbiology," *Bact. Rev.*, *24*, 251–260 (1960).

(12) Messing, R. A., "Immobilized Microbes," in *Annual Reports on Fermentation Processes*, *4*, Academic Press, London, 1980, pp. 105–121.

(13) Siess, M. H., and C. Divies, "Behavior of *S. cerevisiae* Cells Entrapped in a Polyacrylamide Gel and Performing Alcoholic Fermentation," *European J. Appl. Microbiol. Biotechnol.*, *12*, 10–15 (1981).

(14) Freeman, A., and Y. Aharonowitz, "Immobilization of Microbial Cells in Crosslinked, Prepolymerized, Linear Polyacrlyamide Gels: Antibiotic Production by *Streptomyces clavuligerus* Cells," *Biotechnol. Bioeng.*, *23*, 2747–2759 (1981).

(15) Kuu, W. Y., and J. A. Polack, "Improving Immobilized Biocatalysts by Gel Phase Polymerization," *Biotechnol. Bioeng.*, *25*, 1995–2006 (1983).

(16) Drioli, E., G. Iori, and R. Santoro, "Whole Cell Immobilization in Polyurethane Structural Foam," *J. Molecular Catalysis*, *14*, 247–251 (1982).

(17) Cheetam, P. S. J., "Developments in the Immobilization of Microbial Cells and their Applications," *Topics in Enzyme and Biotech*, *4* , 189–238 (1980).

(18) Kierstan, M., and C. Bucke, "The Immobilization of Microbial Cells, Subcellular Organelles, and Enzymes in Calcium Alginate Gels," *Biotechnol.*

Bioeng., *19*, 387–397 (1977).

(19) Tosa, T., T. Sato, T. Mori, K. Yamamoto, I. Takata, Y. Nishida, and I. Chibata, "Immobilization of Enzymes and Microbial Cells Using Carrageenan as a Matrix," *Biotechnol. Bioeng.*, *21*, 1697–1709 (1979).

(20) Nilsson, K., P. Brodelius, and K. Mosbach, "Production of α-Keto Acids with Alginate Entrapped Whole Cells of the Yeast *Trigonopsis variabilis*," *Appl. Biochemistry Biotechnol.*, *7*, 47–49 (1982).

(21) Wada, M., J. Kato, and I. Chibata, "A New Immobilization of Microbial Cells," *European J. Appl. Microbiol. Biotechnol.*, *8*, 241–247 (1979).

(22) Banerjee, M., A. Chakabarty, S. H. Majumdar, "Immobilization of Yeast Cells Containing β-Galactosidase," *Biotechnol. Bioeng.*, *24*, 1839–1850 (1982).

(23) Chibata, I., and T. Tosa, "Immobilized Microbial Cells and their Applications," *TIBS*, April 1980, 88–90 (1980).

(24) Scherer, P., K. Kluge, J. Klein, and H. Sahm, "Immobilization of the Methanogenic Bacterium *Methanosarcina barkeri*," *Biotechnol Bioeng*, *23*, 1057–1065 (1981).

(25) Karel, S. F., and C. R. Robertson, "Protein Synthesis and Degradation in Immobilized Cell Reactors," *78th Annual AIChE Meeting*, Paper 58c, (1985).

(26) Mohan, R. R., and N. N. Li, "Nitrate and Nitrite Reduction by Liquid Membrane Encapsulated Whole Cells," *Biotechnol. Bioeng.*, *17*, 1137–1156 (1975).

(27) Marcipar, A., N. Cochet, L. Brackenridge, J. M. Lebeault, "Immobilization of Yeasts on Ceramic Supports," *Biotechnol. Lett.*, *1*, 65–70 (1979).

(28) Pines, G., and A. Freeman, "Immobilization and Characterization of *S.*

cerevisiae in Crosslinked Polyacrylamide Hydrazide," *Eur. J. Appl. Microbiol. Biotechnol.*, *16*, 15 (1982).

(29) Bandyopadhyay, K. K., and T. K. Ghose, "Studies on Immobilized *S. cerevisiae*. III. Physiology of Growth and Metabolism on Various Supports," *Biotechnol. Bioeng.*, *24*, 805–812 (1982).

(30) Doran, P., and J. E. Bailey, "Effects of Immobilization on Growth, Fermentation Properties, and Macromolecular Composition of *S. cerevisiae* Attached to Gelatin," *Biotechnol. Bioeng.*, *28*, 73–87 (1986).

(31) Mattiason, Bo, and B. Hahn-Hagerdal, "Microenvironment Effects on Metabolic Behavior of Immobilized Cells," *Eur. J. Appl. Microbiol. Biotechnol.*, *16*, 52–55 (1982).

(32) Galazzo, J., J. V. Shanks, and J. E. Bailey, "Comparison of Suspended and Immobilized Yeast Metabolism Using ^{31}P Nuclear Magnetic Resonance Spectroscopy," *Biotechnol. Techniques*, *1 (1)*, 1–6 (1987).

(33) Cregg, J. M., J. F. Tschopp, C. Stillman, R. Siegel, M. Akong, W. S. Craig, R. G. Buckholz, K. R. Madden, P. A. Kellaris, G. R. Davis, B. L. Smiley, J. Cruze, R. Torregrossa, G. Velicelebi, and G. P. Thill, "High-Level Expression and Efficient Assembly of Hepatitus B Surface Antigen in the Methylotrophic Yeast *Pichia pastoris*," *Bio/Technology*, *5 (5)*, 479–485 (1987).

(34) Grosz, R., *Biochemical and Mathematical Modeling of Microaerobic Continuous Ethanol Production by S. cerevisiae*, Ph. D. Thesis, California Institute of Technology, (1987).

(35) Suomalainen, H., E. Oura, "Yeast Nutrition and Solute Uptake," in *The Yeasts*, *2*, A. H. Rose and J. S. Harrison (eds.), Academic Press, London,

1971, pp. 3–74.

(36) Cirillo, V. P., "Relationship Between Sugar Structure and Competition for Sugar Transport System in Baker's Yeast," *J. Bact.*, *95*, 603 (1968).

(37) Heredia, F., A. Sols, and G. De La Fuente, "Specificity of Constitutive Hexose Transport in Yeast," *Eur. J. Biochem.*, *5*, 321 (1968).

(38) Fiechter, A., "Chemostat Studies of Glycolysis in Yeast," in *Continuous Cultivation of Microorganisms*, Proc. 7 th Internat. Symp., Prague, 1980, p. 81.

(39) Kleinzeller, A., and A. Kotyk, "Transport of Monosaccharides in Yeast Cells and its Relationship to Cell Metabolism," in *Aspects of Yeast Metabolism*, A. K. Mills, and H. Krebs (eds.), Blackwell, Oxford, 1968, p. 33.

(40) Rogers, P. J., and P. R. Stewart, "Mitochondrial and Peroxisomal Contributions to the Energy Metabolism of *Saccharomyces cerevisiae* in Continuous Culture," *J. Gen. Microbiol.*, *79*, 205–217 (1973).

(41) Chapman, C., and W. Bartley, "The Kinetics of Enzyme Changes in Yeast under Conditions that Cause Loss of Mitochondria," *Biochem. J.*, *107*, 455 (1968).

(42) Suomalainen, H., T. Nurminen, and E. Oura, "Aspects of Cytology in Metabolism of Yeast," *Prog. Indus. Microbiol.*, *12*, 109 (1973).

(43) Polakis, E. S., and W. Bartley, "Changes in the Enzyme Activities of *Saccharomyces cerevisiae* during Aerobic Growth on Different Carbon Sources," *Biochem. J.*, *97*, 284–297 (1965).

(44) Haarasilta, S., and E. Oura, "On the Activity and Regulation of Anaplerotic and Gluconeogenetic Enzymes during the Growth Process of Baker's Yeast," *Eur. J. Biochem.*, *52*, 1 (1975).

(45) Thomas, D. S., J. A. Hossack, and A. H. Rose, "Plasma-membrane Lipid Composition and Ethanol Tolerance," *Arch. Microbiol.*, *117*, 239–245 (1978).

CHAPTER 2

Diffusion Coefficients of Glucose and Ethanol in Cell-free and Cell-occupied Calcium Alginate Membranes

Betty J. M. Hannoun and Gregory Stephanopoulos
Department of Chemical Engineering, California Institute of Technology, Pasadena, California 91125

Accepted for publication July 23, 1985

The diffusivities of glucose and ethanol in cell-free and cell-occupied membranes of calcium alginate were measured in a diffusion cell. The lag time analysis was used. Diffusivities decreased with increasing alginate concentration and were comparable with those in water for a 2% alginate membrane. Glucose and ethanol concentrations had no effect on the respective diffusion coefficients. The ratio of ethanol diffusivity to glucose diffusivity in 2 and 4% alginate agreed closely with the inverse ratio of the hydrodynamic radii for the two molecules in water, indicating that the hydrodynamic theory of diffusion in liquids may be applicable to diffusion in dilute alginate gels. Also, the presence of 20% dead yeast cells had no effect on the diffusivities. The data reported can be used to study reaction and diffusion in immobilized cell reactors and cell physiology under immobilized conditions.

INTRODUCTION

The immobilization of cells in calcium alginate has been widely studied for the production of biochemicals. Alginate is a naturally occurring polymer consisting of β-D-mannuronic and α-L-guluronic acid units linked by 1,4-glycosidic bonds.[1] Monovalent alginate salts are water soluble, whereas polyvalent cations cause cross-linking between macromolecular chains. By diffusing calcium ions into an alginate solution, a polymer gel is formed. Several factors have contributed to the interest in cell immobilization in calcium alginate. By immobilizing cells, dense cell cultures can be established, leading to faster overall reaction rates. The cells are retained in the reactor and, therefore, used for a longer period of time, reducing the need for new biomass synthesis. Increased yields have been reported for growth and nongrowth associated products.[2-3] Furthermore, a cell-free product stream simplifies downstream processing. Finally, a high percentage of the cells remain viable during calcium alginate immobilization,[4] and the activity of the cells persists for long periods of time.

Despite the potential of immobilized cell processes for improved efficiency, practical problems have often prevented the benefits from being realized. An important disadvantage of immobilized cells is that the transport of nutrients and products to and from the cells can become rate limiting, decreasing the cells' overall productivity.[5] Additionally, rapid cell growth occurs in a small outer shell of alginate beads,[6-7] decreasing product yields. Due to diffusion limitations and cell growth in the outer shell, as little as 10% of the alginate bead may contain active cells. Furthermore, rapid growth near the gel surface leads to cell leakage into the product stream and breakup of the support.

Investigations on the behavior of calcium alginate immobilized cells have been hindered by concentration gradients and cell growth in the alginate. Experimental complexities have prevented researchers from determining the cell count and concentrations of substrates and products near the cells. Measuring substrate and product concentrations in the liquid phase does not adequately describe intramatrix concentrations, as is often assumed. Thus it is difficult to determine the effects of substrate and product concentrations on specific rates of growth, substrate utilization, and product synthesis for immobilized cells.

Experiments were conducted to determine the rates of glucose and ethanol diffusion through calcium alginate under various conditions. Diffusion coefficients have been measured previously by other investigators for a few substrates in matrices suitable for immobilized cells; Table I summarizes the results. Oxygen and sucrose in 2% agar were measured to diffuse at 70 and 72%, respectively, of their diffusion rates in water.[8-9] The diffusion coefficient of glucose was determined to be the same in 2% calcium alginate as it is in water.[10] Oxygen, however, was reported to have a diffusion coefficient in 2% barium alginate of only 25% of its diffusion coefficient in water.[5]

Diffusion coefficients under various conditions are

Biotechnology and Bioengineering, Vol. XXVIII, Pp. 829–835 (1986)

CCC 0006-3592/86/060829-07$04.00

Table I. Substrate diffusion coefficients in immobilization matrices.

Substrate	Matrix	Diffusion coefficient (cm^2/sec)	Fraction of diffusivity in water	Reference
Glucose	2% calcium alginate	6.8×10^{-6}	1.0	10
Sucrose	2% agar	6.7×10^{-6}	0.72	8
Oxygen	2% agar	1.9×10^{-5}	0.70	9
Oxygen	2% barium chloride	7.0×10^{-6}	0.25	5

needed to model reaction and diffusion in immobilized cell reactors. The reactor operating conditions can then be optimized for productivity using reaction-diffusion models. For example, the feed substrate concentration and residence time may be manipulated to control cell growth. Some growth may be desirable to prevent enzyme deactivation, whereas excess growth causes cell leakage, support breakup, and reduced product yields. The accumulation of toxic products inside the matrix can be prevented by maintaining a production rate equal to the rate of product diffusion out of the alginate. Since steep concentration gradients are present in alginate beads, the effect of concentration on the diffusion coefficients needs to be investigated. Additionally, the presence of cells in the gel may alter some properties of the alginate, including diffusion coefficients. In *Saccharomyces cerevisiae* metabolism, the Crabtree effect, Pasteur effect, and product inhibition are controlled by glucose, oxygen, and ethanol concentrations, respectively. The first step in analyzing and explaining these metabolic patterns for immobilized cells is to determine the diffusivities of the effectors under various conditions. The results are reported here for glucose and ethanol diffusion in calcium alginate.

Theory

The diffusion coefficients of glucose and ethanol in calcium alginate were determined using the lag time analysis. An alginate membrane of thickness 4.2 mm is suspended between two well-mixed chambers of concentrations c_1 and c_2 in the component whose diffusivity is to be measured. The system is shown schematically in Fig. 1. Assuming no film mass transfer resistance between the bulk fluids in the two chambers and the membrane, the transient diffusion process inside the membrane is governed by the partial differential equation

$$\frac{\partial c}{\partial t} = D\frac{\partial^2 c}{\partial x^2} \tag{1}$$

where c is the concentration in the membrane, D is the diffusion coefficient, t is time, and x is distance, subject to the boundary conditions

$$\begin{aligned} c &= c_1 \quad \text{at} \quad x = 0 \\ c &= c_2 \quad \text{at} \quad x = l \end{aligned} \tag{2}$$

During the experiment, solute diffuses from the chamber where $c = c_1$ through the membrane into the chamber where $c = c_2$. Thus, the concentrations in the two chambers are not precisely constant as is assumed in the solution of the differential equation. For large enough chambers, however, the changes in concentration over the time of the experiment are small, and as a result the derived solution fits the experimental results well.

The experiment can be designed so that none of the diffusing component is present initially in the membrane. Then the initial condition to eq. (1) is

$$c = 0 \qquad 0 \le x \le l \qquad \text{at } t = 0 \tag{3}$$

The solution to eq. (1) with boundary conditions (2) and initial condition (3) is given by[11]

$$c = c_1 + (c_2 - c_1)\frac{x}{l} + \frac{2}{\pi}\sum_{n=1}^{\infty}\frac{c_2\cos n\pi - c_1}{n}\sin\frac{n\pi x}{l}\exp\frac{-Dn^2\pi^2 t}{l^2} \tag{4}$$

Daynes applied the partial differential equation solution (4) to gas diffusion through a rubber membrane, developing the lag time analysis to measure gaseous diffusion coefficients.[12] The solution (4) is simplified by making the diffusing component concentration zero in one of the chambers ($c_2 = 0$). Then we can write

$$c = c_1\frac{l - x}{l} + \frac{2}{\pi}\sum_{n=1}^{\infty}\frac{-c_1}{n}\sin\frac{n\pi x}{l}\exp\frac{-Dn^2\pi^2 t}{l^2} \tag{5}$$

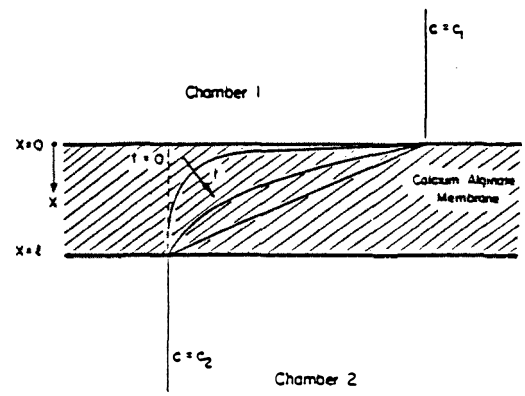

Figure 1. Concentration gradient in a calcium alginate membrane.

It is convenient to measure the concentration of the diffusing component as a function of time in the chamber where c_2 is assumed to be zero. As previously mentioned, the actual deviation from zero is small so that the experimental data fit the theoretical results well. By differentiating eq. (5) we can determine the instantaneous flux into the chamber

$$F|_{x=l} = -D\left(\frac{\partial c}{\partial x}\right)_{x=l} = \frac{Dc_1}{l}\left[1 + 2\sum_{n=1}^{\infty}(-1)^n \exp\frac{-Dn^2\pi^2 t}{l^2}\right] \quad (6)$$

Integrating eq. (6) with respect to t from $t = 0$ to $t = t_s$ and multiplying by the membrane area A determines $Q|_{t_s}$, the total amount of solute transferred through the membrane at the time of sampling. This amount, of course, is the product of the measured concentration in the chamber where $c_2 = 0$ and the chamber volume. Thus, we find

$$Q\Big|_{t_s} = \frac{ADc_1t_s}{l} + \frac{2lA}{\pi^2}\sum_{n=1}^{\infty}\frac{c_1(-1)^n}{n^2} \times\left(1 - \exp\frac{-Dn^2\pi^2t_s}{l^2}\right) = V\cdot c_2\Big|_{t_s} \quad (7)$$

Equivalently

$$Q|_{t_s} = ADt_s\frac{c_1}{l} - \frac{Ac_1l}{6} - \frac{A2lc_1}{\pi^2}\sum_{n=1}^{\infty}\frac{(-1)^n}{n^2}\exp\frac{-Dn^2\pi^2t_s}{l^2} \quad (8)$$

For sufficiently large times the summation term on the right hand side of eq. (8) becomes insignificant. In this case the total amount of solute transferred increases linearly with time

$$Q|_{t_s} = \frac{ADc_1}{l}\left(t_s - \frac{l^2}{6D}\right) \quad (9)$$

A graph of Q versus t approaches a straight line, which intercepts the time axis at $t = l^2/6D$. Figures 2 and 3 are experimental graphs of Q versus t for the diffusion of glucose and ethanol, respectively, in 2% calcium alginate. The intercept of the linear part of the curve is referred to as the lag time. Diffusion coefficients are calculated from the lag time and the membrane thickness.

Rogers et al.[13] took only the leading term of the rapidly converging series in eq. (6) and obtained the equation

$$\ln(t^{1/2}F) = \ln\left[2c_1\left(\frac{D}{\pi}\right)^{1/2}\right] - \frac{l^2}{4Dt} \quad (10)$$

Plotting $\ln(t^{1/2}F)$ versus $1/t$ results in a straight line of slope $-l^2/4D$. Thus, the diffusion coefficient is mea-

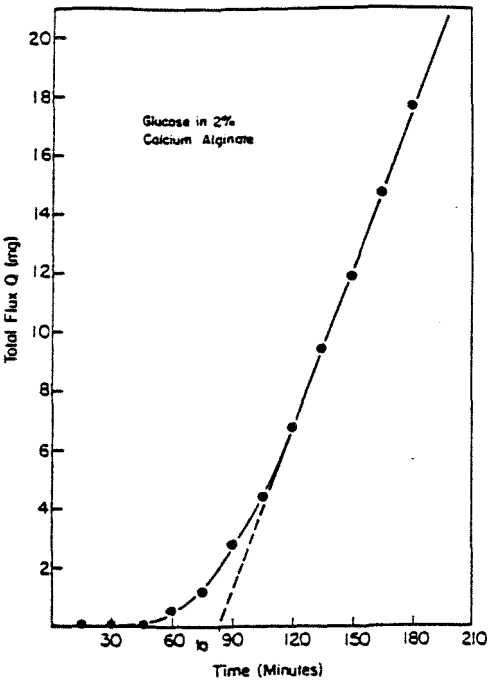

Figure 2. Lag time for glucose diffusion in 2% calcium alginate (C_1 = 10 g/L, t_0 = 81.4 min).

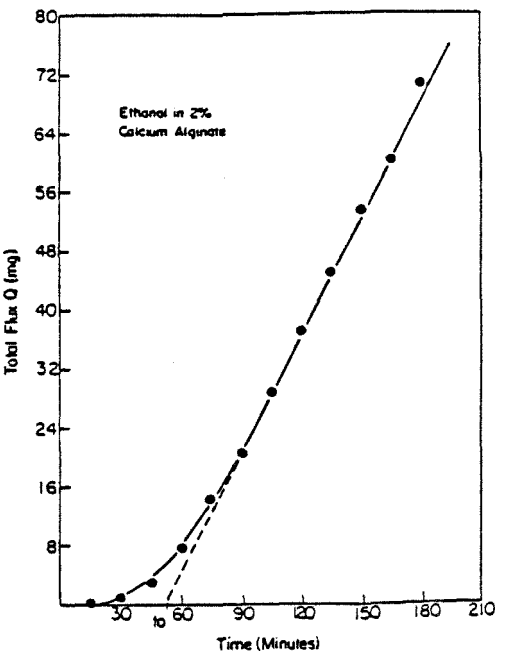

Figure 3. Lag time for ethanol diffusion in 2% calcium alginate (C_1 = 10 g/L, t_0 = 51.1 min).

sured from the slope of the line. Determining F experimentally requires differentiating a graph of Q versus t at various points since $F = (1/A)(dQ/dt)$, where A is the membrane area. Differentiation of the Q versus t graph introduced additional error, however, which led to significant scattering of the data. Therefore, Roger's method of measuring the diffusion coefficients was not applied to the experimental data.

In addition to the lag time analysis and Roger's method, diffusion coefficients are measured by the steady state method.[14] At steady state eq. (1) becomes

$$0 = D\frac{d^2c}{dx^2} \tag{9}$$

Applying the boundary conditions (2) to eq. (9) gives the steady state concentration profile

$$c = c_1 + (c_2 - c_1)\frac{x}{l} \tag{10}$$

The flux at steady state is given by

$$F = -D\left(\frac{dc}{dx}\right) = \frac{D(c_1 - c_2)}{l} = \frac{1}{A}\left(\frac{dQ}{dt}\right) \tag{11}$$

The slope of the straight line in the Q versus t plot is simply (dQ/dt) at steady state. Therefore,

$$D = \frac{l}{(c_1 - c_2)A}\left(\frac{dQ}{dt}\right)_{ss} \tag{12}$$

The disadvantage of the steady state method is that more parameters are required. In addition to the membrane thickness, it is necessary to know the concentration difference across the membrane and the area of the membrane. For solute partition coefficients, K_p, other than 1.0, the concentration gradient across the membrane equals $K_p(c_1 - c_2)$ rather than $c_1 - c_2$. Measuring the concentration difference in the chambers and the partition coefficient introduced additional error in the diffusion coefficient. Furthermore, since a wire mesh was used to support the membrane, the surface area for transport was not known precisely. The steady state method was found to give less consistent results than the lag time analysis for the experimental system used.

MATERIALS AND METHODS

Solutions of 1, 2, and 4% sodium alginate were made by dissolving 1, 2, and 4 g, respectively, of sodium alginate (Fisher Scientific, Pittsburgh, PA) in 100 mL of deionized water. The solutions were then autoclaved to prevent contamination. Membranes of 4.2 mm thickness and 10.9 cm diameter were cast in a metal ring between two porous glass plates and hardened in a bath of 2% (w/v) calcium chloride. Alginate membranes of 1 and 2% were hardened for 2½ h. Alginate membranes of 4% required 3 h in the bath before hardening was complete. Since the diffusion coefficient measured by the lag time analysis is proportional to the square of the membrane thickness, the accuracy of the experimental diffusion coefficients depends on the measurement of the membrane thickness to a large degree. In order to make suitable and consistent membranes for the experiments, the metal ring used to mold the alginate membranes must be uniformly thick and the glass plates must be flat. Slightly warped plates were found to produce nonuniform membranes that introduced reproducibility problems in the measured values of the diffusivities. The membrane thickness could not be measured consistently by micrometer because the gel compressed under very light pressure. The membrane thickness was best controlled by weighing an appropriate amount of the alginate solution before casting between the glass plates.

Membranes containing *S. cerevisiae* cells were prepared as follows. A dense cell suspension was washed with 50% ethanol to kill the yeast. Staining with methylene blue showed cell death to be complete without lysis of the cells. The yeast was centrifuged, then washed with water and centrifuged again. Membranes containing 2% alginate plus yeast were prepared by mixing 20% (wt.) cells, 40% (wt.) of 4% alginate solution, and 40% (wt.) deionized water. The required amount of the mixture was cast to produce a membrane 4.2 mm thick. Membranes of 1% alginate with cells were similarly prepared.

Diffusion Cell

Diffusion experiments were performed in a plexiglass cell consisting of two half-cells; the apparatus is shown in Fig. 4. Each half-cell contained a cylindrical chamber of 152 mL volume. The half-cells were held together with screws so that the chambers connected. A calcium alginate membrane supported by a wire mesh was placed between the chambers and sealed with O-rings. The area around the chambers was sealed with a rubber gasket. The lower chamber, filled initially with deionized water, was connected to a capillary column. Samples were withdrawn from the lower chamber through a septum. The upper chamber contained a solution of glucose or ethanol. Both chambers were magnetically stirred. The capillary column provided a reservoir of water to replace liquid removed during sampling. Diffusion experiments were conducted at 22–26°C.

Analyses

Glucose concentrations were assayed using hexokinase/glucose-6-phosphate dehydrogenase enzyme kits (Sigma Chemical Co., St. Louis, MO). Ethanol concentrations were determined by gas chromatography

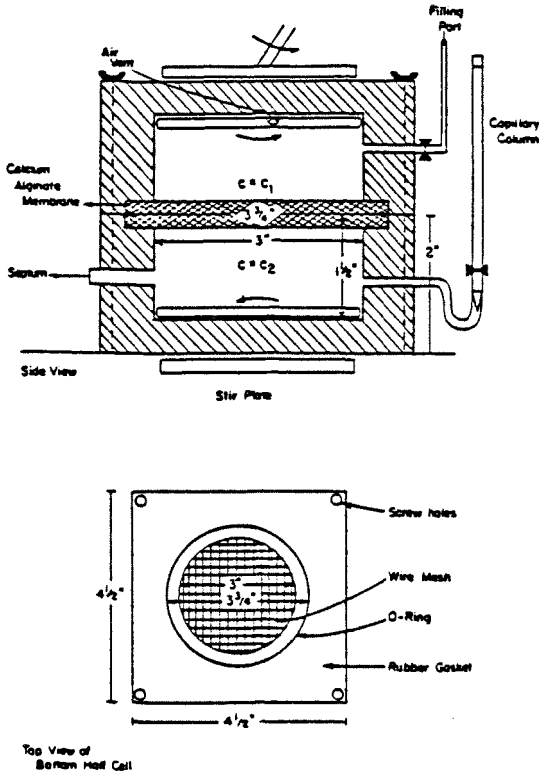

Figure 4. Diffusion Cell.

on a Chromoabsorb 102 column (Varian Associates, Walnut Creek, CA).

RESULTS AND DISCUSSION

The diffusion coefficient of glucose in 2% calcium alginate is 6.1×10^{-6} cm²/sec. Under the same conditions the diffusion coefficient of ethanol is 1.0×10^{-5} cm²/sec. Both values are only slightly lower (9%) than the respective diffusion coefficients in water, as shown in Table II. Tanaka et al. reported similar results for glucose diffusion into and from 2% calcium alginate beads.[10] In dilute water solutions, ethanol with a hydrodynamic radius of 2.25 Å diffuses 1.6 times faster than glucose with a hydrodynamic radius of 3.61 Å. Similarly, the ratio of ethanol diffusivity to glucose diffusivity in 2% calcium alginate is 1.6. The consistency of the diffusivity ratio indicates that the hydrodynamic theory of diffusion in liquids may be applicable to diffusion in dilute alginate gels.

The diffusion coefficients of glucose and ethanol in 1, 2, and 4% alginate are shown in Fig. 5. Increasing the alginate concentration from 1 to 4% leads to a significant decrease in the ethanol diffusion coefficient. The diffusion coefficient of glucose also decreases with increasing alginate concentration. Klein et al. measured the maximal pore size by inverse size exclusion chromatography and determined that calcium alginate gels have maximal pore diameters on the order of 150 Å for 3% Manugel DLB alginate and 7% Manucol LD alginate.[1] Scherer et al. reported that the diameter of calcium alginate pores measured by scanning electron microscopy is on the order of 10 μm.[17] Klein et al. explained the discrepancy by observing that the surface structure of alginate gels has a lower porosity than the bulk phase.[1] Glucose and ethanol with diameters of 7.2 and 4.5 Å, respectively, are an order of magnitude smaller than the surface pores and four orders of magnitude smaller than the bulk pores. Therefore, the slower diffusion rate of glucose and ethanol in more concentrated alginate gels is probably due to a decrease

Table II. Glucose and ethanol diffusion coefficients in 2% alginate and water.

	Diffusion coefficients (cm²/sec)		
Substrate	2% calcium alginate membrane	2% calcium alginate beads	Water
Glucose	6.1×10^{-6}	6.8×10^{-6}[a]	6.7×10^{-6}[b]
Ethanol	1.0×10^{-5}	—	1.1×10^{-5}[c]

[a] Reference 10.
[b] Reference 15.
[c] Reference 16.

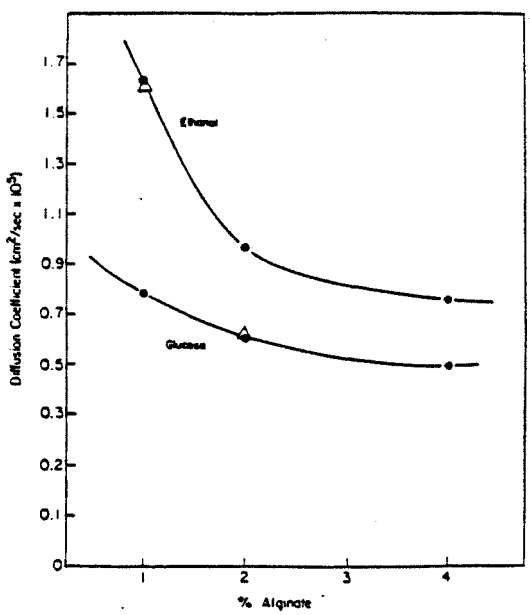

Figure 5. Effect of alginate concentration on glucose and ethanol diffusion coefficients. Cell-free membrane (●); cell-occupied membrane (△) (C_1 = 10 g/L).

in the number and length of the pores rather than a decrease in the pore diameters. In 1 and 2% alginate, glucose and ethanol diffusion is mainly controlled by the rate at which the solute diffuses through the solvent occupying the pores (i.e., water). At 4% alginate concentration the diffusion rate is further restricted by the increased path length required for diffusion through the gel.

The ratio of ethanol diffusivity to glucose diffusivity is plotted as a function of alginate concentration in Fig. 6. At 1% alginate concentration the ratio deviates significantly from the value of 1.6 for dilute water solutions and 2 and 4% alginate gels. For 1% calcium alginate membranes, convective transport may not be negligible as assumed in the lag time analysis. The two chambers of the diffusion cell were well stirred, so solute molecules could have been carried by convection at the edges of the membrane. The effective diffusion distance through the membrane is decreased, leading to an overestimate of the diffusion coefficient. Thus, partial convective transport in 1% alginate can account for the deviation from the hydrodynamic theory.

Concentrations of glucose in the range of 2–100 g/L and ethanol in the range of 10–80 g/L did not affect the diffusion coefficients. The experimental results are shown graphically in Fig. 7.

Yeast cells immobilized in 2% calcium alginate had no effect on the diffusion coefficient of glucose at a cell concentration of 20% by weight. Similarly the diffusion coefficient of ethanol in 1% alginate was unaffected by immobilized cells. Figure 5 illustrates these results. Cell concentrations denser than 20% may reduce the diffusion rate by increasing the tortuosity of the gel. Higher cell loadings were attempted; however, they weakened the membrane, causing deterioration before the flux became linear with time. Cells immobilized in calcium alginate and then allowed to reproduce may significantly affect diffusion coefficients even at low overall cell loadings. Instead of being well distributed throughout the gel, immobilized growing cells

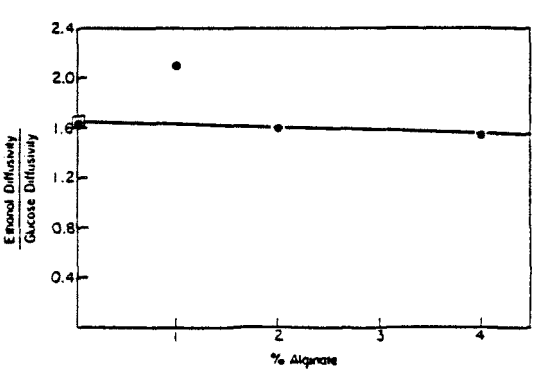

Figure 6. Effect of alginate concentration on the ratio of ethanol diffusivity to glucose diffusivity. Cell-free membrane (●); water □.

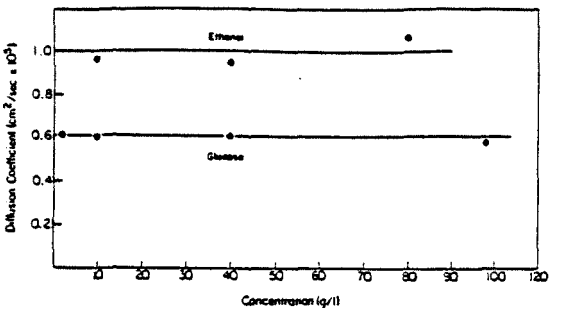

Figure 7. Effect of glucose and ethanol concentrations (c_1) on the diffusion coefficients in 2% alginate.

are found in clumps. Since most cell growth occurs near the gel surface, the cells may form a dense microbial layer slowing the rate of mass transport. Additionally, cells killed by 50% ethanol have permeabilized cell membranes, which may allow glucose and ethanol diffusion through the cell. The intact membrane of living cells presents an additional barrier to solute diffusion.

CONCLUSION

Although alginate gels allow fairly rapid diffusion of small molecules, the productivity of immobilized cells may still be limited by the presence of the alginate matrix. Cells immobilized in calcium alginate obtain nutrients solely by diffusion, whereas in suspended cultures nutrients are carried by convective flow. Diffusion is a significantly slower process than convective transport in a well-stirred reactor. Cell reproduction in the outer shell of alginate beads illustrates the lack of substrate inside the bead. This situation can be described as a reaction front. The rates of cell growth and product synthesis depend on the substrate concentration immediately surrounding the cell. For immobilized cells the substrate concentration falls below a critical value for growth and possibly product synthesis close to the bead's surface. The position of the reaction front, where the limiting substrate concentration falls below a critical value, depends on the substrate diffusion coefficient and the rate of substrate utilization by the cells. To operate an immobilized cell reactor efficiently it is desirable to extend the reaction front to the center of the beads, resulting in a smoother concentration gradient. Rapid cell growth in the outer shell and cell death in the inner core could thus be prevented. Controlling the concentration gradient for productivity optimization requires diffusion coefficients as well as models for the rates of immobilized cell growth, substrate utilization, and product synthesis under varying substrate and product concentrations. Developing the necessary immobilized cell models

is a complicated endeavor. The simplest solution is to try to apply suspended cell models to immobilized cells. Metabolic changes may be induced by entrapping the cells in a polymer, however, making suspended cell models invalid. Another problem is that suspended cell models are usually developed under steady state growth conditions and may not apply to the transient conditions of immobilized cells. Modelling the rates of growth, substrate utilization, and product synthesis for immobilized cells will be aided by knowing diffusion coefficients under various conditions to account for diffusion owing to concentration gradients that cannot easily be eliminated.

This work was supported in part by the Caltech President's Fund No. 228 and an NSF Presidential Young Investigator's Award, CPE-8352314.

NOMENCLATURE

- A membrane area (cm^2)
- c concentration (g/cm^3)
- c_1 concentration at $x = 0$ (g/cm^3)
- c_2 concentration at $x = l$ (g/cm^3)
- D diffusion coefficient (cm^2/sec)
- F flux (g/cm^2 sec)
- K_p partition coefficient of solute between gel and aqueous phases
- l membrane thickness (cm)
- Q total flux or amount of solute transferred (g)
- t time (sec)
- t_0 lag time (min)
- t_s time of sampling (sec)
- x distance (cm)
- V volume of chamber (cm^3)

References

1. J. Klein, J. Stock, and K.-D. Vorlop, *Eur. J. Appl. Microbiol. Biotechnol.*, 18, 86 (1983).
2. A. Shinmyo, H. Kimura, and H. Okada, *Eur. J. Appl. Microbiol. Biotechnol.*, 14 (1982).
3. J. M. Navarro and G. Durand, *Eur. J. Appl. Microbiol. Biotechnol.*, 4, 243 (1977).
4. I. Nilsson, S. Ohlson, L. Häggstrom, N. Molin, and K. Mosbach, *Eur. J. Appl. Microbiol. Biotechnol.*, 10, 261 (1980).
5. H. Hiemstra, L. Dykhuizen, and W. Harder, *Eur. J. Appl. Microbiol. Biotechnol.*, 18, 189 (1983).
6. H. Bettmann and H. J. Rehm, *Appl. Microbiol. Biotechnol.*, 20, 285 (1984).
7. H. Eihmeier, F. Westmeier, and H. J. Rehm, *Appl. Microbiol. Biotechnol.*, 19, 53 (1984).
8. K. Sato and K. Toda, *J. Ferment. Technol.*, 61(3), 239 (1983).
9. K. Toda and M. Shoda, *Biotechnol. Bioeng.*, 17, 481 (1975).
10. H. Tanaka, M. Matsumura, and I. A. Veliky, *Biotechnol. Bioeng.*, 26, 53 (1984).
11. H. S. Carslaw, *Fourier's Series and Integrals* (Macmillan, New York, 1906), p. 263.
12. H. A. Daynes, *Proc. R. Soc.*, 97A, 286 (1920).
13. W. A. Rogers, R. S. Buritz, and D. Alpert, *J. Appl. Phys.*, 25, 868 (1954).
14. J. Crank and G. S. Park, Eds., *Diffusion in Polymers* (Academic Press, New York, 1968), p. 4.
15. L. G. Longsworth, *J. Am. Chem. Soc.*, 75, 5705 (1953).
16. P. A. Johnson and A. L. Babb, *Chem. Revs.*, 56, 387 (1956).
17. P. Scherer, M. Kluge, J. Klein, and H. Sahm, *Biotechnol. Bioeng.*, 23, 1057 (1981).

CHAPTER 3
INTRINSIC GROWTH AND REACTION RATES OF ENTRAPPED CELLS

3.1 INTRODUCTION

In designing and optimizing immobilized cell processes for biochemical production, it is important to characterize the intrinsic, specific growth and reaction rates of the organism at conditions close to the reactor operating conditions. Then the intrinsic reaction rates can be coupled with mass transfer rates to predict the productivity of an immobilized cell reactor. Suspended cell growth and reaction rates cannot be extrapolated to immobilized cells because significant rate changes may occur when cells are immobilized. Furthermore, the method of cell immobilization and the nature of the organism appear to influence the intrinsic, specific rates of growth and reaction. Intrinsic, specific growth and reaction rates for immobilized cells can be used to characterize and optimize immobilized cell reactors.

In the past many investigators used bench-scale immobilized cell reactors to predict the behavior of larger reactors without determining intrinsic reaction rates . Since mass transport rates are functions of reactor size and geometry and volumetric flow rate, the overall reaction rates measured in a bench-scale reactor can be significantly different than the overall reaction rates in a large scale reactor. Therefore, a reliable method for measuring the intrinsic, specific growth rate and reaction rates is necessary to predict the behavior of immobilized cell systems.

Intrinsic reaction rates are difficult to obtain for growing cells entrapped

in a polymeric matrix. Cell growth and intraparticle diffusion make bulk fluid concentration measurements useless in most situations. Many researchers have assumed that the biomass concentration of immobilized cells remains constant for long periods of time in order to model the diffusion and reaction. The biomass concentration will remain constant only if there is no cell growth or if the rate of cell growth equals the rate of attrition. However, the optimum operating conditions may allow cell growth at a rate other than the rate of attrition. New approaches are needed to accurately determine the intrinsic, specific growth rate and reaction rates of entrapped cells.

3.2 THEORY

The simultaneous processes of diffusion and reaction have been analyzed to determine the intrinsic specific growth rate, specific substrate uptake rate, and specific ethanol production rate of *Saccharomyces cerevisiae* immobilized in calcium alginate gel. Transient glucose and ethanol concentration data are used to calculate the intrinsic reaction rates by compensating for the diffusion effects. The method is somewhat analogous to the lag time method, which is used to measure diffusion coefficients from transient, solute concentration data. Details of the lag time method for diffusion coefficients were given in Chapter 2. As illustrated in Figure 2.1 of Chapter 2, cells are immobilized in an alginate membrane, which is situated between two liquid chambers with different substrate concentrations, s_1 and s_2. The alginate membrane is prepared with an initial substrate concentration of s_1, where s_1 is less than s_2. With this initial condition for substrate concentration in the alginate membrane, the results of the mathematical analysis can be simplified to facilitate data

manipulation and interpretation. The chambers are well mixed to minimize external mass transfer resistances between the fluid and the alginate membrane. Substrate then diffuses from the high concentration chamber, through the membrane, and into the low concentration chamber. Some of the substrate is used by the cells in the alginate membrane, but the experiment is designed so that substrate diffuses into the membrane faster than it can be used by the cells.

The growth rate and reaction rates of *S. cerevisiae* can vary with substrate concentration under some conditions. According to the model of Peringer, et al. for *S. cerevisiae* growth in a chemostat at similar glucose concentrations to those used in this investigation, the glucose uptake rate and growth rate will each vary by 9 % for a change in glucose concentration from 1.0 g/l to 50.0 g/l (1). Experiments conducted in batch cultures with *S. cerevisiae* 18790 indicate that there is no variation in the growth rate for glucose concentrations from 1.0 g/l to 50.0 g/l glucose as shown in Figure 3.1. Therefore, substrate concentrations s_1 and s_2 are initialized at 1.0 g/l and 50.0 g/l glucose so that the growth rate and rate of glucose uptake are independent of glucose concentration. Similarly,the product syntheses rates are assumed to be independent of substrate concentration.

The difference in substrate concentrations between the two chambers provides a gradient for substrate transport through the membrane. The concentration gradient across the membrane must be high enough so that glucose diffuses through the membrane faster than it is consumed by the cells. The experiment lasts until the end of the exponential phase or until the substrate concentration in the membrane falls below the limit for zero-order kinetics. Thus we can

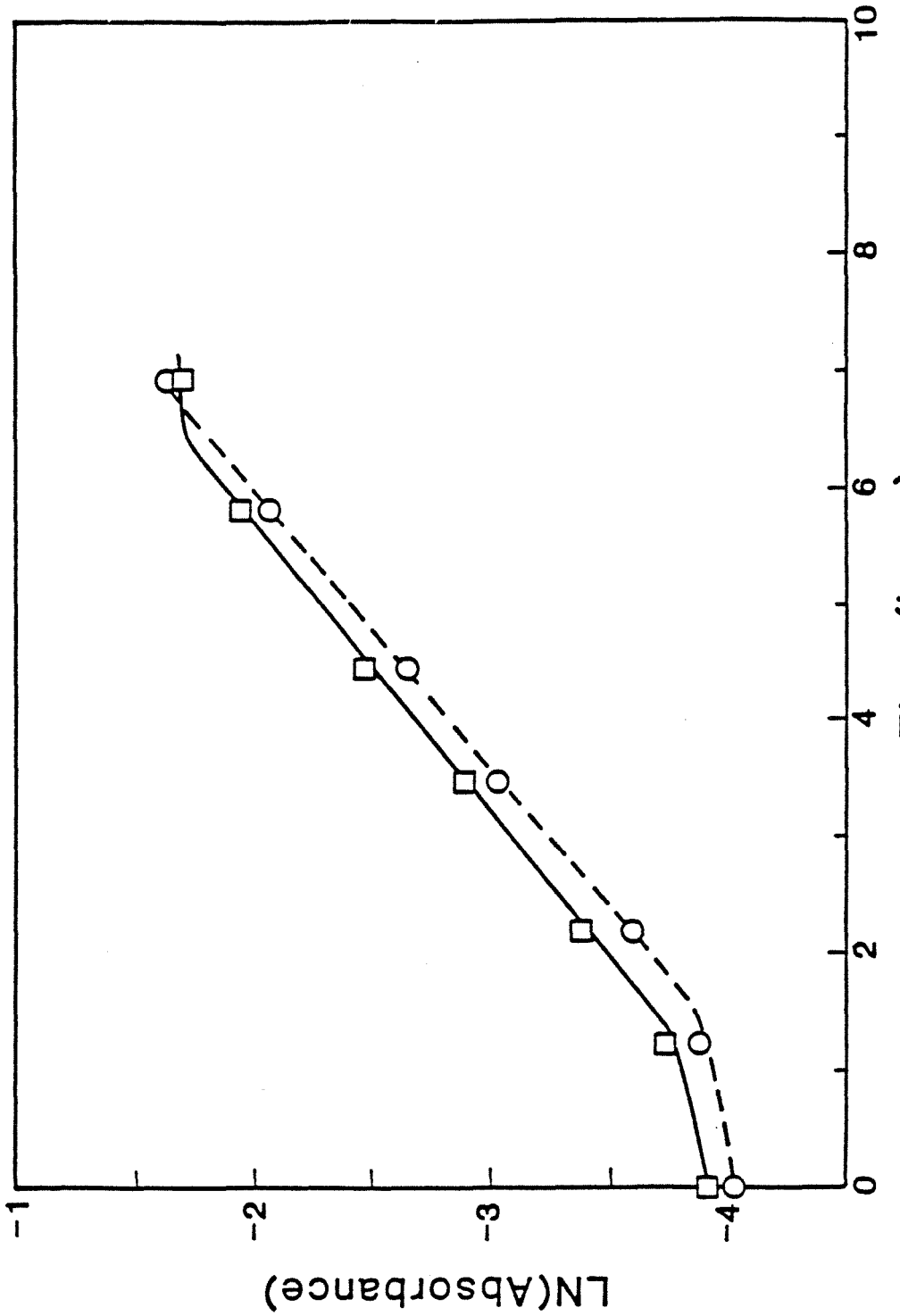

Figure 3.1 Effect of Glucose Concentration on Growth Rate with (□) 1 g/l glucose, or (○) 50 g/l glucose in medium.

assume that the immobilized cells are growing exponentially throughout the experiment. Intrinsic growth and reaction rates were determined using only the data collected during the first eight hours of any experiment.

The mathematical analysis used to determine the intrinsic, specific growth rate and reaction rates assumes that there is no lag phase during the experiment. A lag phase was prevented by harvesting cells from a batch culture during the early exponential phase and then preparing the alginate membrane at $4°C$. Additionally, the glucose concentration in the growth medium was made similar to the initial membrane concentration to minimize the effect of change in the cells' environmemt.

3.2.1 Glucose Uptake

The diffusion and reaction of glucose in an alginate membrane between two chambers is governed by the partial differential equation:

$$\frac{\partial s}{\partial t} = D_g \frac{\partial^2 s}{\partial x^2} - \alpha b_0 e^{\mu t}, \tag{3.1}$$

where s is the glucose concentration in the membrane, D_g is the diffusion coefficient of glucose, x is distance, t is time, α is the specific rate of glucose uptake, b_0 is the initial biomass concentration, and μ is the specific growth rate. The specific growth rate and specific glucose uptake rate are assumed constant, as discussed previously. The glucose concentration is subject to the boundary conditions:

$$\begin{aligned} s &= s_1 \quad \text{at} \quad x = 0 \\ s &= s_2 \quad \text{at} \quad x = L, \end{aligned} \tag{3.2}$$

where L is the thickness of the membrane. When the initial concentration of glucose in the alginate is equal to the glucose concentration in the low

concentration chamber, the following initial condition applies:

$$s = s_1 \quad \text{at} \quad t = 0 \quad \text{for all} \quad x. \tag{3.3}$$

For s_2 greater than s_1, glucose diffuses from the chamber where $s = s_2$ through the alginate membrane into the chamber where $s = s_1$, while part of the glucose is consumed by the cells. In general, the glucose concentrations in the two chambers are not precisely constant because of the flux of glucose. However, as shown in Chapter 2 for the lag time method of measuring diffusion coefficients, when the chambers are large enough, the concentration changes over the course of the experiment are small and can be ignored. Therefore, s_1 and s_2, the glucose concentrations in the chambers, are assumed constant with time, which allows the solution to Equation (3.1) with boundary conditions (3.2) and initial condition (3.3) to be greatly simplified.

Equation (3.1) with boundary conditions (3.2) and initial condition (3.3) can be solved analytically by assuming a solution of the form:

$$s(x,t) = u(x,t) + \bar{s}(x), \tag{3.4}$$

where $u(x,t)$ represents the unsteady-state solution and $\bar{s}(x)$ represents the steady-state solution. The steady-state solution into Equation (3.1) results in the equation:

$$0 = D_g \frac{d^2\bar{s}}{dx^2} \tag{3.5}$$

with boundary conditions:

$$\begin{aligned} \bar{s} &= s_1 \qquad \text{at} \qquad x = 0 \\ \bar{s} &= s_2 \qquad \text{at} \qquad x = L. \end{aligned} \tag{3.6}$$

The solution to Equation (3.5) with boundary conditions (3.6) is given by:

$$\bar{s}(x) = s_1 + \frac{(s_2 - s_1)x}{L}. \tag{3.7}$$

Substituting Equation (3.4) into Equation (3.1) and applying the boundary and initial conditions (3.2) and (3.3) result in the following equation for the transient component, u:

$$\frac{\partial u}{\partial t} = D_g \frac{\partial^2 u}{\partial x^2} - \alpha b_0 e^{\mu t} \tag{3.8}$$

with boundary conditions:

$$\begin{aligned} u(0,t) &= 0 \\ u(L,t) &= 0 \end{aligned} \tag{3.9}$$

and initial condition:

$$u(x,0) = \frac{-(s_2 - s_1)x}{L}. \tag{3.10}$$

The unsteady - state solution, $u(x,t)$, is determined by a sine transform. When the solution for $u(x,t)$ is combined with $\bar{s}(x)$ of Equation (3.7), we obtain the complete solution to Equation (3.1) with boundary conditions (3.2) and initial condition (3.3):

$$\begin{aligned} s(x,t) = s_1 + \frac{(s_2 - s_1)x}{L} + \sum_{\rho=1}^{\infty} \Bigg\{ \Bigg[& \frac{2(s_2 - s_1)(-1)^\rho}{\rho\pi} exp(-D_g \rho^2 \pi^2 t / L^2) \\ & + \frac{2\alpha b_0 L^2 \left((-1)^\rho - 1\right)}{\rho\pi(\mu L^2 + D_g \rho^2 \pi^2)} \left(exp(\mu t) + exp(-D_g \rho^2 \pi^2 t / L^2)\right) \Bigg] \\ & \sin\left(\frac{\rho\pi x}{L}\right) \Bigg\}. \end{aligned} \tag{3.11}$$

Similarly to the lag time method of measuring diffusion coefficients, the time dependent flux into the lower concentration chamber can be determined by

differentiating the concentration expression, Equation (3.11), with respect to x at the boundary $x = 0$ with the following result:

$$F(t) = -D_g \frac{\partial s}{\partial x}\bigg|_{x=0} = \frac{-D_g(s_2 - s_1)}{L} - \sum_{\rho=1}^{\infty}\Bigg\{\Bigg[\frac{2D_g(s_2 - s_1)(-1)^\rho}{L} exp(-D_g\rho^2\pi^2 t/L^2) - \left(\frac{2\alpha b_0 L((-1)^\rho - 1)}{(\mu L^2 + D_g\rho^2\pi^2)}\right) (exp(\mu t) + exp(-D_g(2\rho - 1)^2\pi^2 t/L^2))\Bigg]\Bigg\}. \tag{3.12}$$

Integrating Equation (3.12) from $t = 0$ to $t = \tau$ and multiplying by the membrane surface area give the total amount of glucose that diffused into the low concentration chamber during the experiment, Q:

$$Q = \int_0^\tau \| - D_g A\frac{\partial s}{\partial x}\| = \frac{D_g A(s_2 - s_1)\tau}{L} + A\sum_{\rho=1}^{\infty}\Bigg\{\Bigg[\frac{-2(s_2 - s_1)(-1)^\rho L}{\rho^2\pi^2}\left(\exp(-D_g\rho^2\pi^2\tau/L^2) - 1\right)\Bigg] + \Bigg[\frac{2\alpha b_0 L((-1)^\rho - 1)}{(\mu L^2 + \rho^2\pi^2 D_g)}\left(\frac{\exp(\mu\tau)}{\mu} - \frac{1}{\mu} - \frac{L^2\exp(-D_g\rho^2\pi^2\tau/L^2)}{D_g\rho^2\pi^2} + \frac{L^2}{D_g\rho^2\pi^2}\right)\Bigg]\Bigg\}. \tag{3.13}$$

Experimentally, it is possible to follow the transport of glucose into the low concentration chamber by withdrawing samples and measuring concentration as a function of time.

$$Q = V_c(s_1|_{t=\tau} - s_1|_{t=0}) \tag{3.14}$$

Taking the limit of Equation (3.13) for large times and rearranging terms yields

the following equation:

$$\frac{-Q}{A}+\frac{D_g(s_2-s_1)t}{L}-\frac{(s_2-s_1)L}{6}+\sum_{\rho=1}^{\infty}\frac{4\alpha b_0 L D_g}{\mu L^2+\mu(2\rho-1)^2\pi^2 D_g} = \sum_{\rho=1}^{\infty}\frac{4\alpha b_0 L D_g}{\mu^2 L^2+\mu(2\rho-1)^2\pi^2 D_g}\exp(\mu t). \tag{3.15}$$

Taking the natural logarithm of both sides, we obtain:

$$\ln\left[\frac{-Q}{A}+\frac{D_g(s_2-s_1)t}{L}-\frac{(s_2-s_1)L}{6}+\sum_{\rho=1}^{\infty}\frac{4\alpha b_0 L D_g}{\mu L^2+\mu(2\rho-1)^2\pi^2 D_g}\right] = \ln\left[\sum_{\rho=1}^{\infty}\frac{4\alpha b_0 L D_g}{\mu^2 L^2+\mu(2\rho-1)^2\pi^2 D_g}\right]+\mu t. \tag{3.16}$$

We define the left-hand side of Equation (3.16) to be $\ln Z_g$. The parameters s_1, s_2, L, and b_0 are set by the initial conditions of the experiment. D_g was measured at the experimental conditions as described later in this chapter. Q is measured as a function of time throughout the experiment as indicated in Equation (3.14). Consequently μ and α, the specific growth rate and specific substrate uptake rate, respectively, are the only unknown parameters in Equation (3.16). The measurement of the cumulative amount of glucose transported into the low concentration chamber, Q(t), can then be used to determine μ and α through an iterative procedure. By guessing initial values for μ and α, a plot of the left-hand side of Equation (3.16), $\ln Z_g$, versus time, should yield a straight line with a slope equal to μ, and y-intercept equal to a function of α and μ. Thus, μ, or the slope, is determined by a linear least-squares fit to the data and α is calculated from the y-intercept. The new values of μ and α are then used to recalculate $\ln Z_g$ versus time, and a least-squares routine is applied to again detemine μ and α. The iteration proceeds until the input values of μ and α match the calculated values.

The result of the substrate diffusion-reaction analysis applied to the anaerobic growth of *S. cerevisiae* is shown in Figure 3.2. For time greater than or equal to two hours, the negative exponential terms in Equation (3.13) are negligible as was assumed by taking the limit of Equation (3.13) for large times. The line in the figure represents the best fit to the data. As can be seen from Figure 3.2, the substrate diffusion-reaction theory fits the experimental data well.

3.2.2 Ethanol Production

The ethanol production rate can be determined by a similar analysis; however, different boundary and initial conditions lead to a different solution form. The ethanol concentration throughout the membrane is initially equal to zero and the concentration in both chambers is also equal to zero. Assuming exponential growth and constant specific ethanol production rate, the partial differential equation for ethanol diffusion and production is written:

$$\frac{\partial e}{\partial t} = \frac{\partial^2 e}{\partial x^2} + \nu b_0 e^{\mu t}, \tag{3.17}$$

where e is the ethanol concentration and ν is the specific ethanol production rate. The appropriate boundary conditions are:

$$\begin{aligned} e &= 0 \quad \text{at} \quad x = 0 \\ e &= 0 \quad \text{at} \quad x = L, \end{aligned} \tag{3.18}$$

and the initial condition is:

$$e = 0 \quad \text{at} \quad t = 0 \tag{3.19}$$

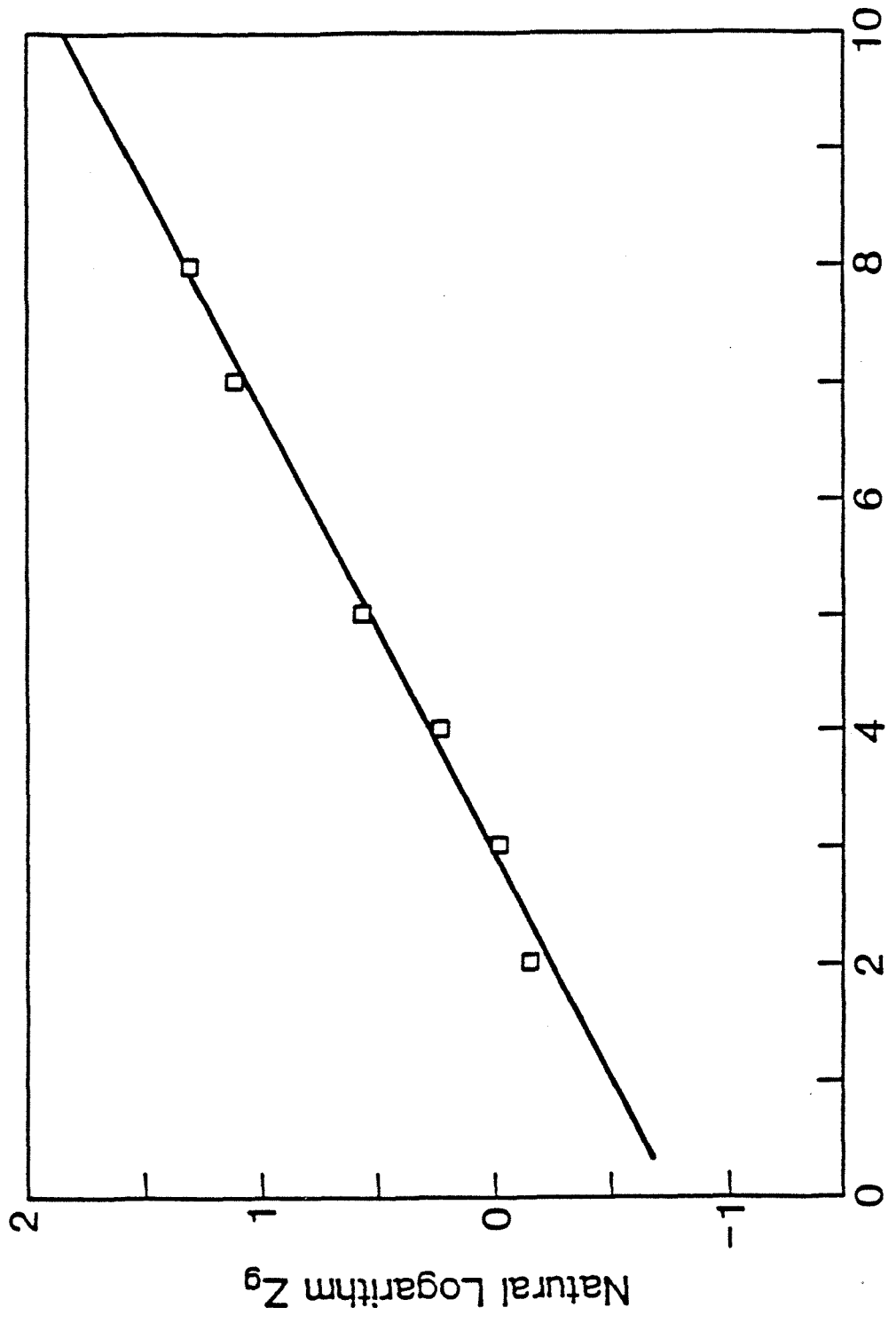

Figure 3.2 **Diffusion-Reaction Experiment for Glucose Uptake and Growth under anaerobic conditions. Run 1.**

Solving Equation (3.17) with boundary conditions (3.18) and initial condition (3.19) by the method of sine transform , the ethanol concentration throughout the membrane is given by:

$$e(x,t) = \sum_{\rho=1}^{\infty} \left\{ \frac{-2L^2 \nu b_0 ((-1)^\rho - 1)}{\rho^3 \pi^2 D_g + \rho \pi \mu L^2} \right. \\ \left. [\exp(\mu t) - \exp(-\rho^2 \pi^2 D_g t / L^2)] \sin\left(\frac{\rho \pi x}{L}\right) \right\}, \tag{3.20}$$

Differentiating with respect to x and evaluating the derivative at the boundaries $x = 0$ and $x = L$ result in the following expression for ethanol flux into the chambers:

$$\begin{aligned} F &= \| - D_g \frac{\partial e}{\partial x}|_{x=0} \| = \| - D_g \frac{\partial e}{\partial x}|_{x=L} \| \\ &= \sum_{\rho=1}^{\infty} \left\{ \frac{-2 D_g L \nu b_0 ((-1)^\rho - 1)}{\rho^2 \pi^2 D_g + \mu L^2} \left[\exp(\mu t) - \exp(-\rho^2 \pi^2 D_g t / L^2\right] \right\}. \end{aligned} \tag{3.21}$$

The total flux into a chamber is obtained by integrating Equation (3.21) over time from $t = 0$ to $t = \tau$ and multiplying by the membrane surface area.

$$\begin{aligned} Q &= \int_0^{\tau} \| - D_g A \frac{\partial e}{\partial x}|_{x=0} \| \partial t \\ &= A \sum_{\rho=1}^{\infty} \left\{ \frac{4 D_g L \nu b_0}{(2\rho - 1)^2 \pi^2 D_g + \mu L^2} \left(\exp(\mu t) - \frac{1}{\mu} \right.\right. \\ &\quad \left.\left. - \frac{L^2}{(2\rho - 1)^2 \pi^2 D_g} + \frac{L^2 \exp(-(2\rho - 1)^2 \pi^2 D_g t / L^2)}{(2\rho - 1)^2 \pi^2 D_g} \right) \right\} \end{aligned} \tag{3.22}$$

The total flux is also determined experimentally as a function of time by sampling for ethanol in the chambers:

$$Q = V_c(e|_{t=\tau}). \tag{3.23}$$

Taking the limit for large times and rearranging Equation (3.22), we obtain:

$$\frac{Q}{A} + \sum_{\rho=1}^{\infty} \left\{ \frac{4D_g L \nu b_0}{(2\rho-1)^2\pi^2 D_g + \mu L^2} \left(\frac{1}{\mu} + \frac{L^2}{(2\rho-1)^2\pi^2 D_g} \right) \right\}$$
$$= \sum_{\rho=1}^{\infty} \left\{ \left(\frac{4D_g L \nu b_0}{(2\rho-1)^2\pi^2 D_g \mu + \mu^2 L^2} \right) \exp(\mu t) \right\}. \tag{3.24}$$

Again, we take the natural logarithm of both sides of Equation (3.24), obtaining:

$$\ln\left[\frac{Q}{A} + \sum_{\rho=1}^{\infty} \left\{ \frac{4D_g L \nu b_0}{(2\rho-1)^2\pi^2 D_g + \mu L^2} \left(\frac{1}{\mu} + \frac{L^2}{(2\rho-1)^2\pi^2 D_g} \right) \right\} \right]$$
$$= \ln\left[\sum_{\rho=1}^{\infty} \left\{ \left(\frac{4D_g L \nu b_0}{(2\rho-1)^2\pi^2 D_g \mu + \mu^2 L^2} \right) \exp(\mu t) \right\} \right]. \tag{3.25}$$

The left-hand side of Equation (3.25) is defined as $\ln Z_e$. As in the glucose diffusion-reaction analysis, the growth rate and ethanol production rate can be determined by plotting $\ln Z_e$ versus time. An iterative procedure is again required. The ethanol production rate and growth rate of *S. cerevisiae* were determined under anaerobic conditions. The experimental data and the lines representing the best fit to the data are plotted in Figures 3.3–3.6 for two different experiments. The ethanol flux was measured in both reaction chambers during each experiment. Again, the negative exponential terms are negligible for time greater than or equal to two hours.

In Figures 3.3 and 3.4 the ethanol production rates were determined during the glucose diffusion - reaction experiments when the glucose concentration varied from 1.0 g/l to 50.0 g/l in the alginate membrane. Additionally, the ethanol production rate can be determined from experiments with equal concentrations of glucose in the two chambers. Experiments with 25.0 g/l

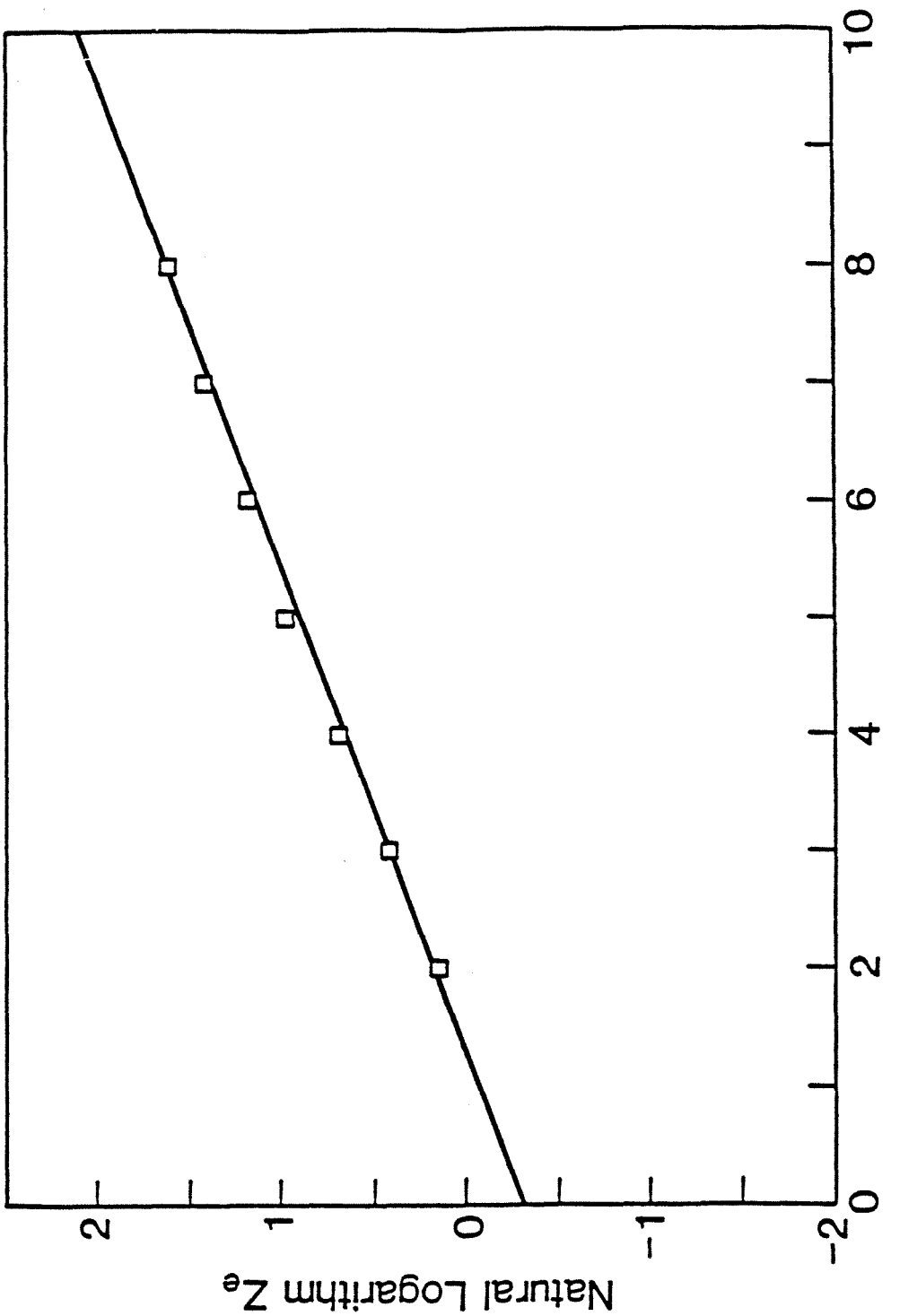

Figure 3.3 **Diffusion-Reaction Experiment for Ethanol Production and Growth under anaerobic conditions with asymmetric glucose concentrations. Run 1, chamber 1.**

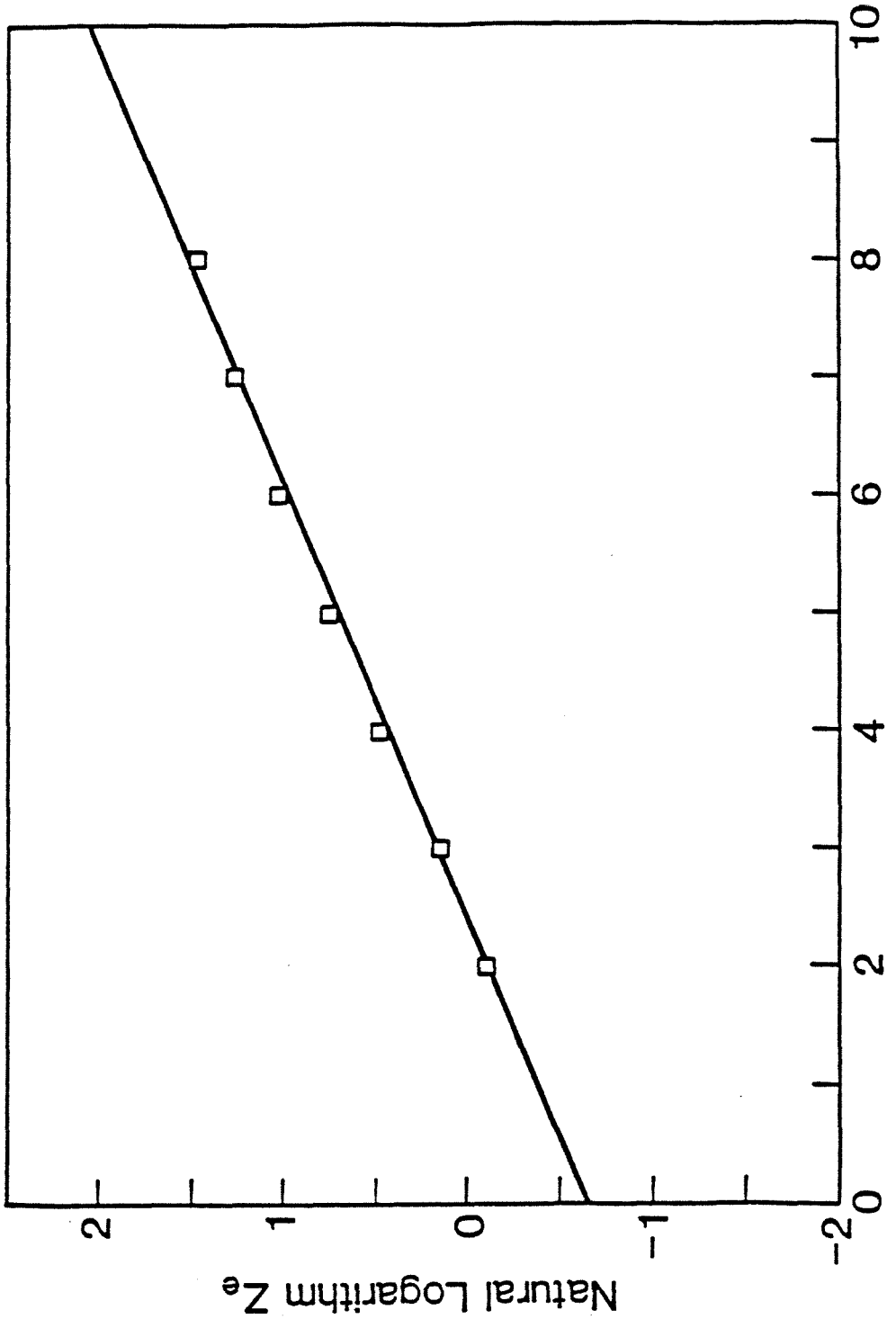

Figure 3.4 **Diffusion-Reaction Experiment for Ethanol Production and Growth under anaerobic conditions with asymmetric glucose conentrations. Run 1, chamber 2.**

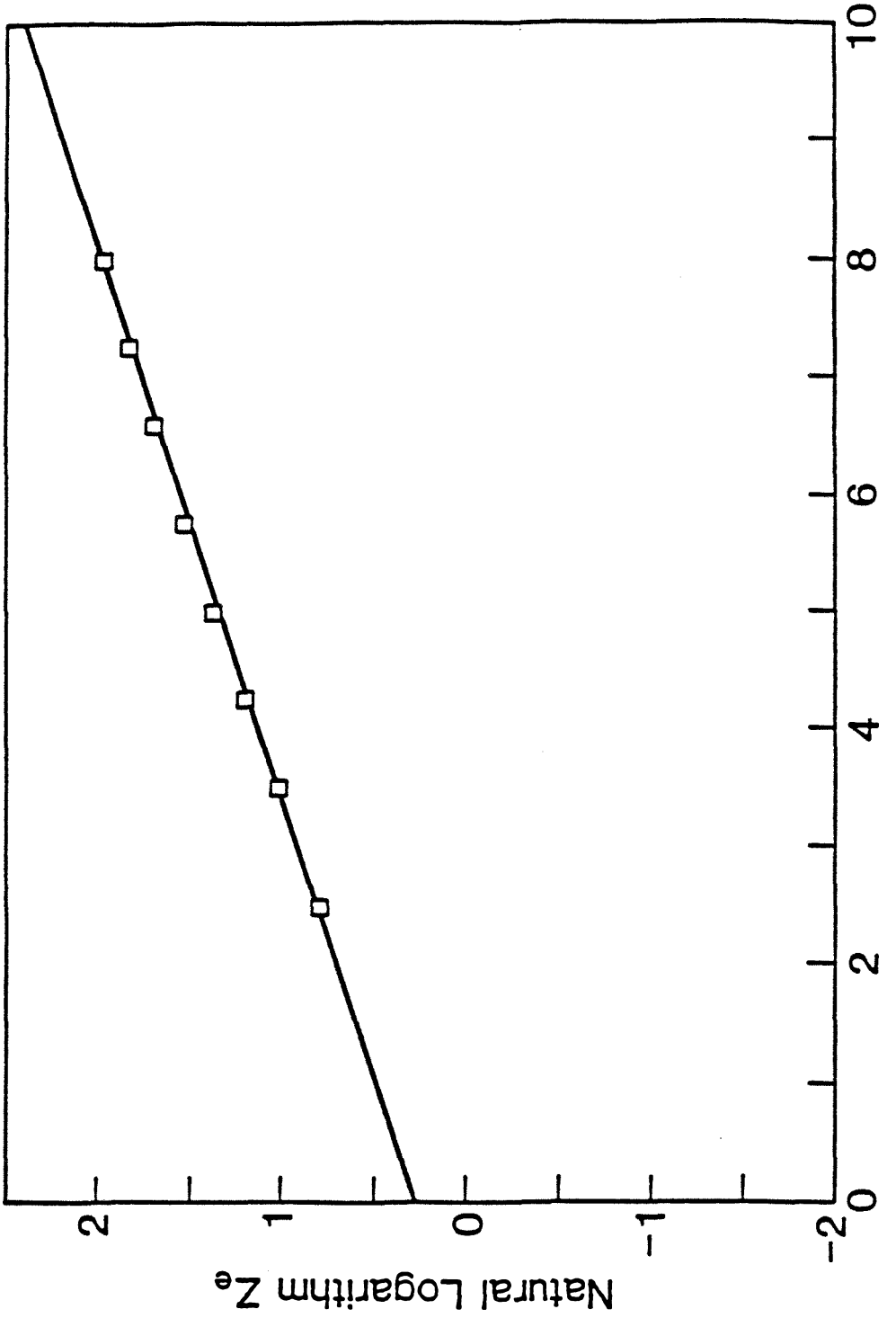

Figure 3.5 **Diffusion-Reaction Experiment for Ethanol Production and Growth under anaerobic conditions with symmetric glucose concentrations. Run 2, chamber 1.**

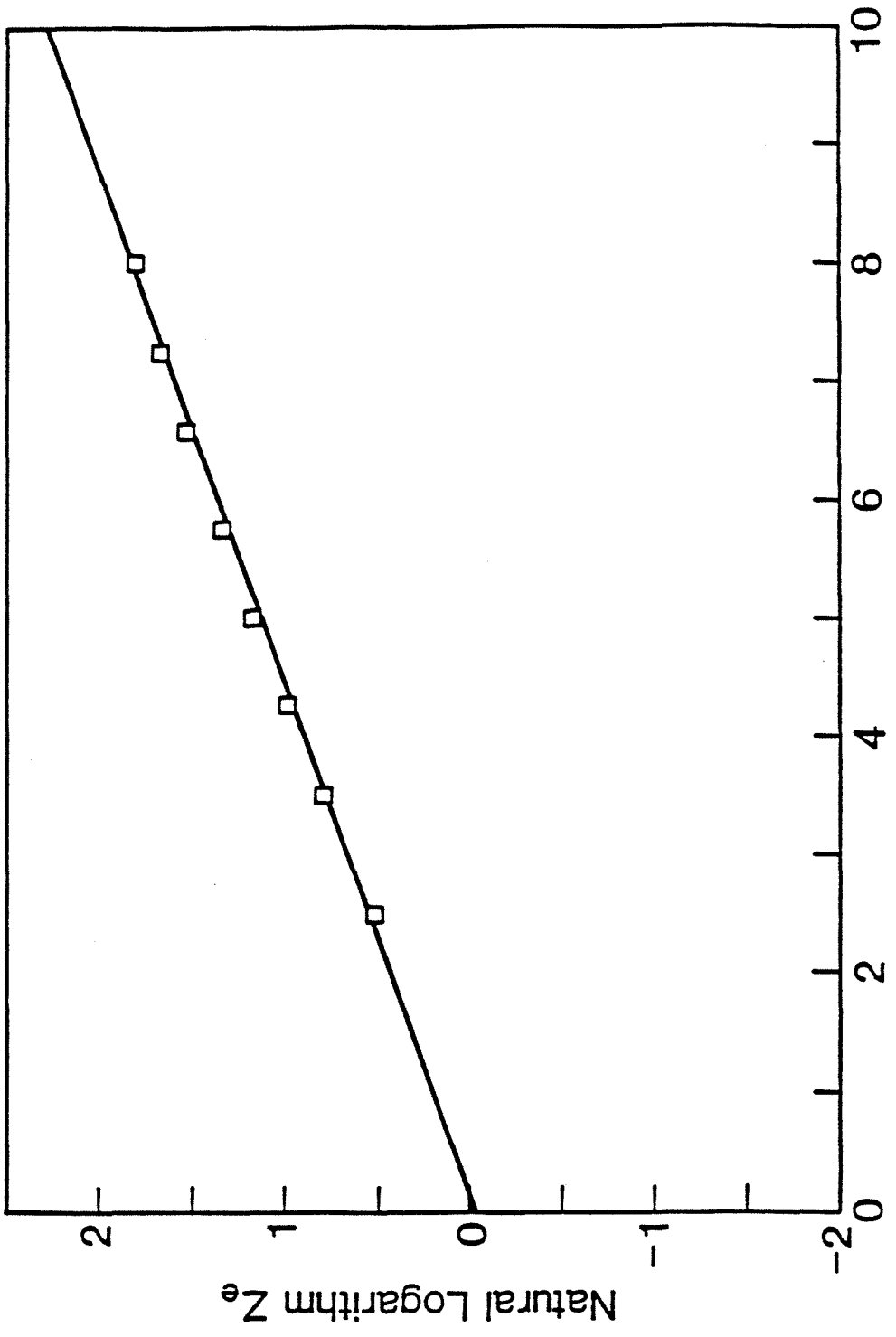

Figure 3.6 **Diffusion-Reaction Experiment for Ethanol Production and Growth under anaerobic conditions with symmetric glucose concentrations. Run 2, chamber 2.**

of glucose in each chamber were carried out to determine ethanol production rates with symmetric glucose concentrations on each side of the membrane. Figures 3.5 and 3.6 are plots of $\ln Z_e$ versus time for the symmetric glucose experiments under anaerobic conditions. The ethanol diffusion-reaction theory characterizes the experimental data well with and without an imposed glucose gradient.

3.3 MATERIALS AND METHODS

3.3.1 Cell Cultivation

Saccharomyces cerevisiae 18790 was grown in defined medium using glutamate as the nitrogen source (DGM, defined glutamate medium). The medium composition is given in Table 3.1. The medium was sterilized by passing it through a 0.22 μm filter. Yeast extract - peptone medium inhibited the diffusion of glucose through the alginate gel, making a defined medium necessary. Glutamate was used as the nitrogen source because ammonium ion concentrations of 15 mM and higher caused deterioration of the alginate gel during the diffusion - reaction experiments. To further improve the stability of the alginate gel, 0.04 % calcium chloride was added to the medium. The growth rate of *S.cerevisiae* 18790 was inhibited by calcium chloride concentrations greater than 0.1 %. Figure 3.7 shows the effect of calcium chloride concentration on growth rate.

Prior to each experiment, *S. cerevisiae* was carefully cultivated to provide a consistent biomass sample for each experiment. A petri plate colony was used to inoculate the preculture medium, which consisted of DGM 2.5 times the usual concentration and 50.0 g/l glucose. The preculture was incubated at

Table 3.1

DEFINED GLUTAMATE MEDIUM

$MgCl_2 \bullet 6H_2O$	0.52 g/l
EDTA	0.10 g/l
glutamate	1.98 g/l
$H_3PO_4(85\%)$	1.6 ml/l
KCl	0.12 g/l
$CaCl_2 \bullet 2H_2O$	0.54 g/l
$NaCl$	0.06 g/l
$MnSO_4 \bullet H_2O$	0.024 g/l
$CuSO_4 \bullet 5H_2O$	0.50 mg/l
H_3BO_4	0.50 mg/l
$Na_2MoO_4 \bullet 2H_2O$	2.0 mg/l
$NiCl_2 \bullet 2H_2O$	2.5 μg/l
$ZnSO_4 \bullet 7H_2O$	0.012 g/l
$CoSO_4 \bullet 7H_2O$	2.3 μg/l
KI	0.1 mg/l
$FeSO_4(NH_4)_2SO_4 \bullet 6H_2O$	0.035 g/l
m-inositol	0.125 g/l
pyroxidine	6.25 mg/l
Ca-D-pantothenate	6.25 mg/l
thiamine-HCl	5.0 mg/l
nicotinic acid	5.0 mg/l
biotin	0.125 mg/l
glucose	0–50 g/l
pH = 4.5	

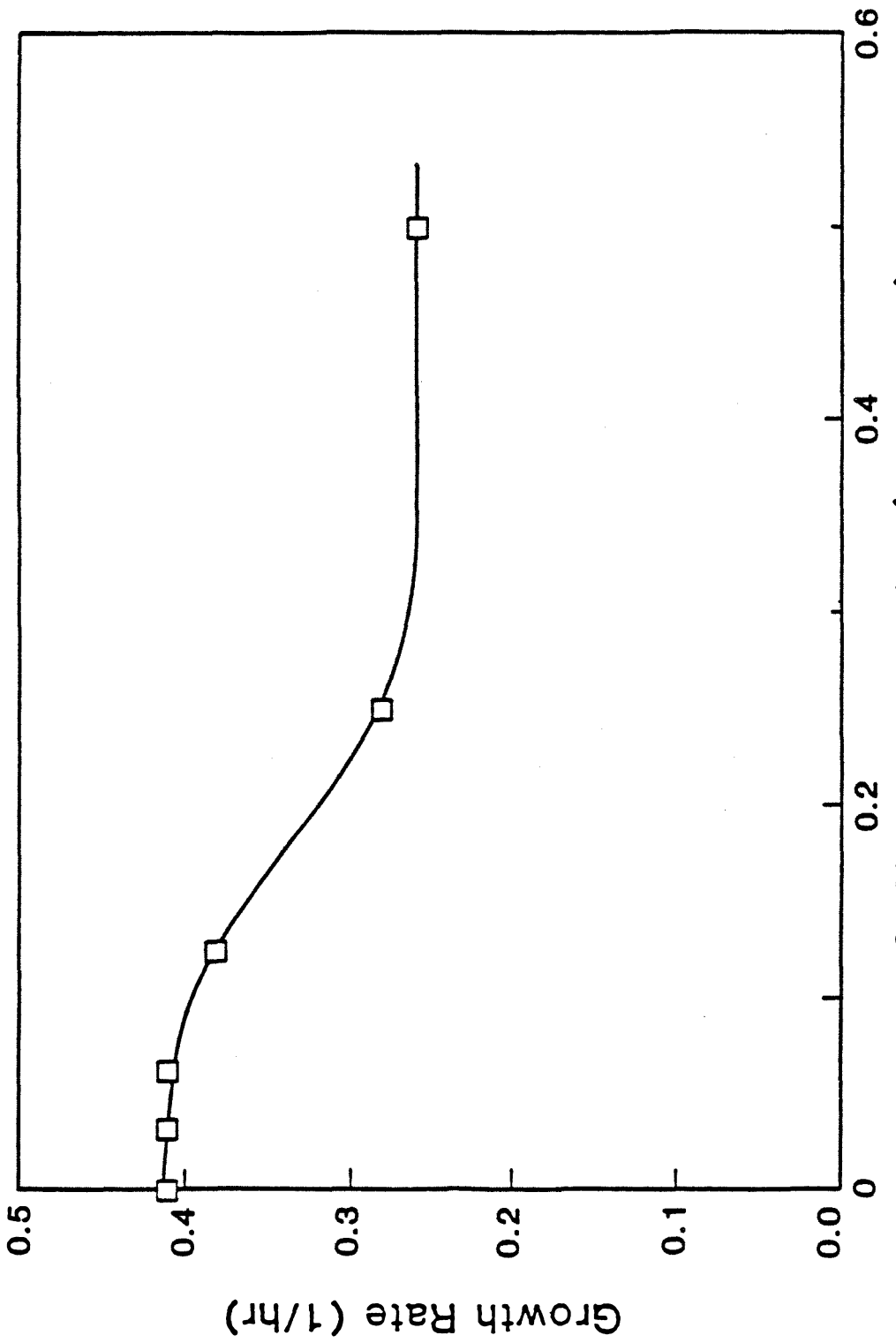

Figure 3.7 Effect of Calcium Chloride Concentration on Growth Rate.

30°C for approximately 18 hours. One ml of the preculture was then used to inoculate 100 ml of DGM with 1.0 g/l glucose. After approximately 4 hours of growth at 30°C, the cells were harvested for use in the diffusion-reaction experiment. For ethanol production experiments with 25.0 g/l glucose in each chamber, the preculture was transferred into 100 ml of DGM with 25.0 g/l glucose. Cultivating the cells in a medium similar to the experimental medium helped prevent a lag phase after the membrane was prepared. The analytical solution for diffusion and reaction in the alginate membrane assumes a constant exponential growth rate. Therefore, it is essential to eliminate the lag phase. Prior to harvesting, the optical density of the cell culture was measured several times on a Bausch and Lomb Spectronic 21 to insure that the cells were in exponential phase.

3.3.2 Calcium Alginate Preparation

The cells for the diffusion–reaction experiment were harvested by centrifuging the appropriate volume of cell culture to obtain a final concentration of 0.4 mg/ml (dry weight) in the alginate membrane. The cells were centrifuged for 8 minutes at 4000 rpm and 4°C in a Beckman centrifuge. Then the cell pellet was resuspended in 4 ml of 2.0 g/l glucose solution and mixed well with 4.0 g of 4 % alginate solution. Both the glucose and alginate solutions were also at 4°C. The mixing was done on a stir plate at high speed for 3 minutes. Glucose solutions were filter sterilized. The alginate solution was prepared by dissolving 4 g of sodium alginate in 100 ml of deionized water and autoclaving for 20 minutes at 121°C.

The alginate membrane was prepared by hardening sodium alginate at

4°C in a mold. The cell and alginate mixture was poured into a ring (0.4 cm height x 2.5 cm diameter) on top of a fritted glass plate and covered with a second fritted glass plate. Rubber bands were used to hold the glass plates and the ring together. The glass plates had been previously soaked in a 500 ml bath of 2 % calcium chloride and 1 g/l glucose at 4°C to prevent the alginate from being absorbed by the plates. The mold containing the alginate was then placed in the calcium chloride and glucose bath over another metal ring with holes. The bath was stirred magnetically in the refrigerator at 4°C while the alginate was hardening. This arrangement allowed calcium ions to diffuse into the alginate through the fritted glass plates on each side of the membrane. The apparatus is shown in Figure 3.8. After hardening 1.5 hours, the alginate was loosened from the mold and hardened another half-hour. The 2 % calcium alginate membrane contained about 0.4 mg/ml biomass (dry weight) and 1.0 g/l glucose. The exact biomass concentration was calculated for each membrane from the absorbance of the cell culture at the time of harvesting.

In order to demonstrate the absence of a lag phase after cell harvesting, a control experiment was carried out. Cells were cultivated and harvested according to the method described above. After being stored at 4°C for 2 hours, the cell pellet was suspended in defined glutamate medium with 1 g/l glucose. The initial absorbance of the culture was measured, and then absorbance was measured as a function of time until glucose became growth-limiting. As shown in Figure 3.9, there was no lag phase.

3.3.3 Diffusion-Reaction Experiments

A glass reactor was employed for the diffusion-reaction experiments. The

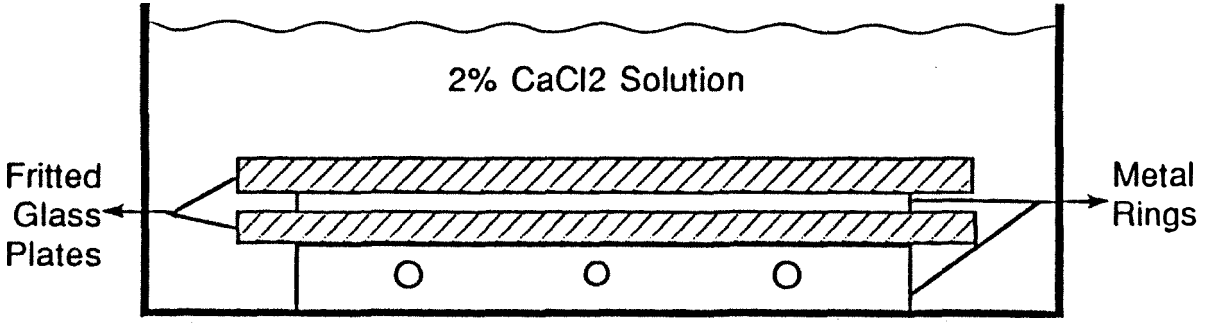

Apparatus for Membrane Preparation

Figure 3.8 **Apparatus for Preparation of Calcium Alginate Membrane.**

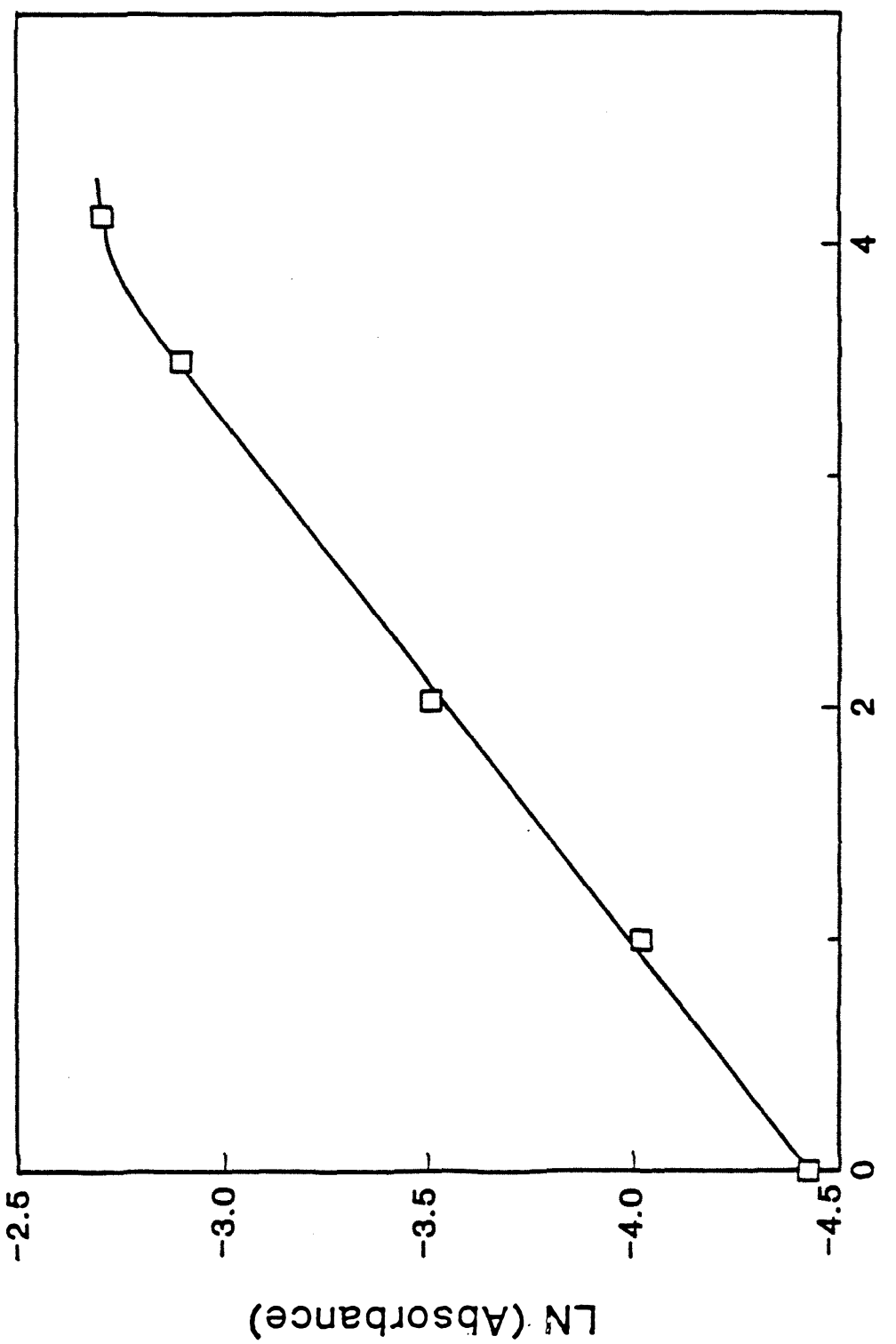

Figure 3.9 Growth of Cells after Harvesting Procedure for immobilization in alginate membrane. The lag phase has been eliminated.

reactor consisted of two chambers (6 cm diameter x 15 cm height) connected by a #25 glass O-ring joint 2.4 cm in diameter. A schematic diagram of the reactor is given in Figure 3.10. The top of each chamber was closed by a rubber stopper with four ports (medium inlet, gas inlet, gas outlet, and sampling ports). The gas flow rate into each chamber was controlled using Brooks flowmeters. Fritted tubes were used to bubble nitrogen through each reactor chamber at a rate of 40 ml/min to maintain anaerobic conditions. Samples were withdrawn from each chamber with a sterile needle and syringe. The alginate membrane was held between the two chambers of the reactor by the O-ring joint. A light gauze mesh on each side helped support the alginate membrane. One O-ring was used to seal the joint, and a ball and socket clamp held the reactor together. The reactor was immersed in a $30°C$ water bath and each chamber was stirred using magnetic stir plates.

After the alginate membrane was arranged in the reactor, 250 ml of DGM were pumped simultaneously into each chamber from Erlenmyer flasks. The rate of solute transport through the alginate membrane is extremely sensitive to pressure variations across the membrane. Therefore, the liquid chambers of the reactor must be filled at the same rate to avoid leaks or pressure variations. Nitrogen gas was bubbled through the medium before it was pumped into the reactor. The high concentration chamber contained 50.0 g/l glucose, and the low concentration chamber had 1.0 g/l glucose. Time equal to zero was defined when the liquid level reached the center of the alginate membrane in each chamber. When all the medium was in the reactor (t= 2 minutes), the gas flow was switched from the medium flasks to the reactor chambers and initial samples were taken from each chamber. Samples of 2.5 ml were taken from

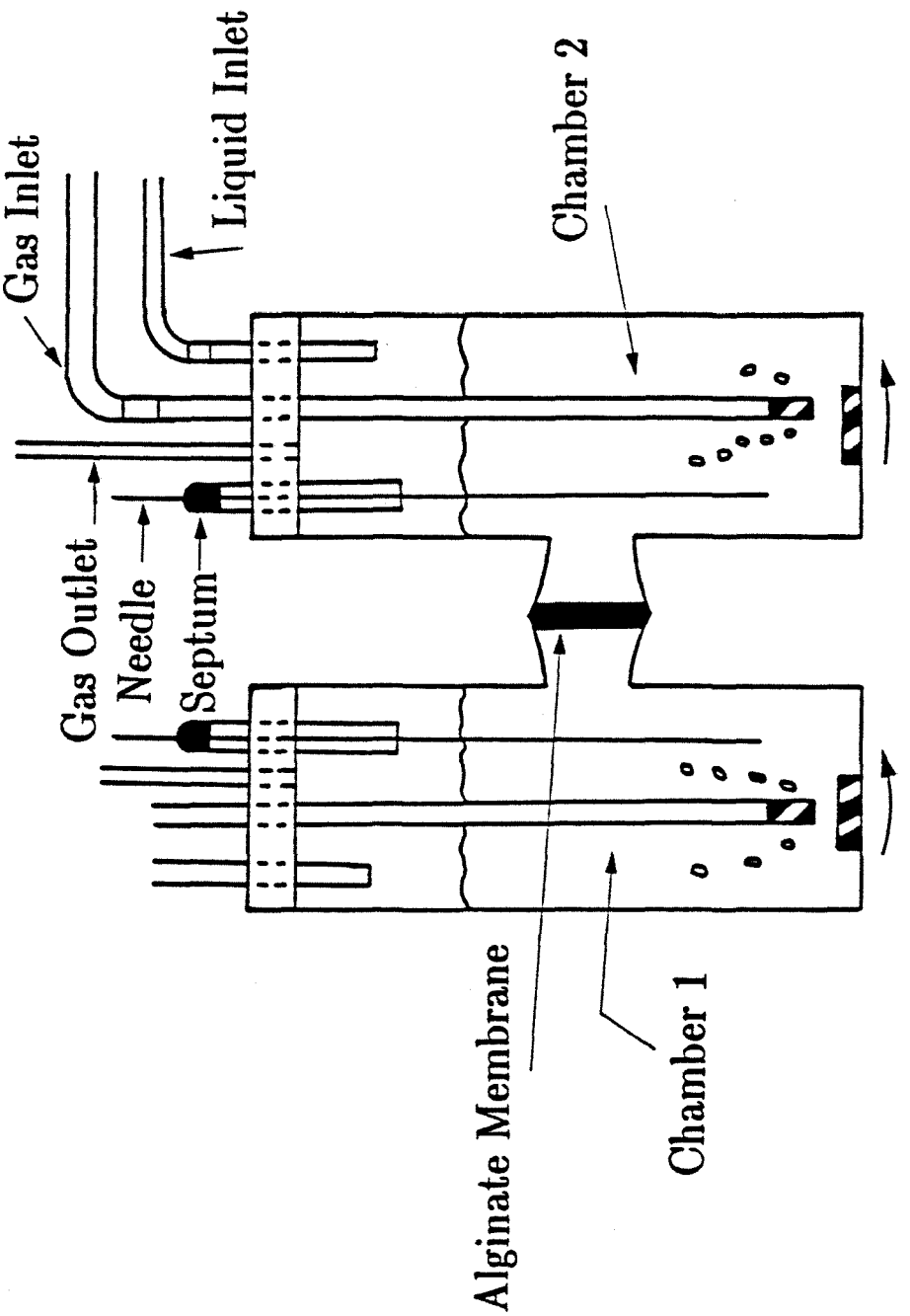

Figure 3.10 Diffusion Reactor for measuring intrinsic, specific rates of growth, glucose uptake, and ethanol production for entrapped cells.

each chamber to maintain equal pressure in the two chambers. The samples were filtered and stored at 4°C for glucose and ethanol analyses later in the day or on the following day. More samples were taken over a period of about eight hours.

Experiments were also carried out with DGM and 25 g/l glucose in each chamber. The experimental procedures are the same as for the diffusion-reaction experiments except that, when preparing the alginate membrane, the cell pellet was resuspended in 4 ml of 50.0 g/l glucose solution instead of the 2.0 g/l glucose solution. The alginate was hardened in 2 % calcium chloride with 25 g/l glucose to produce an alginate membrane with 25 g/l glucose. Samples of 1.5 ml were withdrawn from the reactor and analyzed for ethanol only.

3.3.4 Measurements of Final Biomass Dry Weight

After completing a diffusion-reaction experiment, the alginate membrane was frozen immediately. Later a disc (1.7 cm diameter x 0.4 cm height) was cut from the frozen membrane with a sharpened steel tube. Tripolyphosphate solution was used to dissolve the alginate membrane. Tripolyphosphate disrupts the crosslinking of the alginate chains without affecting the viability of the cells. Tripolyphosphate, 85 % purity, was obtained from Sigma Chemical Company, St. Louis, Mo.. The solution was filter-sterilized before use. The alginate sample was suspended in 20 ml of 100 g/l tripolyphosphate solution and agitated at 5°C for 7.5 hours. The partially dissolved alginate was then centrifuged at 5000 rpm for 8 minutes at 4°C. The cells and any undissolved alginate were washed with 10 ml of 100 g/l tripolyphosphate and centrifuged

again at the same conditions. Next the cell and alginate pellet was suspended in another 20 ml of tripolyphosphate solution and agitated for 3.75 hours at $5°C$, completely dissolving the alginate. After centrifuging the cells a third time, the cells were washed with 10 ml of deionized, filtered water to remove any tripolyphosphate residue. The cells were then centrifuged and resuspended in 5 ml of deionized, filtered water. The cell suspension was poured into tin dishes, which had previously been dried and weighed. Another 1 ml of water was used to wash the centrifuge tubes containing the cells. The tin dishes were placed in a drying oven at $100°C$ for 24 hours. Then the dishes were cooled in a dessicator and weighed. The supernatant liquid from the first two centrifuge runs was saved and later examined for cells; however, none was found, indicating that all the cells were collected. An average growth rate was calculated from the initial biomass concentration, the final biomass concentration, and the time of the experiment.

3.3.5 Diffusion Coefficient Measurements

Experiments were carried out in the diffusion reactor shown in Figure 3.10 to measure the diffusivity of glucose and ethanol in 2 % calcium alginate at 22° and 30°. The experimental procedure was similar to the procedure for the diffusion-reaction experiments described earlier in this chapter. Diffusion coefficients were determined by both the lag time method and the steady-state method as described in Chapter 2. The alginate membrane was prepared without cells by mixing 4.0 g of 4 % sodium alginate and 4.0 g of deionized water. Thus, the solute concentration in the membrane was zero, initially. The diffusivity of glucose was measured with 50.0 g/l glucose in the high concentration

chamber and 0.0 g/l glucose in the low concentration chamber. Similarly, the diffusivity of ethanol was determined with 100.0 g/l ethanol and 0.0 g/l ethanol in the high and low concentration chambers, respectively. Either deionized water or defined glutamate medium was used as the aqueous phase. The concentration of solute was measured in the low concentration chamber as a function of time. The reactor was kept at either $22°C$ or $30°C$ by immersing it in a water bath.

3.3.6 Suspended Cell Experiments

A control experiment was run with suspended cells. The cells were cultivated as in the diffusion - reaction experiments. After centrifuging at 4000 rpm for 8 minutes and $4°C$, the cells were resuspended in 4 ml of 2.0 g/l glucose solution. The cell and glucose solution was used to inoculate 250 ml of DGM containing 2.0 g/l glucose. The experiment was carried out in a 500 ml flask covered by a rubber stopper. There were three ports in the vessel for gas inlet, gas outlet, and sampling. The flask was immersed in a $30°C$ water bath and the medium was magnetically stirred. Anaerobic conditions were maintained by bubbling nitrogen gas through the medium. The gas flow rate was controlled with a Brooks flowmeter. Samples (2.5 ml) were withdrawn with a sterile needle and syringe over a period of eight hours. After measuring the optical density, samples were filtered and stored at $4oC$ for glucose and ethanol analyses later in the day and on the following day.

3.3.7 Analyses

Biomass was determined by measuring the absorbance of the culture at

590 nm on a Bausch and Lomb Spectronic 21 spectrophotometer. The absorbance was correlated with the dry weight by filtering samples and drying the biomass to a constant weight. The correlation is shown in Figure 3.11. Biomass was also correlated with the number of cells. Cell counts were done with a Levy-Hausser counting chamber.

The glucose concentration of filtered samples was measured with hexokinase glucose-6-phosphate dehydrogenase enzyme assays (Sigma Chemical Co., St. Louis, Mo.). The change in NADH concentration was monitered by the change in absorbance at 340 nm using a Shimadzu UV 260 spectrophotometer. 20 μl of sample were added to 3 ml of enzyme solution. The reaction proceeded for 10 minutes at 25°C in 3 ml disposable cuvettes. Each sample was analyzed six times with a standard deviation of 2 %.

Ethanol concentrations were determined by gas chromatography (Shimadzu). 1.0 μl samples were injected into a Porapak Q column held at 120°C. The injector and the flame ionization detector were maintained at 190°C. Chromatagrams were analyzed on a Shimadzu Chromatapac, using the one-point calibration method. A calibration was run every time the gas chromatograph was started. Samples were analyzed twice with an accuracy of 1 %.

3.4 RESULTS AND DISCUSSION

3.4.1 Diffusion Coefficients

The diffusion reactor was used to determine the diffusion coefficients of glucose and ethanol in 2 % calcium alginate at 22°C and 30°C. The results are listed in Table 3.2. Diffusion coefficients were measured at 22°C for comparison

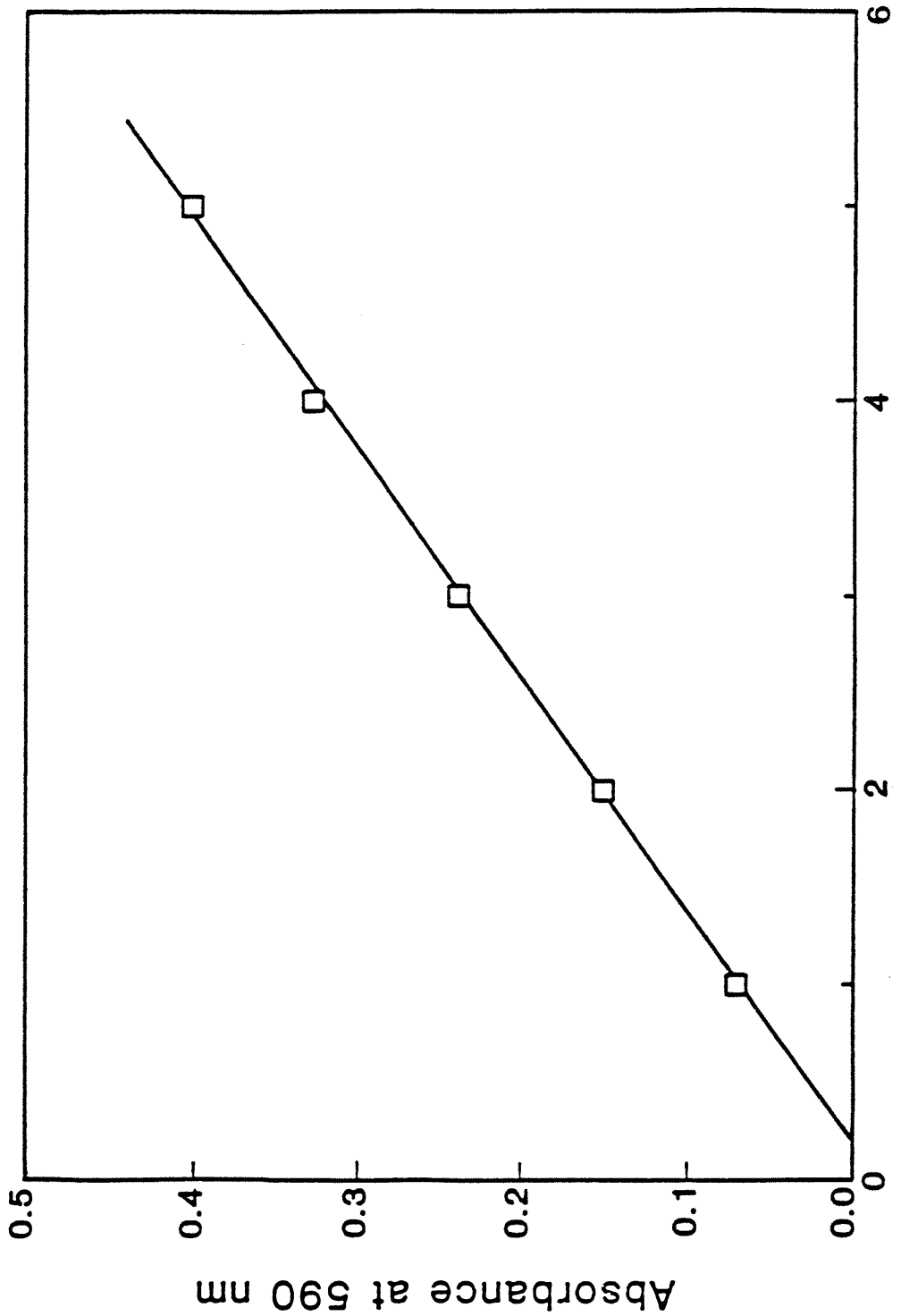

Figure 3.11 Absorbance-Dry Weight Correlation for *S. cerevisiae* 18790.

Table 3.2

DIFFUSION COEFFICIENTS OF GLUCOSE AND ETHANOL IN 2% CALCIUM ALGINATE

	Diffusion Coefficient at 22°$C(cm^2/sec)$	Diffusion Coefficient at 30°$C(cm^2/sec)$
Glucose	6.1 x 10^{-6}	7.8 x 10^{-6}
Ethanol	1.0 x 10^{-5}	1.2 x 10^{-5}

with the results reported in Chapter 2, which were obtained in another system. The data from Chapter 2 were reproduced, indicating that the membrane sealed properly in the reactor. In several runs, defined glutamate medium was used as the aqueous phase to determine if any of the medium components interfered with glucose or ethanol diffusion in 2 % calcium alginate. However, there was no change in the diffusion coefficients of either glucose or ethanol when defined glutamate medium was used. Since the diffusion-reaction experiments were to be run at 30°C , the diffusion coefficients of glucose and ethanol were also measured at this temperature.

The lag time method and the steady-state method described in Chapter 2 were used to determine the diffusion coefficients. The two methods gave similar results. The diffusion coefficients appear to remain constant over the course of the experiments, since the solute concentration in the low concentration increases linearly with time for large times. As the experiment progresses, the solute concentration in the membrane increases. Therefore, the concentration of glucose and ethanol in the membrane does not affect the diffusion coefficients. In Chapter 2 it was shown that there was no change in the diffusion coefficients for glucose concentrations from 2 g/l to 100 g/l and ethanol concentrations from 10 g/l to 80 g/l. It appears that the insensitivity of the diffusion coefficients to solute concentration can be extended to lower solute concentrations.

The diffusion cofficients for glucose and ethanol at 30°C are 28 % and 20 % higher, respectively, than the diffusion coefficients at 22°C. The variation in the diffusion coefficients with temperature agrees with that predicted by the Stokes-Einstein equation for glucose and ethanol diffusion in water. The

Stokes-Einstein equation, which is derived from the hydrodynamic theory for diffusion of a particle in a stationary medium, predicts a 24 % and 20 % increase in the diffusivity of glucose and ethanol, respectively, for a change in temperature from 22°C to 30°C. As was observed in Chapter 2, the hydrodynamic theory accurately describes the diffusion of both glucose and ethanol in calcium alginate gel. The relatively large pore size of the alginate gel accounts for the suitability of the hydrodynamic theory, since the pores are filled with water.

The diffusion coefficients of glucose and ethanol in calcium alginate were shown in Chapter 2 to be unaffected by the presence of 40 g/l biomass (dry weight) in the alginate membrane. Onuma, et al. measured the effect of bacterial biomass concentration on the diffusion coefficients of glucose and oxygen through microbial aggregates (2). They found that the effect of biomass concentration depended on the C/N ratio of the aggregate. From the correlations they reported, a biomass concentration of 40 g/l would result in a 3 % decrease in the diffusion coefficient of glucose for a C/N ratio of 12. When the C/N ratio increases to 83, a 40 g/l biomass concentration leads to a 20 % decrease in the diffusion coefficient. Similar results were obtained for oxygen diffusion coefficients. Yeast with a C/N ratio of 5 probably does not affect solute diffusivity significantly at a biomass concentration of 40 g/l. Since the biomass concentration never exceeded 8 g/l in any of the diffusion-reaction experiments, the glucose and ethanol diffusion coefficients measured without cells in the membrane can be applied to the diffusion-reaction experiments where cells are present.

3.4.2 Intrinsic Growth and Reaction Rates

Specific rates of growth, glucose uptake, and ethanol production of *S. cerevisiae* 18790 immobilized in 2 % calcium alginate were determined using the diffusion-reaction analysis previously described. One experiment was conducted with a glucose gradient and another was conducted without an imposed glucose gradient. The second experiment was conducted with 25 g/l glucose in each of the liquid chambers, so only the growth rate and the ethanol production rate were determined. The average growth rate during each experiment was measured from the initial and final biomass concentration in the alginate membrane and the duration of the experiment. The biomass measurements provided an independent test of the diffusion-reaction analysis. Table 3.3 lists the results of the two experiments. The growth rates determined by the diffusion-reaction analysis are within 10 % of the average specific growth rate determined by the biomass measurements. The imposed glucose gradient appears to have no significant effect on the specific growth rate and specific ethanol production rate as measured by the diffusion-reaction analysis. The intrinsic specific reaction rates and the biomass and product yields for immobilized and suspended cells at 0 mg/l dissolved oxygen are presented in Table 3.4. The suspended cell rates were determined by shake flask experiments, which were previously described. The immobilized cell rates represent the average of the two experiments. A 20 % decrease in the growth rate occurs when *S. cerevisiae* is immobilized in 2 % calcium alginate. The glucose uptake rate and ethanol production rate increase by a factor of 4.3 and 4.0, respectively, for cells immobilized in alginate. While the ethanol yield appears independent of the state of the cell, the biomass yield for immobilized cells decreases to

Table 3.3

GROWTH AND REACTION RATES FROM DIFFUSION-REACTION EXPERIMENTS UNDER ANAEROBIC CONDITIONS

	Run 1	Run 2
μ (1/hr)	0.26	0.22
α (g/g-hr)	5.6	—
ν (g/g-hr)	2.2	2.7
μ_* (1/hr)	0.26	1.27

* Determined from final biomass concentration.

Table 3.4

SPECIFIC REACTION RATES AND YIELDS FOR IMMOBILIZED AND SUSPENDED CELLS UNDER ANAEROBIC CONDITIONS

	Immobilized	Suspended
μ (1/hr)	0.24	0.31
α (g/g-hr)	5.6	1.3
ν (g/g-hr)	2.4	0.6
Y_b (C mole/mole)	0.31	1.7
Y_e (mole/mole)	1.7	1.8

approximately one-fifth of its value for suspended cells. The decrease in the biomass yield may be related to the increases in the specific rates of glucose uptake and ethanol production by immobilized cells.

The most extreme effect of immobilizing *S. cerevisiae* in 2 % calcium alginate is the decrease in the biomass yield to one-fifth the value for suspended cells. Since the biomass yield depends strongly on the ATP concentration of the cell (3), a low ATP concentration may be responsible for the low biomass yield of entrapped cells. Stouthammer measured the growth yield based on ATP of a wide variety of microorganisms to be approximately one-third of its theoretical value (4). He concluded that a large amount of ATP must be either wasted or utilized in unknown functions. He further suggested that large quantities of ATP can be wasted by membrane ATPases, which hydrolyze ATP and leak protons across the membrane. Proton leakage results in a decay of the energized membrane. Furthermore, proton translocating membrane ATPases have been found in anaerobic cultures of *S. cerevisiae* (5). In an experimental investigation with *E. coli*, Stouthammer and Bettenhaussen demonstrated that 51 % of the ATP generated by anaerobically growing cells was used to energize the cell membrane (6). Therefore, a great deal of ATP can be utilized in yeast to maintain a proton gradient, which is continuously degraded by membrane ATPases. The control of ATP wastage by the leakiness of the membrane has been demonstrated in *E. coli* (4).

Several researchers have suggested that immobilization leads to permeabilization of the cell membrane (7,8). Cell immobilization may increase the leakiness of the cell membrane by making the cell membrane more permeable to protons. Then ATP would be utilized much faster in immobilized cells than

in suspended cells, resulting in a lower ATP concentration and a lower biomass yield for immobilized cells.

The 20 % reduction in growth rate of *S. cerevisiae* immobilized in calcium alginate compared to suspended cultures is probably due to the physical constraint of the alginate matrix. The semisolid gel surrounding the cells hinders cell growth. Doran and Bailey measured a 45 % decrease in the growth rate of the same organism when it was crosslinked to the surface of gelatin beads. Observing high intracellular concentrations of reserve carbohydrates and multiple DNA and RNA copies, they concluded that gelatin crosslinking prevents bud emergence during some reproductive cycles of the organism (9). A similar phenomenon may occur when cells are entrapped in alginate. The smaller change in growth rate of alginate-entrapped cells versus cells crosslinked to gelatin may be due to the gentler nature of alginate immobilization. Alginate is crosslinked by divalent cations, whereas Doran and Bailey used glutaraldehyde to crosslink the gelatin producing molecular bonds. Since molecular bonds are stronger than ionic bonds, the growth rate of gelatin immobilized cells is more greatly affected than the growth rate of alginate-entrapped cells.

Immobilization of *S. cerevisiae* in 2 % calcium alginate greatly enhances the specific glucose uptake rate and ethanol production rate of the cells. The yield of ethanol remains essentially the same for free and immobilized cells, indicating that control between the different metabolic pathways operates normally in immobilized cells. In this investigation the glucose uptake rate and ethanol production rate increased by a factor of 4.3 and 4.0, respectively, when the cells were immobilized and cultured anaerobically. For crosslinked gelatin immobilized *S. cerevisiae* 18790, Doran and Bailey reported an increase in glucose

uptake of 2.0 times the rate for suspended cells at anaerobic conditions. They found that the ethanol production rate increased by a factor of 1.4 for immobilized cells (9). These researchers suggested that the faster fermentation rates of immobilized cells may be due at least partially to the high intracellular DNA content, which they observed since polyploidy in yeast has been shown to enhance the fermentation rate. Galazzo, et al. measured the uptake rate and ethanol production rate of *S. cerevisiae* 18790 immobilized in calcium alginate under anaerobic, nongrowth conditions. They reported that the glucose uptake rate and ethanol production rate of immobilized cells both increased by a factor of 2.2 over the rates of suspended cells (10). Because of the suppression of growth, however, the ethanol production rate measured by Galazzo, et al. for suspended cells was only 7.3 % of the ethanol production rate measured in this investigation. Using NMR techniques, Galazzo, et al. reported a decrease of 0.2 pH units in the intracellular pH of immobilized cells compared to suspended cells. By increasing the activity of the glycolytic enzymes, the decrease in intracellular pH can account for the faster glucose uptake rate and ethanol production rates which they observed (10).

Immobilization can affect cells in various ways. In this investigation, immobilized cell reaction rates were enhanced by a factor of approximately four, whereas Doran and Bailey (9) and Galazzo, et al. (10) measured roughly an increase of a factor of two for the same organism under different conditions. In this study and in the study by Doran and Bailey, the immobilized cells were growing at a lower rate than suspended cells under the same conditions. The reduction in the growth rate was 20 % in this study and 45 % in the study by Doran and Bailey. Thus, the immobilized cells in this investigation probably

contain fewer DNA copies than the immobilized cells analyzed by Doran and Bailey. If polyploidy alone was affecting the fermentation rate of immobilized cells, the reaction rate enhancement in this investigation should be lower than the reaction rate enhancement measured by Doran and Bailey. Instead, we measured a larger change in the reaction rates than did Doran and Bailey. Galazzo, et al. utilized nongrowing cells in their investigation; thus, multiple DNA copies were probably not present at all. The increase in the reaction rates which they observed can be explained by the decrease in the intracellular pH of 0.2 pH units. A decrease in the intracelllular pH of immobilized cells can be produced by a cell membrane that is more permeable to protons. Furthermore, growing cells immobilized in calcium alginate may maintain an even lower intracellular pH than nongrowing cells because growth may enhance the leakiness of the plasma membrane. The increase of a factor of four in the fermentation rate of immobilized cells that we measured may be due to several different effects of immobilization. The cells probably contain multiple DNA copies and a lower intracellular pH than suspended cells. The intracellular pH appears to be the more significant factor in the present investigation. A faster rate of ATP utilization can also cause an increase in the fermentation rate of immobilized cells as will be shown below.

Ryu, et al. measured an intrinsic glucose uptake rate of 5.9 g/g-hr for *S. cerevisiae* immobilized in 2 % calcium alginate (11). The suspended cell glucose uptake rate is not given for the same strain and the same growth conditions; however, the results of Ryu, et al. are very similar to the value of 5.6 g/g-hr obtained in this investigation. A fivefold increase in the glucose uptake rate of adsorbed *S. carlsbergensis* was reported by Navarro and Durand. Similarly,

they found the alcohol production rate increased by a factor of six compared with free cells (12). Other researchers have reported significant increases (13) and decreases (14) in the substrate consumption rate of immobilized cells for a variety of organisms and immobilization methods.

The enhanced glucose uptake rate and ethanol production rate of immobilized cells may be caused at least partially by a permeabilized cell membrane. Glycolysis in *S. cerevisiae* appears to be controlled at several points in the reaction pathway. The rate of glucose transport into the cell may limit glycolysis (15,16). Initially, one may think that permeabilizing the cell membrane by immobilization causes a faster glucose uptake rate. However, there is significant evidence that glucose is transported into the cell by a carrier protein. Thus, increasing the membrane permeability should have no direct effect on the rate of glucose uptake. Glucose-6-phosphate has been shown to inhibit glucose transport into the cell (17). Additionally, glucose-6-phosphate is the substrate for the allosteric enzyme phosphofructokinase, which is the second important point of glycolytic control. ATP inhibits the activity of phosphofructokinase, while ADP is an activator. Various other metabolites also activate or deactivate phosphofructokinase(18). A permeabilized cell membrane may utilize more energy for maintenance, as previously mentioned. Thus, in immobilized cells the level of ATP may be reduced compared to free cells, resulting in a higher phosphofructokinase activity. As the phosphofructokinase activity increases, the glucose-6-phosphate concentration will decrease, causing a concomitant increase in the rate of glucose transport into the cell. There is evidence for a third control point at pyruvate kinase, which is also activated by ADP (19). Since utilization of ATP leads to an increase in the ADP concentra-

tion in the cell, pyruvate kinase may also be activated by the immobilization of the cells.

3.5 CONCLUSION

The intrinsic reaction rates measured by the diffusion-reaction analysis indicate that marked differences exist between immobilized and suspended cells of *S. cerevisiae* entrapped in 2 % calcium alginate. Immobilized cells metabolize glucose significantly faster than suspended cells without a concomitant increase in the growth rate. Therefore, the ATP produced during glycolysis must be utilized rapidly in immobilized cells for cell maintenance or in ATP wasting reactions. The large increase in the specific ethanol production rate of the immobilized cells is important commercially. Overall production rates of immobilized cell processes can be significantly higher than suspended cell processes because of increases in the intrinsic reaction rates and higher cell densities in immobilized cell reactors. Since cell growth is not as important in immobilized cell systems, the decrease in the growth rate and biomass yield of immobilized *S. cerevisiae* will not strongly affect the overall productivity of an immobilized cell reactor.

REFERENCES

(1) Peringer, P., H. Blachere, G. Corrieu, and A. G. Lane, "Mathematical Model of the Kinetics of *Saccharomyces cerevisiae*," *Biotechnol. Bioeng. Symp.*, *4*, 27–42 (1973).

(2) Onuma, M., T. Omura, T. Umita, and J. Aizawa, "Diffusion Coefficient and Its Dependency on Some Biochemical Factors," *Biotechnol. Bioeng.*, *27*, 1533–1539 (1985).

(3) Stouthammer, A. H., and C. Bettenhaussen, "Utilization of Energy for Growth and Maintenance in Continuous and Batch Cultures of Microorganisms," *Biochim. Biophys. Acta*, *301*, 53–70 (1973).

(4) Stouthammer, A. H., "The Search for Correlation Between Theoretical and Experimental Growth Yields," in *Microbial Biochemistry*, J. R. Quayle (ed.), University Park Press, Baltimore, 1979, p. 1.

(5) Serrano, R., "Effect of ATPase Inhibitors on the Proton Pump of Respiratory Deficient Yeast," *Eur. J. Biochem.*, *105*, 419 (1980).

(6) Stouthammer, A. H., and C. W. Bettenhaussen, "A Continuous Culture Study of ATPase-Negative Mutant of *E. coli*," *Arch. Microbiol.*, *113*, 185 (1977).

(7) Marcipar, A., N. Cochet, L. Brackenridge, J. M. Lebeault, "Immobilization of Yeasts on Ceramic Supports," *Biotechnol. Lett.*, *1*, 65–70 (1979).

(8) Mattiason, B., "Immobilized Viable Cells," in *CRC Handbook of Immobilized Cells and Organelles*, *2*, 1983, pp. 23–40.

(9) Doran, P., and J. E. Bailey, "Effects of Immobilization on Growth, Fermentation Properties, and Macromolecular Composition of *S. cerevisiae* At-

tached to Gelatin," *Biotechnol. Bioeng.*, *28*, 73–87 (1986).

(10) Galazzo, J., J. V. Shanks, and J. E. Bailey, "Comparison of Suspended and Immobilized Yeast Metabolism Using ^{31}P Nuclear Magnetic Resonance Spectroscopy," *Biotechnol. Techniques*, *1 (1)*, 1–6 (1987).

(11) Ryu, D. D. Y., H. S. Kim, and H. Taguchi, "Intrinsic Fermentation Kinetic Parameters of Immobilized Yeast Cells," *J. Ferment. Technol.*, *62 (3)*, 255–261 (1984).

(12) Navarro, J. M., and G. Durand, "Modification of Yeast Metabolism by Immobilization onto Porous Glass," *Eur. J. Appl. Microbiol. Biotechnol.*, *4*, 243–254 (1977).

(13) Tyagi, R. D., and T. K. Ghose, "Studies on Immobilized *S. cerevisiae* I. Analysis of Continuous Rapid Ethanol Fermentation in Immobilized Cell Reactor," *Biotechnol. Bioeng.*, *24*, 781–795 (1982).

(14) Lancy, E. D., and O. H. Tuovinen, "Ferrous Ion Oxidation by *Thiobacillus ferroxidans* Immobilized in Calcium Alginate," *Appl. Microbiol. Biotechnol.*, *20*, 94–99 (1984).

(15) van Steveninck, and J. A. Rothstein, "Sugar Transport and Metal Binding in Yeast," *J. Gen. Physiol.*, *49*, 235–246 (1965).

(16) van Uden, N., "Transport-limited Fermentation and Growth in *S. cerevisiae* and its Competitive Inhibition," *Arch. Mikrobiol.*, *58*, 155–168 (1967).

(17) Sols, A., "Regulation of Carbohydrate Transport and Metabolism in Yeast," in *Aspects of Yeast Metabolism*, A. K. Mills and H. Krebs (eds.), Blackwell, Oxford, 1967, p. 47.

(18) Krebs, H. A., "Pasteur Effect and Relation Between Respiration and Fermentation in Living Systems," in *Essays in Biochemistry*, eds. Campbell, P.

N., and F. Dickens, *8*, Academic Press, New York, 1972, p. 34.

(19) den Hollander, J. A., K. Ugurbil, T. R. Brown. M. Bednar, C. Redfiled, and R. G. Shulman, "Studies of Aerobic and Anaerobic Glycolysis in *Saccharomyces cerevisiae*," *Biochemistry*, *25*, 203 (1986).

CHAPTER 4

EFFECT OF OXYGEN ON GROWTH AND REACTION RATES

4.1 INTRODUCTION

An understanding of how oxygen affects the metabolic rates of immobilized *S. cerevisiae* is important in developing and optimizing processes for ethanol production. Dissolved oxygen concentration is an important operating parameter because it influences the specific rates of growth, glucose uptake, and ethanol production. Although the production of alcohol in yeast is generally considered to be inhibited by oxygen, a low oxygen concentration is required by the yeast to maintain cell viability in continuous processes. In fact, the role of oxygen in the metabolism of yeast is quite complicated. While the glucose uptake rate and ethanol production rate generally decrease when oxygen is supplied to a culture, dissolved oxygen concentrations in the 5–10 ppb range have been shown to increase the specific glucose uptake rate and specific ethanol production rate over the rates at anaerobic conditions (1). Additionally, small amounts of oxygen have been shown to increase the percent of unsaturated fatty acids in the cell membrane as well as the total number of fatty acids (2). Membranes containing fatty acids with a higher number of unsaturated bonds have been shown to improve the ethanol tolerance of the cell (3). Generally, the growth rate of *S. cerevisiae* increases with dissolved oxygen concentration.

The productivity of continuous immobilized cell processes may benefit from the availability of dissolved oxygen through changes in the growth and reaction rates and improved cell viability. In this chapter we look at how diffusion-reaction experiments can be used to examine the effects of oxygen on

the growth and reaction rates of immobilized cells. The effects of dissolved oxygen concentration on the specific growth rate, specific glucose uptake rate, and specific ethanol production rate will dictate the rate at which oxygen should be supplied to a reactor in order to optimize the ethanol productivity.

4.2 THEORY

In order to examine the effects of oxygen on the intrinsic, specific growth and reaction rates of immobilized cells, a series of experiments were conducted at various aeration conditions. The diffusion-reaction analysis for determining the intrinsic specific growth rate, specific glucose uptake rate, and specific ethanol production rate of immobilized cells is detailed in Chapter 3. Diffusion-reaction experiments were conducted with various dissolved oxygen concentrations in the liquid reactor chambers to investigate the effects of oxygen on the specific growth rate, specific glucose uptake rate, and specific ethanol production rate of immobilized cells. However, the oxygen concentration in the alginate membrane is not equal to the bulk oxygen concentration in the reactor chambers. Because of the rapid utilization rate of oxygen by *S. cerevisiae* compared to the rate of oxygen diffusion, a steep oxygen gradient develops in the membrane during the diffusion-reaction experiments (except at 0 mg/l dissolved oxygen). In the absence of reliable techniques for the direct measurement of the intramembrane dissolved oxygen concentration, the transient oxygen concentration profile in the alginate membrane was computed numerically by solving the diffusion-reaction equation for oxygen. The computed dissolved oxygen profiles in the membrane were then used to interpret the experimental results for specific growth rate, specific glucose uptake rate, and

specific ethanol production rate as a function of dissolved oxygen concentration.

4.2.1 Oxygen Diffusion and Reaction Model

Oxygen diffusion and reaction in an alginate membrane is described by the following second-order partial differential equation:

$$\frac{\partial O_2}{\partial t} = D_O \frac{\partial^2 O_2}{\partial x^2} - b\theta, \tag{4.1}$$

where O_2 is the dissolved oxygen concentration as a % of air saturation, b is the biomass concentration (g/l), θ is the specific oxygen utilization rate (%-l/g-hr), D_O is the diffusion coefficient of oxygen (cm^2/hr), x is position (cm), and t is time (hr). The diffusion coefficient of oxygen in calcium alginate was estimated from the diffusion coefficient of oxygen in water. It was assumed that the ratio of oxygen diffusivity in alginate to oxygen diffusivity in water is the same as the ratios for glucose and ethanol diffusivities in alginate and water. The boundary conditions for the oxygen concentration partial differential equation are:

$$\begin{aligned} O_2 &= O_{2,b} \quad \text{at} \quad x = 0 \\ O_2 &= O_{2,b} \quad \text{at} \quad x = L, \end{aligned} \tag{4.2}$$

where $O_{2,b}$ is the dissolved oxygen concentration in the bulk fluid. Initially the dissolved oxygen in the alginate membrane equals the dissolved oxygen concentration at air saturation:

$$O_2 = 100 \quad \text{at} \quad t = 0 \quad \text{for all} \quad x. \tag{4.3}$$

The biomass concentration in the alginate membrane is governed by the partial differential equation:

$$\frac{\partial b}{\partial t} = \mu t, \tag{4.4}$$

where μ is the growth rate of the organism (1/hr). The initial biomass concentration is:

$$b = b_0 \quad \text{at} \quad t = 0. \tag{4.5}$$

Peringer, et al. developed an expression for the specific rate of oxygen utilization by *S. cerevisiae* (4). The expression is given by:

$$\theta = \theta_m \left(\frac{O_2}{K_L + O_2} \right) \left(\frac{s}{K_s + s} \right), \tag{4.6}$$

where θ_m is the maximum, specific oxygen utilization rate (%-l/g-hr), s is the glucose concentration (g/l), O_2 is the dissolved oxygen concentration (% air saturation), K_L is the Michaelis constant for oxygen (1.36 % air saturation), and K_s is the Michaelis constant for glucose (0.1 g/l). Peringer's model applies to glucose-repressed *S. cerevisiae* cells, which are used in this investigation. Although the model was developed for suspended cells, it may prove useful in describing the behavior of immobilized cells. Since it was not possible to measure the intrinsic, specific oxygen uptake rate for growing, entrapped cells, we attempted to apply a suspended cell rate expression.

The oxygen concentration profile in the alginate membrane was computed numerically by integrating Equations (4.1) and (4.4) with boundary conditions (4.2) and initial conditions (4.3) and (4.5). Equation (4.6) was used for the specific oxygen utilization rate in Equation (4.1). The equation was solved for an average glucose concentration of 25 g/l. In the experiments, the glucose

concentration varied between 1 and 50 g/l. Glucose concentration has little effect on the oxygen uptake rate and therefore has almost no effect on the computed oxygen profile in the membrane. The growth rate was taken to be 0.24 1/hr, which equals the experimentally measured value under anaerobic conditions. Thus, the biomass concentration is an analytical function of time, $b = b_0 \exp \mu t$. The Crank-Nicholson method of finite differences with a degree of implicitness of one-half was used to solve the parabolic partial differential equation. A time step of 1.0×10^{-3} hr and a distance step of 8.0×10^{-4} cm were used. The Crank-Nicholson method is universally stable. The predicted oxygen profiles are shown in Figure 4.1 for a typical diffusion-reaction experiment with a bulk oxygen concentration of 7.5 mg/l, which is equal to 100 % air saturation.

The accuracy of the numerical solution was examined by solving the diffusion-reaction equation analytically for a constant oxygen uptake rate. The exact same equation was integrated numerically and the solutions were compared. The constant oxygen uptake rate chosen for the analytical solution was the maximum value of the oxygen uptake rate in the model of Peringer, et al. As shown in Figure 4.2 for a bulk oxygen concentration of 7.5 mg/l, the numerical solution is extremely accurate.

4.2.2 Effect of Bulk Oxygen Concentration on Oxygen Profiles

In order to interpret experimental results for the effect of bulk oxygen concentration on the intrinsic, specific rates of growth, glucose uptake, and ethanol production, it is necessary to know how the bulk oxygen concentration affects the oxygen concentration profiles in the alginate membrane. At first, we would expect that a higher bulk oxygen concentration always leads to a higher

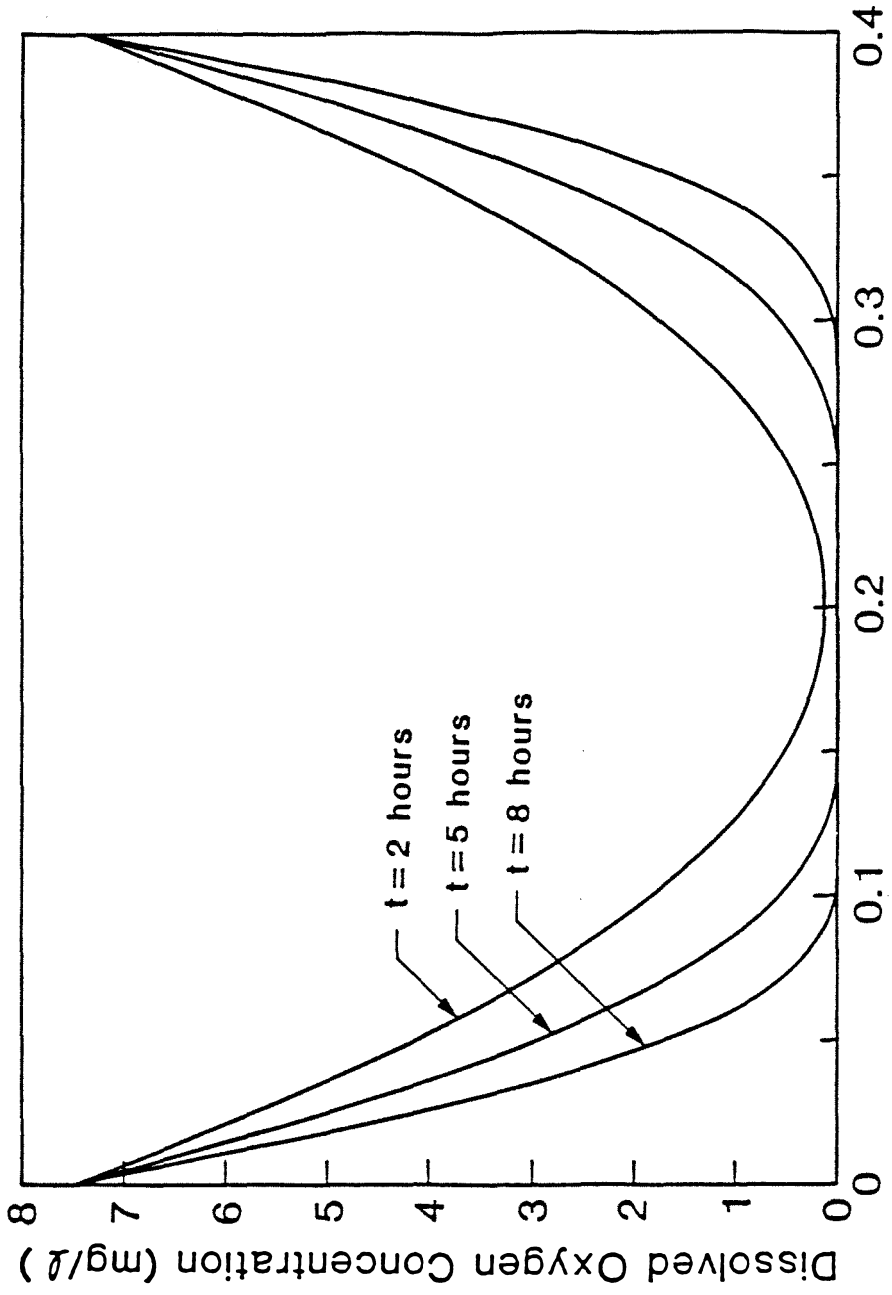

Figure 4.1 **Oxygen Concentration Profile in alginate membrane at $t = 2$, 5, and 8 hours for a growth rate of 0.24 1/hr and a nonconstant oxygen uptake rate.**

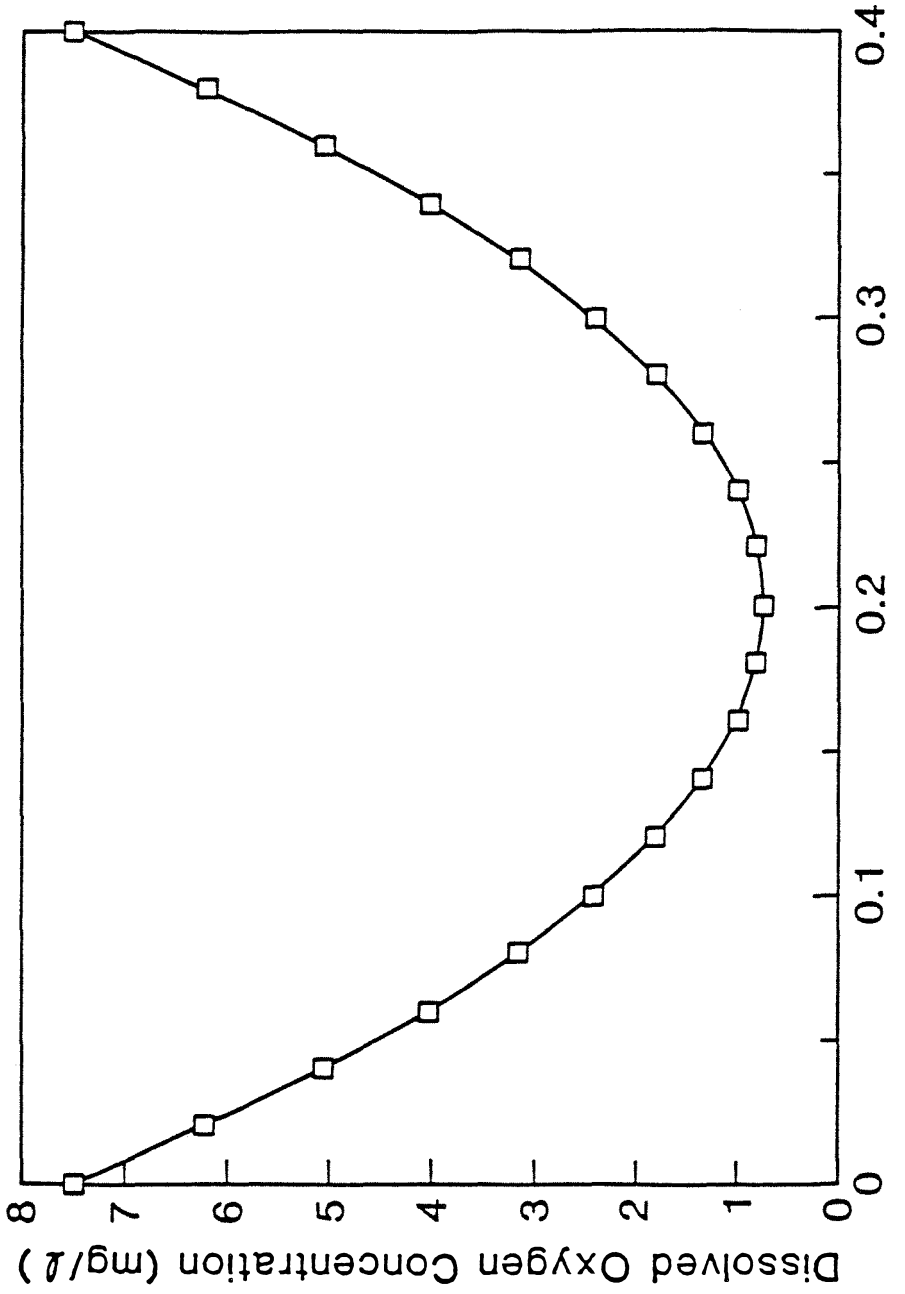

Figure 4.2 **Comparison of Numerical and Analytical Solution for oxygen concentration profile in alginate membrane at time equals 1 hour with a growth rate of 0.24 1/hr and an oxygen uptake rate of 61.44 mg/g-hr, (—) analytical solution, (□) numerical solution.**

oxygen concentration throughout the membrane. However, we must consider the effect of dissolved oxygen concentration on the growth rate of the organism. The growth rate increases with dissolved oxygen concentration, resulting in more biomass. As the biomass concentration increases, the total rate of oxygen uptake in the membrane increases. High biomass concentrations in the alginate membrane can lead to the formation of anoxic regions in the membrane. It is impossible to predict *a priori* how the bulk oxygen concentration will actually affect the oxygen profile in the membrane.

First, we considered the effect of bulk oxygen on the oxygen profiles when the growth rate is considered to be independent of the oxygen concentration. Figure 4.3 shows the oxygen concentration profiles predicted by Equations (4.1) and (4.4) with boundary conditions (4.2) and initial conditions (4.3) and (4.5) at time equal to 8 hours for various bulk oxygen concentrations. The bulk oxygen concentration in Figure 4.3 equals the concentration at the edges of the alginate membrane, since external mass transfer limitations were assumed negligible. The glucose concentration was taken to be 25 g/l and the growth rate was considered constant at 0.24 1/hr. The fraction of cells growing under aerobic conditions always increases with bulk oxygen concentration. Similar results were found at times less than 8 hours.

Secondly, we examined how the bulk oxygen concentration affects the membrane oxygen profiles when the growth rate varies with dissolved oxygen concentration. Peringer, et al. derived an expression for the growth rate of suspended *S. cerevisiae* as a function of dissolved oxygen concentration. The expression was multiplied by a factor of 1.15 to agree with the anaerobic immobilized cell growth rate of 0.24 1/hr measured experimentally in Chapter 3.

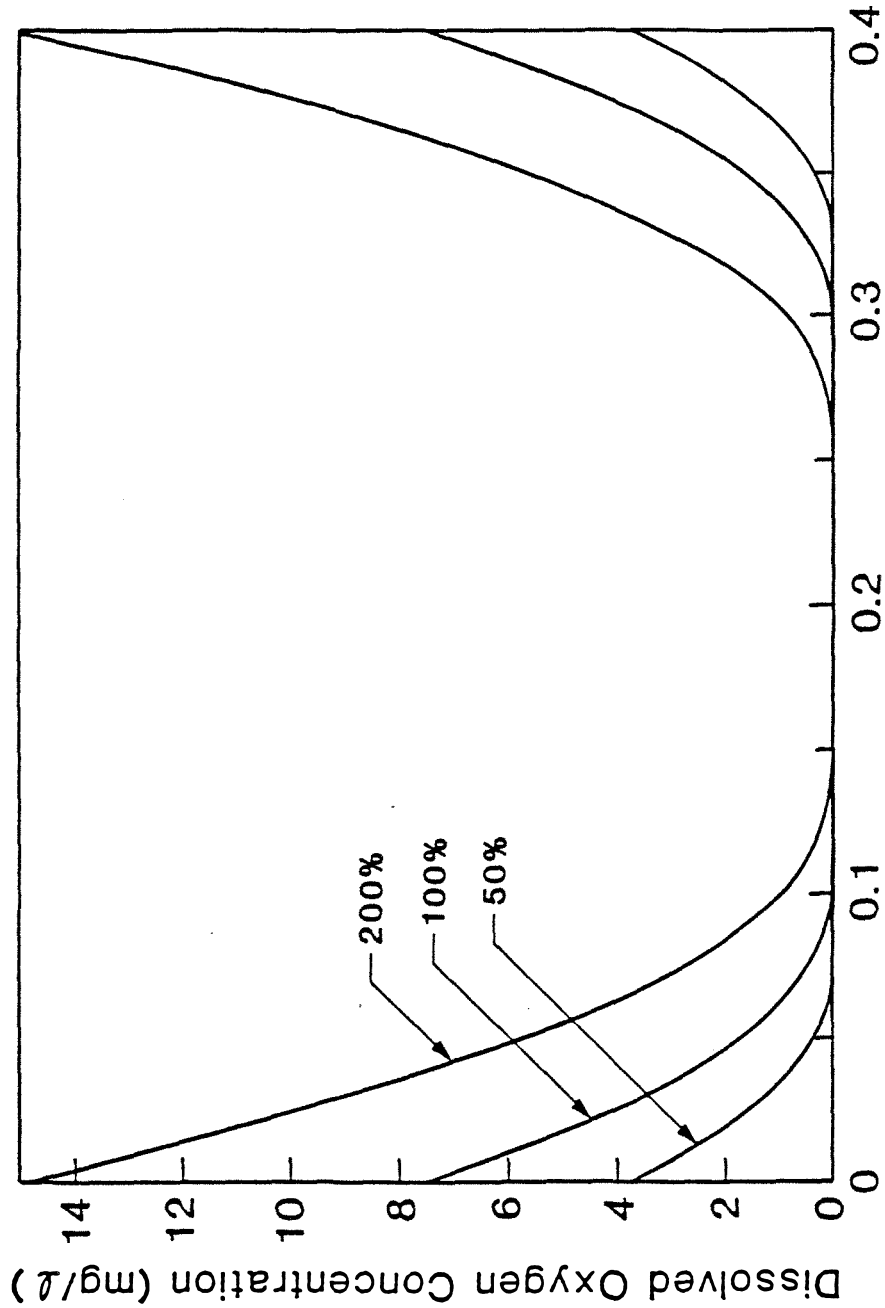

Figure 4.3 **Oxygen Concentration Profiles in alginate membrane for various bulk oxygen concentrations (% air saturation) at time equals 8 hours for a growth rate of 0.24 1/hr and a nonconstant oxygen uptake rate.**

The growth rate is given by:

$$\mu = \left(\frac{s}{K_s + s}\right)\left[\frac{\mu_G}{1 + bO_2} + \frac{\mu_R O_2}{K_L + O_2}\right] \tag{4.7}$$

where μ is the growth rate, μ_G is the growth rate that is due to glycolysis (0.24 1/hr), μ_R is the growth rate due to respiration (0.12 1/hr), K_s is the Michaelis constant for glucose (0.1 g/l), p is a quantitative index of the Pasteur effect (5 x 10^{-4} 1/% air saturation), and K_L is the Michaelis constant for oxygen (1.36 % air saturation). Equations (4.1) and (4.4) were numerically integrated with boundary conditions (4.2) and initial conditions (4.3) and (4.5). Equation (4.6) was used for the specific oxygen utilization rate expression and Equation (4.7) was used for the specific growth rate. The predicted oxygen profiles at time equal to 8 hours are shown in Figure 4.4 for various bulk dissolved oxygen concentrations. The results indicate that the fraction of cells under aerobic conditions increases as the bulk oxygen concentration increases. Similar results were obtained at previous times. Thus, the effect of oxygen concentration on growth rate does not cause larger anoxic regions at higher bulk oxygen concentrations for the growth and reaction rates in this investigation.

4.2.3 Effect of Bulk Oxygen Concentration on Average Respiration Rate

The specific oxygen utilization rate of *S. cerevisiae* increases with dissolved oxygen concentration as expressed in Equation (4.6). Since the specific oxygen utilization rate approaches its maximum value at a low dissolved oxygen concentration, an increase in the total amount of oxygen in the alginate membrane

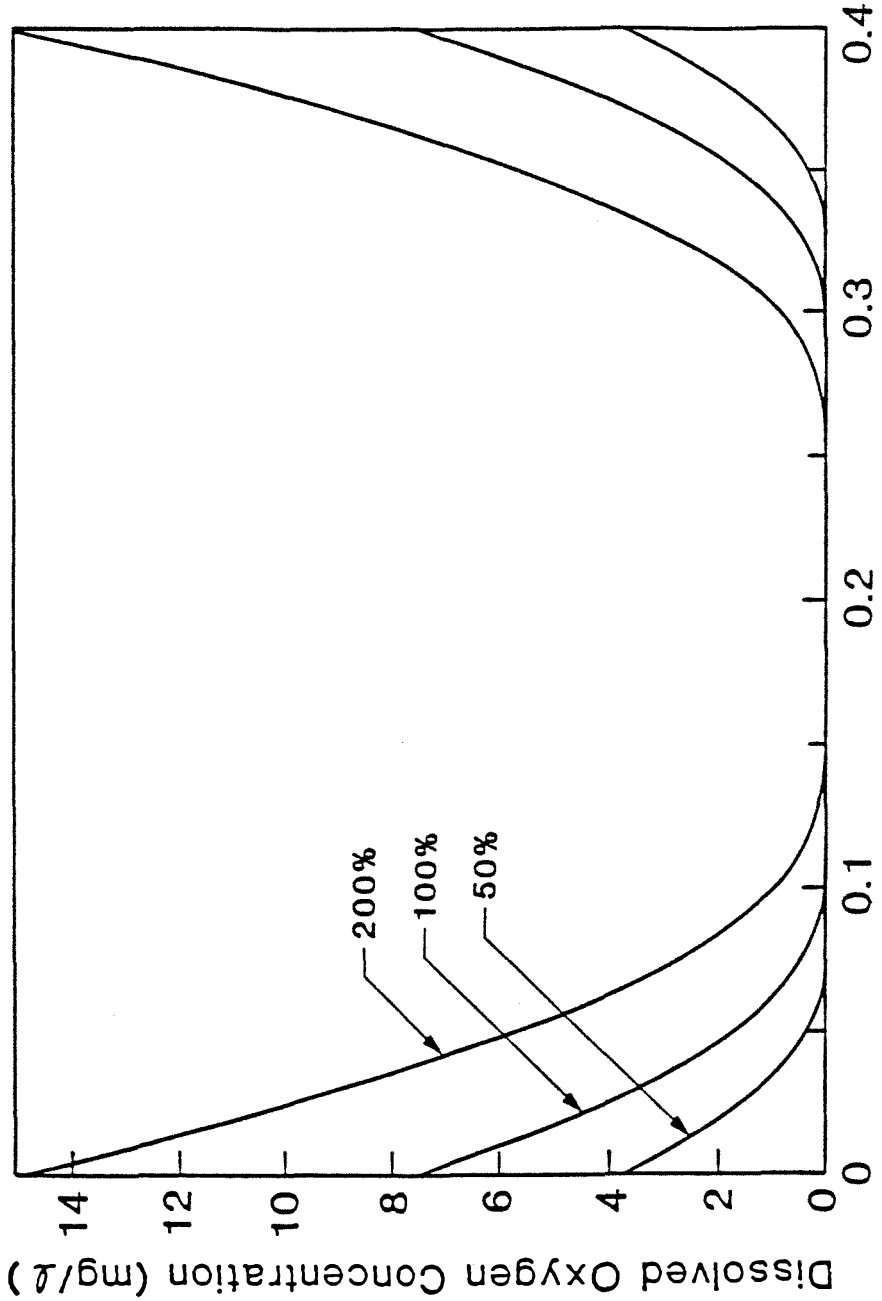

Figure 4.4 **Oxygen Concentration Profiles in alginate membrane for various bulk oxygen concentrations (% air saturation) at time equals 8 hours for a nonconstant growth rate and a nonconstant oxygen uptake rate.**

may not necessarily lead to a comparable increase in the total respiratory activity of the cells. The specific growth rate, glucose uptake rate, and ethanol production rate of *S. cerevisiae* may change roughly in proportion to the specific oxygen utilization rate rather than in proportion to the change in dissolved oxygen concentration. Thus, the oxygen utilization rate may be a more significant indicator than the amount of oxygen in describing the effect of the bulk oxygen concentration on the behavior of entrapped cells. An average rate of oxygen utilization during the diffusion-reaction experiment can be calculated from the oxygen concentration profile and the oxygen utilization rate as a function of oxygen concentration. The average oxygen utilization rate is defined as the mean specific oxygen utilization rate, weighted with respect to the biomass concentration and then normalized by the total amount of biomass. The following equation is used to calculate the average oxygen utilization rate:

$$\bar{\theta} = \frac{\sum_{j=1}^{J} \sum_{i=1}^{N} \theta_{i,j} b_{i,j} \delta x_i \delta t_j}{\sum_{j=1}^{J} \sum_{i=1}^{N} b_{i,j} \delta x_i \delta t_j}, \tag{4.8}$$

where $\theta_{i,j}$ is the specific oxygen utilization rate in the (i,j)th interval, where the intervals are discretized in time and space, $b_{i,j}$ is the biomass concentration in the (i,j)th interval, δx_i is the step size in position, and δt_j is the step size in time. The effect of the bulk dissolved oxygen concentrationon on the average oxygen utilization rate is shown in Figure 4.5 as obtained from the solution of Equations (4.1) and (4.4) with boundary conditions (4.2) and initial conditions (4.3) and (4.5) and with the oxygen utilization rate given by Equation (4.6) and the growth rate given by Equation (4.7). An increase in the average respiration rate of the immobilized cells is predicted as the bulk oxygen concentration goes from 0 to 15.0 mg/l dissolved oxygen or 200 % air saturation. Therefore,

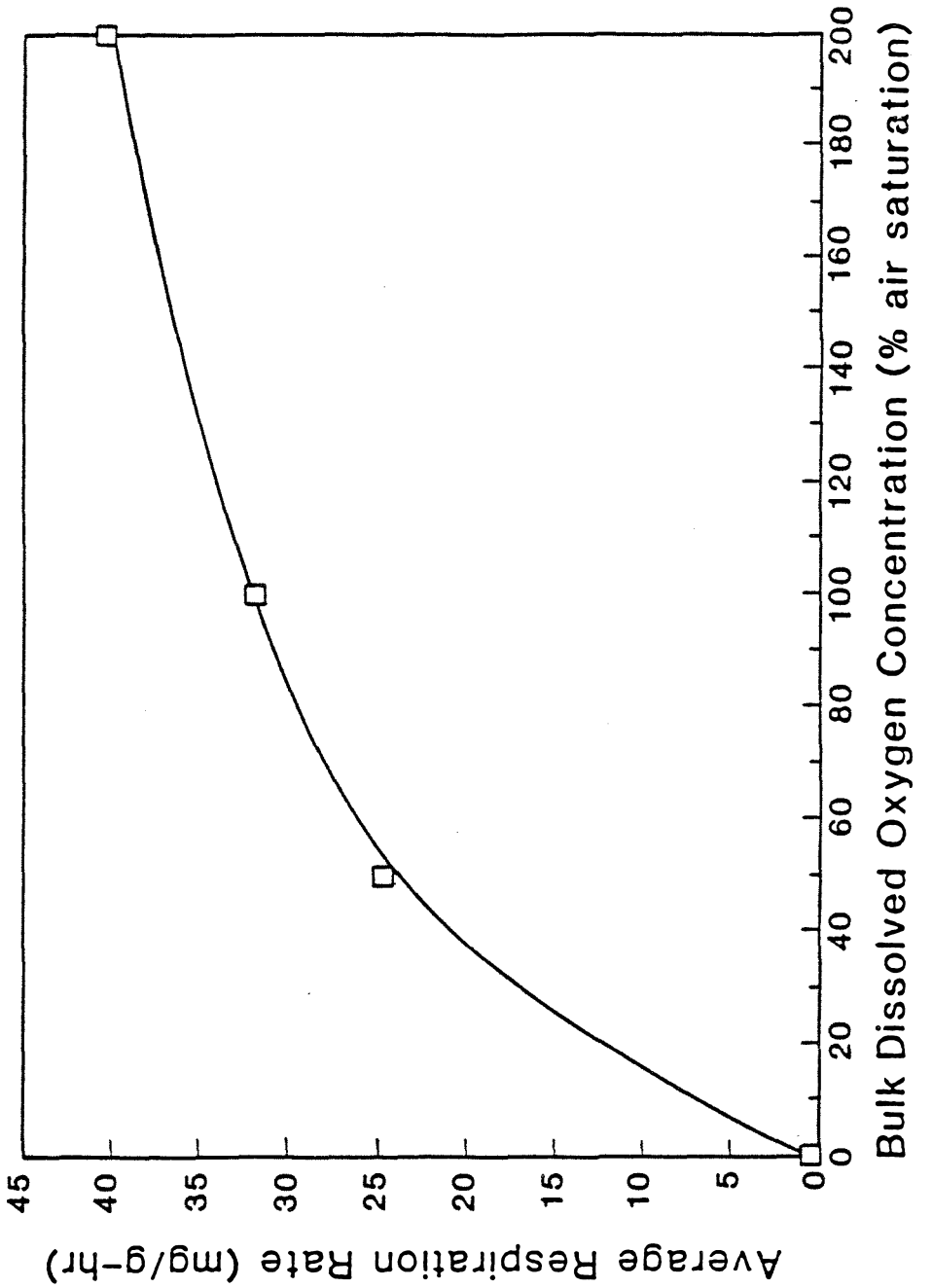

Figure 4.5 **Effect of Bulk Dissolved Oxygen Concentration on Average Respiration Rate of *S. cerevisiae* 18790 immobilized in alginate.**

changes in the specific growth rate, specific glucose uptake rate, and specific ethanol production rate with bulk oxygen concentration are anticipated in the diffusion-reaction experiments.

4.2.4 Effect of Oxygen Profiles on Experimental Results

Before applying the experimental method developed in Chapter 3 to aerobic reactor conditions, we must consider how oxygen gradients in the membrane will affect experimental results. The growth rate, glucose uptake rate, and ethanol production rate of immobilized cells are expected to vary with dissolved oxygen concentration. In Chapter 3 the diffusion-reaction analysis was derived for constant values of the growth rate, glucose uptake rate, and ethanol production rate. If these reaction parameters are weak functions of dissolved oxygen concentration, the diffusion-reaction analysis may still be applied directly to the experimental data. In this case one would expect the growth rate, glucose uptake rate, and ethanol production rate determined by the diffusion-reaction analysis to be close to some weighted average of the rates over the course of the experiment. On the other hand, if the growth rate, glucose uptake rate, and ethanol production rate are strong functions of the dissolved oxygen concentration, they will vary significantly during the experiments. The diffusion-reaction analysis can then produce misleading results if it is applied directly to the experimental data. For example, if the intrinsic, specific glucose uptake rate increases as the dissolved oxygen concentration decreases, then the glucose uptake rate will be increasing over the course of the experiment. Let the constant value of the glucose uptake rate in the glucose

diffusion-reaction equation be replaced by an expression exponential in time:

$$\alpha = \alpha_0 \exp^{dt}, \tag{4.8}$$

where α is the glucose uptake rate, α_0 is the initial glucose uptake rate, d is an arbitrary constant, and t equals time. If the diffusion-reaction analysis is applied as derived in Chapter 3, the slope of the plot, $\ln Z_g$ versus time, will equal the growth rate plus the exponential factor, d, of the glucose uptake rate expression. The glucose uptake rate determined by the diffusion-reaction analysis will be equal to the glucose uptake rate at time equal to zero. For d greater than zero, the growth rate will be overestimated and the glucose uptake rate will be underestimated.

The effect of nonconstant values of the growth rate, glucose uptake rate, and ethanol production rate on the diffusion-reaction analysis was further investigated numerically. The diffusion reaction equations for biomass, glucose, and ethanol (Equations 3.1–3.4) were solved numerically where the growth rate, glucose uptake rate, and ethanol production rate were taken to be functions of both time and space. Various functions were generated for growth rate, glucose uptake rate, and ethanol production rate. The growth rate was considered as a decreasing function of time, and the glucose uptake rate and ethanol production rate were considered as increasing functions of time to simulate the situation where the oxygen concentration in the membrane decreases as a function of time because of increasing biomass. Similarly, the growth rate was considered to decrease towards the center of the membrane, and the glucose uptake rate and ethanol production rate were taken to increase towards the center of the membrane because towards the end of the diffusion-reaction

experiments, the oxygen concentration is lowest in the center of the membrane.

The diffusion reaction equations (Equations 3.1–3.4) were solved simultaneously by the Crank-Nicholson method of finite differences. The total flux of glucose and ethanol versus time data that were measured in previous experiments for the determination of the specific growth rate, glucose uptake rate, and ethanol production rate, were also simulated using the numerical solution. Then the simulated flux versus time data was analyzed by the same procedure as the experimental data to determine μ_{DR}, α_{DR}, and ν_{DR}, where μ_{DR} is the specific growth rate calculated by the diffusion-reaction analysis, α_{DR} is the specific glucose uptake rate calculated by the diffusion-reaction analysis, and ν_{DR} is the specific ethanol production rate calculated by the diffusion-reaction analysis. In general, spatial variations in the reaction rates resulted in values of μ_{DR}, α_{DR}, and ν_{DR} which were close to the average values of the growth rate, glucose uptake rate, and ethanol production rate, respectively. For simulations with symmetric and asymmetric glucose concentrations across the membrane, the growth rate, glucose uptake rate, and ethanol production rate closest to the chamber where the flux measurements were made, had more effect on the values of μ_{DR}, α_{DR}, and ν_{DR} than the growth rate, glucose uptake rate, and ethanol production rate in the center of the membrane and on the other edge of the membrane. Time variations in the growth rate, glucose uptake rate, and ethanol production rate had a more significant effect than spatial variations on μ_{DR}, α_{DR}, and ν_{DR} When the glucose uptake rate and ethanol production rate increased with time, μ_{DR} was higher than the growth rate at any time during the experiment and α_{DR} and ν_{DR} were lower than the rates at any time during the experiment. Therefore, time variations in the growth and reaction rates

can cause the diffusion-reaction analysis to produce biased results.

A first step in evaluating the effect of oxygen on the growth rate, glucose uptake rate, and ethanol production rate of immobilized cells is to carry out the diffusion-reaction experiments at various bulk oxygen concentrations. If oxygen has little or no effect on the growth and reaction rates of immobilized cells, then similar results will be obtained at all bulk oxygen concentrations. If the effect of oxygen on the growth rate, glucose uptake rate, and ethanol production rate is important, the predicted growth and reaction rates will vary with bulk dissolved oxygen concentration. Since oxygen causes an increase in the growth rate of suspended cells and a decrease in the glucose uptake rate and ethanol production rate of suspended cells, it can be anticipated that there will be some decrease in the growth rate and increase in the glucose and ethanol reaction rates during the diffusion-reaction experiments as oxygen is depleted from the membrane. This will cause an overestimate of the growth rate and an underestimate of the reaction rates at higher bulk dissolved oxygen concentrations, if the variation in the growth rate and reaction rates with dissolved oxygen is significant.

4.3 MATERIALS AND METHODS

The diffusion-reaction experiments were conducted as described in Chapter 3. The bulk oxygen concentration was controlled by bubbling gas through each chamber of the reactor at a rate of 40 ml/min. The dissolved oxygen concentration in the bulk fluid was maintained throughout the experiment at either 3.75, 7.50, or 15.0 mg/l, which equal 50, 100, and 200 % air saturation, respectively. Experiments were conducted with either an imposed glucose gra-

dient or with symmetric glucose concentrations as described in Chapter 3. Final biomass densities were also measured according to the procedure described in Chapter 3.

Suspended cell experiments were also carried out as described in Chapter 3 for dissolved oxygen concentrations of 50 % and 100 % air saturation. The dissolved oxygen concentration was fixed by bubbling gas through the medium at a rate of 40 ml/min.

4.4 RESULTS AND DISCUSSION

The diffusion-reaction analysis was applied to the experimental data of the diffusion-reaction experiments. The values of the growth rate, glucose uptake rate, and ethanol production rate determined by the diffusion-reaction analysis are referred to as μ_{DR}, α_{DR}, and ν_{DR}, respectively. The $\ln Z_g$ versus time plots are shown in Figures 4.6–4.8 for three diffusion-reaction experiments with an imposed glucose gradient and dissolved oxygen concentrations of 50 %, 100 %, and 200 % air saturation, respectively. Figures 4.9–4.14 are plots of $\ln Z_e$ versus time for the same three experiments where the ethanol concentration is measured in both reactor chambers. Four diffusion-reaction experiments were also conducted with symmetric glucose concentrations in the reactor chambers. The $\ln Z_e$ versus time is plotted in Figures 4.15–4.22 for these four experiments with dissolved oxygen concentrations of 50 %, 100 %, 200 %, and 200 % air saturation, respectively. The lines in Figures 4.6–4.22 represent the best fit to the experimental data. The lines fit the experimental data quite well for all times. Although the growth rate, glucose uptake rate, and ethanol production rate vary over the course of the experiments as will be shown later, the

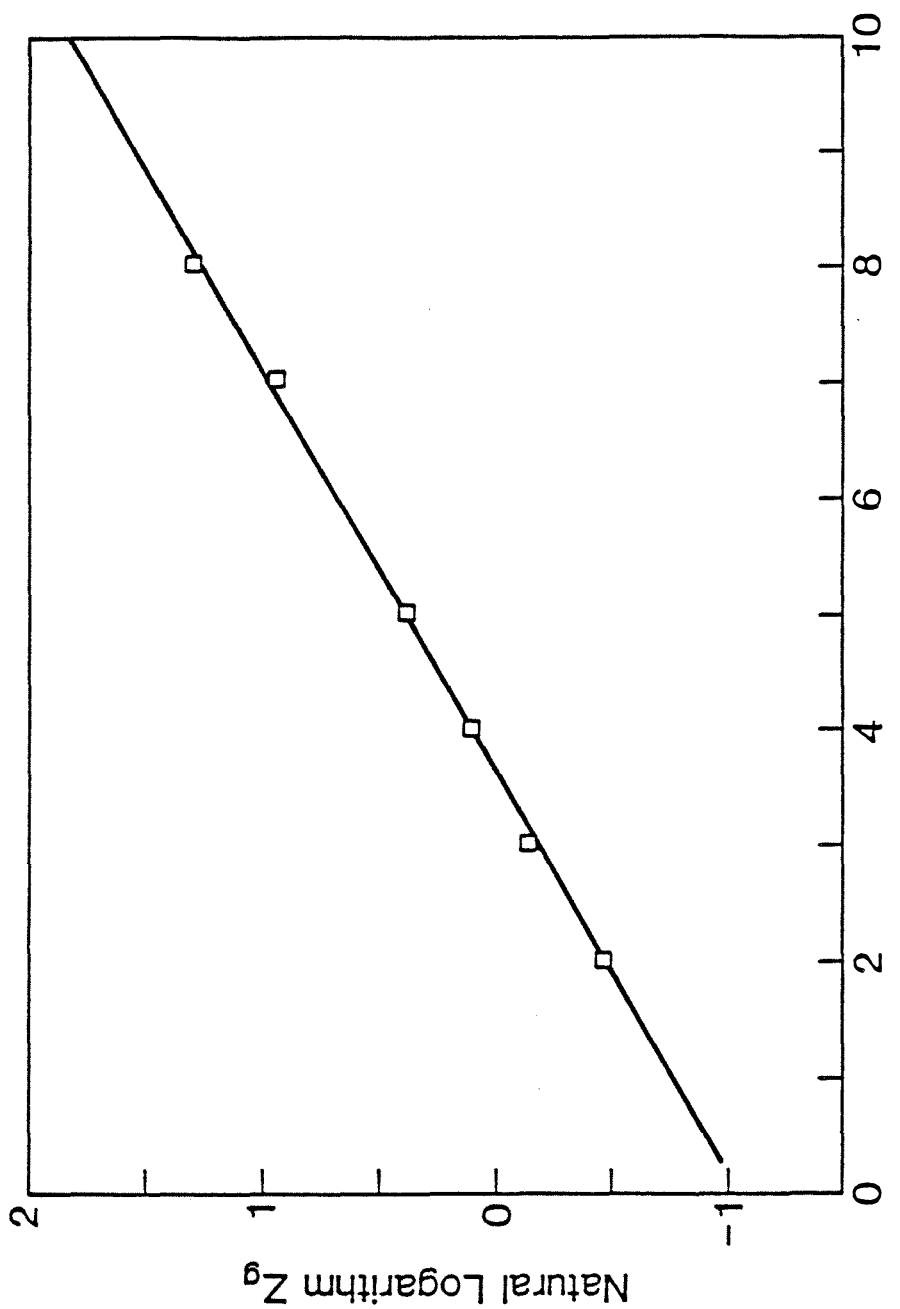

Figure 4.6 **Diffusion-Reaction Experiment for Glucose Uptake and Growth with a bulk dissolved oxygen concentration of 50% air saturation. Run 3.**

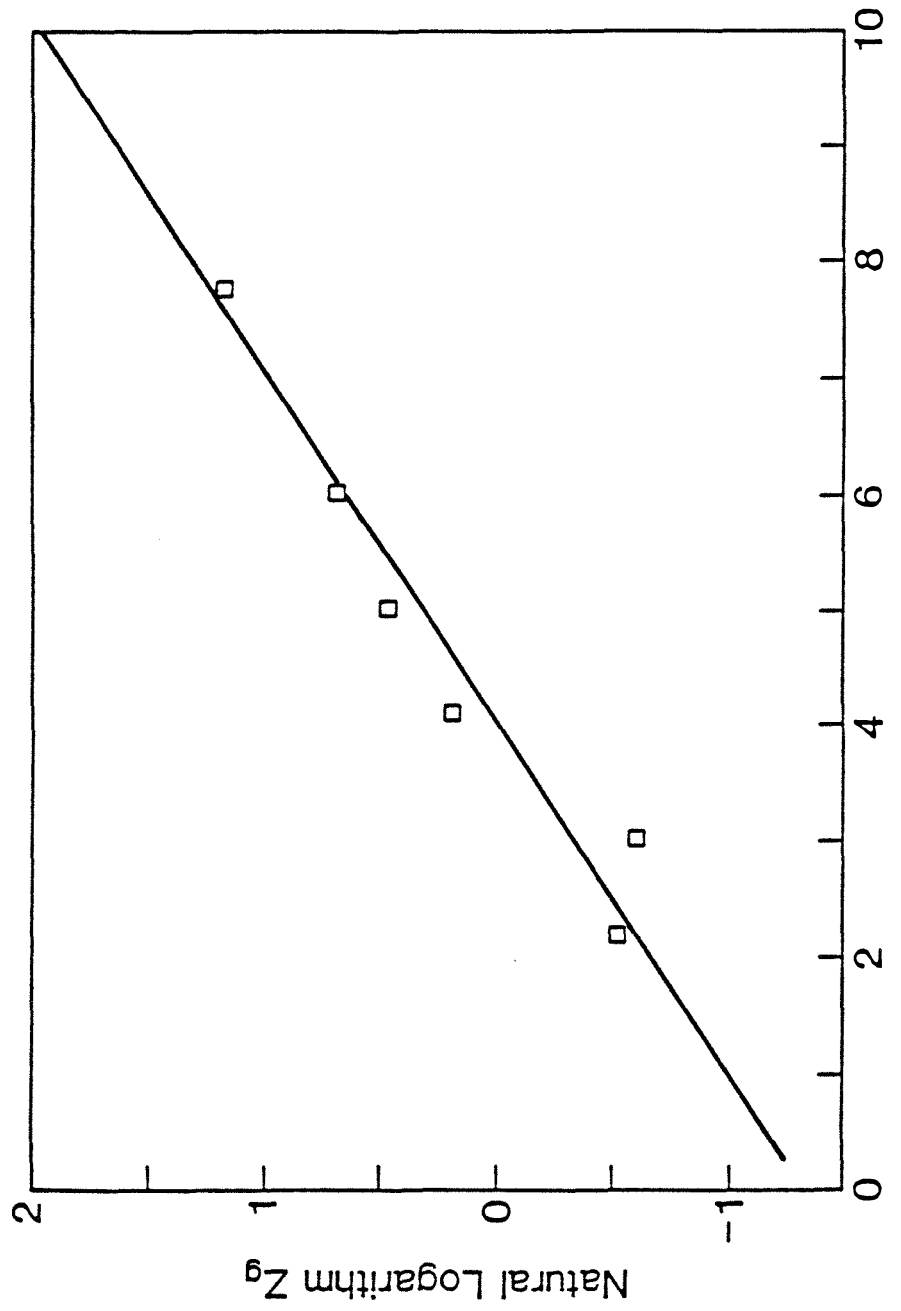

Figure 4.7 **Diffusion-Reaction Experiment for Glucose Uptake and Growth with a bulk dissolved oxygen concentration of 100% air saturation. Run 5.**

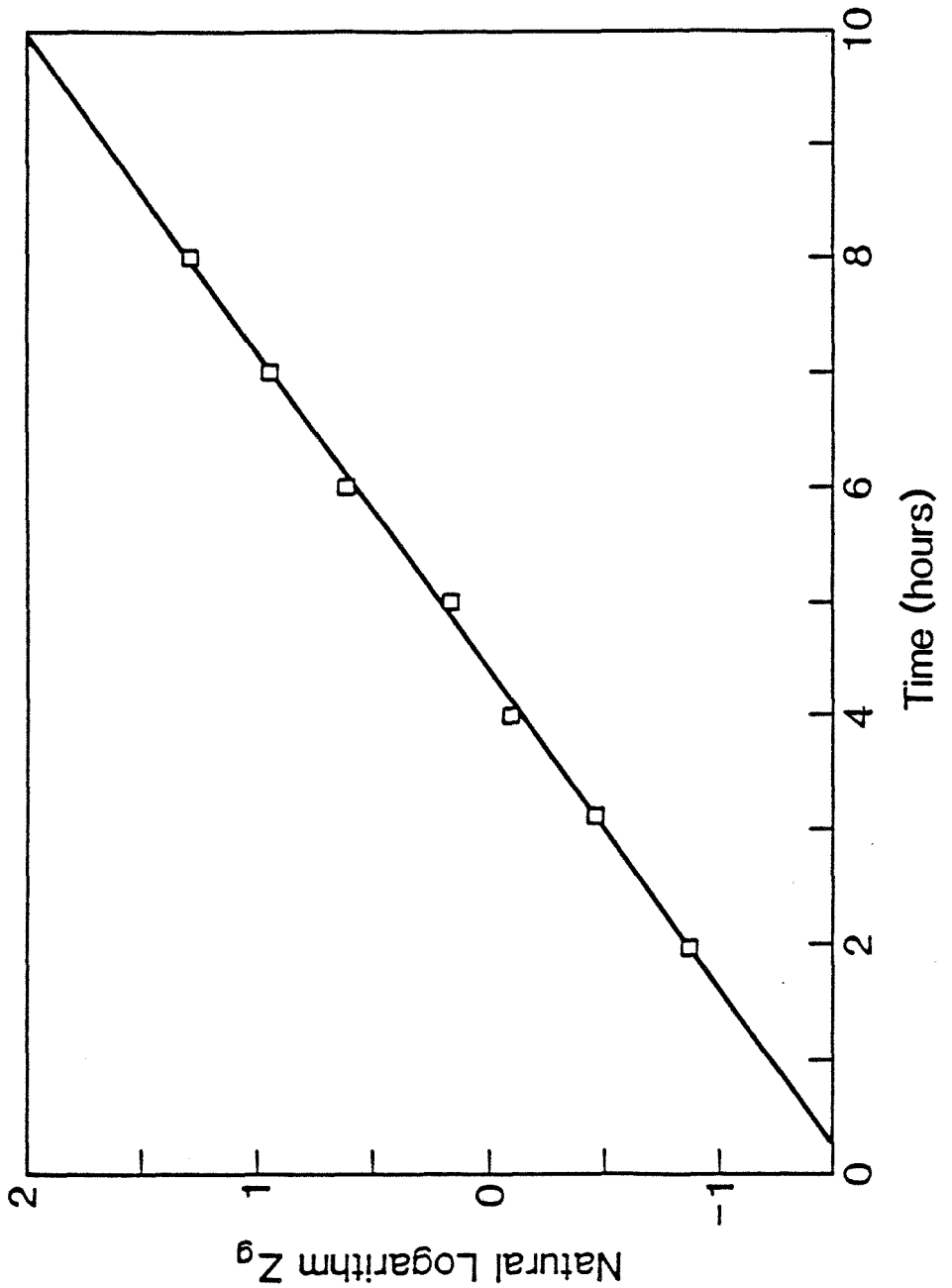

Figure 4.8 **Diffusion-Reaction Experiment for Glucose Uptake and Growth with a bulk dissolved oxygen concentration of 200% air saturation. Run 7.**

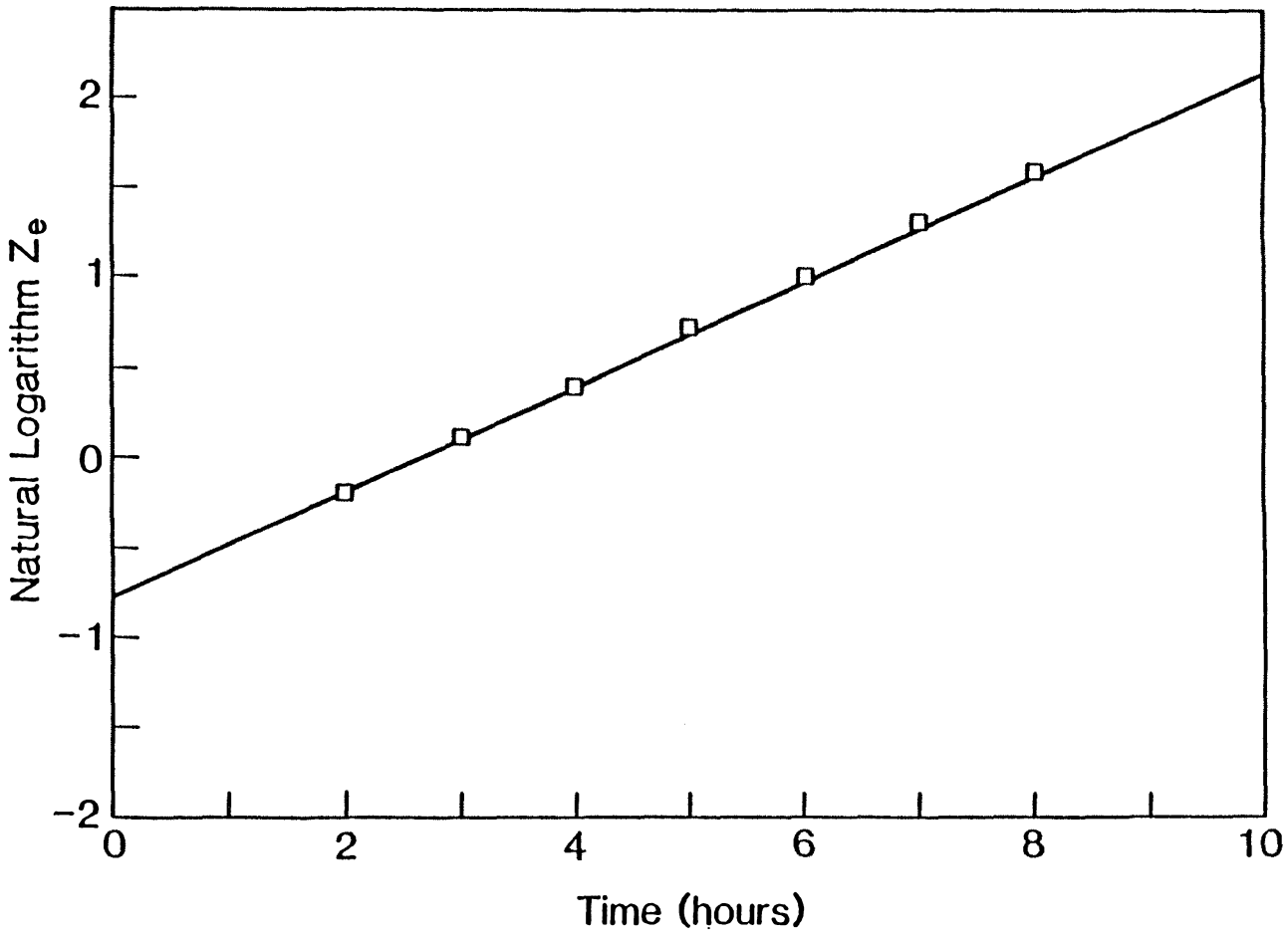

Figure 4.9 **Diffusion-Reaction Experiment for Ethanol Production and Growth with a bulk dissolved oxygen concentration of 50% air saturation and asymmetric glucose concentrations. Run 3, chamber 1.**

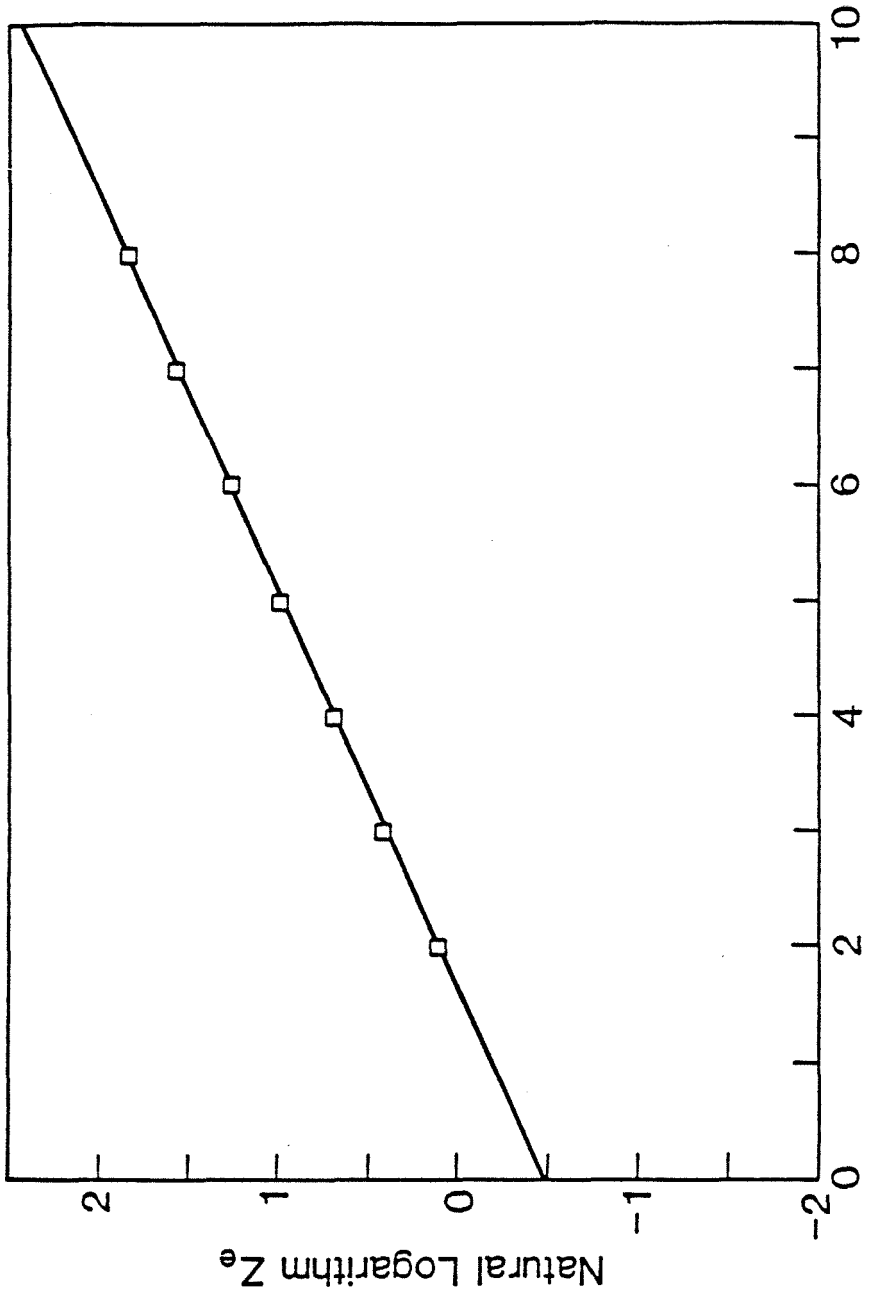

Figure 4.10 **Diffusion-Reaction Experiment for Ethanol Production and Growth with a bulk dissolved oxygen concentration of 50% air saturation and asymmetric glucose concentrations. Run 3, chamber 2.**

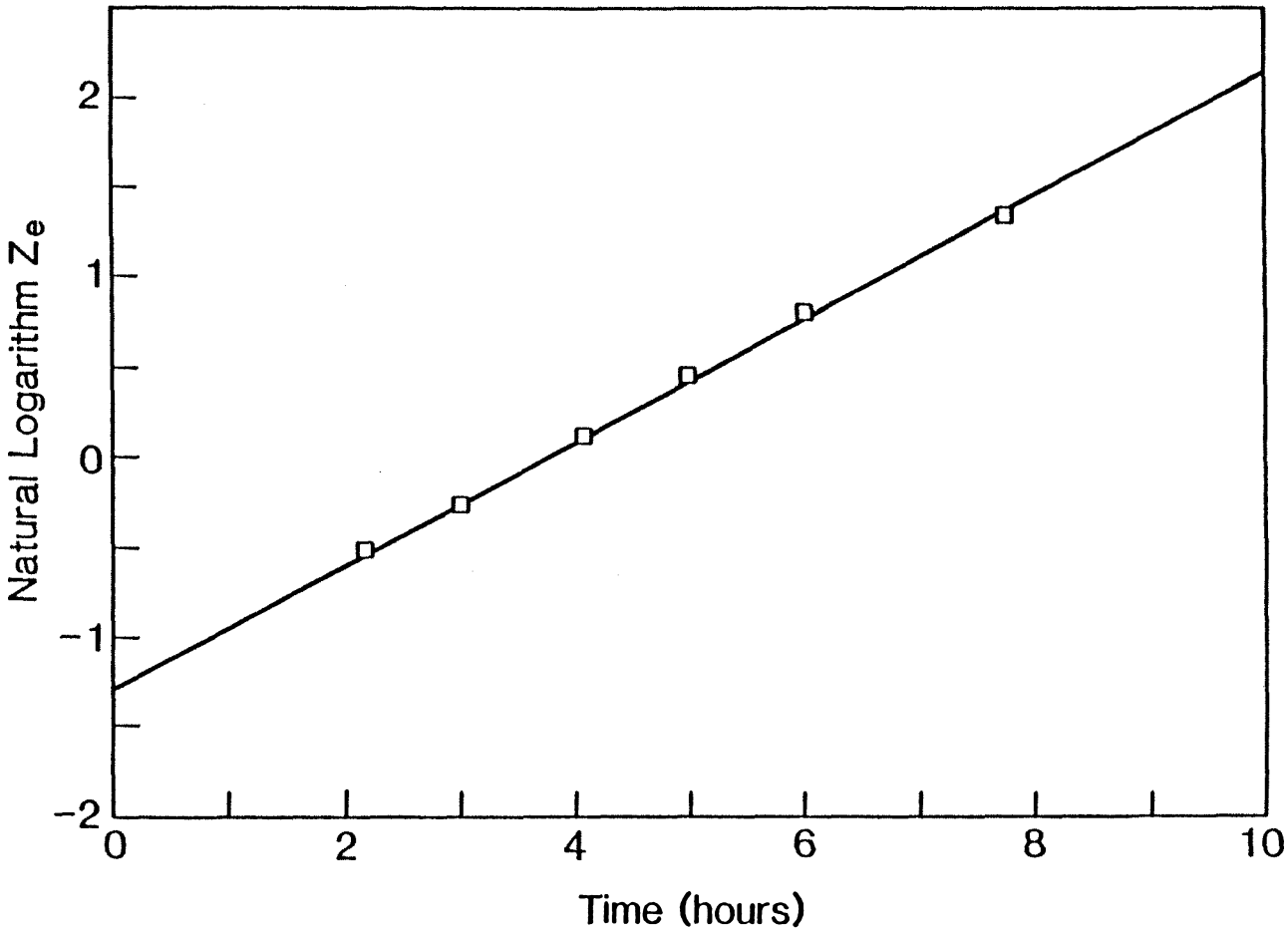

Figure 4.11 **Diffusion-Reaction Experiment for Ethanol Production and Growth with a bulk dissolved oxygen concentration of 100% air saturation and asymmetric glucose concentrations. Run 5, chamber 1.**

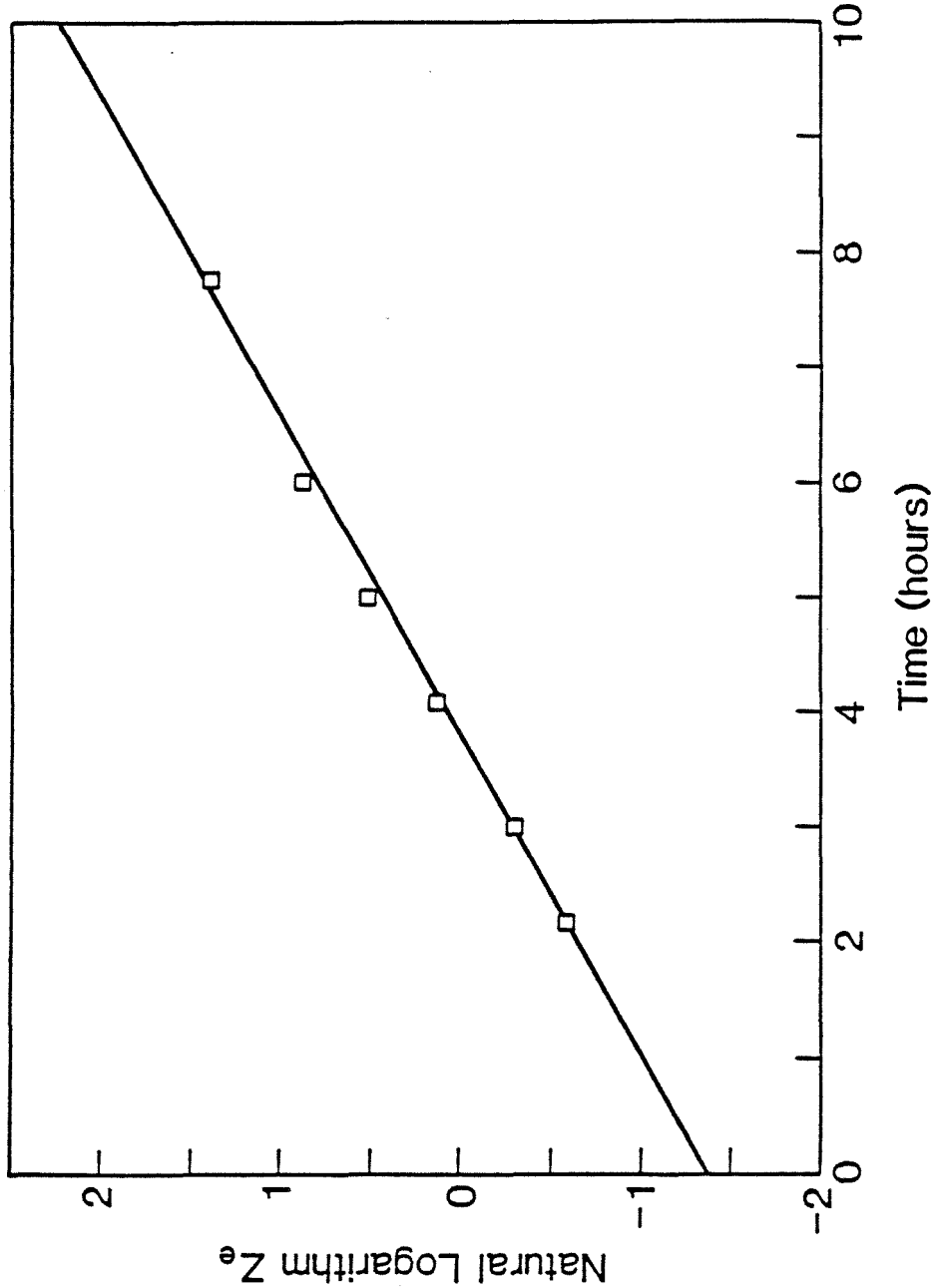

Figure 4.12 **Diffusion-Reaction Experiment for Ethanol Production and Growth with a bulk dissolved oxygen concentration of 100% air saturation and asymmetric glucose concentrations. Run 5, chamber 2.**

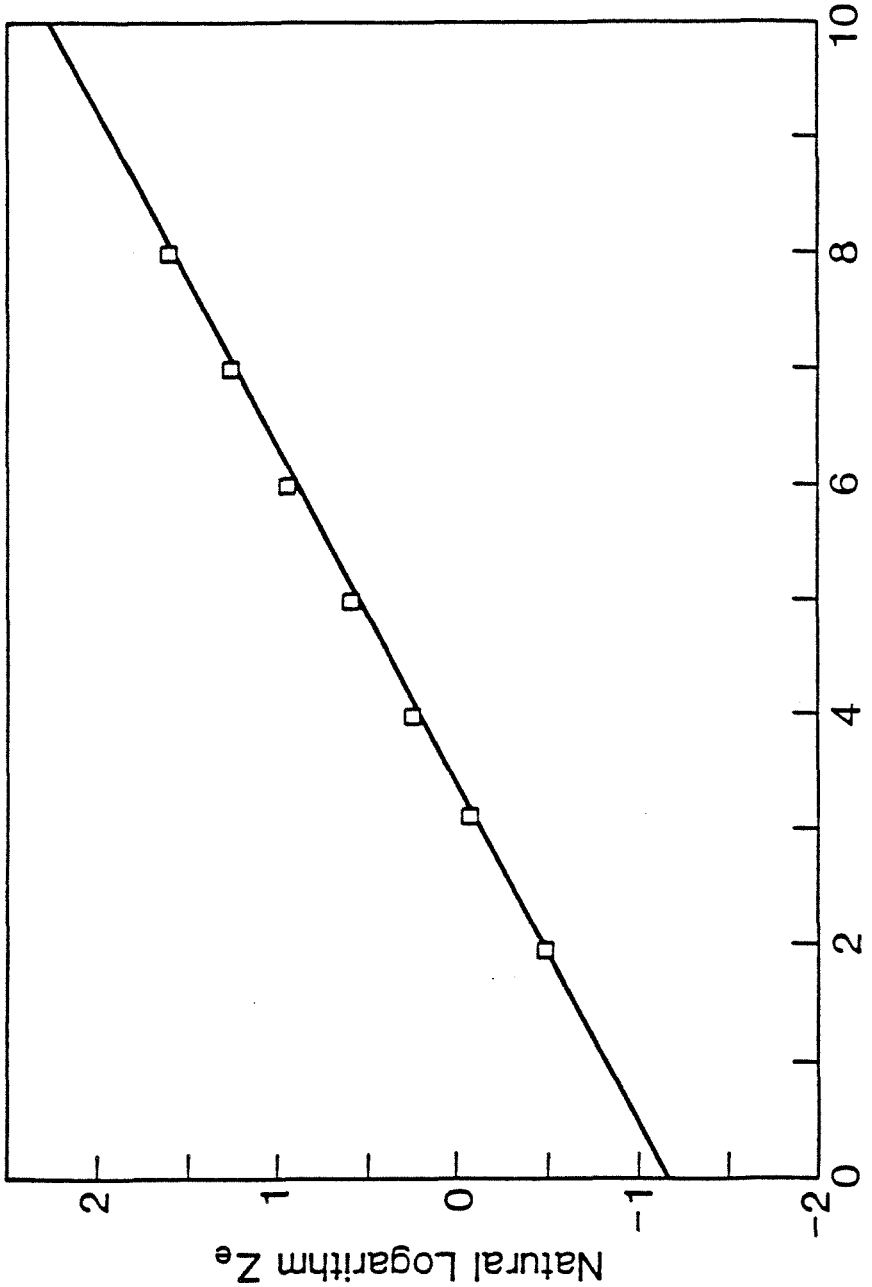

Figure 4.13 **Diffusion-Reaction Experiment for Ethanol Production and Growth with a bulk dissolved oxygen concentration of 200% air saturation and asymmetric glucose concentrations. Run 7, chamber 1.**

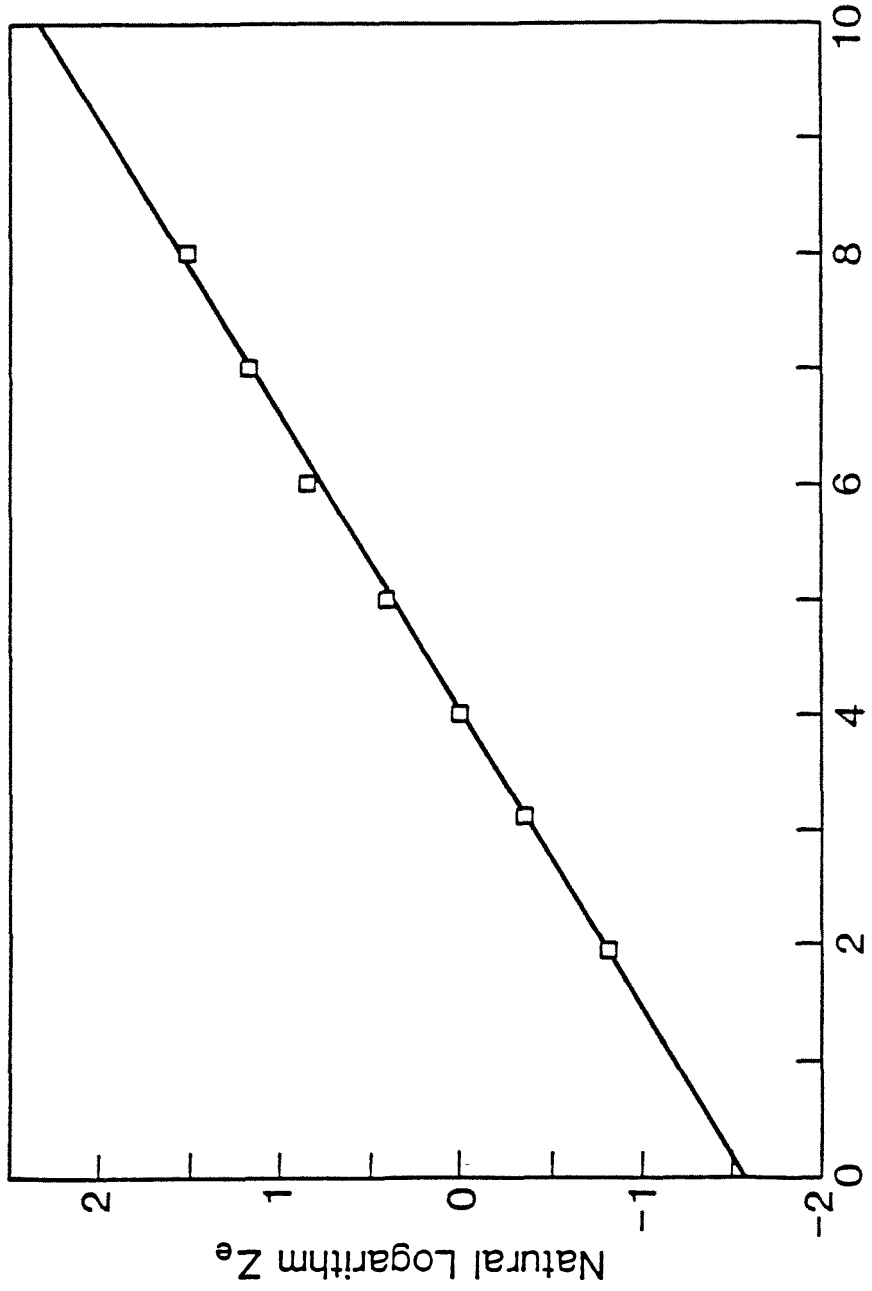

Figure 4.14 **Diffusion-Reaction Experiment for Ethanol Production and Growth with a bulk dissolved oxygen concentration of 200% air saturation and asymmetric glucose concentrations. Run 7, chamber 2.**

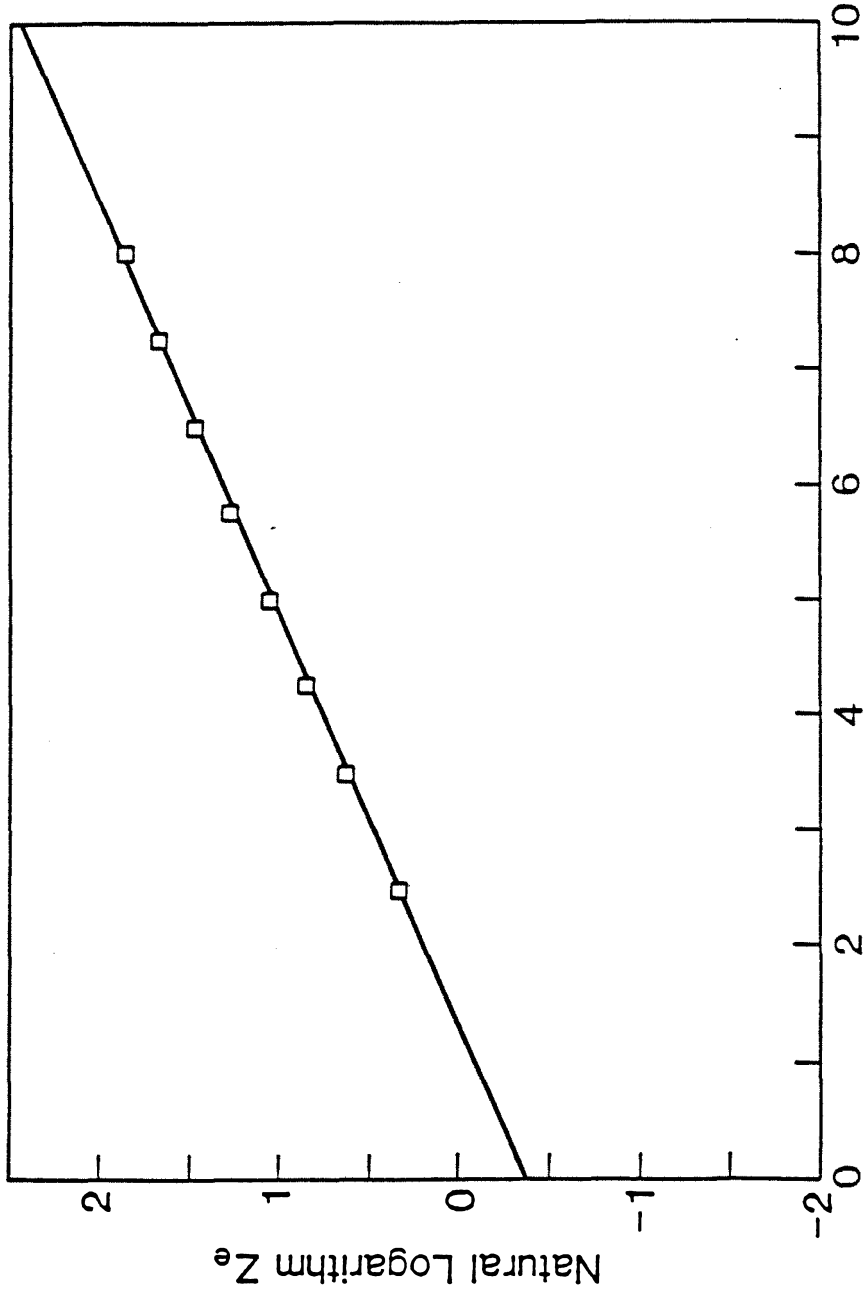

Figure 4.15 **Diffusion-Reaction Experiment for Ethanol Production and Growth with a bulk dissolved oxygen concentration of 50% air saturation and symmetric glucose concentrations. Run 4, chamber 1.**

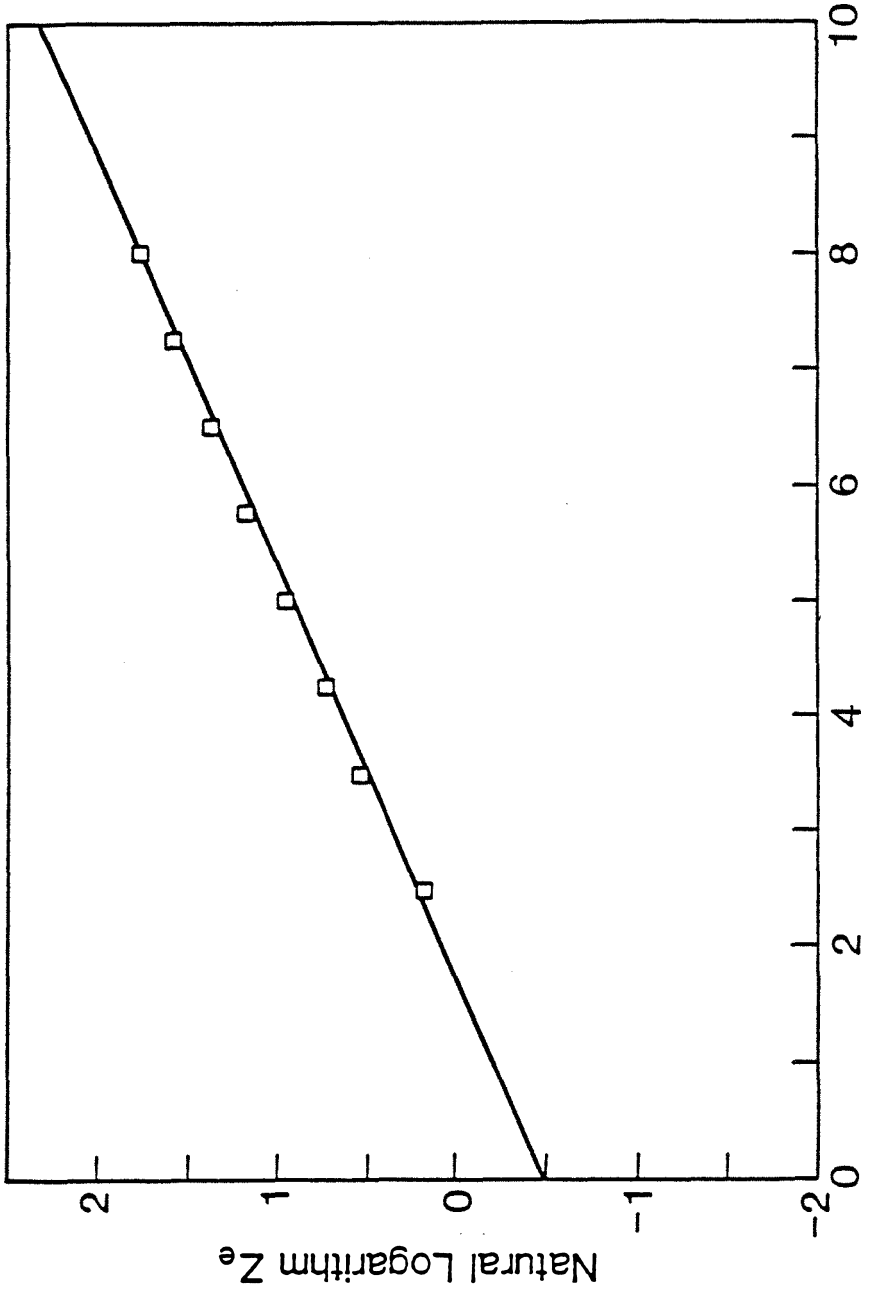

Figure 4.16 **Diffusion-Reaction Experiment for Ethanol Production and Growth with a bulk dissolved oxygen concentration of 50% air saturation and symmetric glucose concentrations. Run 4, chamber 2.**

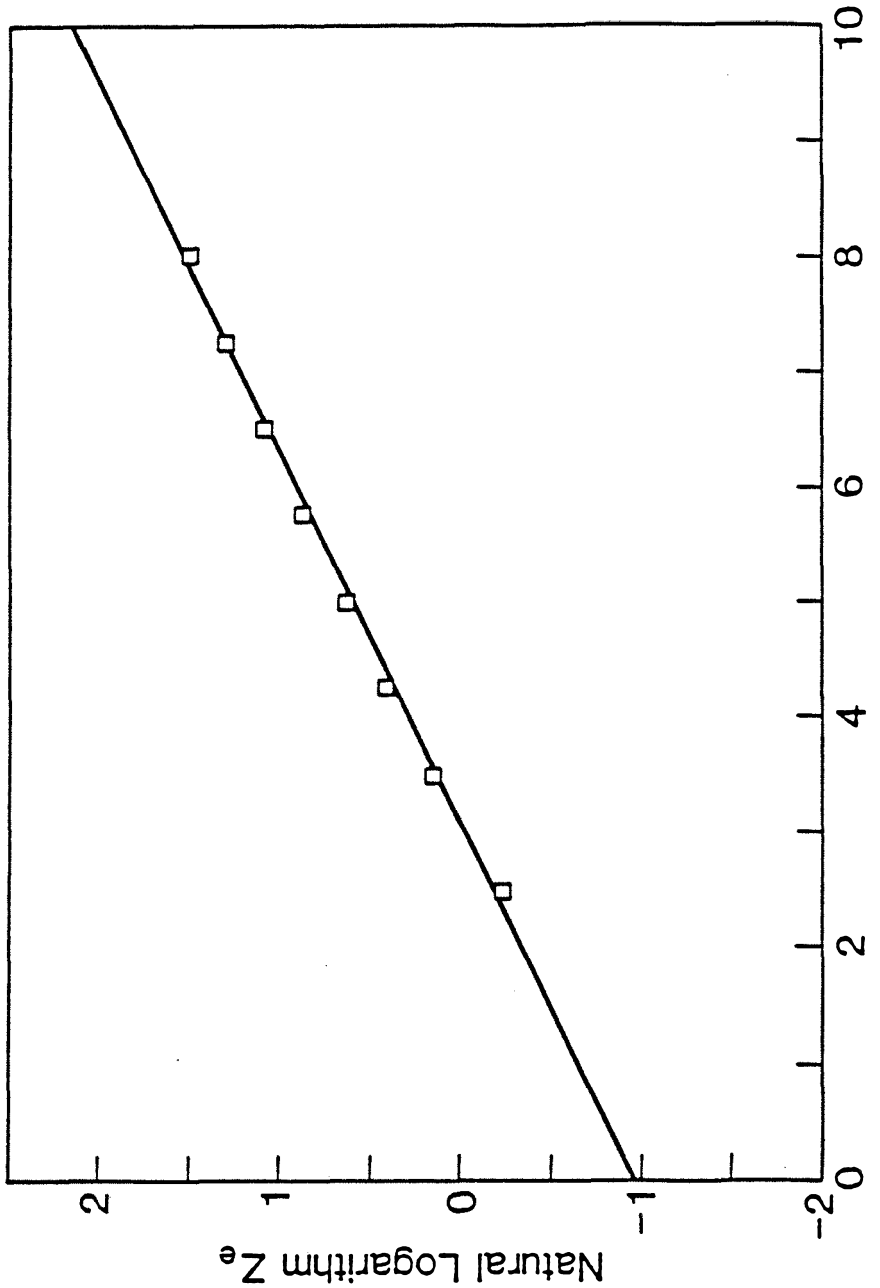

Figure 4.17 **Diffusion-Reaction Experiment for Ethanol Production and Growth with a bulk dissolved oxygen concentration of 100% air saturation and symmetric glucose concentrations. Run 6, chamber 1.**

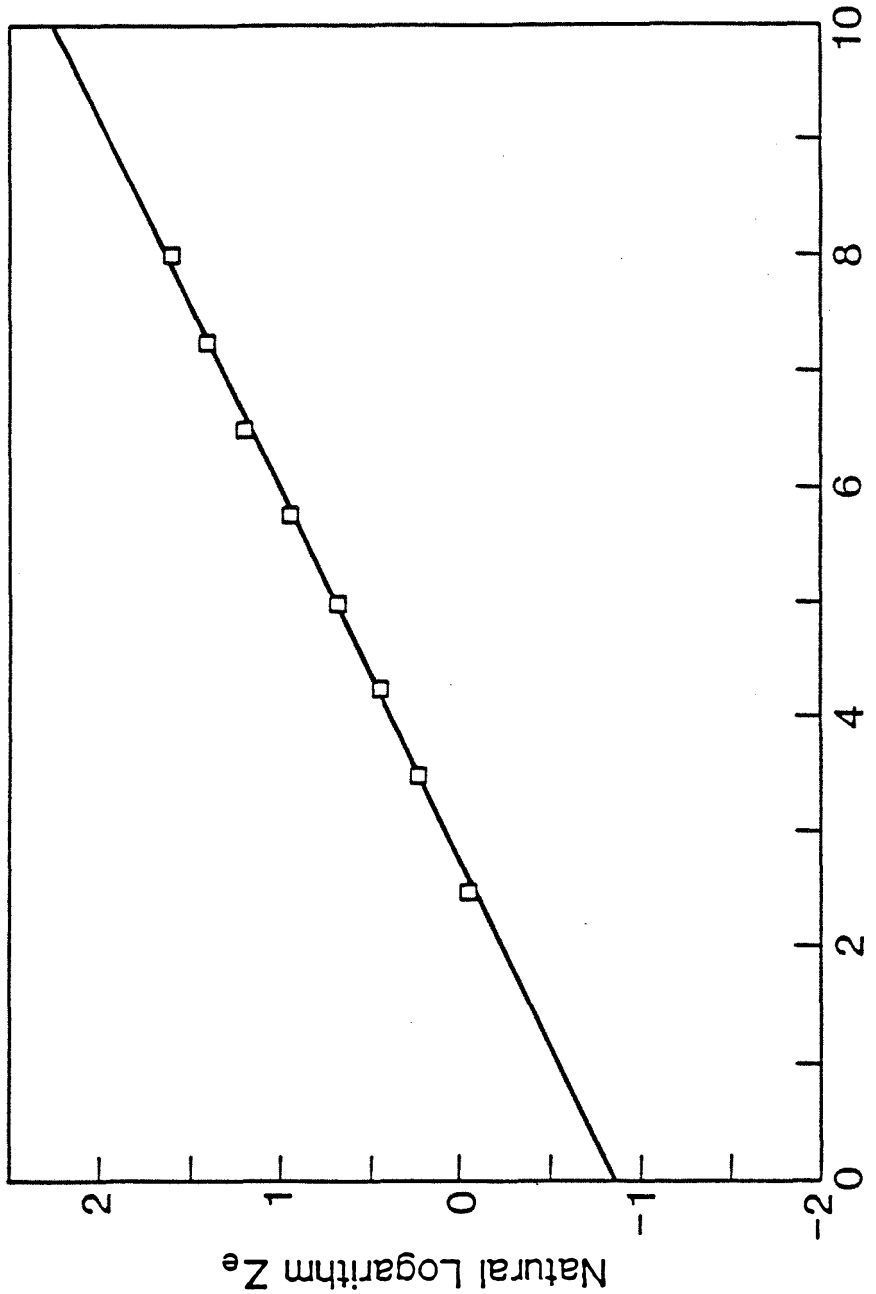

Figure 4.18 **Diffusion-Reaction Experiment for Ethanol Production and Growth with a bulk dissolved oxygen concentration of 100% air saturation and symmetric glucose concentrations. Run 6, chamber 2.**

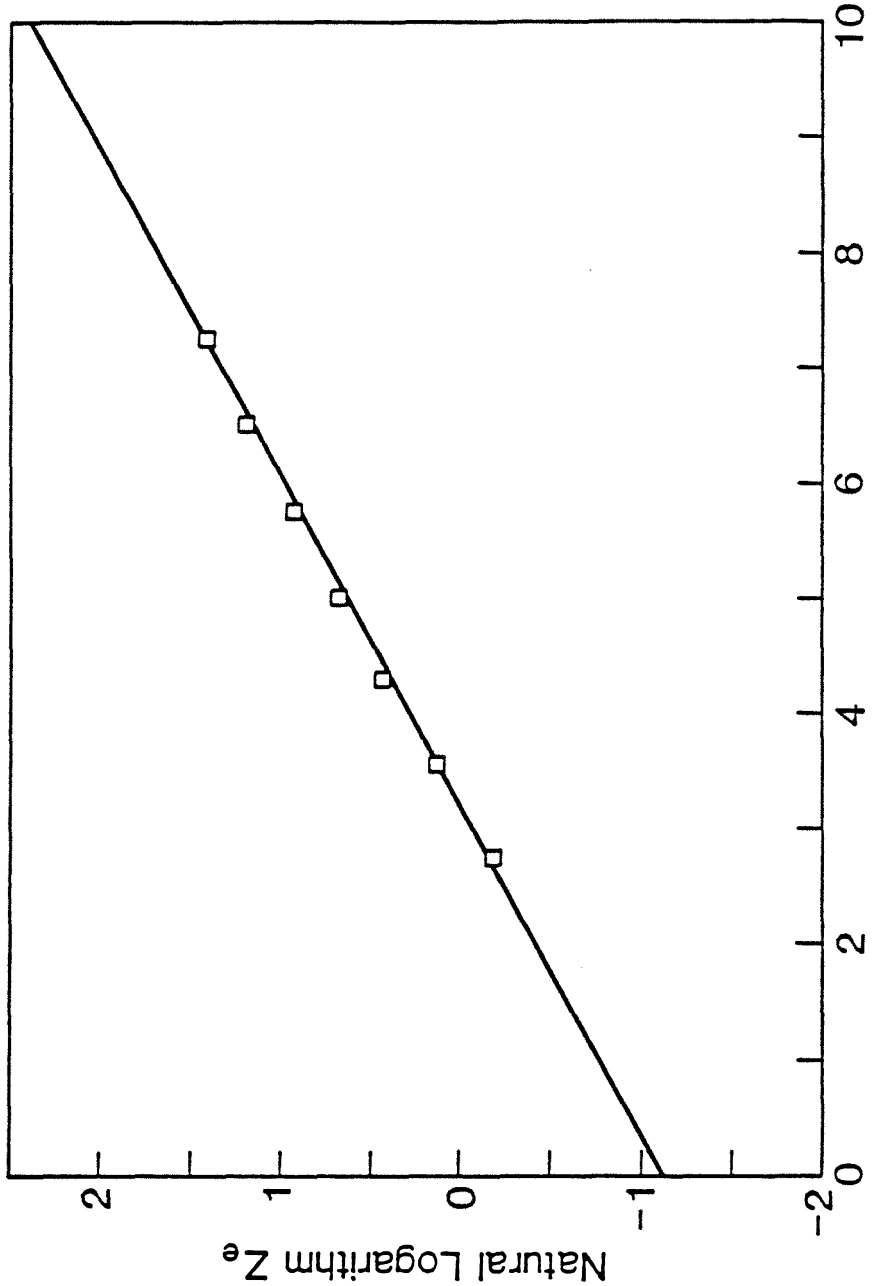

Figure 4.19 **Diffusion-Reaction Experiment for Ethanol Production and Growth with a bulk dissolved oxygen concentration of 200% air saturation and symmetric glucose concentrations. Run 8, chamber 1.**

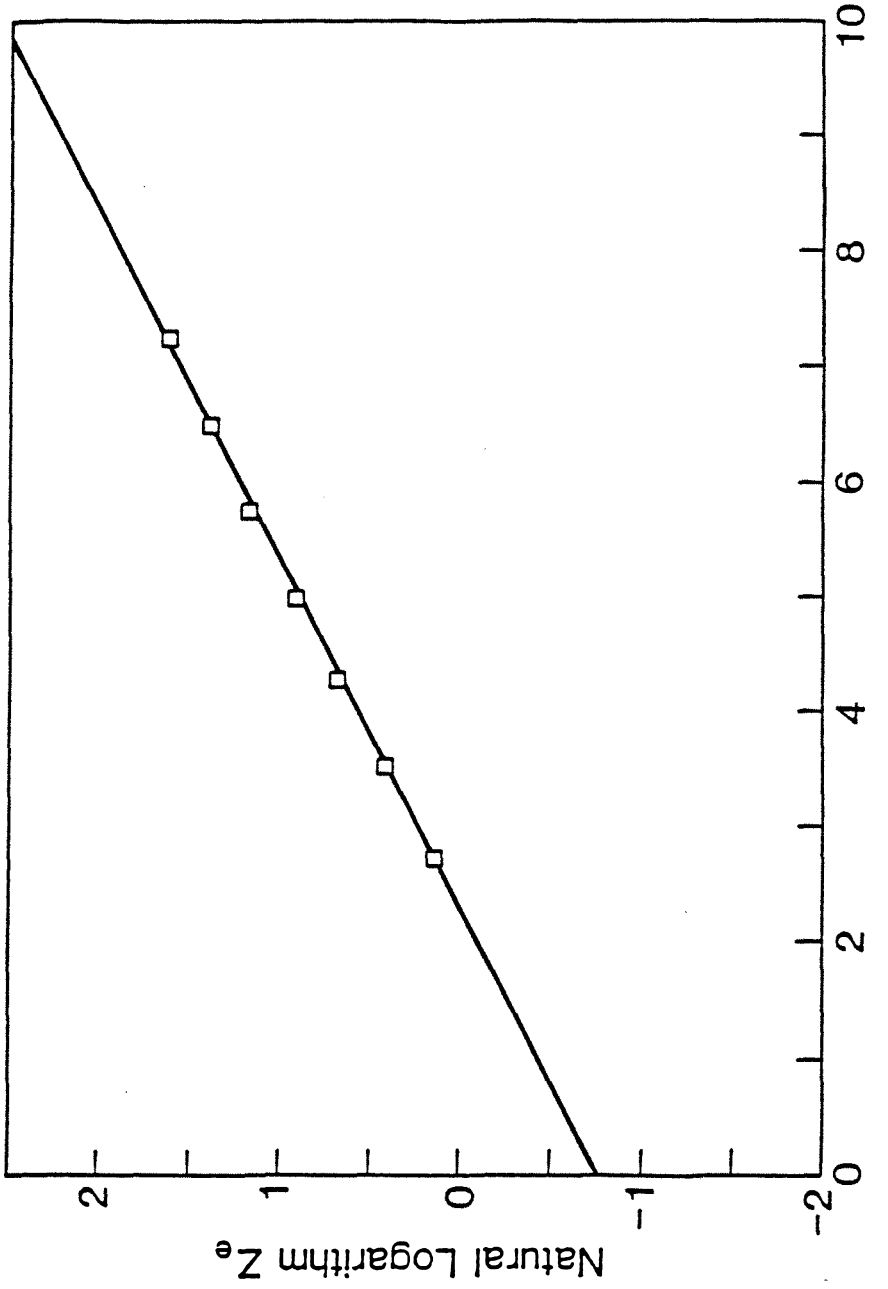

Figure 4.20 **Diffusion-Reaction Experiment for Ethanol Production and Growth with a bulk dissolved oxygen concentration of 200% air saturation and symmetric glucose concentrations. Run 8, chamber 2.**

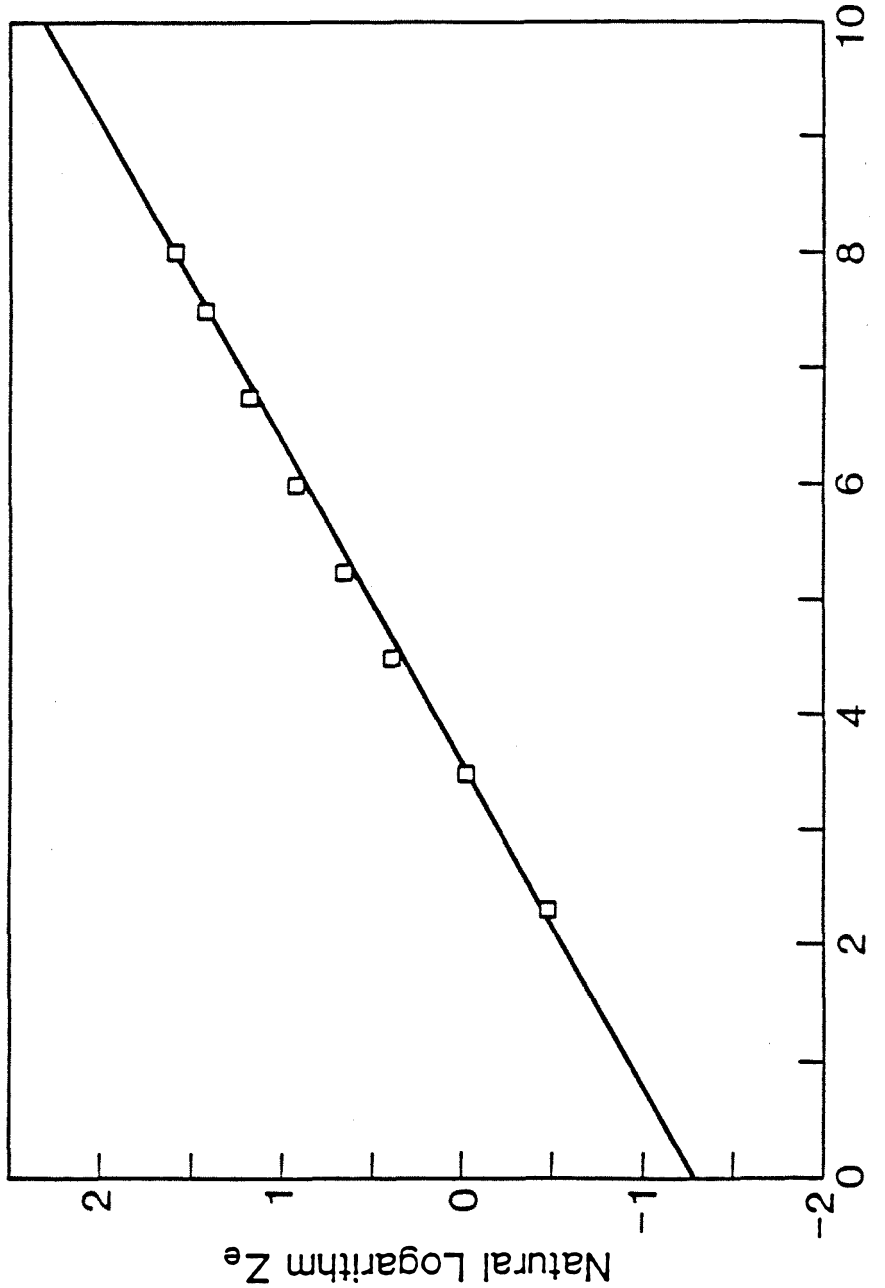

Figure 4.21 **Diffusion-Reaction Experiment for Ethanol Production and Growth with a bulk dissolved oxygen concentration of 200% air saturation and symmetric glucose concentrations. Run 9, chamber 1.**

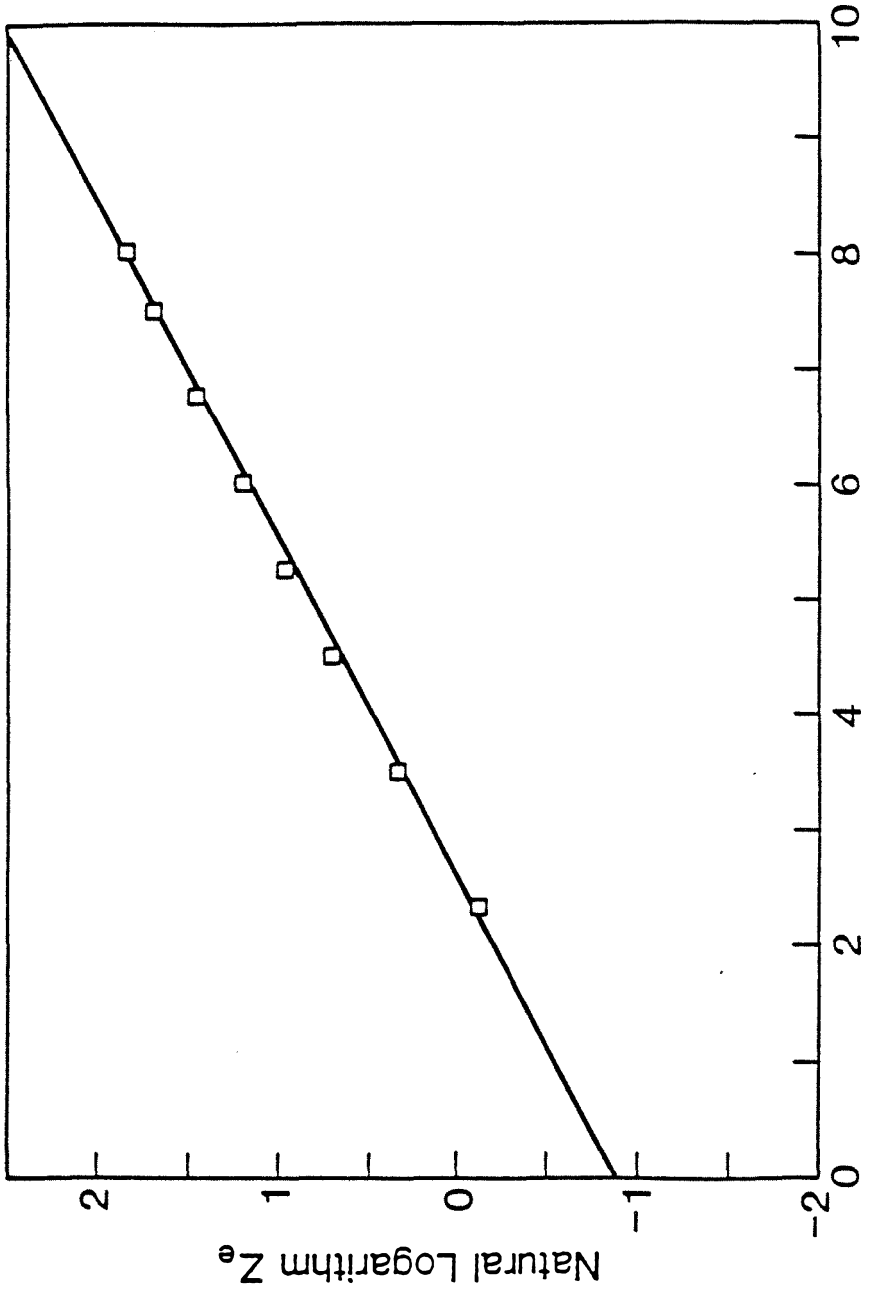

Figure 4.22 **Diffusion-Reaction Experiment for Ethanol Production and Growth with a bulk dissolved oxygen concentration of 200% air saturation and symmetric glucose concentrations. Run 9, chamber 2.**

diffusion-reaction method still produces a linear ln Z versus time plot. The ln Z_g and ln Z_e data remain linear with respect to time throughout the entire experiment for all the diffusion-reaction experiments. The procedure for analyzing the experimental glucose and ethanol flux versus time data requires iterating until the input values of μ_{DR}, α_{DR}, and ν_{DR} equal the output values, where the values are determined from a linear least-squares fit to the data. These criteria probably produce a line for nonconstant rates of growth, glucose uptake, and ethanol production. μ_{DR}, α_{DR}, and ν_{DR} were determined from the slopes and intercepts of Figures 4.6–4.22.

In practice, the end point of the experiments was determined by using α_{DR} and μ_{DR} to calculate the glucose concentration in the alginate membrane as a function of time. When the glucose concentration fell below 1.0 g/l somewhere in the membrane, the previous data point was considered the last data point. Then μ_{DR}, α_{DR}, and ν_{DR} were calculated again if necessary. Therefore, the glucose concentration in the alginate membrane was greater than or equal to 1 g/l for all times. Thus, the glucose concentration did not significantly affect the growth rate, glucose uptake rate, or ethanol production rate of the cells.

ν_{DR} as a function of dissolved oxygen concentration is more scattered than either μ_{DR} or α_{DR}. ν_{DR} was taken as the average of values measured in the two reactor chambers. There was no consistent difference in the value of ν_{DR} measured in the high glucose concentration chamber and in the low glucose concentration chamber. The values of ν_{DR} in the two chambers differ by as much as 25 % with an average standard deviation of 0.28 g/g-hr. μ_{DR} was taken as the average of the value determined from the glucose concentration measurement and the two values determined from the ethanol concentration

measurements. μ_{DR} varied by less than 5 % in any single experiment with an average standard deviation of 0.013 1/hr. α_{DR} was determined only from the glucose concentration measurements in the low glucose concentration chamber.

Table 4.1 summarizes the results of all the diffusion-reaction experiments including the experiments presented in Chapter 3 for anaerobic conditions. The effect of bulk dissolved oxygen concentration on μ_{DR}, α_{DR}, and ν_{DR} are shown in Figures 4.23, 4.24, and 4.25, respectively, along with the specific growth rates, specific glucose uptake rates, and specific ethanol production rates measured for suspended cells. The specific growth rate, glucose uptake rate, and ethanol production rate of immobillized cells appear to vary significantly with the dissolved oxygen concentration. Therefore, the values of μ_{DR}, α_{DR}, and ν_{DR} need to be checked for accuracy in representing the actual specific growth rate, glucose uptake rate, and ethanol production rate. As discussed in the previous section, oxygen gradients and their effects on growth and metabolism can cause the growth rate to be overestimated and the glucose uptake rate and ethanol production rate to be underestimated. In both cases the effect of dissolved oxygen on the growth rate and reaction rates will be exaggerated.

The average growth rate was determined during each diffusion-reaction experiment from the initial and final biomass concentration in the alginate membrane. The average growth rate represents the instantaneous growth rate averaged over space and time. These results are compared to the value of μ_{DR} calculated from the diffusion-reaction experiment in Table 4.2. The diffusion-reaction analysis leads to an overestimation of the intrinsic, specific growth rate when oxygen is supplied to the alginate membrane at high rates. As described previously, the overestimation of the growth rate is due to the sig-

Table 4.1

SUMMARY OF DIFFUSION-REACTION EXPERIMENTS

Run Number	DO Conc. (% air sat.)	μ (1/hr)	α (g/g-hr)	ν (g/g-hr)
1	0	0.26	5.6	2.2
2	0	0.22	—	2.7
3	50	0.29	4.7	2.2
4	50	0.28	—	2.6
5	100	0.34	4.3	1.3
6	100	0.31	—	1.8
7	200	0.35	3.6	1.3
8	200	0.34	—	1.9
9	200	0.36	—	1.7

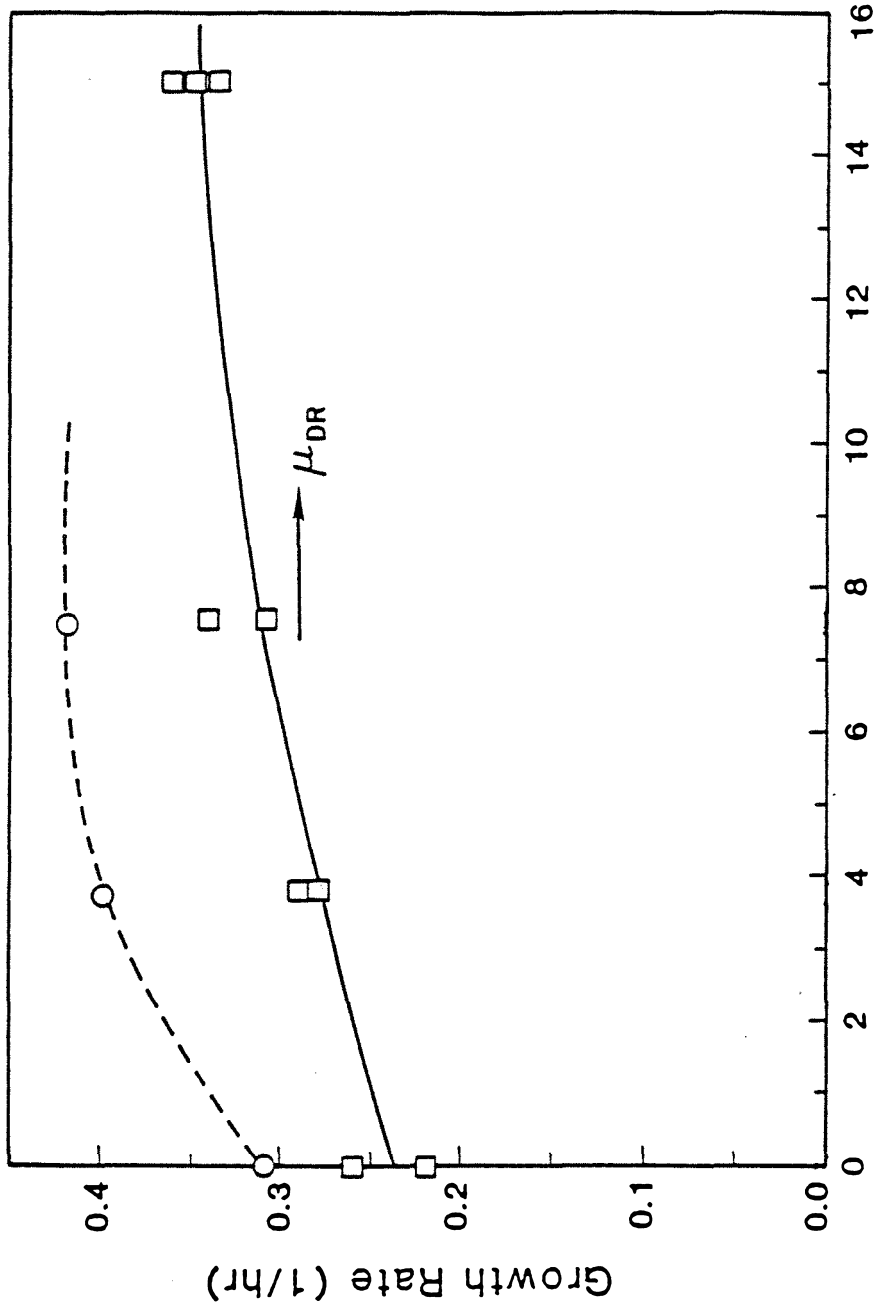

Figure 4.23 Effect of Dissolved Oxygen Concentration on Growth Rate of (O) suspended and (□) immobilized *S. cerevisiae*.

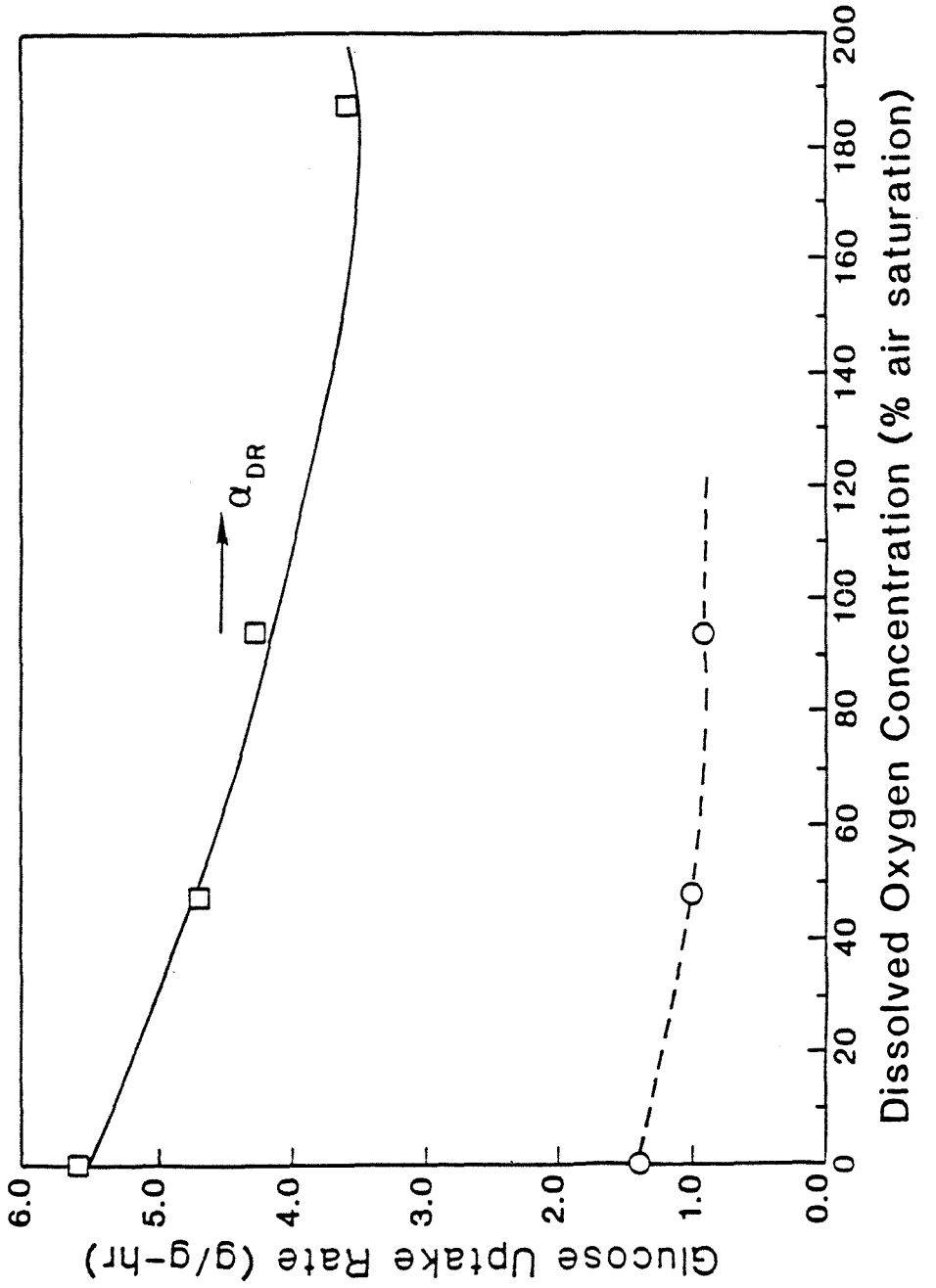

Figure 4.24 Effect of Dissolved Oxygen Concentration on Glucose Uptake Rate of (O) suspended and (□) immobilized *S. cerevisiae*.

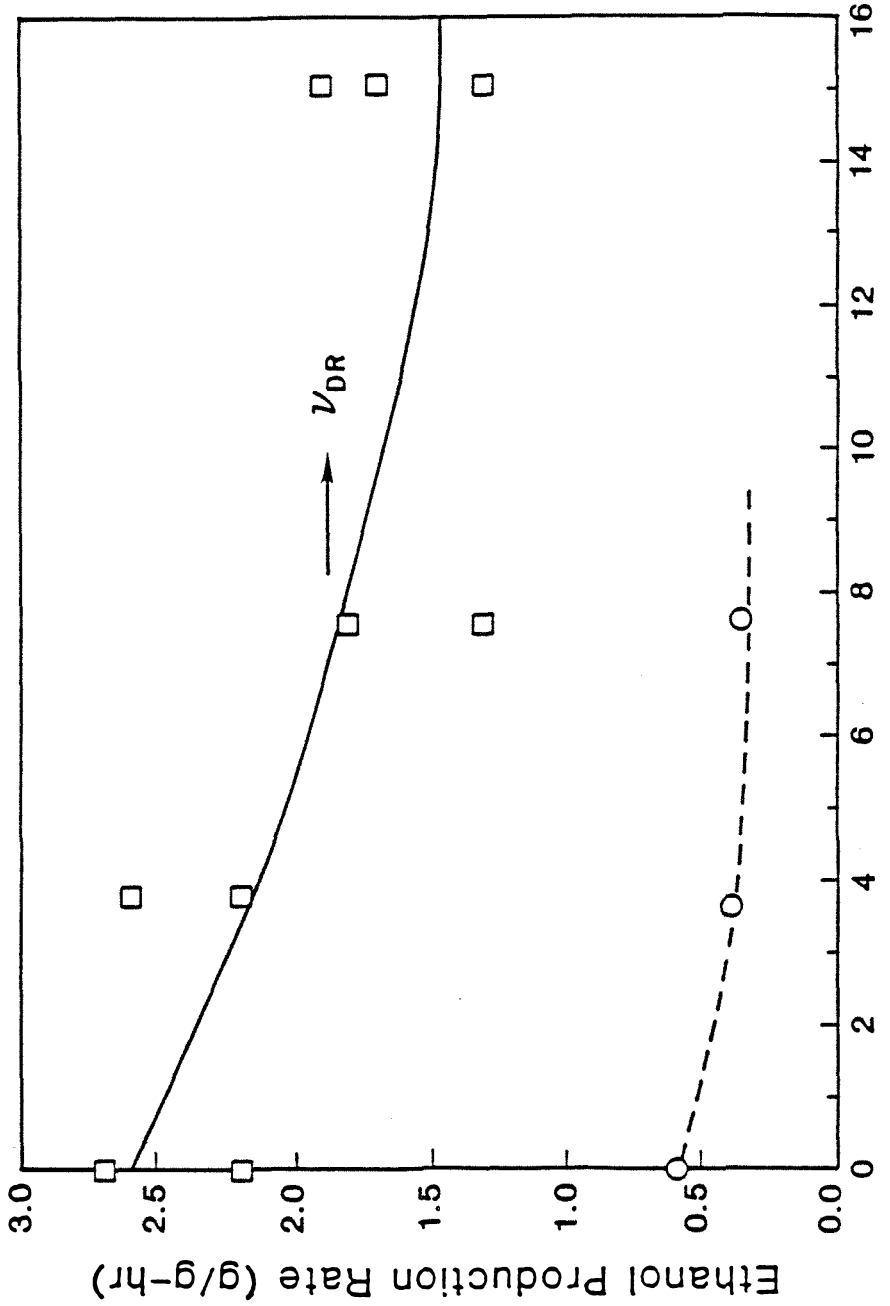

Figure 4.25 **Effect of Dissolved Oxygen Concentration on Ethanol Production Rate of (○) suspended and (□) immobilized *S. cerevisiae*.**

Table 4.2

AVERAGE GROWTH RATE AND μ_{DR} FROM DIFFUSION-REACTION EXPERIMENTS

Run Number	DO Conc. (% air sat.)	μ_{DR} (1/hr)	$\bar{\mu}$ (1/hr)
1	0	0.26	0.26
2	0	0.22	0.27
3	50	0.29	0.29
4	50	0.28	0.30
5	100	0.34	—
6	100	0.31	0.29
7	200	0.35	0.31
8	200	0.34	—
9	200	0.36	0.29

nificant effect of oxygen on the growth rate. Similarly, it is expected that α_{DR} and ν_{DR} underestimate the glucose uptake rate and ethanol production rate, respectively, when oxygen is supplied to the cells. At a dissolved oxygen concentration of 200 % air saturation, μ_{DR} is 17 % higher than the average growth rate determined from the biomass concentration. The trends in the growth rate, glucose uptake rate, and ethanol production rate as a function of dissolved oxygen are illustrated by the diffusion-reaction experiments even though the magnitudes of the numbers are not accurate at high aeration levels. In the following chapter an attempt will be made to further quantify the effects of dissolved oxygen concentration on the behavior of immobilized cells.

The growth rate of immobilized cells varies with dissolved oxygen concentration. As shown in Table 4.2, both methods of measuring the growth rate indicate that increasing the oxygen concentration increases the intrinsic, specific growth rate. Suspended cells of *S. cerevisiae* 18790 also show an increase in growth rate, from 0.32 1/hr to 0.42 1/hr, when the bulk dissolved oxygen concentration goes from 0 to 100 % air saturation.

The faster growth rate of aerobic cells may be due to partial activation of the respiratory pathway by oxygen. In this investigation, high glucose concentrations were employed, so catabolite repression is maximally operative. However, high glucose concentrations alone may not be able to fully suppress respiratory enzyme activity. Rsearchers have shown that oxygen partially alleviates glucose repression of respiratory enzymes and cytochromes (5,6). When oxygen is unavailable to the cells, energy is supplied via the glycolytic pathway and the growth rate is limited by the rate of energy production. As reviewed in Chapter 1, the glycolytic pathway leads mainly to ethanol and carbon diox-

ide production via substrate-level phosphorylation. The respiratory pathway utilizes oxygen as the terminal electron acceptor and breaks glucose down to carbon dioxide and water. Glycolysis produces a net of two ATP molecules per molecule of glucose, whereas respiration leads to a net of thirty-six ATP molecules per molecule of glucose. The growth yield of *S.cerevisiae* increases with the ATP content of the cells (7). Thus, in batch cultures a faster growth rate can occur for the same or a decreasing glucose uptake rate when oxygen is available. Similarly, immobilized cells exhibit a faster growth rate when more energy is available.

Oxygen may also have led to an increased growth rate through its effect on the plasma-membrane composition. In the presence of oxygen, *S. cerevisiae* synthesizes essential membrane lipids and fatty acids. Cells growing anaerobically become depleted in fatty acids and sterols unless medium supplements are provided (2). In this investigation, a defined medium without fatty acid and sterol supplements was used. Providing oxygen to the cells allowed synthesis of essential plasma-membrane components, which may have increased the growth rate of the organism.

The fact that the growth rate of immobilized *S. cerevisiae* increases with dissolved oxygen concentration indicates that growth is probably not limited by nitrogen or another essential nutrient. Various researchers have attributed the slower growth and reaction rates of immobilized cells to low concentrations of essential nutrients, since immobilization may inhibit the transport of nutrients to the cell surface. Under the conditions employed in this investigation, the growth rate is not limited by essential nutrient concentration, but by the cell's ability to synthesize ATP and/or membrane lipids.

For all dissolved oxygen concentrations, the growth rate of immobilized cells remains below the growth rate of suspended cells. The reduction in the growth rate is probably due to the physical restriction of the semisolid alginate matrix.

Figures 4.24 and 4.25 show that α_{DR} and ν_{DR} decrease with increasing dissolved oxygen concentration. Although the numbers probably underestimate the glucose uptake rate and ethanol production rate at higher bulk dissolved oxygen concentrations, the trend with respect to oxygen concentration is illustrated. Similarly, suspended cells of *S. cerevisiae* 18790 undergo a decrease in the glucose uptake rate and ethanol production rate when the oxygen concentration increases from 0 to 100 % air saturation.

The ethanol yields of immobilized and suspended cells appear to be independent of the dissolved oxygen concentration as shown in Figure 4.26. The ethanol yield is the ratio of the specific ethanol production rate to the specific glucose uptake rate. Since there is some experimental error in each of these measurements, the ethanol yield data are more scattered than either the glucose uptake rate data or the ethanol production rate data. As mentioned previously, both the glucose uptake rate and ethanol production rate are probably underestimated at high dissolved oxygen concentrations. If the degree of error is the same for both the glucose uptake rate and ethanol production rate, there will be no effect on the ethanol yield.

According to Figure 4.27, the biomass yield of immobilized cells increases slightly with dissolved oxygen concentration. However, this may not actually be the case because the diffusion-reaction method leads to an overestimation of the growth rate and an underestimation of the glucose uptake rate. The

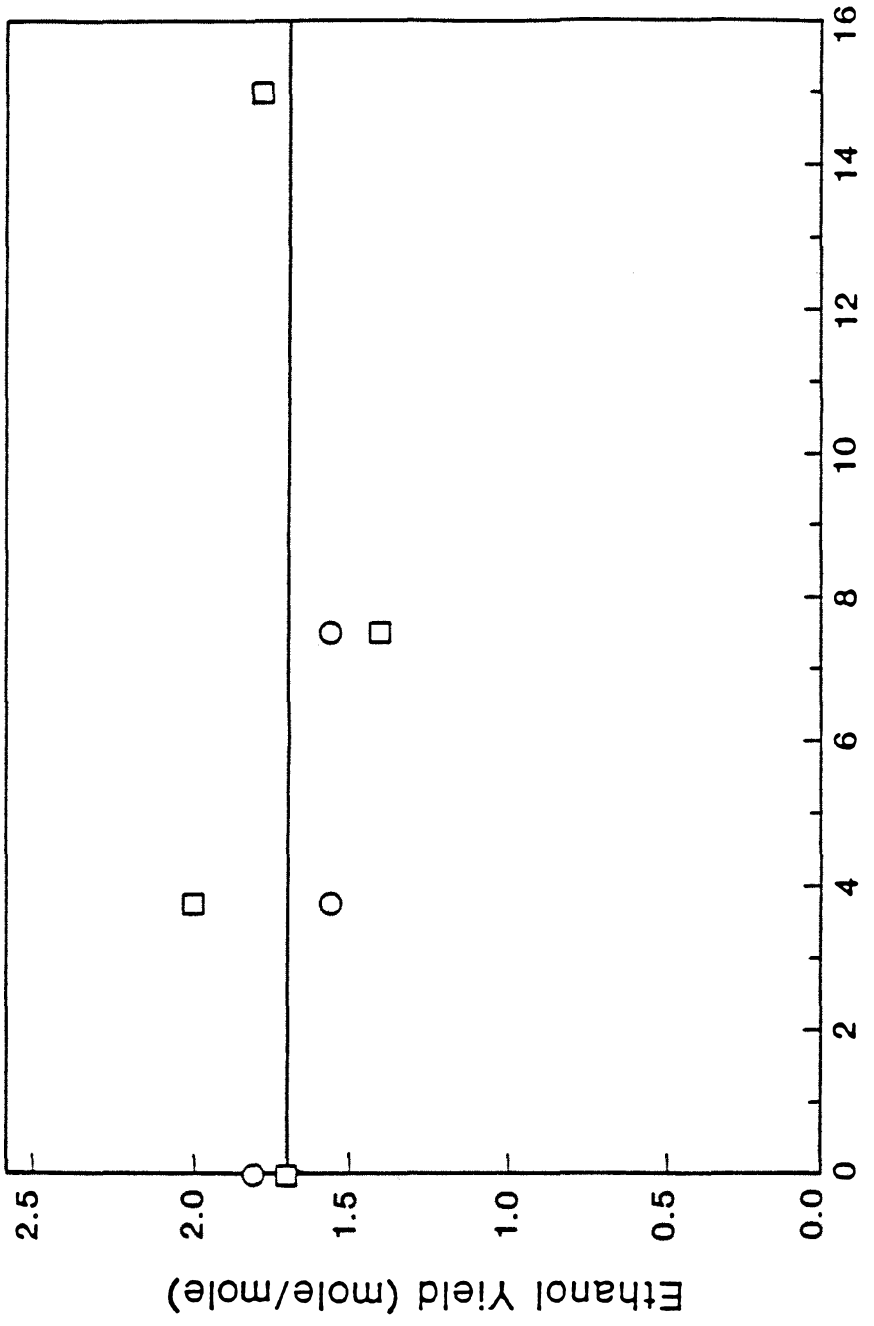

Figure 4.26 **Effect of Dissolved Oxygen Concentration on Ethanol Yield of (○) suspended and (□) immobilized *S. cerevisiae*.**

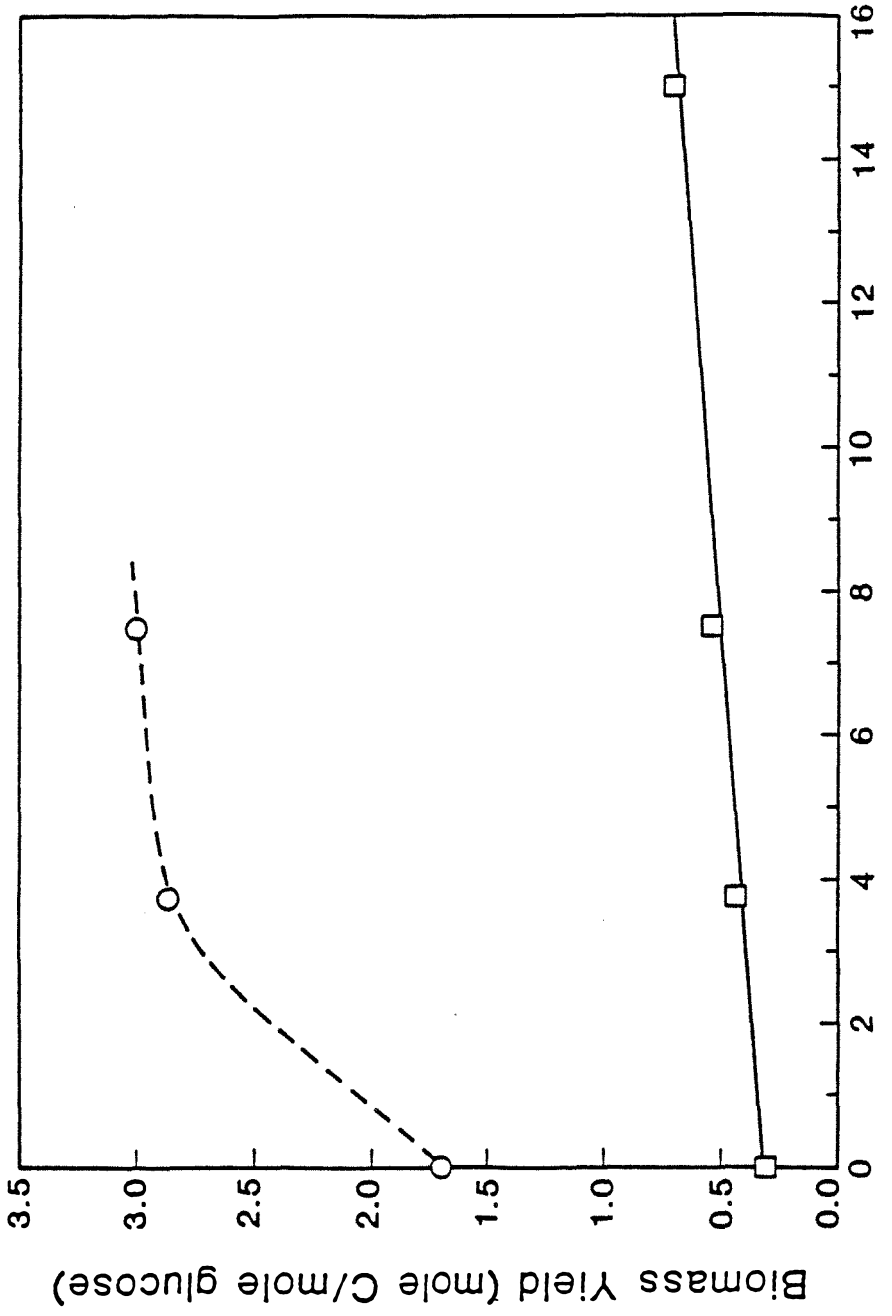

Figure 4.27 **Effect of Dissolved Oxygen Concentration on Biomass Yield of (○) suspended and (□) immobilized *S. cerevisiae*.**

biomass yield is the ratio of growth rate to glucose uptake rate. Therefore, the biomass yield may either increase slightly, decrease, or remain constant with dissolved oxygen concentration. In any case, the biomass yield of immobilized cells does not increase as rapidly with dissolved oxygen concentration as the biomass yield of suspended cells.

The suppression of glucose uptake by oxygen is known as the Pasteur effect. Oxygen activates the enzymes of the tricarboxylic acid (TCA) cycle and the respiratory pathway. The extra energy supplied by respiration leads to an increase in the ATP concentration in the cell. ATP is known to inhibit the allosterically regulated enzyme, phosphofructokinase, which converts fructose-6-phosphate to fructose diphosphate in the early stages of the glycolytic pathway. Furthermore, ADP decreases in concentration when the energy level increases and ADP is an activator of phosphofructokinase(8). Therefore, ATP and ADP combine to reduce the rate of glycolysis at phosphofructokinase. Furthermore, glucose-6-phosphate, which accumulates when phosphofructokinase is inhibited, has been shown to inhibit glucose transport into the cell (9). Therefore, the energy produced by respiration inhibits glycolysis, which then slows the rate of glucose uptake.

High glucose concentrations, such as are employed in this investigation, mitigate the Pasteur effect. Glucose represses the activity of tricarboxylic acid cycle enzymes as well as respiratory enzymes; however, as mentioned previously, glucose repression of the enzymes may not be complete when oxygen is present. The ethanol yield is constant for immobilized cells at all dissolved oxygen concentrations as shown in Figure 4.25. The high ethanol yield indicates that metabolism is primarily fermentative in the presence of oxygen.

Since the ATP yield from respiration is 18 times higher than the ATP yield from glycolysis, a small amount of respiration may cause an increase in the ATP concentration of immobilized cells and a decrease in the glucose uptake rate at high dissolved oxygen concentrations. However, the level of respiration may be too low to noticeably affect the ethanol yield at high oxygen concentrations. For example, if only 3 % of the glucose is metabolized by oxidative phosphorylation at high oxygen concentrations, 51 % more ATP will be produced by the cell than if glucose metabolism was by glycolysis alone. A low level of activation of the respiratory pathway may cause the decrease in the glucose uptake rate and ethanol production rate with increasing dissolved oxygen concentration.

Immobilized cells at all dissolved oxygen concentrations metabolize glucose and produce ethanol significantly faster than anaerobic suspended cells. Although the ATP concentration of immobilized cells increases when more oxygen is available, the ATP concentration must still be lower in immobilized cells growing aerobically than in suspended cells growing anaerobically. It thus appears that the limited respiratory activity of immobilized, glucose-repressed cultures cannot provide immobilized cells with all the energy they require for maintainance and growth.

4.5 CONCLUSION

Increasing the dissolved oxygen concentration of immobilized cells leads to an increase in the growth rate and a decrease in the glucose uptake rate and ethanol production rate. Suspended cells undergo similar metabolic changes in the presence of oxygen. By partially activating oxidative-phosphorylation,

oxygen causes an increase in the rate of ATP production. The higher ATP production rate is evidenced by a faster growth rate and a lower glucose uptake rate at higher dissolved oxygen concentrations. Plasma-membrane fatty acids and sterols, which are synthesized in the presence of oxygen, may also contribute to the faster growth rate at high dissolved oxygen concentrations.

REFERENCES

(1) Grosz, R., *Biochemical and Mathematical Modeling of Microaerobic Continuous Ethanol Production by S. cerevisiae*, Ph. D. Thesis, California Institute of Technology, 1987.

(2) Rogers, P. J., and P. R. Stewart, "Mitochondrial and Peroxisomal Contributions to the Energy Metabolism of *Saccharomyces cerevisiae* in Continuous Culture," *J. Gen. Microbiol.*, *79*, 205–217 (1973).

(3) Thomas, D. S., J. A. Hossack, and A. H. Rose, "Plasma-membrane Lipid Composition and Ethanol Tolerance," *Arch. Microbiol.*, *117*, 239–245 (1978).

(4) Peringer,P., H. Blachere, G. Corrieu, and A. G. Lane, "Mathematical Model of the Kinetics of *Saccharomyces cerevisiae*," *Biotechnol. Bioeng. Symp.*, *4*, 27–42 (1973).

(5) Chapman, C., and W. Bartley, "The Kinetics of Enzyme Changes in Yeast under Conditions that Cause Loss of Mitochondria," *Biochem. J.*, *107*, 455 (1968).

(6) Suomalainen, H., T. Nurminen, and E. Oura, "Aspects of Cytology in Metabolism of Yeast," *Prog. Indus. Microbiol.*, *12*, 109 (1973).

(7) Stouthammer, A. H., and C. Bettenhaussen, "Utilization of Energy for Growth and Maintenance in Continuous and Batch Cultures of Microorganisms," *Biochim. Biophys. Acta*, *301*, 53–70 (1973).

(8) Krebs, H. A., "Pasteur Effect and Relation Between Respiration and Fermentation in Living Systems," in *Essays in Biochemistry*, eds. Campbell, P. N., and F. Dickens, *8*, Academic Press, New York, 1972, p. 34.

(9) Sols, A., "Regulation of Carbohydrate Transport and Metabolism in

Yeast," in *Aspects of Yeast Metabolism*, A. K. Mills and H. Krebs (eds.), Blackwell, Oxford, 1967, p. 47.

CHAPTER 5

MATHEMATICAL MODEL FOR IMMOBILIZED *S. cerevisiae*

5.1 INTRODUCTION

The growth and metabolism of cells entrapped in a polymeric matrix are governed by the environmental conditions at the immediate cell surroundings rather than by the conditions farther away in the bulk fluid. The space surrounding the entrapped cells is referred to as the microenvironment of the cell, whereas the fluid phase is called the macroenvironment of the cell. Often the microenvironment of a cell is drastically different from the macroenvironment. Characterizing the microenvironment of immobilized cells is important in explaining the cells' metabolic activities under immobilization conditions, as well as in guiding equipment scale-up and operation.

One approach to characterizing the behavior of immobilized cells is to minimize the differences between the microenvironment and the macroenvironment of immobilized cells. Then the substrate and product concentrations measured in the bulk fluid are fairly accurate representations of the intramatrix concentrations. In some cases it may not be feasible to eliminate diffusion effects. The rapid utilization rate of oxygen by *S. cerevisiae* causes the oxygen concentration to decrease steeply within the immobized cell matrix for even a low biomass concentration. A second approach is to measure microenvironmental conditions *in situ*. In order to obtain the necessary spatial resolution without disrupting the immobilized cell preparation, chemical sensors with a tip size of only a few microns are required. Such probes must be small to minimize disruption of the cells' microenvironment, yet large enough to in-

sure a signal representative of a statistically large number of cells. Although improvements are being made in the field of microprobes, few sensors are available commercially and "in house" development and production can be quite costly.

A third approach to characterizing the microenvironment of entrapped cells is to employ mathematical models to describe diffusion and reaction in the polymeric matrix. This is the approach taken in the present investigation. Models are solved to predict substrate and product concentrations in the matrix as a function of time and space. The metabolic rates of the immobilized cells are then related to microenvironmental conditions.

A mathematical model for the growth and metabolism of *S. cerevisiae* immobilized in calcium alginate has been discussed in Chapters 3 and 4. In this chapter the growth rate and reaction rate terms in the model are expanded to include the effects of microenvironmental glucose, ethanol, and oxygen concentrations. The model parameters in the growth and reaction terms are then adjusted so that the mathematical model predicts the experimental results of the diffusion-reaction analysis. Next, the mathematical diffusion-reaction model is applied to the growth and metabolism of *S. cerevisiae* immobilized in calcium alginate spheres with a higher biomass loading than was used in the diffusion-reaction experiments. The ability of the mathematical model to describe the growth and metabolism of *S. cerevisiae* immobilized in calcium alginate spheres is finally investigated experimentally.

5.2 MATHEMATICAL DIFFUSION-REACTION MODEL

A mathematical model was developed to characterize the behavior of

immobilized cells with respect to glucose, ethanol, and oxygen concentrations in the microenvironment of the cells. Transients are included in the model because immobilized cells do not neccesarily reach a steady state because of cell growth. The equations for growth and reaction of *S. cerevisiae* immobilized in a calcium alginate membrane are:

$$\frac{\partial b}{\partial t} = \mu b \tag{5.1}$$

$$\frac{\partial s}{\partial t} = D_g \frac{\partial^2 s}{\partial x^2} - \alpha b \tag{5.2}$$

$$\frac{\partial e}{\partial t} = D_e \frac{\partial^2 e}{\partial x^2} + \nu b \tag{5.3}$$

$$\frac{\partial O_2}{\partial t} = D_O \frac{\partial^2 O_2}{\partial x^2} - \theta b, \tag{5.4}$$

where s is the glucose concentration (g/l), e is the ethanol concentration (g/l), O_2 is the dissolved oxygen concentration (% air saturation), b is the biomass concentration (g/l), μ is the specific growth rate (g/g-hr), α is the specific glucose uptake rate (g/g-hr), ν is the ethanol production rate (g/g-hr), θ is the specific oxygen utilization rate (% saturation-l/g-hr), D_g is the diffusion coefficient of glucose (0.028 cm^2/hr), D_e is the diffusion coefficient of ethanol (0.043 cm^2/hr), D_O is the diffusion coefficient of oxygen (0.088 cm^2/hr), x is position (cm), and t is time (hr). The diffusion coefficients of glucose and ethanol in calcium alginate were measured experimentally by the lag time method. The results of those measurements are discussed in Chapters 2 and 3. The diffusion coefficient of oxygen in calcium alginate was estimated from the diffusion coefficient of oxygen in water. It was assumed that alginate decreases the diffusion coefficient of oxygen in water by the same percentage as it decreases the diffusion coefficients of glucose and ethanol in water. The boundary conditions

are given by:

$$s = s_1 \quad \text{at} \quad x = o \quad \text{and} \quad s = s_2 \quad \text{at} \quad x = L \tag{5.5}$$

$$e = 0 \quad \text{at} \quad x = 0 \quad \text{and} \quad x = L \tag{5.6}$$

$$O_2 = O_{2,b} \quad \text{at} \quad x = 0 \quad \text{and} \quad x = L, \tag{5.7}$$

and the initial conditions are:

$$b = b_0 \quad \text{at} \quad t = 0 \tag{5.8}$$

$$s = s_1 \quad \text{at} \quad t = 0 \tag{5.9}$$

$$e = 0 \quad \text{at} \quad t = 0 \tag{5.10}$$

$$O_2 = 100 \quad \text{at} \quad t = 0, \tag{5.11}$$

where s_1 is the glucose concentration in chamber 1, s_2 is the glucose concentration in chamber 2, and $O_{2,b}$ is the bulk dissolved oxygen concentration in both of the reactor chambers. The specific growth rate, specific glucose uptake rate, specific ethanol production rate, and specific oxygen utilization rate can all be functions of the glucose, ethanol, and oxygen concentrations.

Equations (5.1)–(5.4) with boundary conditions (5.5)–(5.7) and initial conditions (5.8)–(5.11) can be solved analytically only when μ, α, ν, and θ are constants. For nonconstant growth and reaction rates, a numerical solution is required. The Crank-Nicholson method of finite differences was used to solve Equations (5.1)–(5.4) simultaneously for nonconstant growth and reaction rates with boundary conditions (5.5)–(5.7) and initial conditions (5.8)–(5.11). A time step of 0.001 hr and a distance step of 0.008 cm were used. The

numerical solution was verified by comparing analytical and numerical solutions for constant reaction rates as discussed in Chapter 4. The reaction rate terms in equations (5.1)-(5.4) were evaluated using the solute concentrations at the previous time step in order to decrease the computation time. Several calculations were carried out where the reaction terms were determined iteratively using current solute concentrations; however, there was no difference in the numerical results. The computer program used to solve the partial differential equations is included in the Appendix.

There are few models in the literature for the growth and metabolism of *S. cerevisiae* in suspension as a function of dissolved oxygen concentration. Most of the models that do include oxygen effects apply only to a limited range of dissolved oxygen concentration. Peringer, et al. developed a model for the specific growth rate, glucose uptake rate, and oxygen utilization rate of *S. cerevisiae* as a function of glucose and dissolved oxygen concentrations. The model applies to glucose-repressed cultures at any dissolved oxygen concentration (1). Furthermore, the model is relatively simple and thus can be easily incorporated into the equations that describe the the behavior of immobilized cells.

Peringer's model for the growth and metabolism of suspended *S. cerevisiae* is based on balancing the ATP requirements of the cell with the ATP production rate. ATP wasting reactions are not accounted for in the model. The total rate of ATP production is taken as the sum of the ATP production rate via the glycolytic pathway and oxidative-phosphorylation. Since the amount of glucose metabolized by oxidative-phosphorylation is small relative to the amount metabolized by the glycolytic pathway, the glucose uptake rate expression is

modeled by the glycolytic pathway reactions. Because of the observed linear relationship between the inverse of the respiration rate and the inverse of the dissolved oxygen tension, the rate of oxidative-phosphorylation is modeled as a Michaelis-Menten reaction with oxygen as the substrate. The growth rate of *S. cerevisiae* is taken to be proportional to the ATP utilization rate, which equals the ATP production rate via glycolysis and oxidative-phosphorylation. Although the model developed by Peringer, et al. has some biochemical justification, it is a phenomenological model.

The model of Peringer, et al. consists of the following equations:

$$\mu = \left[\frac{\mu_G}{1 + pO_2} + \frac{\mu_R}{K_L + O_2}\right]\left(\frac{s}{K_s + s}\right) \tag{5.12}$$

$$\alpha = \left[\frac{\alpha_m}{1 + pO_2}\right]\left(\frac{s}{K_s + s}\right) \tag{5.13}$$

$$\theta = \left[\frac{\theta_m O_2}{K_L + O_2}\right]\left(\frac{s}{K_s + s}\right), \tag{5.14}$$

where s is the glucose concentration (g/l) and O_2 is the dissolved oxygen concentration (% air saturation). Peringer et al. conducted batch and continuous suspended cell experiments with high glucose concentrations to measure the model parameters. They reported the following parameter values, which de-

pend on the physiological conditions of the culture:

$$\mu_G = 0.208 \quad 1/\text{hr}$$

$$\mu_R = 0.103 \quad 1/\text{hr}$$

$$p = 4.93x10^{-4} \quad 1/\% \text{ air saturation}$$

$$K_s = 0.1g/l$$

$$\alpha_m = 2.08 \quad \text{g/g-hr}$$

$$\theta_m = 8.19x10^3 \quad (\%\text{-l/g-hr})$$

$$K_L = 1.36\%,$$

where p is a measure of the Pasteur effect, K_s is the Michaelis constant for the substrate, K_L is the Michaelis constant for oxygen,μ_G represents the maximum growth rate from glycolysis, μ_R represents the maximum growth rate from oxidative-phosphorylation, α_m is the maximum glucose uptake rate, and θ_m is the maximum oxygen utilization rate (1).

The model developed by Peringer, et al. for the metabolism of *S. cerevisiae* at high glucose concentrations was modified as follows to fit the observed behavior of immobilized cells. The diffusion-reaction model consisting of Equations (5.1)–(5.4) with boundary conditions (5.5)–(5.7) and initial conditions (5.8)–(5.11) was numerically integrated with growth and reaction rate expressions given by Equations (5.12)–(5.14). The ethanol production rate was taken to be 0.43 times the glucose uptake rate as measured experimentally under anaerobic conditions. The simulated flux versus time data from the numerical solution were analyzed according to the iterative diffusion-reaction analysis presented in Chapter 3. From these simulations, values for μ_{DR}, α_{DR}, and ν_{DR} were determined for various bulk dissolved oxygen concentrations and com-

pared with the corresponding experimental values reported in Chapters 3 and 4. The parameter values and the growth and reaction rate expressions in Equations (5.12)–(5.14) were subsequently adjusted until the simulated specific rate values agreed satisfactorily with the experimental values of μ_{DR}, α_{DR}, and ν_{DR}. The final form of the model for immobilized cells is by no means a unique representation of the metabolic rates of immobilized cells but accurately predicts the results of the diffusion-reaction experiments at all bulk dissolved oxygen concentrations. As was discussed in Chapter 4, μ_{DR}, α_{DR}, and ν_{DR} do not necessarily represent the average specific growth rate, glucose uptake rate, and ethanol production rate, respectively. The model was also used to calculate the average specific growth rate, glucose uptake rate, and ethanol production rate, and these values were compared to μ_{DR}, α_{DR}, and ν_{DR}.

The first step in fitting Peringer's model to the immobilized cell experiments was to add a term to each rate expression for ethanol inhibition. Since ethanol must diffuse away from the surface of entrapped cells rather than be carried off by convection as in suspension cultures, the ethanol concentration in the alginate matrix may be significantly higher than in the bulk fluid. Therefore, it is necessary to determine the ethanol concentration as a function of time and position in the membrane and account for the effect of ethanol on the specific growth rate, glucose uptake rate, ethanol production rate, and oxygen utilization rate. Researchers agree that the growth and reaction rates of *S. cerevisiae* decrease monotonically with increasing ethanol concentration and that ethanol inhibition is noncompetitve (2–8). The quantitative effect of ethanol on the growth and fermentation rates of *S. cerevisiae* is somewhat more controversial.

A linear relationship between the ethanol concentration and the growth and reaction rates has been proposed by various researchers (2–4). The growth and reaction rates have also been modeled as exponential (5,6) and hyperbolic (7,8) functions of the ethanol concentration. Furthermore, ethanol appears to inhibit the growth rate of *S. cerevisiae* more than the fermentation rate (3,5). A linear relationship was used in the present investigation to model ethanol inhibition of the growth rate, glucose uptake rate, and ethanol production rate. The ethanol concentration at which growth and fermentation cease was measured experimentally by Bazua and Wilke to be 93 g/l (9). The value which they reported is close to the average of the values several other researchers have reported for the ethanol concentration that prevents cell activity (2-8). Therefore, 93 g/l ethanol concentration was used in the mathematical model as the ethanol concentration at which growth, glucose uptake, ethanol production, and oxygen utilization stop. Immobilization has not been shown to alter the ethanol tolerance of *S. cerevisiae* significantly. Low oxygen concentrations can affect the plasma membrane composition of a culture growing anaerobically without sterol and unsaturated fatty acid supplements since oxygen is required for the cell to synthesize these compounds (10). Thomas, et al. demonstrated that unsaturated fatty acids improve the ethanol tolerance of *S. cerevisiae* and that linoleyl (2 double bond) residues are more effective than oleyl (1 double bond) residues. They also showed that sterols enhance the cell viability in the presence of ethanol with ergosterol and stigmasterol being more effective than cholesterol and camposterol (11). The direct effect of oxygen concentration on ethanol inhibition expression has not been quantified experimentally. Therefore, the ethanol inhibition expression was considered independent of oxygen.

In modeling the behavior of *S. cerevisiae* immobilized in calcium alginate, the ethanol production rate was taken to be proportional to the glucose uptake rate. The proportionality constant was determined from the ethanol yield under anaerobic conditions. The experimental results presented in Chapter 4 indicate that the ethanol yield remains constant for all bulk oxygen concentrations. This is due to the high glucose concentration, which limits the rate of oxidative-phosphorylation. The amount of glucose completely oxidized to carbon dioxide and water is small compared to the amount of glucose metabolized to ethanol and carbon dioxide through the glycolytic pathway.

The oxygen utilization rate of immobilized cells was taken to be identical to the expression given in Equation (5.14) for suspended cells. Marcipar, et al. measured approximately a sevenfold increase in the oxygen utilization rate of yeast adsorbed onto ceramic (12). Entrapped cells may behave quite differently than adsorbed cells, so it is impossible to extrapolate the rate increase to calcium alginate immobilized cells. At the glucose concentrations employed in this investigation, the respiration rate of *S. cerevisiae* remains low for all dissolved oxygen concentrations. Oxygen is utilized for biosynthetic reactions, such as sterol and fatty acid synthesis, and for residual respiration. Since immobilized cells take up glucose faster than suspended cells, there may be a concomitant increase in the oxygen uptake rate of immobilized cells if some of the excess glucose is oxidized to carbon dioxide and water. However, the high ethanol yield of immobilized cells at all dissolved oxygen concentrations indicates that the respiration rate of immobilized cells compared to free cells probably does not increase more than the glucose uptake rate increases. Therefore, in assuming an immobilized cell oxygen uptake rate expression identical

to the suspended cell rate expression, there is limited potential for error. The sensitivity of the immobilized cell model to the oxygen uptake rate expression will be discussed further later.

The effect of the glucose concentration on the rate expressions was also assumed to be the same as in Peringer's model. According to Peringer's model for glucose concentrations in the range used in this investigation, there is only a small variation in the reaction rates, which is due to glucose concentration. The experimental results of Chapter 4 indicate that the growth rate and ethanol production rate of immobilized cells are not affected by the presence of a glucose gradient from 50 g/l to 1 g/l or a symmetric glucose concentration of 25 g/l.

The specific growth rate and specific glucose uptake rate of immobilized cells under anaerobic conditions were used to determine μ_G and α_m, respectively, in Peringer's model. The intrinsic specific growth rate and intrinsic specific glucose uptake rate were measured experimentally as reported in Chapter 3 for immobilized *S. cerevisiae*. Since the dissolved oxygen concentration was zero (anaerobic conditions) during the experiments, the growth rate and glucose uptake rate were constant throughout the experiment. If O_2 is set equal to zero in Peringer's model, the anaerobic, intrinsic specific growth rate of immobilized *S. cerevisiae* equals μ_G and the anaerobic, intrinsic specific glucose uptake rate equals α_m at high glucose concentrations and low ethanol concentrations. Thus, μ_G and α_M were initially estimated to be 0.24 1/hr and 5.6 g/g-hr, respectively.

For high dissolved oxygen concentrations the growth rate expression in equation (5.12) approaches an upper limit because of saturation kinetics. The

maximum specific growth rate is approximately μ_G plus μ_R for small values of K_s, p, and K_L. From the plot of growth rate versus bulk dissolved oxygen concentration in Chapter 4, the maximum specific growth rate was estimated to be about 0.38 1/hr. Therefore, μ_G plus μ_R is approximately equal to 0.38 1/hr. Since μ_G was determined to be 0.24 1/hr from the anaerobic growth rate, μ_R equals 0.14 1/hr.

The form of the glucose uptake rate expression developed by Peringer, et al. cannot describe the effect of oxygen observed experimentally for immobilized cells. From the plot of glucose uptake rate versus bulk dissolved oxygen concentration in Figure 4.4, it appears that the glucose uptake rate decreases with dissolved oxygen concentration and approaches a saturation rate at high dissolved oxygen concentrations. Therefore, the following expression was substituted for glucose uptake rate in Peringer's model:

$$\alpha = [\alpha_m - \frac{O_2}{K_L + O_2}] \left(\frac{s}{K_s + s} \right). \tag{5.15}$$

The maximum specific glucose uptake rate is still equal to 5.6 g/g-hr from the experiment conducted under anaerobic conditions.

The modified model for the growth and reaction rates of immobilized *S. cerevisiae* as a function of microenvironmental substrate and product concentrations was used to predict μ_{DR}, α_{DR}, and ν_{DR} at several bulk dissolved oxygen concentrations. Then μ_{DR}, α_{DR}, and ν_{DR} were plotted as a function of bulk dissolved oxygen concentration, and the results were compared to the experimental results of Chapters 3 and 4. Initially, there was a significant discrepancy between the experimental and simulated values of μ_{DR}, α_{DR}, and ν_{DR}. The model parameters were adjusted until a reasonable fit was obtained

between the experimental and simulated results. The Michaelis constant for oxygen, K_L, was varied independently in different reaction expressions. The final form of the model is given by the following equations:

$$\mu = \frac{s}{K_s + s}\left[\frac{\mu_G}{1 + pO_2} + \frac{\mu_R O_2}{K_{L,\mu} + O_2}\right] \tag{5.16}$$

$$\alpha = \frac{s}{K_s + s}\left[\alpha_m - \frac{1}{K_{L,\alpha} + O_2}\right] \tag{5.17}$$

$$\nu = 0.43\alpha \tag{5.18}$$

$$\theta = \frac{s}{K_s + s}\left[\frac{\theta_m O_2}{K_{L,O_2} + O_2}\right], \tag{5.19}$$

with the following parameter values:

$$\mu_G = 0.24 \quad 1/\text{hr}$$

$$\mu_R = 0.12 \quad 1/\text{hr}$$

$$p = 5.0x10^{-4} \quad 1/\% \text{ air saturation}$$

$$K_{L,\mu} = 14.0\%$$

$$K_s = 0.1l/g$$

$$\alpha_m = 5.8 \quad \text{g/g-hr}$$

$$K_{L,\alpha} = 14.0\%$$

$$\theta_m = 8.19x10^3 \quad (\%\text{-l/g-hr})$$

$$K_{L,O_2} = 1.36\%,$$

Figures 5.1–5.3 show the agreement between the experimental results of Chapters 3 and 4 and the model predictions for growth rate, glucose uptake rate, and ethanol production rate, respectively. The fitted model predicts μ_{DR}, α_{DR}, and ν_{DR} extremely well.

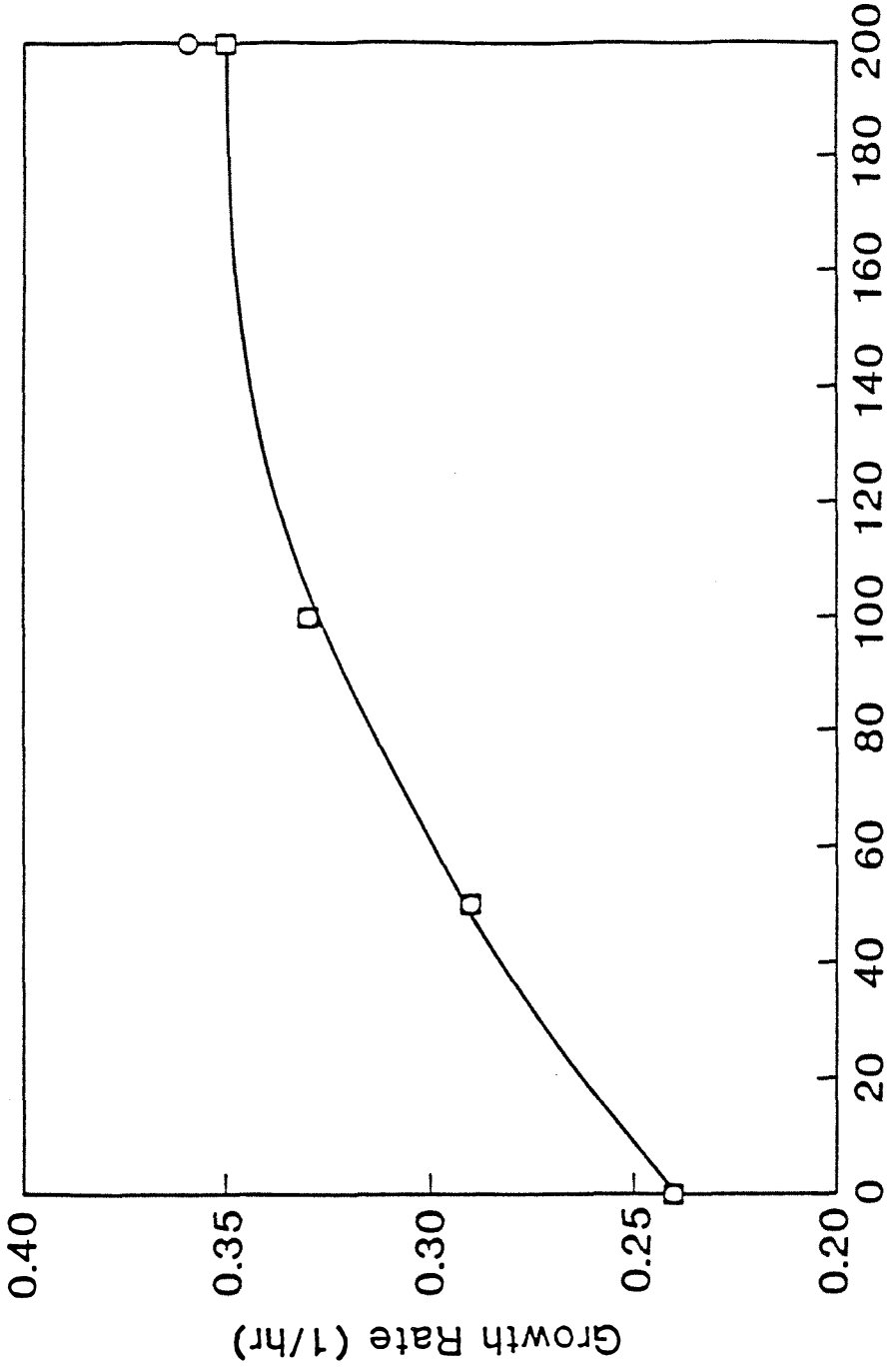

Figure 5.1 **Effect of Bulk Dissolved Oxygen Concentration on Growth Rate of immobilized *S. cerevisiae* according to (□) experiments and (○) mathematical model.**

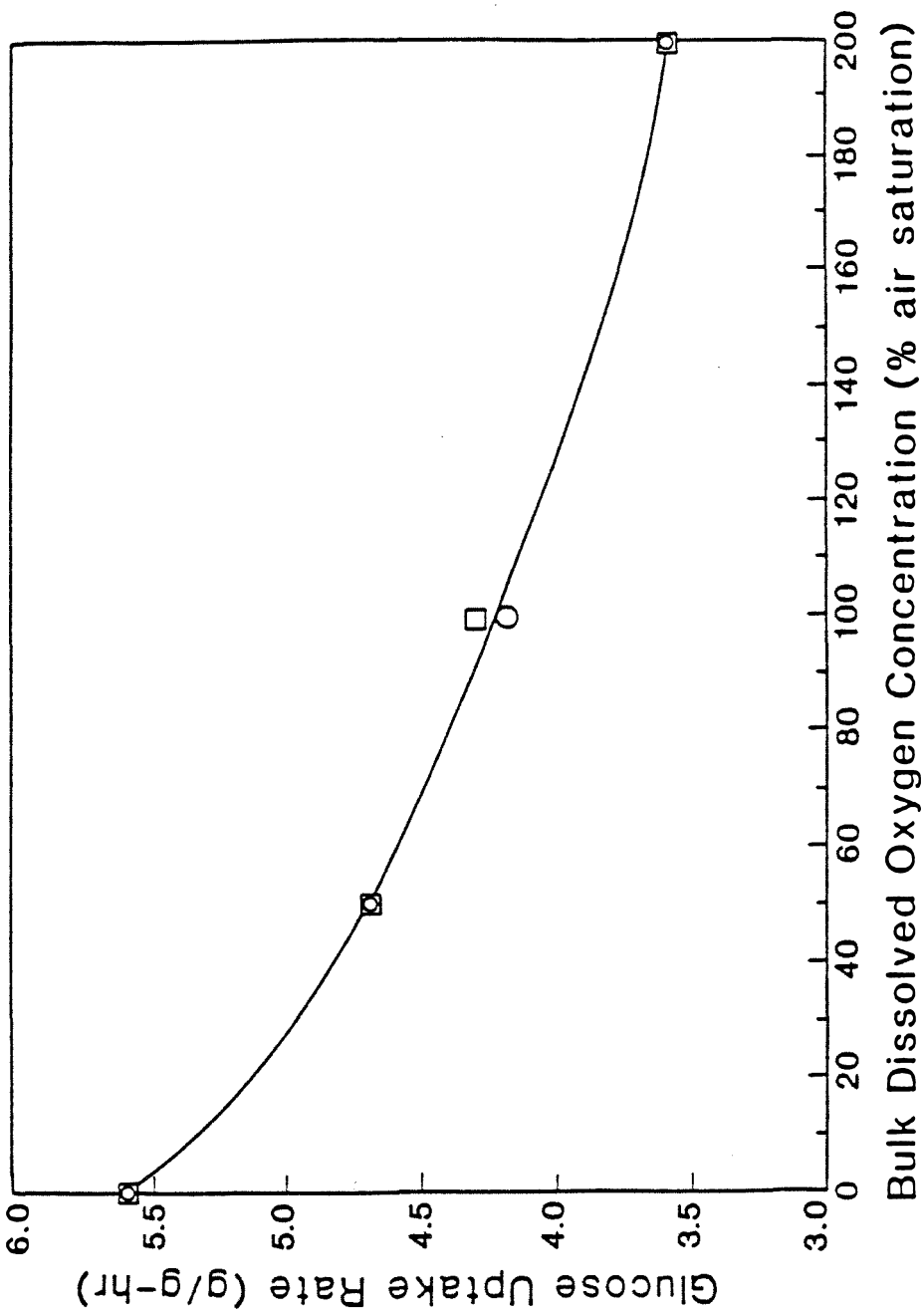

Figure 5.2 **Effect of Bulk Dissolved Oxygen Concentration on Glucose Uptake Rate of immobilized *S. cerevisiae* according to (□) experiments and (○) mathematical model.**

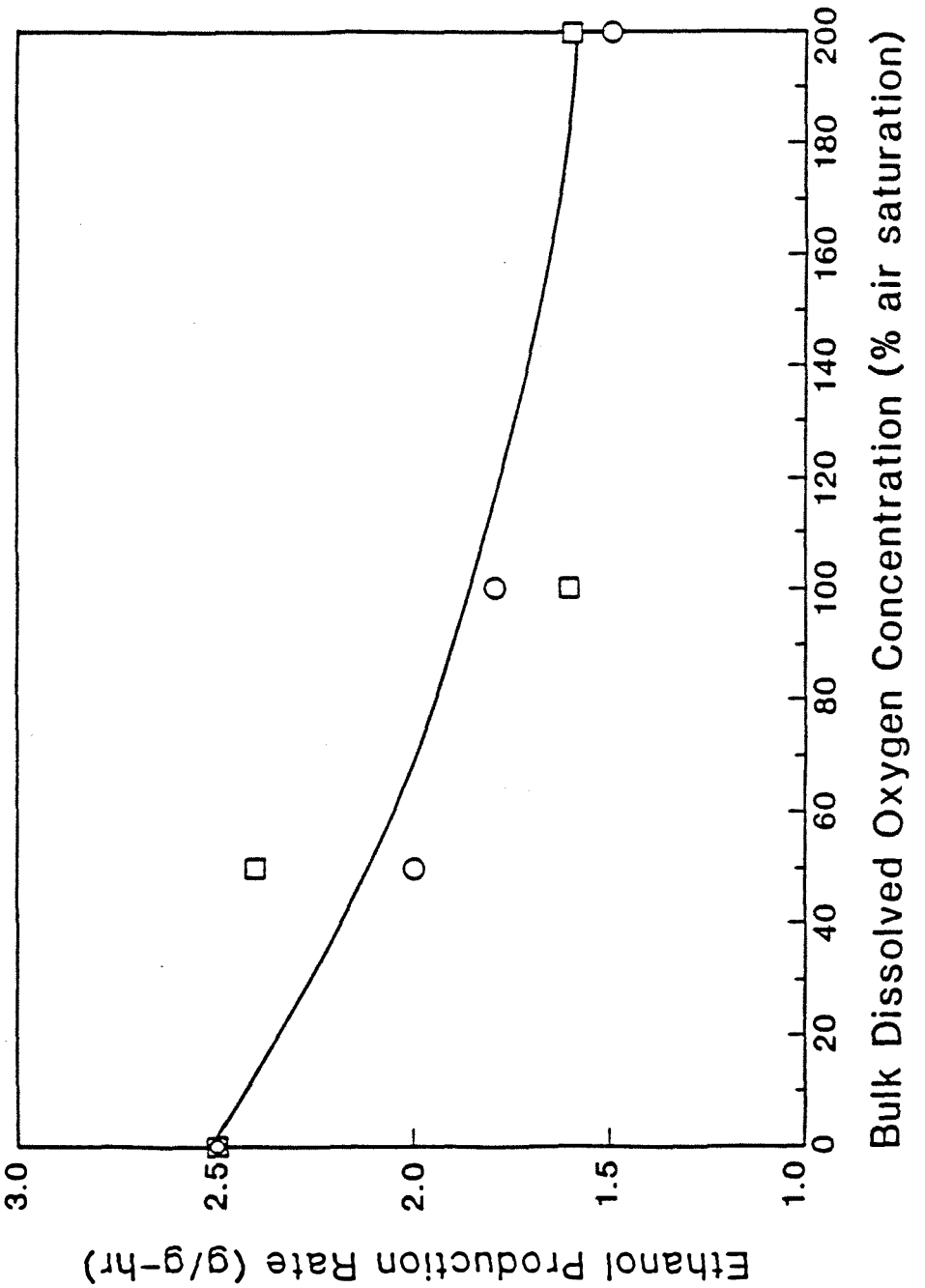

Figure 5.3 Effect of Bulk Dissolved Oxygen Concentration on Ethanol Production Rate of immobilized *S. cerevisiae* according to (□) experiments and (○) mathematical model.

The sensitivity of the model to the fitted parameters was investigated by varying the parameter values individually. The model was used to predict the growth rate and glucose uptake at various bulk dissolved oxygen concentrations. The results are shown in Figures 5.4–5.9 for the effect of p, $K_{L,\mu}$, and $K_{L,\alpha}$ on the growth rate and glucose uptake rate. The specific growth rate is more sensitive to p and $K_{L,\mu}$ than is the specific glucose uptake rate. p and $K_{L,\mu}$ influence the growth rate directly, whereas they affect the glucose uptake rate by influencing the dissolved oxygen concentration in the alginate membrane. $K_{L,\alpha}$ affects the glucose uptake rate more than it affects the growth rate for the same reason. Neither the growth rate nor the glucose uptake rate is extremely sensitive to changes in p, $K_{L,\mu}$, or $K_{L,\alpha}$. In order to see a significant change in the growth or reaction rates, the parameters were varied by an order of magnitude for p and 50% for $K_{L,\mu}$ and $K_{L,\alpha}$.

The effect of the assumed oxygen uptake rate was also examined by varying the maximum oxygen uptake rate, θ_m, and the saturation constant, K_{L,O_2}. The results are shown in Figures 5.10–5.13. The maximum oxygen uptake rate and the saturation constant each affect the growth rate and glucose uptake rate significantly for changes in θ_m and K_L, O_2 of 50% or more. For some values of p, $K_{L,\mu}$, θ_m, and K_{L,O_2} a maximum is predicted in the growth rate with respect to bulk dissolved oxygen concentration. The experimental results indicate that growth rate increases monotonically with bulk dissolved oxygen concentration. Similarly, a minimum glucose uptake rate is predicted for certain values of θ_m and K_{L,O_2}. A minimum glucose uptake rate was not detected from the experimental results. Although the modified model is not a unique solution to fit the behavior of immobilized cells, the model describes adequately the growth

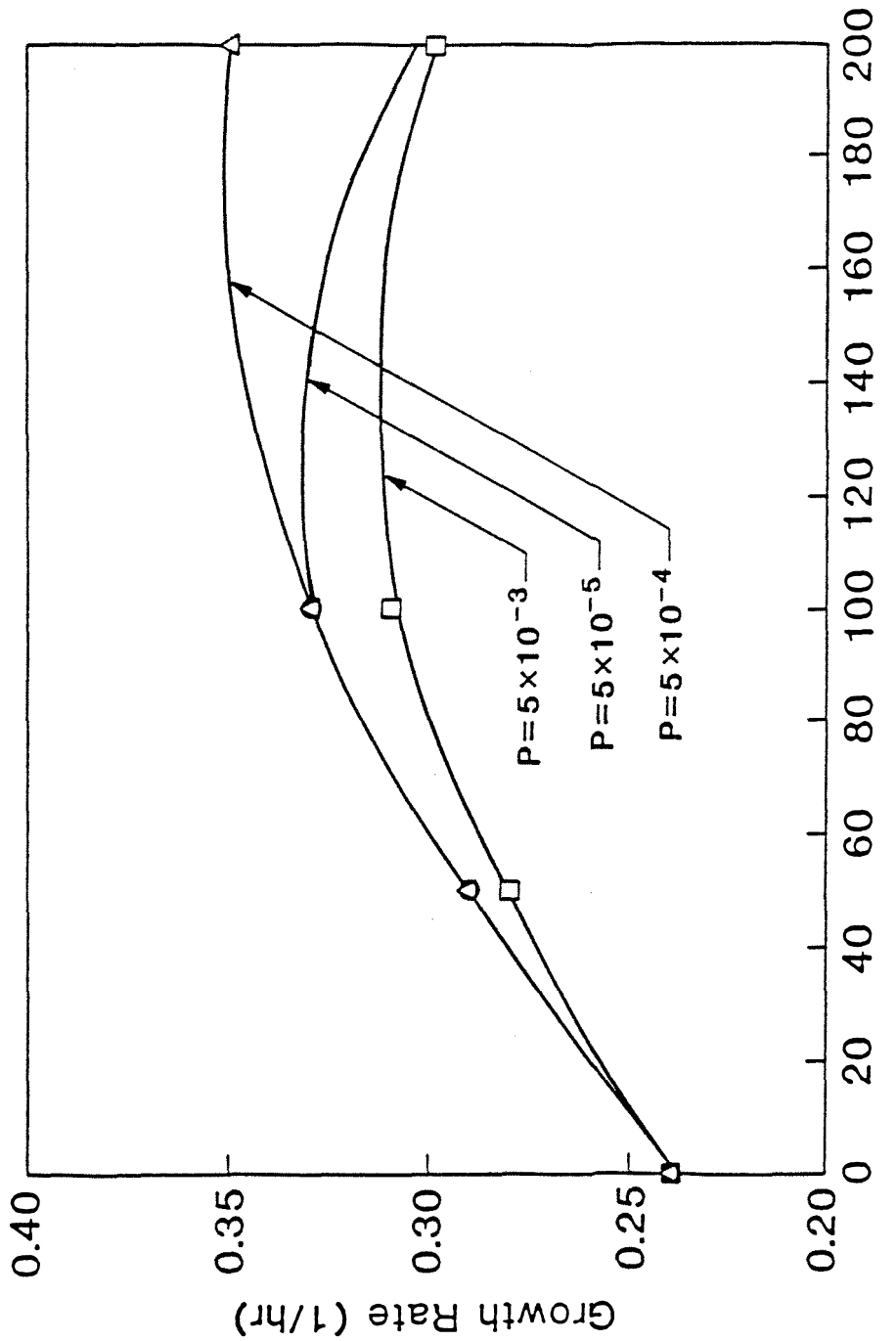

Figure 5.4 **Effect of Model Parameter, P, on Predicted Growth Rate as a function of bulk dissolved oxygen concentration, (□) $p = 5 \times 10^{-3}$ (1/%), (Δ) $p = 5 \times 10^{-4}$ (1/%), (○) $p = 5 \times 10^{-5}$ (1/%).

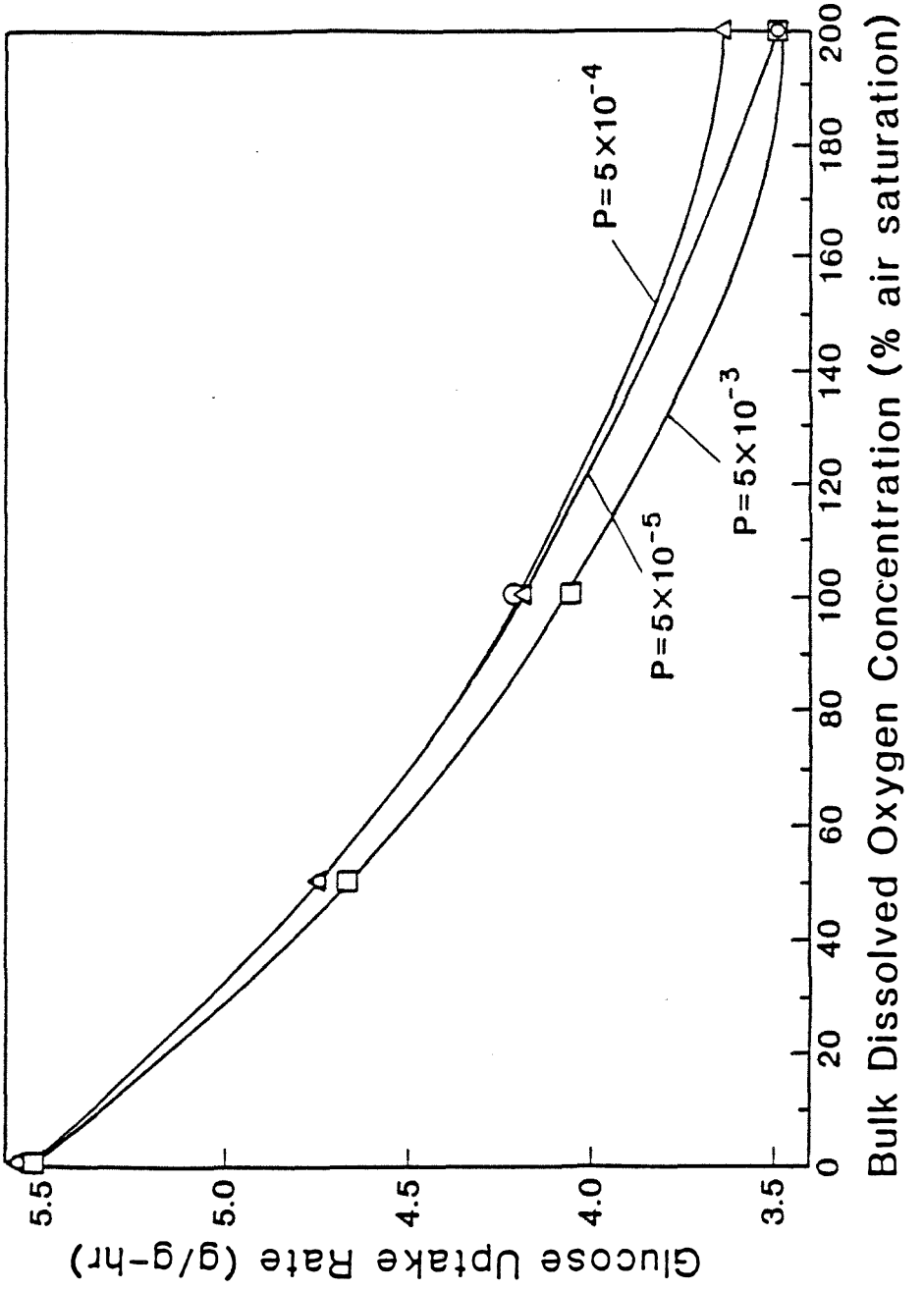

Figure 5.5 **Effect of Model Parameter, p, on Predicted Glucose Uptake Rate as a function of bulk dissolved oxygen concentration, (□) p = 5 x 10^{-3} (1/%), (Δ) p = 5 x 10^{-4} (1/%), (○) p = 5 x 10^{-5} (1/%).**

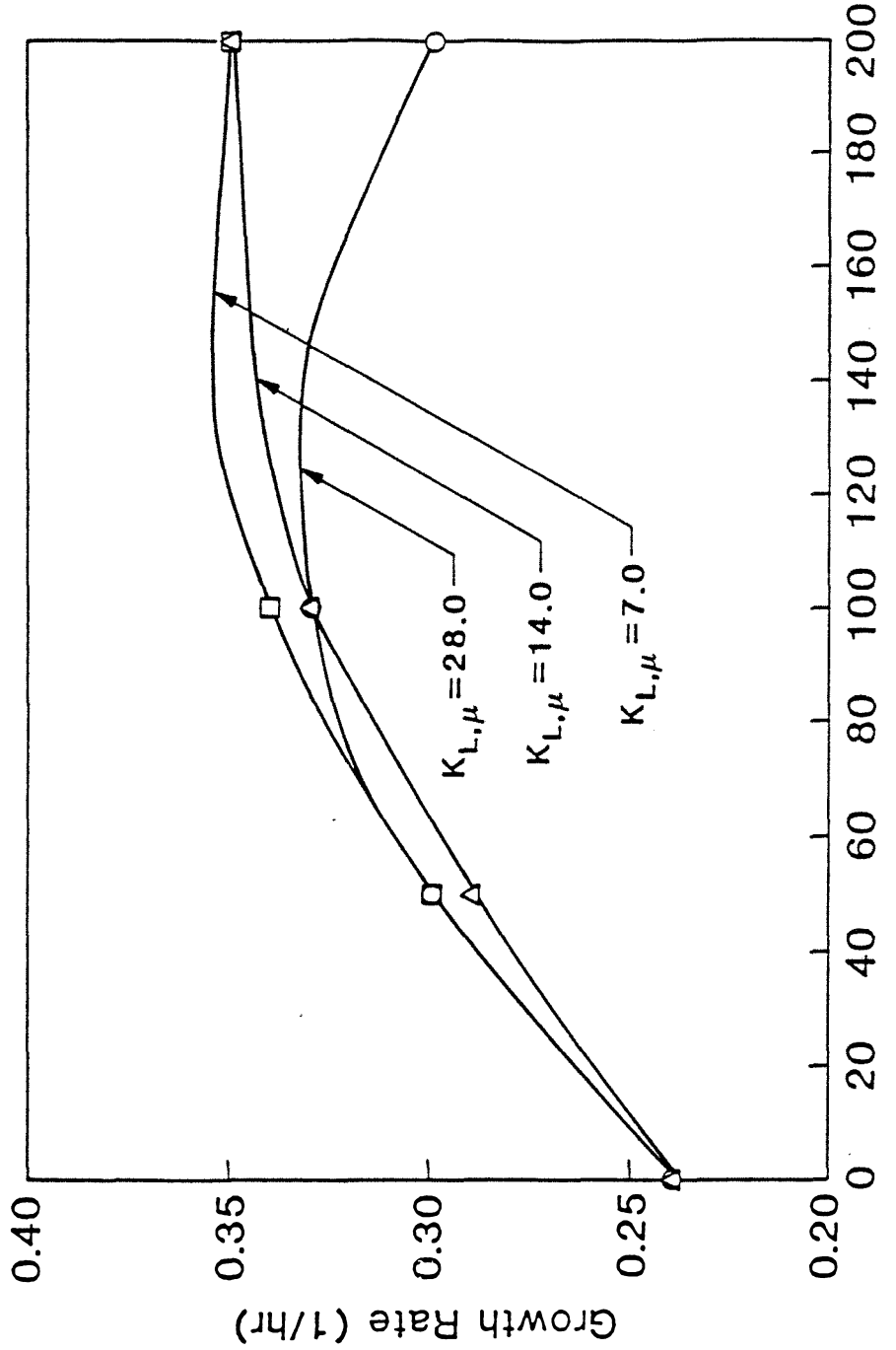

Figure 5.6 **Effect of Model Parameter, $K_{L,\mu}$, on Predicted Growth Rate as a function of bulk dissolved oxygen concentration, (□) $K_{L,\mu}$ = 7.0%, (Δ) $K_{L,\mu}$ = 14.0%, (○) $K_{L,\mu}$ = 28.0%.**

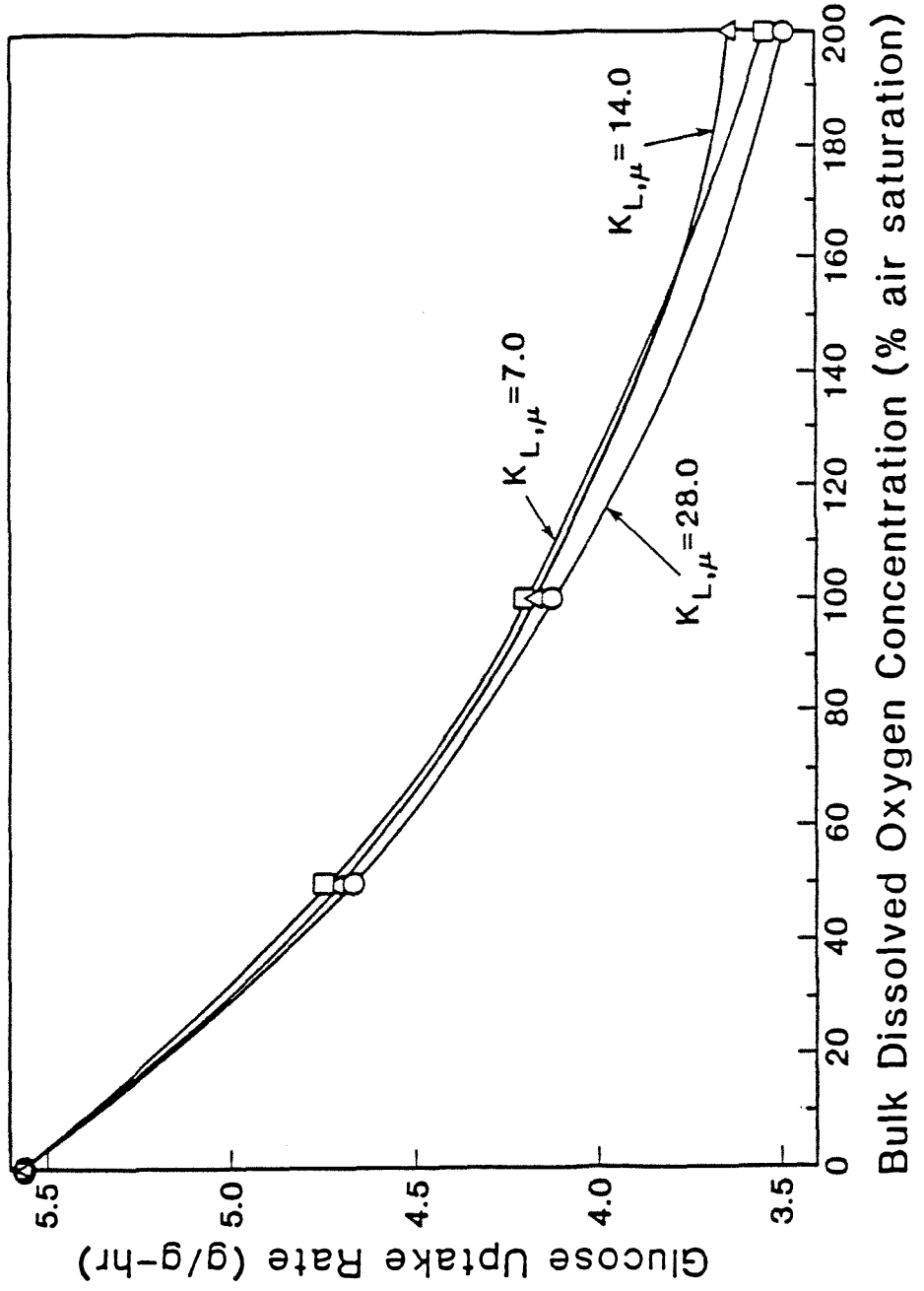

Figure 5.7 **Effect of Model Parameter, $K_{L,\mu}$, on Predicted Glucose Uptake Rate as a function of bulk dissolved oxygen concentration, (□) $K_{L,\mu}$ = 7.0%, (Δ) $K_{L,\mu}$ = 14.0%, (○) $K_{L,\mu}$ = 28.0%.**

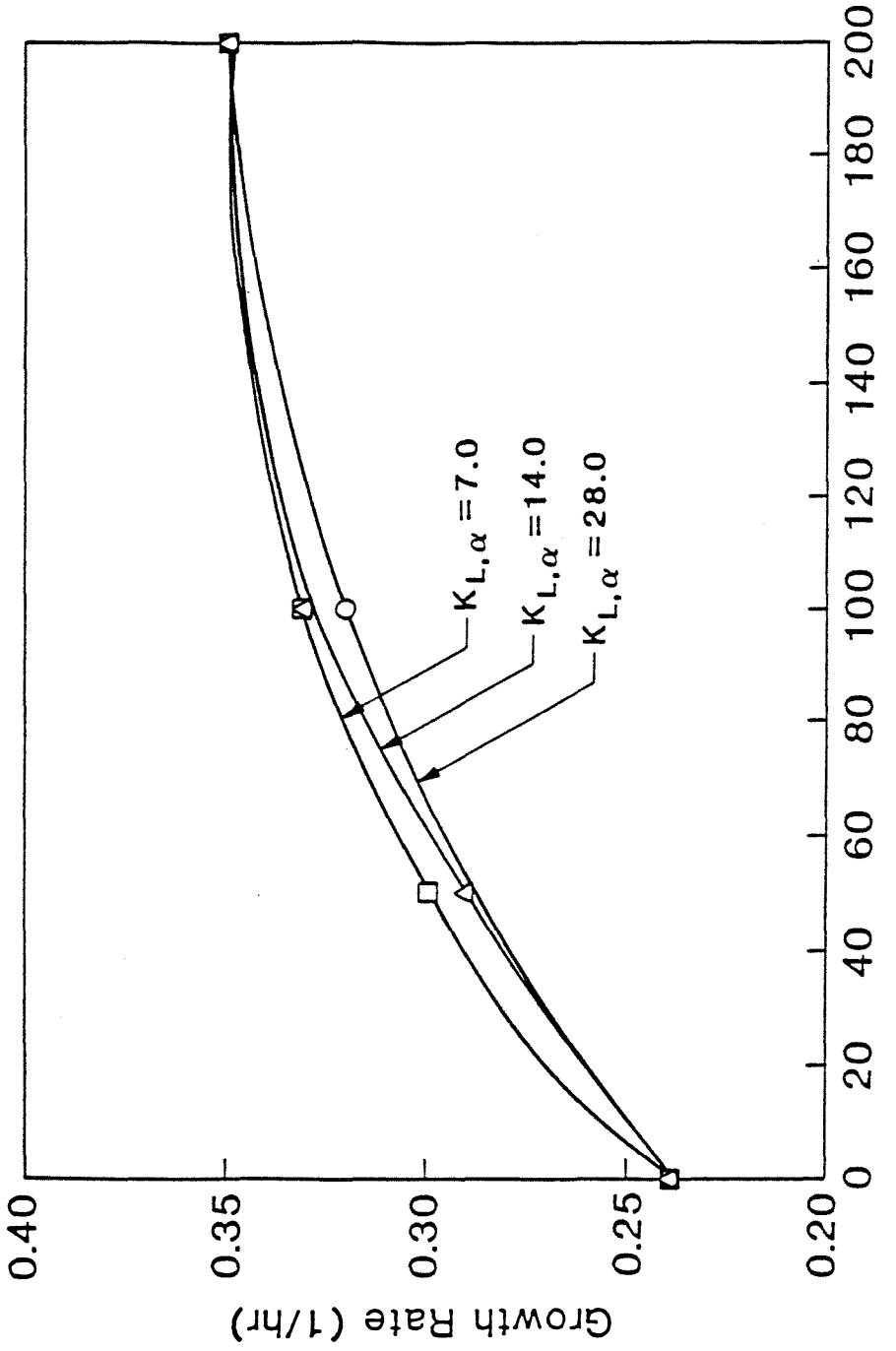

Figure 5.8 **Effect of Model Parameter, $K_{L,\alpha}$, on Predicted Growth Rate as a function of bulk dissolved oxygen concentration, (□) $K_{L,\alpha}$ = 7.0%, (Δ) $K_{L,\alpha}$ = 14.0%, (○) $K_{L,\alpha}$ = 28.0%.**

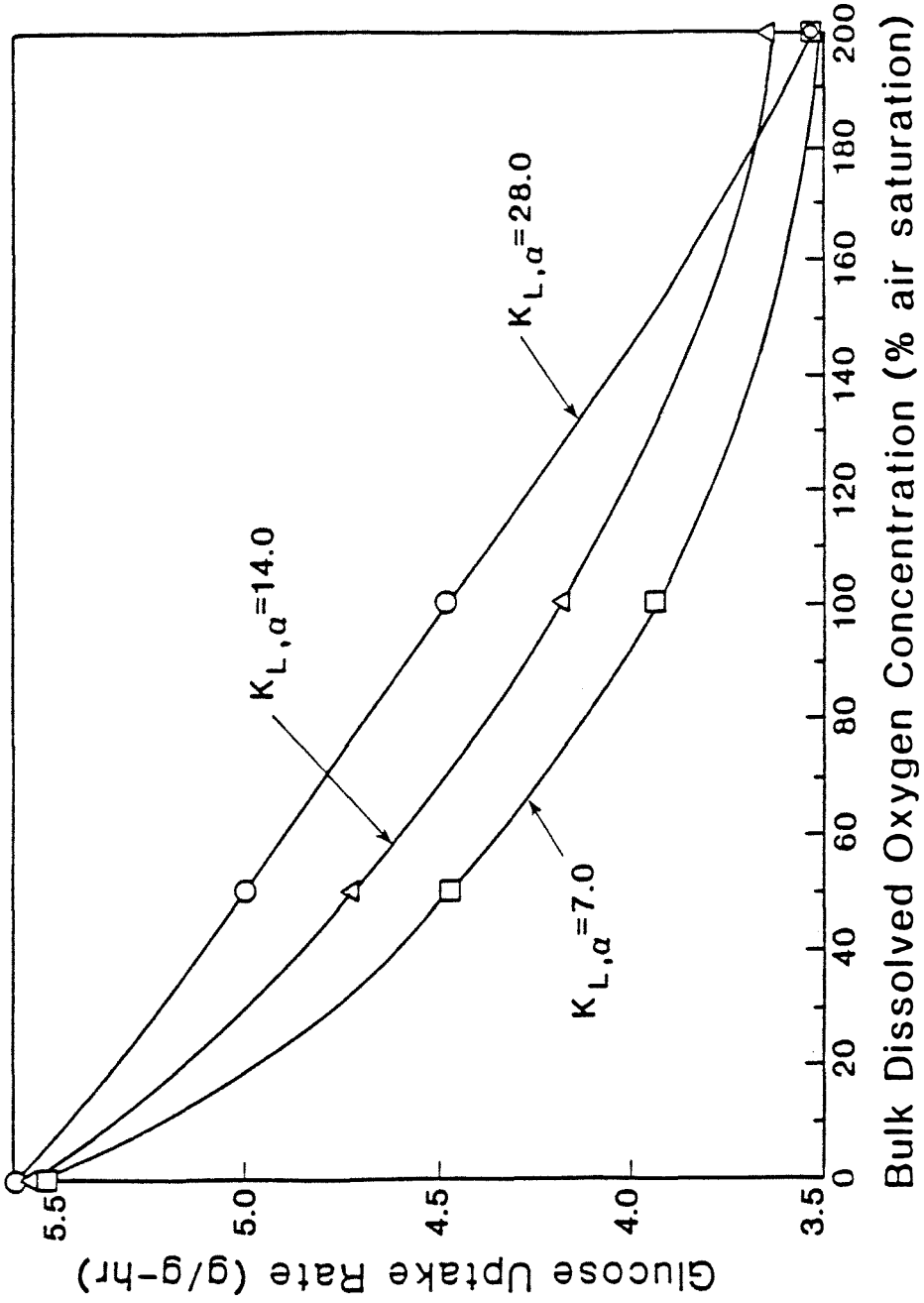

Figure 5.9 **Effect of Model Parameter, $K_{L,a}$, on Predicted Glucose Uptake Rate as a function of bulk dissolved oxygen concentration, (□) $K_{L,a}$ = 7.0%, (Δ) $K_{L,a}$ = 14.0%, (○) $K_{L,a}$ = 28.0%.**

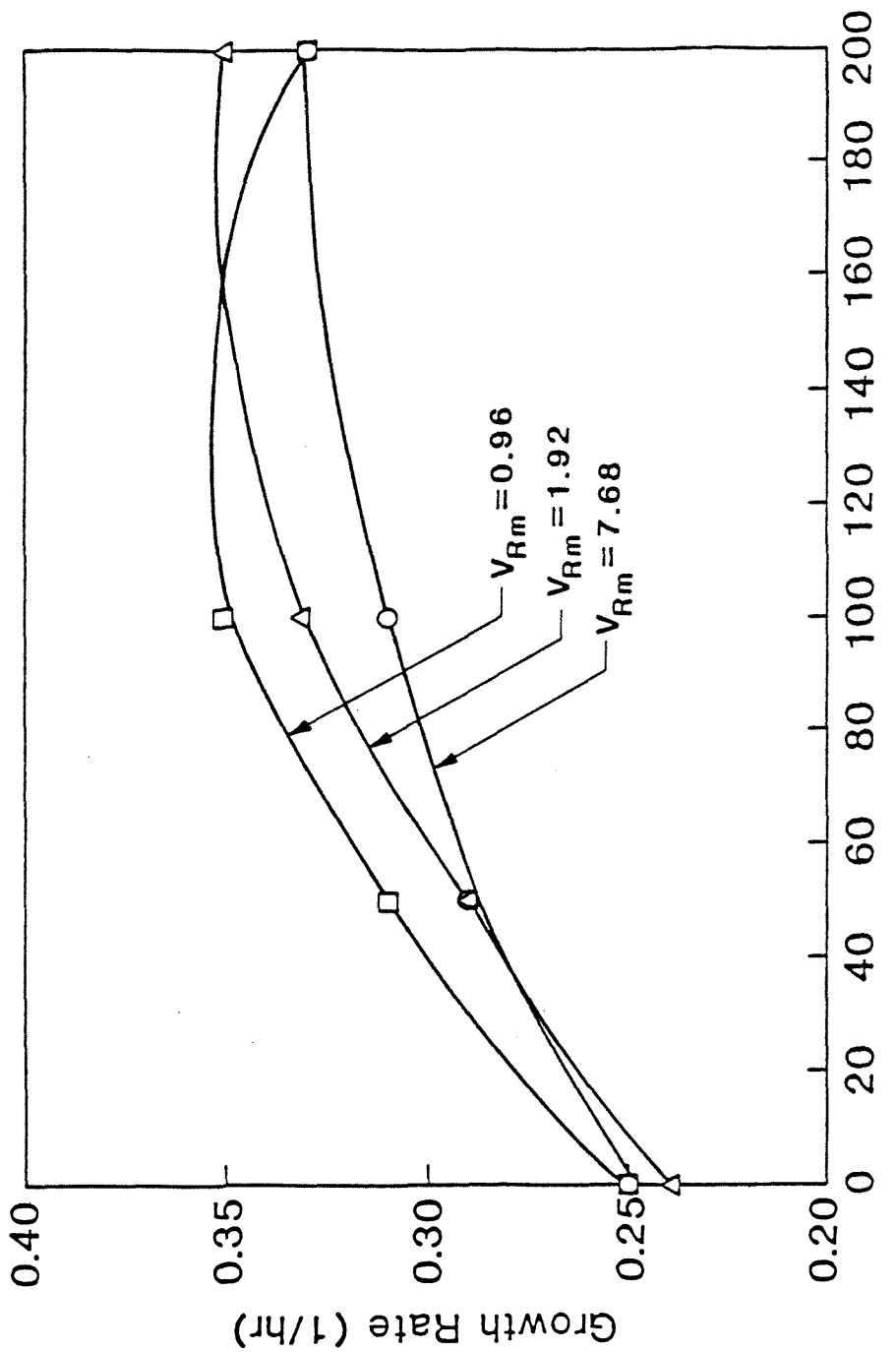

Figure 5.10 **Effect of Model Parameter, θ_m, on Predicted Growth Rate as a function of bulk dissolved oxygen concentration, (□) $\theta_m = 0.96\% - l/g - hr$, (Δ) $\theta_m = 1.92\% - l/g - hr$, (○) $\theta = 7.68\% - l/g - hr$.**

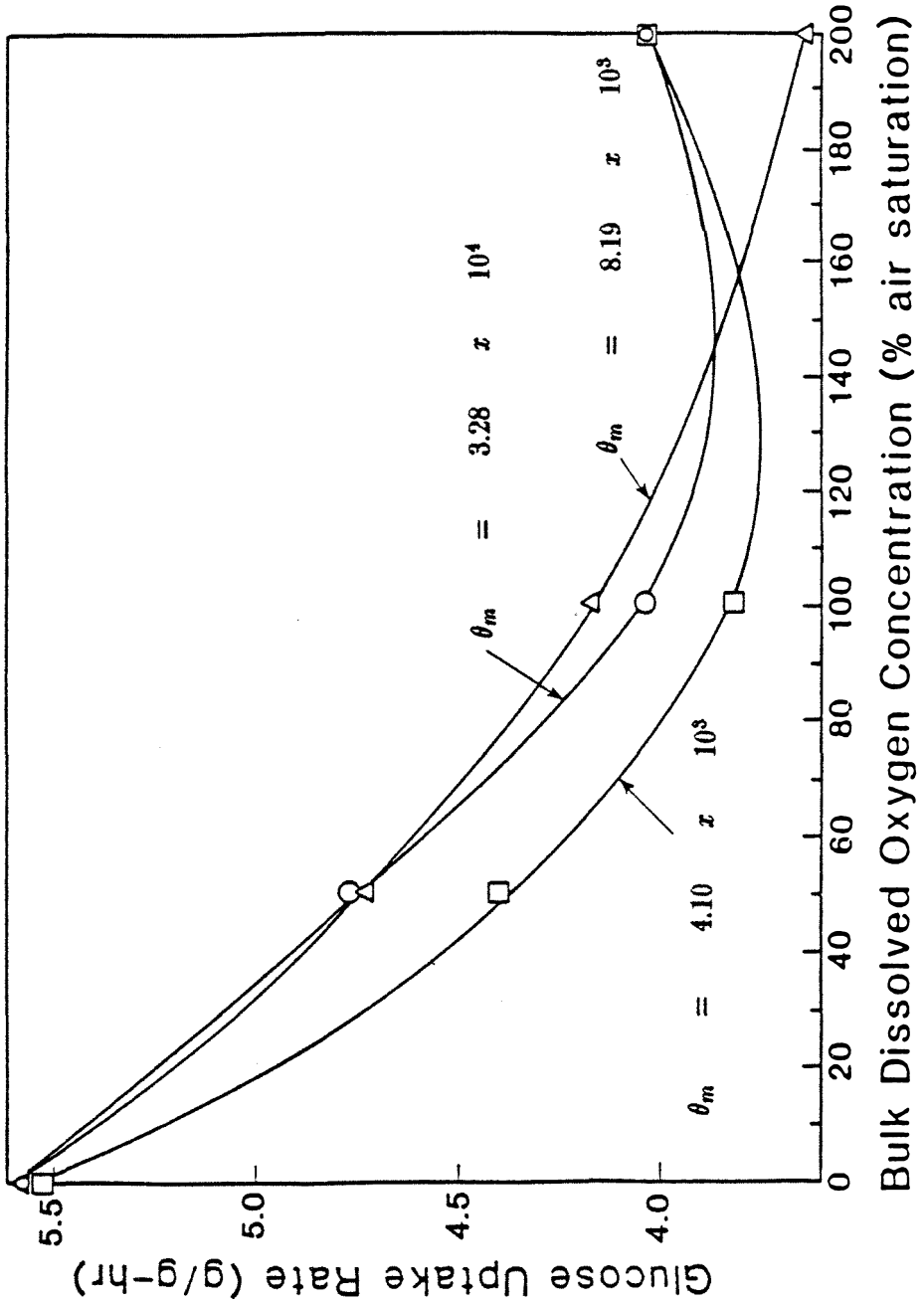

Figure 5.11 **Effect of Model Parameter, θ_m, on Predicted Glucose Uptake Rate as a function of bulk dissolved oxygen concentration, (□) $\theta_m = 4.10x10^3\% - l/g - hr$, (Δ) $\theta_m = 8.19x10^3\% - l/g - hr$, (○) $\theta = 3.28x10^4\% - l/g - hr$.**

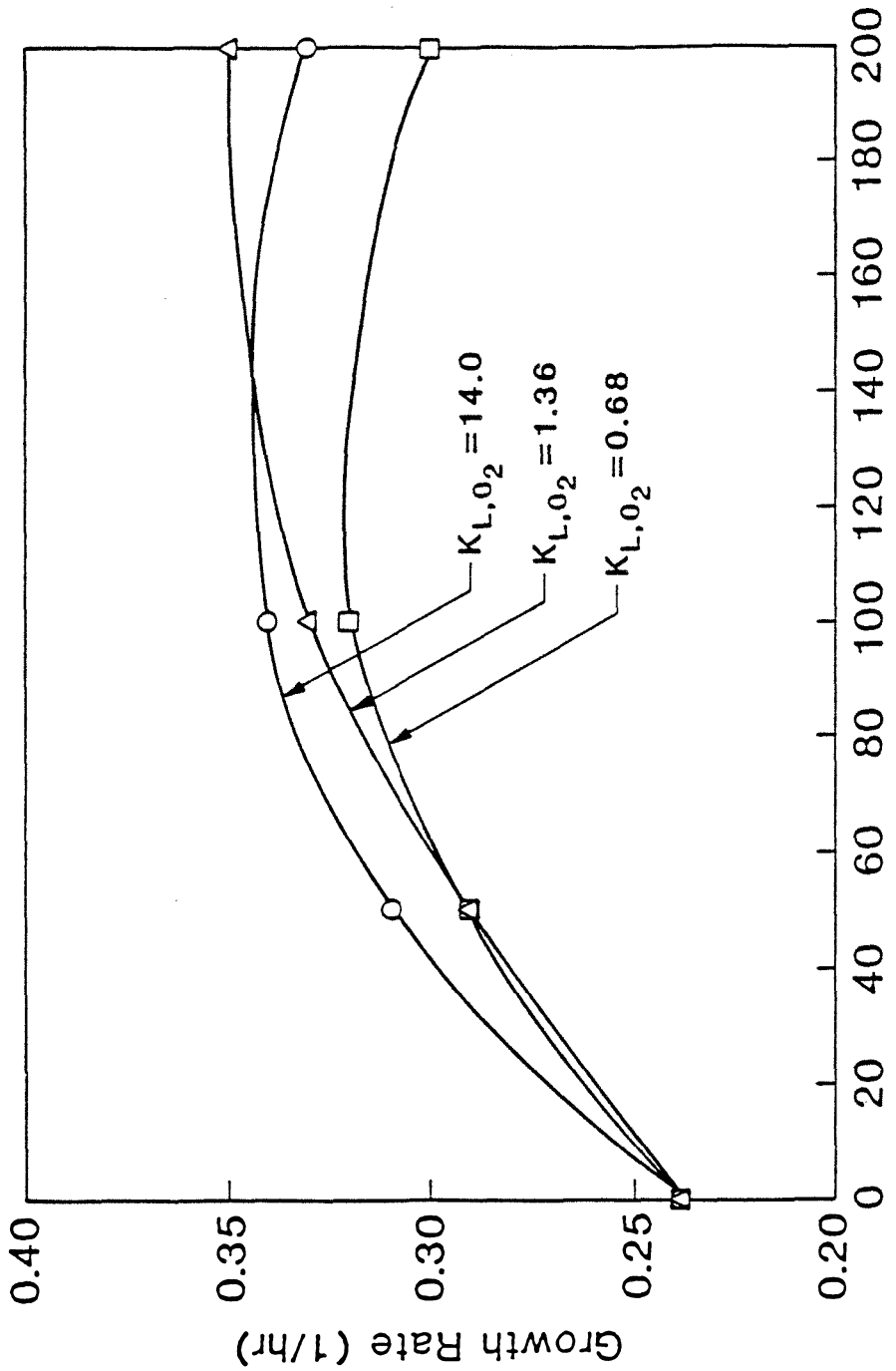

Figure 5.12 **Effect of Model Parameter, K_{L,O_2}, on Predicted Growth Rate as a function of bulk dissolved oxygen concentration, (□) K_{L,O_2} = 0.68%, (Δ) K_{L,O_2} = 1.36%, (○) K_{L,O_2} = 14.0%.**

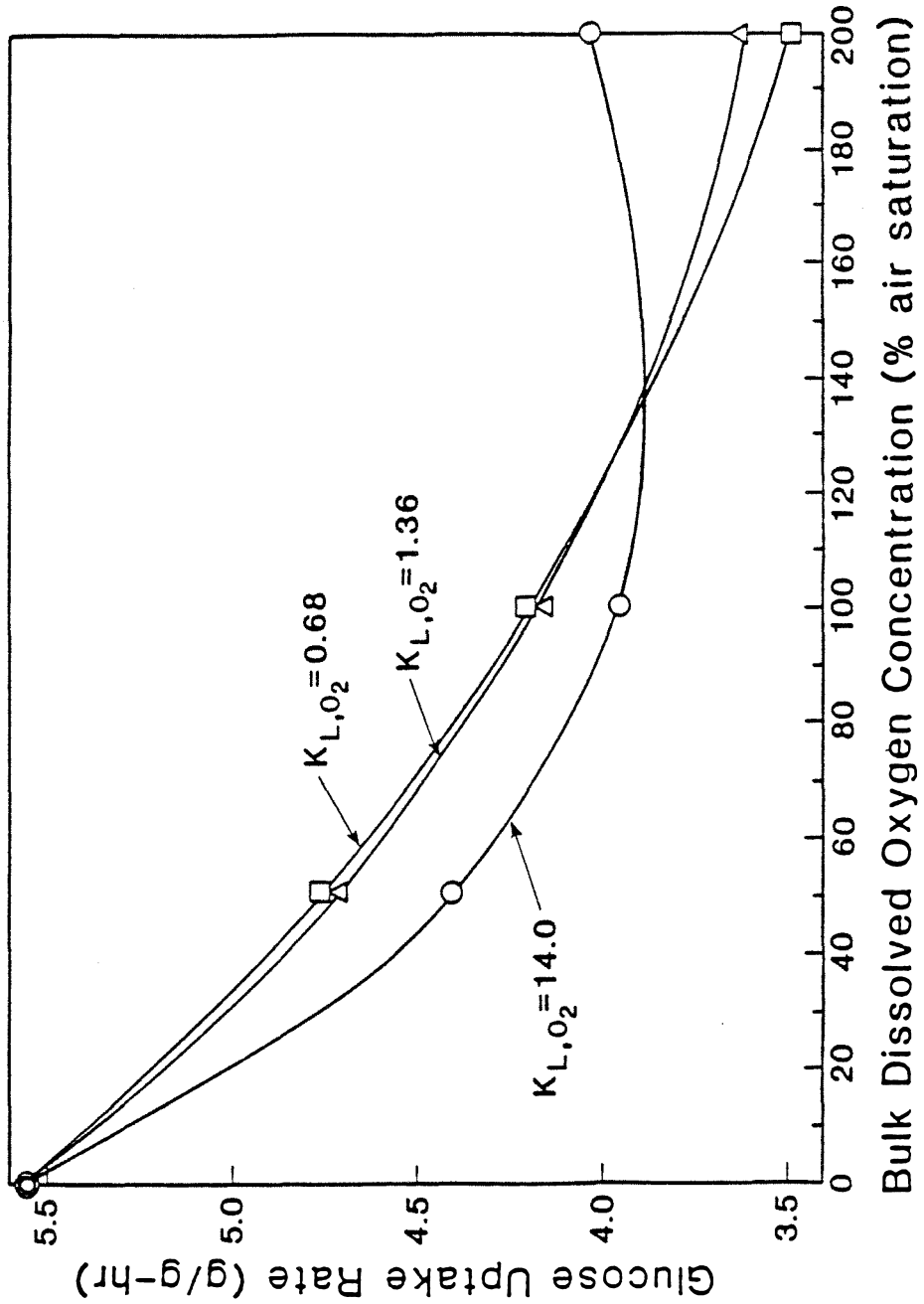

Figure 5.13 **Effect of Model Parameter, K_{L,O_2}, on Predicted Glucose Uptake Rate as a function of bulk dissolved oxygen concentration, (□) K_{L,O_2} = 0.68%, (Δ) K_{L,O_2} = 1.36%, (○) K_{L,O_2} = 14.0%.**

and reaction rates of *S. cerevisiae* immobilized in calcium alginate.

The diffusion-reaction model was used to predict the biomass concentration as a function of time and position during the diffusion-reaction experiments. The average growth rate was then calculated from initial and final biomass concentrations. The results from the diffusion-reaction model are compared to the experimental results in Table 5.1. There is close agreement between the model and the experimental results. Thus, the model predicts the actual growth rate as well as it predicts μ_{DR}. The average glucose uptake rate and ethanol production rate were also calculated from the diffusion-reaction model for immobilized cells using the following equations:

$$\bar{\alpha} = \frac{\sum_{j=1}^{J}\sum_{i=1}^{N} \alpha_{i,j} b_{i,j} \delta x_i \delta t_j}{\sum_{j=1}^{J}\sum_{i=1}^{N} b_{i,j} \delta x_i \delta t_j} \tag{5.20}$$

$$\bar{\nu} = \frac{\sum_{j=1}^{J}\sum_{i=1}^{N} \nu_{i,j} b_{i,j} \delta x_i \delta t_j}{\sum_{j=1}^{J}\sum_{i=1}^{N} b_{i,j} \delta x_i \delta t_j}, \tag{5.21}$$

Table 5.2 compares the average glucose uptake rate with α_{DR} and the average ethanol production rate with ν_{DR} for 0, 50, 100, and 200 % air saturation. At high dissolved oxygen concentrations, α_{DR} and ν_{DR} consistently underestimate the average glucose uptake rate and average ethanol production rate, respectively. As discussed in Chapter 4, the difference between α_{DR} and average glucose uptake rate results from time variations in the intrinsic specific glucose uptake rate during aerobic diffusion-reaction experiments. Similarly, time variations in the intrinsic ethanol production rate account for differences between ν_{DR} and the average ethanol production rate.

From the values of $K_{L,\mu}$ and $K_{L,\alpha}$ of 14.0 % for immobilized cells, it appears that the intrinsic growth rate and intrinsic glucose uptake rate of immobilized

Table 5.1

AVERAGE GROWTH RATE FROM EXPERIMENTS AND MODEL

DO Conc. (% air sat.)	μ^1 (1/hr) experiment	μ^2 (1/hr) model
0	0.26	0.24
50	0.29	0.26
100	0.29	0.28
200	0.30	0.30

[1] Determined from final biomass concentration.

[2] Predicted by mathematical model.

Table 5.2

REACTION RATES FROM DIFFUSION-REACTION EXPERIMENTS AND AVERAGE REACTION RATES FROM MODEL

DO Conc. (% air sat.)	α_{DR} (g/g-hr)	$\bar{\alpha}$ (g/g-hr)	ν_{DR} (g/g-hr)	$\bar{\nu}$ (g/g-hr)
0	5.6	5.7	2.5	2.5
50	4.7	5.2	2.4	2.2
100	4.3	4.8	1.6	2.1
200	3.6	4.3	1.6	1.9

cells may be less sensitive to oxygen at low oxygen concentrations than suspended cells with a $K_{L,\mu}$ and a $K_{L,\alpha}$ of 1.36 %. Higher energy requirements of immobilized cells can account for this difference. When oxygen becomes available to immobilized and suspended glucose repressed cells, a low level of respiratory enzyme activity may develop. ATP is produced at a faster rate because respiration provides 18 times more ATP per molecule of glucose than fermentation. The extra ATP produced may be degraded faster by immobilized cells than by suspended cells because immobilized cells appear to waste more ATP than suspended cells. The ATP concentration will increase more slowly in immobilized cells than in suspended cells when oxygen becomes available for respiration. Since the growth rate is related to the ATP concentration in the cells, the growth rate of immobilized cells will increase more slowly with dissolved oxygen concentration than the growth rate of suspended cells. The rate of glucose uptake is inversely related to the ATP concentration since ATP inhibits glycolysis. Thus, the glucose uptake rate will decrease more slowly in immobilized cells than in suspended cells when oxygen becomes available.

5.3 COMPARISON BETWEEN MODEL AND EXPERIMENT

The diffusion-reaction model was applied to *S. cerevisiae* immobilized in calcium alginate beads. The model was used to predict the behavior of a well-stirred and aerated, immobilized cell batch reactor. Alginate beads occupied roughly 5 % of the reactor's working volume, allowing complete mixing of the liquid phase. Uniform bulk fluid concentrations were assumed throughout the reactor. Alginate beads with a diameter of 3.4 mm were used in the reactor.

The appropriate diffusion-reaction equations for the alginate phase are:

$$\frac{\partial b}{\partial t} = \mu b \tag{5.22}$$

$$\frac{\partial s}{\partial t} = D_g \left(\frac{\partial^2 s}{\partial r^2} + \frac{2}{r} \frac{\partial s}{\partial r} \right) - \alpha b \tag{5.23}$$

$$\frac{\partial e}{\partial t} = D_e \left(\frac{\partial^2 e}{\partial r^2} + \frac{2}{r} \frac{\partial e}{\partial r} \right) + \nu b \tag{5.24}$$

$$\frac{\partial O_2}{\partial t} = D_O \left(\frac{\partial O_2}{\partial r^2} + \frac{2}{r} \frac{\partial O_2}{\partial r} \right) - \theta b. \tag{5.25}$$

The appropriate boundary conditions are:

$$\frac{\partial s}{\partial r} = 0 \quad \text{at} \quad r = o \qquad s = s_b \quad \text{at} \quad r = R \tag{5.26}$$

$$\frac{\partial e}{\partial r} = 0 \quad \text{at} \quad r = 0 \qquad e = e_b \quad \text{at} \quad r = R \tag{5.27}$$

$$\frac{\partial O_2}{\partial r} = 0 \quad \text{at} \quad r = 0 \qquad O_2 = O_{2,b} \quad \text{at} \quad r = R, \tag{5.28}$$

and the initial conditions are:

$$b = b_0 \quad \text{for all r at} \quad t = 0 \tag{5.29}$$

$$s = s_b \quad \text{for all r at} \quad t = 0 \tag{5.30}$$

$$e = o \quad \text{for all r at} \quad t = 0 \tag{5.31}$$

$$O_2 = O_{2,b} \quad \text{for all r at} \quad t = 0. \tag{5.32}$$

The glucose and ethanol concentrations in the bulk phase are given by:

$$s_b|_{t+dt} = s_b|_t - \frac{Q_s}{V_R(1 - A_g)} \tag{5.33}$$

$$e_b|_{t+dt} = e_b|_t - \frac{Q_e}{V_R(1 - A_g)}, \tag{5.34}$$

where:

$$Q_s = D_g \frac{\partial s}{\partial r}\|_{r=R} \frac{3 V_R A_g dt}{R} \tag{5.35}$$

$$Q_e = D_e \frac{\partial e}{\partial r}\|_{r=R} \frac{3V_R A_g dt}{R}. \tag{5.36}$$

The computer program used to calculate the bulk glucose and ethanol concentrations as a function of time is included in the Appendix.

5.3.1 Materials and Methods

5.3.1.1 Cell Cultivation

S. cerevisiae 18790 was grown in defined glutamate medium. The growth medium composition is given in Table 3.1 of Chapter 3. A petri plate colony was used to inoculate 7 ml of preculture medium, which was 2.5 times the concentration of the growth medium and contained 50.0 g/l glucose. The preculture was incubated for 11 hours at 30°*C*. Then 1 ml of the preculture was transferred to each of two flasks with 250 ml of growth medium and 50.0 g/l glucose. The cells were incubated for approximately 10 hours at 30°*C*. The cell density of the culture was measured by absorbance on a Klett meter. The cells were growing exponentially at a rate of 0.42 1/hr when the cell density reached the desired level. A 1 ml sample was removed from each of the growth flasks (originally 250 ml volume) and put on ice for cell counting with a Levy-Hausser counting chamber. The biomass concentration was determined from a correlation between the cell number and dry weight, which was previously established.

5.3.1.2 Alginate Bead Preparation

Cells were harvested by centrifuging the cell culture for 8 minutes at 4°*C* and 4,000 rpm. The cell pellet was washed with 10 ml of sterile deionized water and recentrifuged for 8 minutes at 4°*C* and 4,000 rpm. The cells were

then suspended in 7.5 ml of sterile deionized water and added to 7.5 ml of 4% sodium alginate. The alginate and cell mixture was stirred well and pumped slowly through a Pasteur pipette. Alginate beads were dropped into 2% calcium alginate and hardened for 1.5 hours at $4°C$. The average diameter of the calcium alginate beads was 3.4 mm.

5.3.1.3 Immobilized Cell Experiments

The immobilized cell experiments were carried out in a 250 ml flask closed with a rubber stopper. There were three ports in the stopper for aerating the medium, removing gas, and taking samples. The reactor was stirred magnetically and maintained at $30°C$ with a water bath. The experiments started with the addition of calcium alginate beads (approximately 5 % vol/vol) to defined glutamate medium already in the reactor. Samples (0.5 ml) were withdrawn periodically with a sterile needle and syringe and then filter-sterilized. The samples were analyzed for both glucose and ethanol at a later time. The initial glucose concentration in the reactor was close to 25 g/l.

5.3.1.4 Analyses

The glucose concentration in the bulk fluid of the reactor was assayed enzymatically (Sigma Chemical Co., St. Louis, Mo.). Samples were diluted to bring the glucose concentration into the range of 1–10 g/l. 1.5 ml of reagent and 10 μl of sample were mixed in a microcuvette. The absorbance was measured at 340 nm on a Hitachi Model 100–30 spectrophotometer after 10 minutes. A blank consisting of reagent and deionized water was used to zero the spectrophotometer.

The alcohol dehydrogenase enzyme assay (Sigma Chemical Co.) was used to measure the ethanol concentration in the bulk fluid. 3 ml of reagent were mixed with 10 μl of diluted sample in a cuvette. The absorbance was read on a Hitachi Model 100–30 spectrophotometer at 340 nm after 12 minutes of reaction. The spectrophotometer was zeroed using a blank of reagent plus 10 μl of deionized water.

5.3.2 Experimental Results

The experimental glucose and ethanol concentrations in the bulk fluid of the immobilized cell batch reactor are shown in Figure 5.14 as a function of time for the first batch reactor experiment. The initial biomass concentration in the experiment was 11.0 g DW/l. The lines in the figure represent the time trajectories predicted by the immobilized cell diffusion-reaction model for the experimental conditions. Figure 5.15 shows the glucose and ethanol concentrations in the batch reactor during the second experiment, where the initial biomass concentration was 5.9 g DW/l. The experimental data from both batch reactor runs follow the trends predicted by the diffusion-reaction model for immobilized cells. The diffusion-reaction model was developed from experiments conducted with final biomass concentrations of 8 g/l or less. In the batch experiment with alginate beads, the final biomass concentration reached 150 g/l. Thus, the model developed at low biomass concentrations applies well at higher biomass concentrations.

5.4 CONCLUSION

The growth and reaction rates of viable cells entrapped in a matrix can

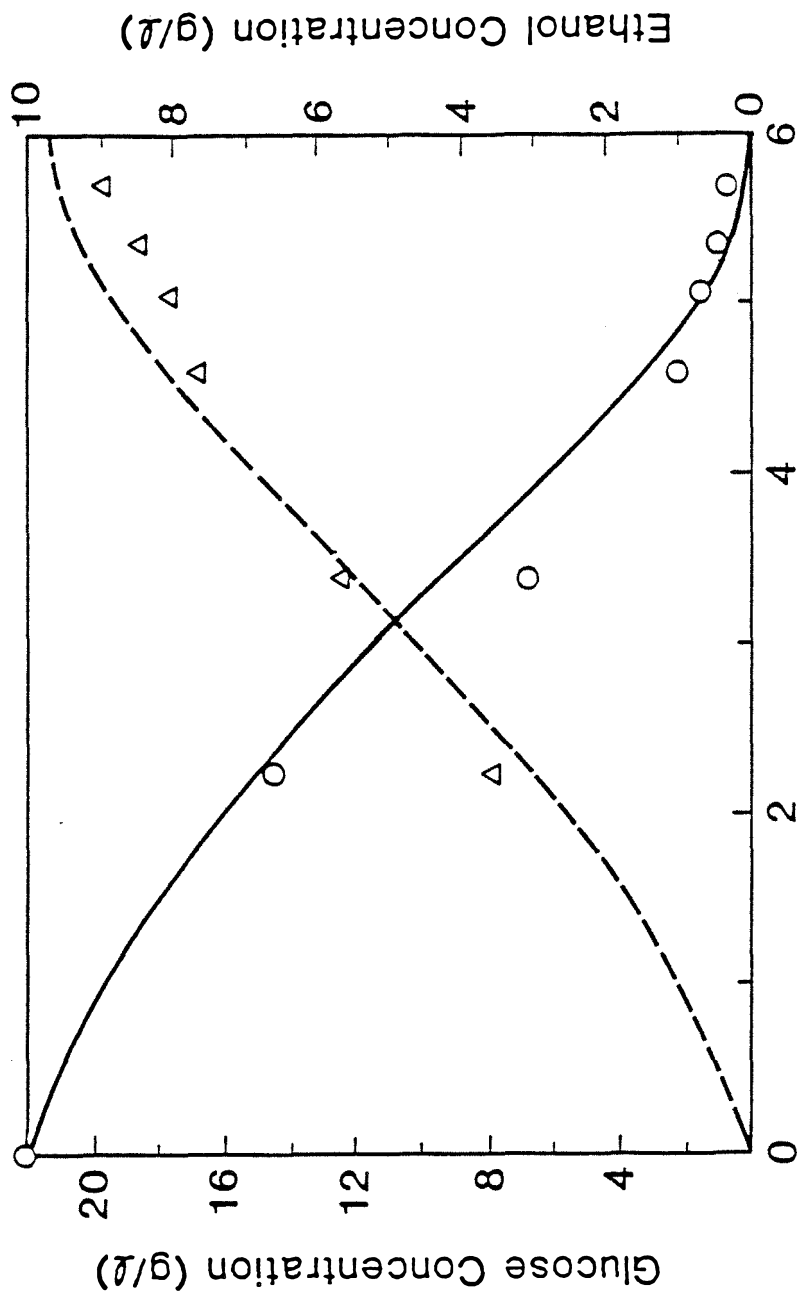

Figure 5.14 **Bulk Glucose and Ethanol Concentrations in Batch Reactor as a function of time for *S. cerevisiae* immobilized in alginate beads, (○) glucose concentration, (Δ) ethanol concentration. Initial biomass concentration is 11.0 g DW/l.**

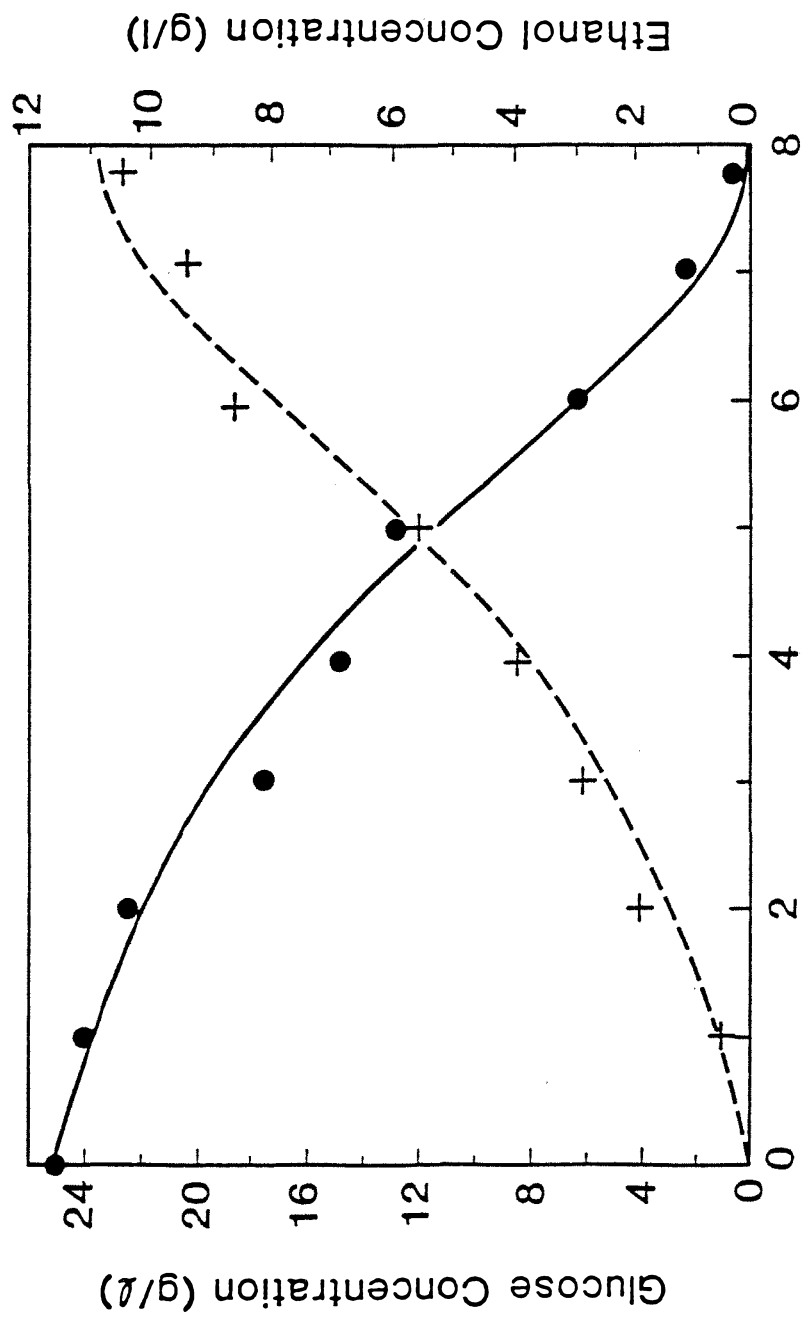

Figure 5.15 **Bulk Glucose and Ethanol Concentrations in Batch Reactor as a function of time for *S. cerevisiae* immobilized in alginate beads, (•) glucose concentration, (+) ethanol concentration. Initial biomass concentration is 5.9 g DW/l.**

be accurately modeled by combining the intrinsic kinetic expressions with diffusion rates. Because of biochemical changes from cell immobilization, suspended cell rate expressions cannot always be applied to the intrinsic kinetics of immobilized cells. Instead, the intrinsic kinetics of immobilized cells must be determined experimentally with cells immobilized under the desired conditions.

REFERENCES

(1) Peringer,P., H. Blachere, G. Corrieu, and A. G. Lane, "Mathematical Model of the Kinetics of *Saccharomyces cerevisiae*," *Biotechnol. Bioeng. Symp.*, *4*, 27–42 (1973).

(2) Holzberg, I., R. K. Finn, and K. H. Steinkraus, "A Kinetic Study of the Alcoholic Fermentation of Grape Juice." *Biotechnol. Bioeng.*, *9*, 413 (1967).

(3) Tyagi, R. D., and T. K. Ghose, "Rapid Ethanol Fermentation of Cellulose Hydrolysate. II. Product and Substrate Inhibition and Optimization of Fermentor Design," *Biotechnol. Bioeng.*, *21*, 1401 (1980).

(4) Zines, D. O., and P. L. Rogers, "A Chemostat Study of Ethanol Inhibition," *Biotechnol. Bioeng.*, *13*, 293 (1971).

(5) Aiba, S., M. Shoda, and M. Nagatani, "Kinetics of Product Inhibition in Alcohol Fermentation," *Biotechnol. Bioeng.*, *10*, 845–864 (1968).

(6) Leão, C., and N. Van Uden, "Effects of Ethanol and Other Alkanols on the General Amino Acid Permease of *Saccharomyces cerevisiae*," *Biotechnol. Bioeng.*, *26*, 403–405 (1984).

(7) Righelato, R. C., D. Rose, and A. W. Westwood, "Kinetics of Ethanol Production by Yeast in Continuous Culture," *Biotechnol. Lett.*, *3*, 3–8 (1981).

(8) Aiba, S., and M. Shoda, "Reassessment of the Product Inhibition in Alcohol Fermentation," *J. Ferment. Technol.*, *47*, 790–794 (1969).

(9) Bazua, C. D., and C. R. Wilke, "Ethanol Effects on the Kinetics of a Continuous Fermentation with *Saccharomyces cerevisiae*," *Biotechnol. Bioeng. Symp.*, *7*, 105–118 (1977).

(10) Rogers, P. J., and P. R. Stewart, "Mitochondrial and Peroxisomal Contri-

butions to the Energy Metabolism of *Saccharomyces cerevisiae* in Continuous Culture," *J. Gen. Microbiol.*, *79*, 205–217 (1973).

(11) Thomas, D. S., J. A. Hossack, and A. H. Rose, "Plasma-membrane Lipid Composition and Ethanol Tolerance," *Arch. Microbiol.*, *117*, 239–245 (1978).

(12) Marcipar, A., N. Cochet, L. Brackenridge, J. M. Lebeault, "Immobilization of Yeasts on Ceramic Supports," *Biotechnol. Lett.*, *1*, 65–70 (1979).

CHAPTER 6

UNSTEADY-STATE IMMOBILIZED CELL REACTOR MODEL

6.1 INTRODUCTION

S. cerevisiae immobilized in calcium alginate can be employed commercially for ethanol production from glucose. Bench-scale experiments indicate that the intrinsic specific ethanol production rate increases by a factor of four when *S. cerevisiae* is entrapped in alginate. An intrinsic, specific ethanol production rate of 2.4 g/g-hr was measured experimentally for anaerobic, alginate-entrapped cells, while the specific ethanol production rate of suspended cells was measured at 0.6 g/g-hr under anaerobic conditions. Higher biomass concentrations can be maintained in continuous immobilized cell reactors than in chemostats because immobilized cells are not transported out of the reactor with the product stream. For a continuous, immobilized cell reactor containing 50% alginate by volume and a cell concentration of 100 g DW/l alginate or 50 g DW/l reactor, an ethanol productivity of 120 g/l-hr would result if the rate of ethanol production were 2.4 g/g-hr everywhere in the reactor. A chemostat with the same ethanol productivity would require a biomass concentration of 200 g DW/l reactor for an ethanol production rate of 0.6 g/g-hr. Such dense suspended cell concentrations are not experimentally feasible. The higher productivity of immobilized cell reactors makes them attractive for the commercial production of ethanol.

Mathematical models can offer useful insights in the design and operation of chemical reactors. The scale-up of laboratory results can be facilitated

by developing models that account for both mass transport in the alginate bead and chemical reaction. Models can also be used in identifying design parameters that limit the overall reactor productivity. Lastly, a model can be used to predict the effects of changing the operating conditions and to identify the operating conditions for optimal reactor performance.

Steady-state immobilized cell reactor models can be found in the literature for a variety of reactor configurations (1–3). All of these models, however, fail to account for any changes in the biomass, substrate, and product concentrations in the reactor with time. Immobilization in calcium alginate does not prevent cell growth. In this investigation, immobilized cells grew at 80% of the rate of suspended cells. Other researchers have reported immobilized cell growth rates of 55% and 170% of suspended cell rates (4,5). As the biomass concentration in the reactor increases with time, the substrate concentration in the alginate beads decreases and the product concentration increases. Because of cell growth and substrate uptake, the substrate concentration may become depleted in the interior of the bead, leading to inactivation of some cells, while other cells continue growing in the outer region of the bead. The depletion of nutrients and the accumulation of toxic products inside the beads may also cause changes in the intrinsic, specific growth and reaction rates of entrapped cells. Thus, the operating state of an immobilized cell reactor is inherently unsteady because of changes in the biomass, substrate, and product concentration profiles in the reactor.

If cell growth is prevented by removing an essential nutrient from the medium or by adding growth inhibitory compounds, the activity of the immobilized cells will deteriorate with time. Deactivation of immobilized cells will

also cause unsteady-state reactor behavior. Nevertheless, some researchers have observed constant glucose and ethanol effluent concentrations from an immobilized cell reactor over a period of time (6,7). When the rate of cell growth equals the rate of cell attrition, the reactor may be operating at a steady state or a pseudosteady state. For entrapped cells the distribution of the cells in the matrix can continue to change even when the total number of active cells remains constant. If substrate and product transport limitations develop, the changing distribution of cells can influence the overall reaction rates. Thus a "steady state" may deteriorate with time to an unsteady state.

In order to describe accurately the behavior of an immobilized cell bioreactor containing entrapped cells, time variations must be taken into consideration. Steady-state operation may not be reached for a long time and in some instances the reactor may never reach steady state. Economically, it is important to optimize the reactor productivity over all times including the start-up period. Furthermore, the start-up conditions of the reactor may also be significantly different than the operating conditions at later stages. For example, a reactor containing a low biomass concentration during start-up will require a longer residence time initially to produce a concentrated product stream. Another reason to model the unsteady-state behavior of an immobilized cell reactor is to include the effect of oxygen on the reactor performance. Oxygen is utilized rapidly compared to the rate at which it can be transported to the cells. Cells without oxygen grow more slowly than aerobic cells but produce ethanol at a faster rate. Thus, providing oxygen to an immobilized cell reactor during some stages of operation may improve the overall reactor productivity.

6.2 DESCRIPTION OF THE REACTOR MODEL

Designing an immobilized cell reactor for ethanol production requires intrinsic kinetic data and mass transfer coefficients. In order to predict the behavior of a heterogeneous catalytic reactor it is necessary to model diffusion and reaction inside the catalyst pellets to determine the bulk fluid concentrations throughout the reactor. Accordingly, a reactor containing cells entrapped in an alginate matrix is described by two sets of equations. One set of equations describes diffusion and reaction inside the alginate beads, and the second set of equations models the bulk fluid concentrations. The following partial differential equations describe the biomass, glucose, ethanol, and oxygen concentrations in the alginate beads with time and position:

$$\frac{\partial b}{\partial t} = \mu b \tag{6.1}$$

$$\frac{\partial s}{\partial t} = D_g \left(\frac{\partial^2 s}{\partial r^2} + \frac{2}{r} \frac{\partial s}{\partial r} \right) - \alpha b \tag{6.2}$$

$$\frac{\partial e}{\partial t} = D_e \left(\frac{\partial^2 e}{\partial r^2} + \frac{2}{r} \frac{\partial e}{\partial r} \right) + \nu b \tag{6.3}$$

$$\frac{\partial O_2}{\partial t} = D_O \left(\frac{\partial O_2}{\partial r^2} + \frac{2}{r} \frac{\partial O_2}{\partial r} \right) - \theta b. \tag{6.4}$$

The appropriate boundary conditions are:

$$\frac{\partial s}{\partial r} = 0 \quad \text{at} \quad r = o \qquad s = s_b \quad \text{at} \quad r = R \tag{6.5}$$

$$\frac{\partial e}{\partial r} = 0 \quad \text{at} \quad r = 0 \qquad e = e_b \quad \text{at} \quad r = R \tag{6.6}$$

$$\frac{\partial O_2}{\partial r} = 0 \quad \text{at} \quad r = 0 \qquad O_2 = O_{2,b} \quad \text{at} \quad r = R, \tag{6.7}$$

and the initial conditions are:

$$b = b_0 \quad \text{for all r at} \quad t = 0 \tag{6.8}$$

$$s = s_b \quad \text{for all r at} \quad t = 0 \tag{6.9}$$

$$e = o \quad \text{for all r at} \quad t = 0 \tag{6.10}$$

$$O_2 = O_{2,b} \quad \text{for all r at} \quad t = 0. \tag{6.11}$$

The intrinsic kinetics developed in Chapter 5 for ethanol production by *S. cerevisiae* immobilized in calcium alginate is employed in the reactor model. The growth rate, glucose uptake rate, ethanol production rate, and oxygen utilization rate are given by the following equations:

$$\mu = \frac{s}{K_s + s}\left[\frac{\mu_G}{1 + pO_2} + \frac{\mu_R O_2}{K_{L,\mu} + O_2}\right]\left(1 - \frac{e}{93.6}\right) \tag{6.12}$$

$$\alpha = \frac{s}{K_s + s}\left[\alpha_m - \frac{1}{K_{L,\alpha} + O_2}\right]\left(1 - \frac{e}{93.6}\right) \tag{6.13}$$

$$\nu = 0.43\alpha \tag{6.14}$$

$$\theta = \frac{s}{K_s + s}\left[\frac{\theta_m O_2}{K_{L,O_2} + O_2}\right]\left(1 - \frac{e}{93.6}\right), \tag{6.15}$$

with the following parameter values:

$$\mu_G = 0.24 \quad 1/\text{hr}$$

$$\mu_R = 0.12 \quad 1/\text{hr}$$

$$p = 5.0x10^{-4} \quad 1/\% \text{ air saturation}$$

$$K_{L,\mu} = 14.0\%$$

$$K_s = 0.1l/g$$

$$\alpha_m = 5.8 \quad \text{g/g-hr}$$

$$K_{L,\alpha} = 14.0\%$$

$$\theta_m = 8.19x10^3 \quad \%\text{-l/g-hr}$$

$$K_{L,O_2} = 1.36\%.$$

Equations (6.1)–(6.4) were solved simultaneously with boundary conditions (6.5)–(6.7) and initial conditions (6.8)–(6.11). The rate expressions in Equations (6.12)–(6.15) were substituted into the appropriate diffusion-reaction equations. The Crank-Nicholson method of finite differences was used to solve the system of equations. The boundary conditions at the bead surface change with time because of the unsteady-state reactor operation. Therefore, at each time step the concentration profiles in the alginate bead are computed by iterating for the bulk fluid concentrations and the bead concentrations. A time-step size of 0.005 hr was used. Because of steep gradients in the alginate beads, the bead radius was divided into 500 steps.

6.2.1 Plug Flow Reactor

A substrate mass balance on the fluid phase of a heterogeneous plug flow reactor generates the following first-order partial differential equation:

$$\frac{\partial s}{\partial t} = \frac{-F}{A(1-A_g)}\frac{\partial s}{\partial z} - D_g\left(\frac{\partial s}{\partial r}\|_{r=R}\right)\frac{3A_g}{R(1-A_g)}, \tag{6.16}$$

where F is the volumetric flow rate (cm^3/hr), A is the cross-sectional area of the reactor (cm^2), A_g is the volume fraction of the reactor occupied by alginate, R is the bead radius (cm), D_g is the diffusion coefficient of glucose (cm^2/hr), s is the bulk fluid substrate concentration in the reactor (g/l), z is the distance from the reactor inlet (cm), t is time (hr). Similar equations describe the ethanol and oxygen concentrations in the plug flow reactor:

$$\frac{\partial e}{\partial t} = \frac{-F}{A(1-A_g)}\frac{\partial e}{\partial z} - D_e\left(\frac{\partial e}{\partial r}\|_{r=R}\right)\frac{3A_g}{R(1-A_g)} \tag{6.17}$$

$$\frac{\partial O_2}{\partial t} = \frac{-F}{A(1-A_g)}\frac{\partial O_2}{\partial z} - D_{O_2}\left(\frac{\partial O_2}{\partial r}\|_{r=R}\right)\frac{3A_g}{R(1-A_g)}, \tag{6.18}$$

where e is the bulk fluid ethanol concentration, D_e is the diffusion coefficient of ethanol (cm^2/hr), O_2 is the dissolved oxygen concentration in the bulk fluid (% air saturation), and D_{O_2} is the oxygen diffusion coefficient (cm^2/hr). The following boundary conditions describe the feed-stream concentrations at the reactor inlet:

$$s(0,t) = s_{feed} \tag{6.19}$$

$$e(0,t) = 0 \tag{6.20}$$

$$O_2 = O_{2,feed}. \tag{6.21}$$

The initial reactor conditions are given by:

$$s(x,0) = s_{feed} \tag{6.22}$$

$$e(x,0) = 0 \tag{6.23}$$

$$O_2(x,0) = O_{2,feed}. \tag{6.24}$$

Equations (6.16)–(6.18) were solved simultaneously by the Keller box finite difference method (6) with boundary conditions (6.19)–(6.21) and initial conditions (6.22)–(6.24). The numerical solution describes the glucose, ethanol, and dissolved oxygen concentrations in the bulk fluid of the plug flow reactor. The substrate, ethanol, and oxygen gradients at the bead surface, which appear in the second term on the right-hand side of each of the reactor Equations (6.16)–(6.18), were determined from the numerical solution to Equations (6.1)–(6.4) for diffusion and reaction inside the alginate bead. Because the fluxes of glucose, ethanol, and oxygen into or from the beads are numerical functions, commercial software packages for solving partial differential equations were not applicable. For each step in time the bulk fluid concentrations

in the reactor were calculated using the bead concentrations at the previous time step. Then the bead concentration profiles were updated and the bulk fluid concentrations were computed again for the same time step. The iteration proceeded until the bulk fluid concentrations changed by less than 1.0 x 10^{-5} g/l. Equations (6.16)–(6.18) were solved for a time step of 0.005 hr and a reactor step size of 6.08 cm. The program listing used to compute the reactor concentrations is given in the Appendix.

6.2.2 Continuous Stirred Tank Reactor

Unsteady-state mass balances on the fluid phase of a heterogeneous, continuous stirred tank reactor result in the following partial differential equations for glucose, ethanol, and dissolved oxygen concentrations in the bulk fluid:

$$\frac{\partial s}{\partial t} = \left(\frac{F}{V_R(1-A_g)}\right)(s_{feed} - s) - 3D_g \frac{\partial s}{\partial r}\Big|_{r=R} \frac{A_g}{R(1-A_g)} \tag{6.25}$$

$$\frac{\partial e}{\partial t} = \left(\frac{F}{V_R(1-A_g)}\right)(-e) - 3D_e \frac{\partial e}{\partial r}\Big|_{r=R} \frac{A_g}{R(1-A_g)} \tag{6.26}$$

$$\frac{\partial O_2}{\partial t} = \left(\frac{F}{V_R(1-A_g)}\right)(O_{2,feed} - O_2) - 3D_O \frac{\partial O_2}{\partial r}\Big|_{r=R} \frac{A_g}{R(1-A_g)}, \tag{6.27}$$

where s is the bulk fluid glucose concentration (g/l), e is the bulk fluid ethanol concentration (g/l), O_2 is the dissolved oxygen concentration (% air saturation), F is the volumetric flow rate (cm^3/hr), V_R is the volume of the reactor (cm^3), A_g is the volume fraction of the reactor occupied by alginate, R is the bead radius (cm), D_g is the diffusion coefficient of glucose (cm^2/hr), D_e is the diffusion coefficient of ethanol (cm^2/hr), D_O is the diffusion coefficient of oxygen (cm^2/hr), and t is time (hr). The appropriate initial conditions are:

$$s(0) = s_{feed} \tag{6.28}$$

$$e(0) = 0 \tag{6.29}$$

$$O_2(0) = O_{2,feed}. \tag{6.30}$$

The glucose, ethanol, and dissolved oxygen concentrations are functions of time only since the reactor is thoroughly mixed. Equations (6.25)–(6.27) were solved with initial conditions (6.28)–(6.30) by the Keller box method of finite differences as described in the previous section for the plug flow reactor. The program listing for the continuous stirred tank reactor is also included in the Appendix.

6.3 REACTOR PERFORMANCE

The mathematical models described in the previous sections were employed to simulate the operation of a heterogeneous PFR and a heterogeneous CSTR. There are three criteria that are important in evaluating the reactor performance. They are: 1) effluent ethanol concentration, 2) ethanol productivity, and 3) ethanol yield. The ethanol concentration in the effluent stream determines the cost of recovering the product since more dilute ethanol streams require more energy to purify. The ethanol productivity is the effluent ethanol concentration times the volumetric flow rate divided by the volume of the reactor. Ethanol productivity is a measure of the rate at which a product is available for a given reactor size, or capital investment. The ethanol yield equals the effluent ethanol concentration divided by the feed glucose concentration and is a measure of how efficiently the feed stream is utilized.

An immobilized cell PFR and an immobilized cell CSTR were designed to produce approximately 500 g ethanol per hour when the biomass concentration

reaches its maximum level. In all of the reactor simulations it is assumed that alginate beads containing 10.0 g DW/l are available at the start of the reactor operation. Alginate occupies 50 % of the PFR volume and 10 % of the CSTR volume, since the PFR is a packed bed and the CSTR requires thorough mixing. The maximum biomass concentration permitted anywhere in the alginate beads is 200 g DW/l or approximately 100 % of the bead volume. The PFR volume is 2.17 liters with a cross-sectional area to length ratio of 0.6. The CSTR requires a volume of 10.85 liters to produce ethanol at a rate similar to the rate for the 2.17 liter PFR.

The effects of four operating conditions on the reactor performances were investigated. The diameter of the alginate beads, the reactor residence time, the glucose feed concentration, and the concentration of dissolved oxygen during start-up were varied in PFR and CSTR simulations.

6.3.1 Plug Flow Reactor

The behavior of a heterogeneous plug flow reactor was modeled for the first 20 hours of operation. First, the effects of the alginate bead size, glucose feed concentration, and residence time were investigated for anaerobic reactor conditions. Next, the effect of supplying oxygen to the feed stream was examined. Oxygen increases the growth rate of *S. cerevisiae* but decreases the specific glucose uptake rate and specific ethanol production rate. Thirdly, the reactor residence time was decreased for the first eight hours of operation in order to improve the ethanol yield and productivity during start-up.

The effluent ethanol concentrations of a plug flow reactor with bead diameters of 1 mm, 2 mm, and 5 mm and a volumetric flow rate of 12.7 l/hr are

shown in Figure 6.1 for a glucose feed concentration of 100 g/l. The area under the curves is proportional to the reactor productivity, since the flow rate and reactor volume are constant. The ethanol yield is also proportional to the area under the curve since the yield is based on feed glucose, not on the amount of glucose utilized in the reactor. For the first two hours of operation the bead size does not affect the reactor performance because initially the beads contain 100 g/l glucose. However, after two hours the effluent ethanol concentration, ethanol productivity, and ethanol yield decrease when the bead diameter is increased from 1 mm to 5 mm. As the biomass concentration in the reactor increases and the bulk glucose concentration decreases, the effect of the bead size becomes more significant. At steady state, a 5 mm diameter bead results in 66 % of the ethanol productivity and yield achieved with a 1 mm diameter bead. A 2 mm diameter bead has 95% of the ethanol productivity and yield of a 1 mm diameter bead.

Figure 6.2 shows the effect of bead diameter at the same flow rate of 12.7 l/hr but for a glucose feed concentration of 200 g/l. The results are similar to, but slightly less significant than, the results for a feed glucose concentration of 100 g/l. At steady state a 5 mm diameter bead has an ethanol concentration, productivity, and yield of 75 % of that for a 1 mm diameter bead. A 2 mm diameter bead has 96 % of the ethanol concentration of a 1 mm diameter bead at steady state. Thus, for higher glucose feed concentrations, the diameter of the alginate bead has less effect on the reactor performance.

The effect of alginate bead size on reactor performance is shown in Figure 6.3 for a feed glucose concentration of 200 g/l and a flow rate of 4.0 l/hr, which is roughly one-third of the flow rate in Figures 6.1 and 6.2. Although steady

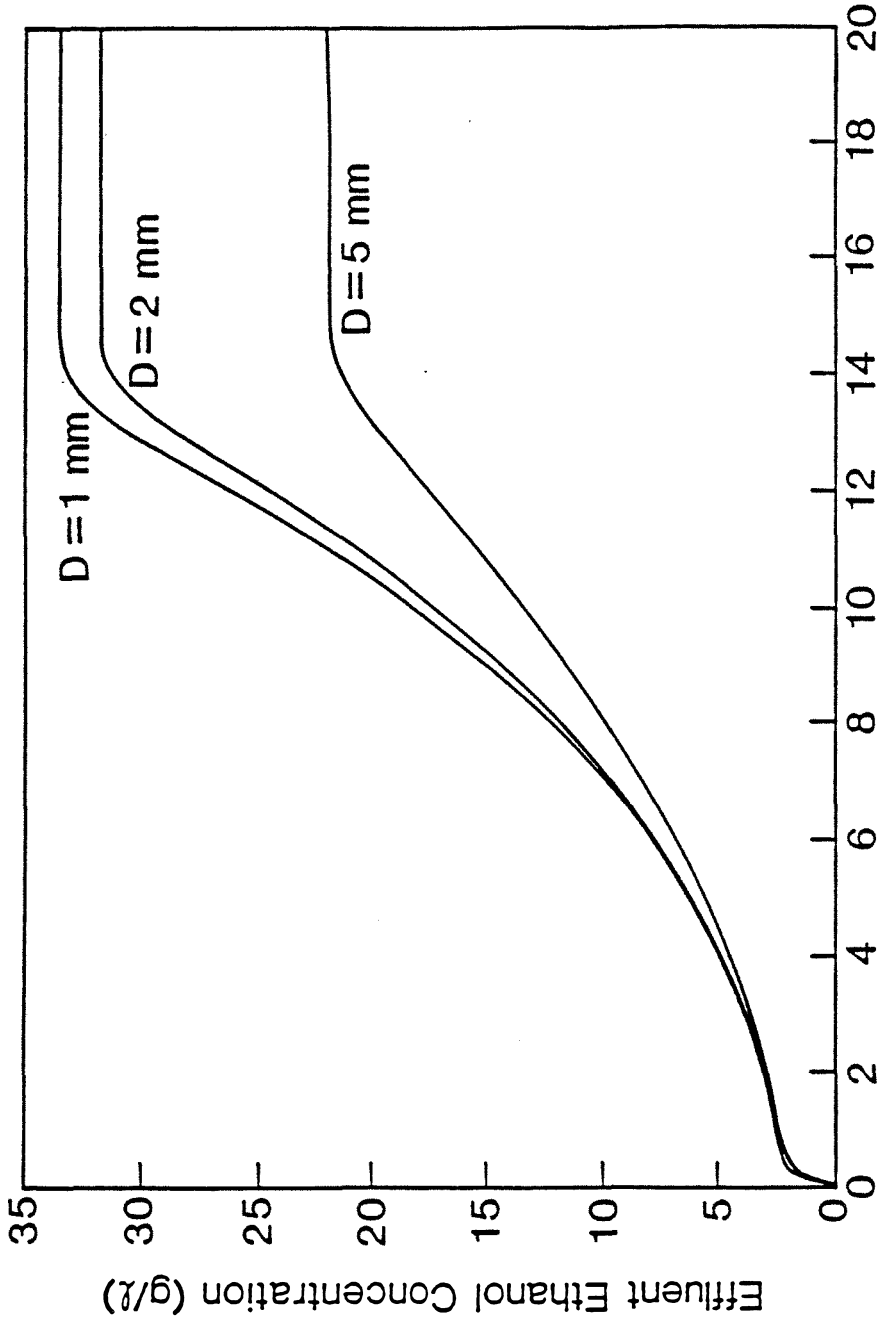

Figure 6.1 **Effect of Bead Diameter on Effluent Ethanol Concentration of an immobilized cell PFR with a feed glucose concentration of 100 g/l and a residence time of 0.17 hours.**

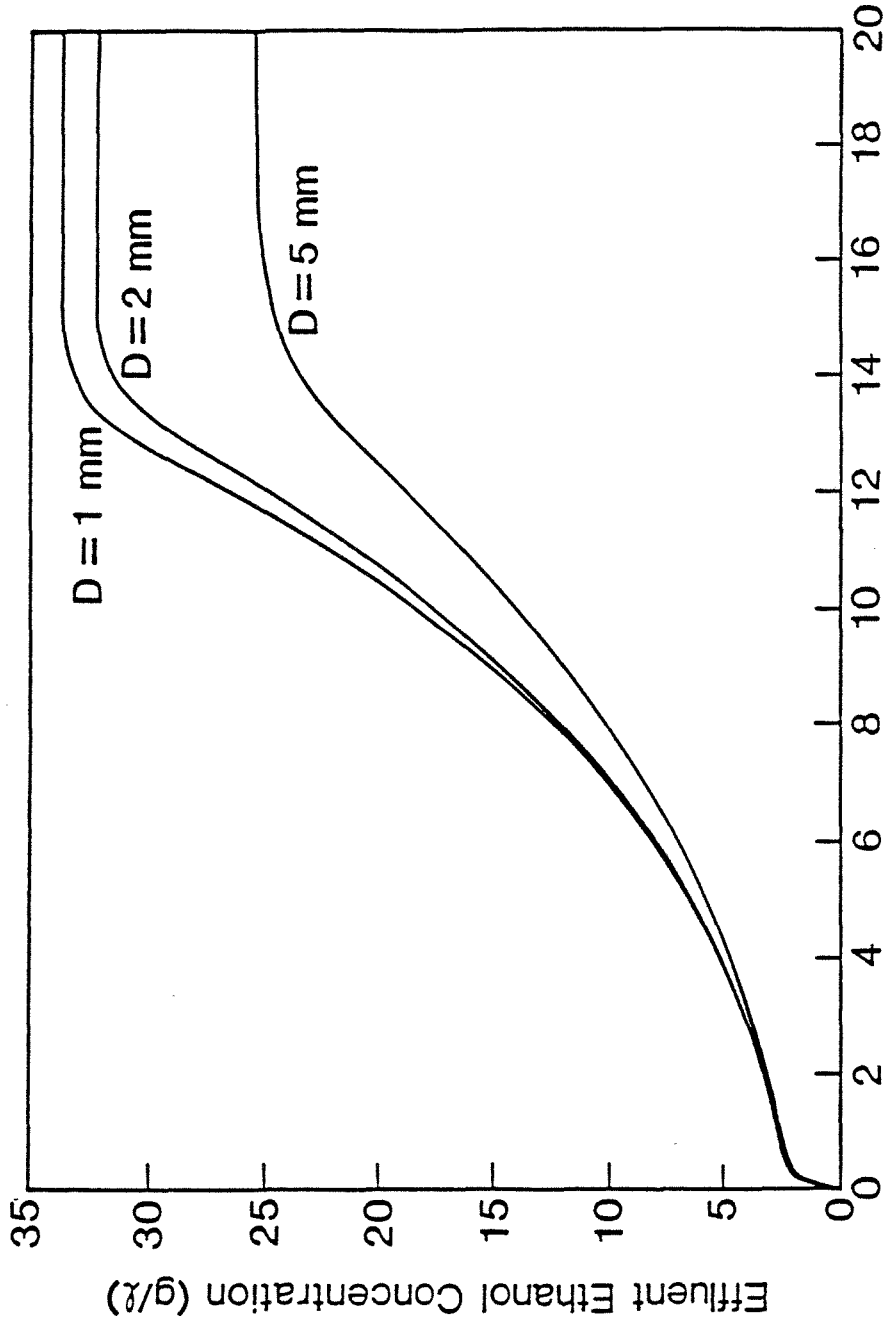

Figure 6.2 **Effect of Bead Diameter on Effluent Ethanol Concentration of an immobilized cell PFR with a feed glucose concentration of 200 g/l and a residence time of 0.17 hours.**

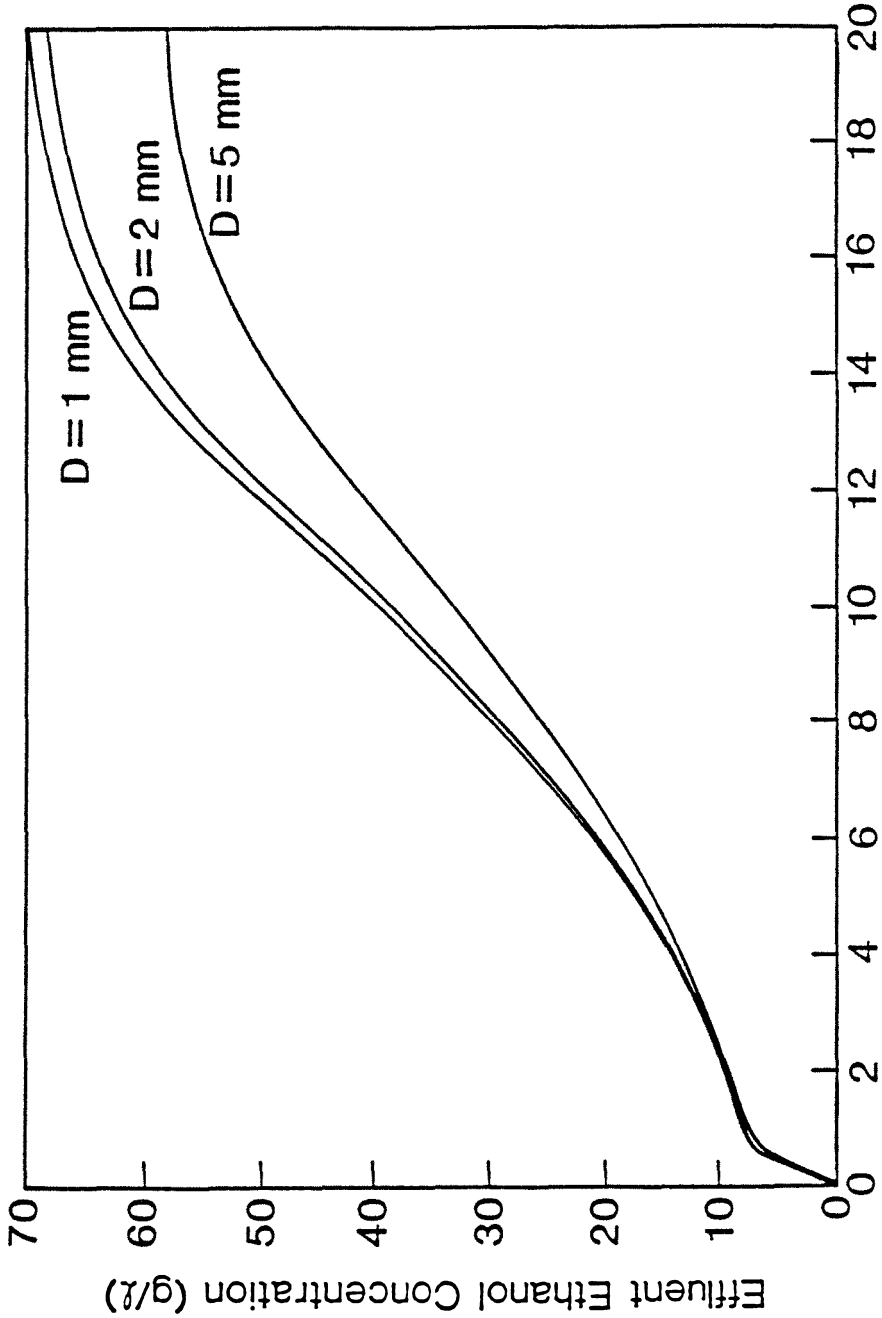

Figure 6.3 **Effect of Bead Diameter on Effluent Ethanol Concentration of an immobilized cell PFR with a feed glucose concentration of 200 g/l and a residence time of 0.54 hours.**

state has not been reached after 20 hours of reactor operation, Figure 6.3 illustrates that the effect of alginate bead size is similar at lower flow rates.

Further reactor simulations were performed with 1 mm and 2 mm diameter beads. 2 mm diameter beads are probably optimum because smaller alginate beads are more difficult to produce and are weaker mechanically. The decrease in the reactor performance caused by the bead size is relatively small for 2 mm diameter beads.

Figures 6.4–6.7 show the effects of varying the reactor residence time for 1 mm and 2 mm diameter beads in a plug flow reactor with glucose feed concentrations of 100 g/l and 200 g/l. Residence time appears to affect the reactor performance similarly for both bead diameters and both glucose feed concentrations. As the residence time increases, the effluent ethanol concentration also increases during both the initial and steady-state reactor operation. Doubling the reactor residence time results in a 69% increase in the ethanol yield but a 17% decrease in the ethanol productivity of the reactor for 2 mm diameter beads and 100 g/l glucose feed concentration.

The ethanol productivity at steady state is shown in Figure 6.8 as a function of the reactor residence time for 1 mm and 2 mm diameter beads and glucose feed concentrations of 100 g/l and 200 g/l. For all reactor conditions the ethanol productivity of the reactor decreases monotonically with respect to residence time. At low residence times the ethanol productivity is more sensitive to the residence time than at higher residence times. Increasing the feed glucose concentration from 100 g/l to 200 g/l has no effect on the steady-state reactor productivity at low residence times, but improves the reactor productivity at high residence times. On the other hand, decreasing the bead

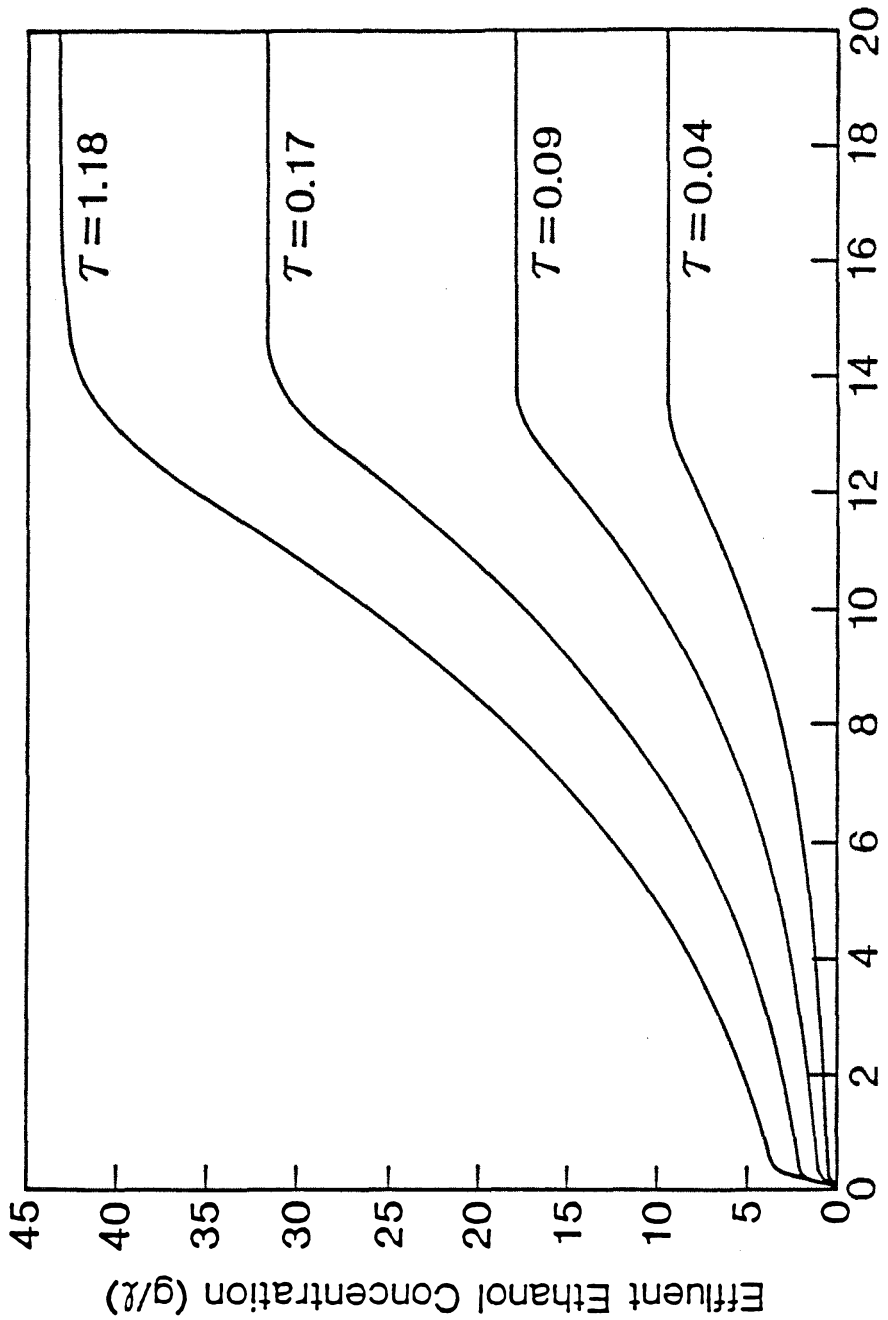

Figure 6.4 **Effect of Residence Time on Effluent Ethanol Concentration of an immobilized cell PFR with a feed glucose concentration of 100 g/l and a bead diameter of 2 mm.**

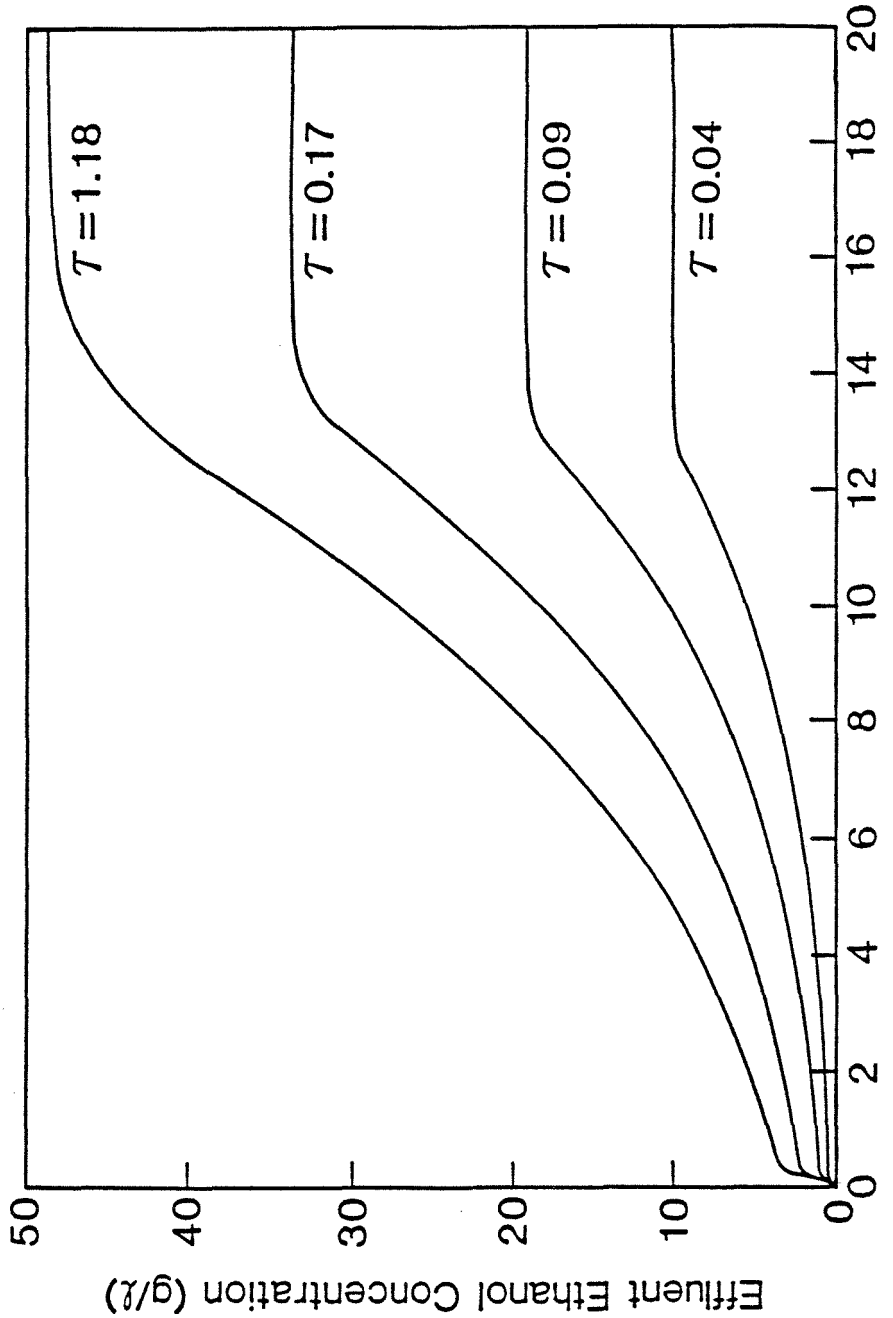

Figure 6.5 **Effect of Residence Time on Effluent Ethanol Concentration of an immobilized cell PFR with a feed glucose concentration of 100 g/l and a bead diameter of 1 mm.**

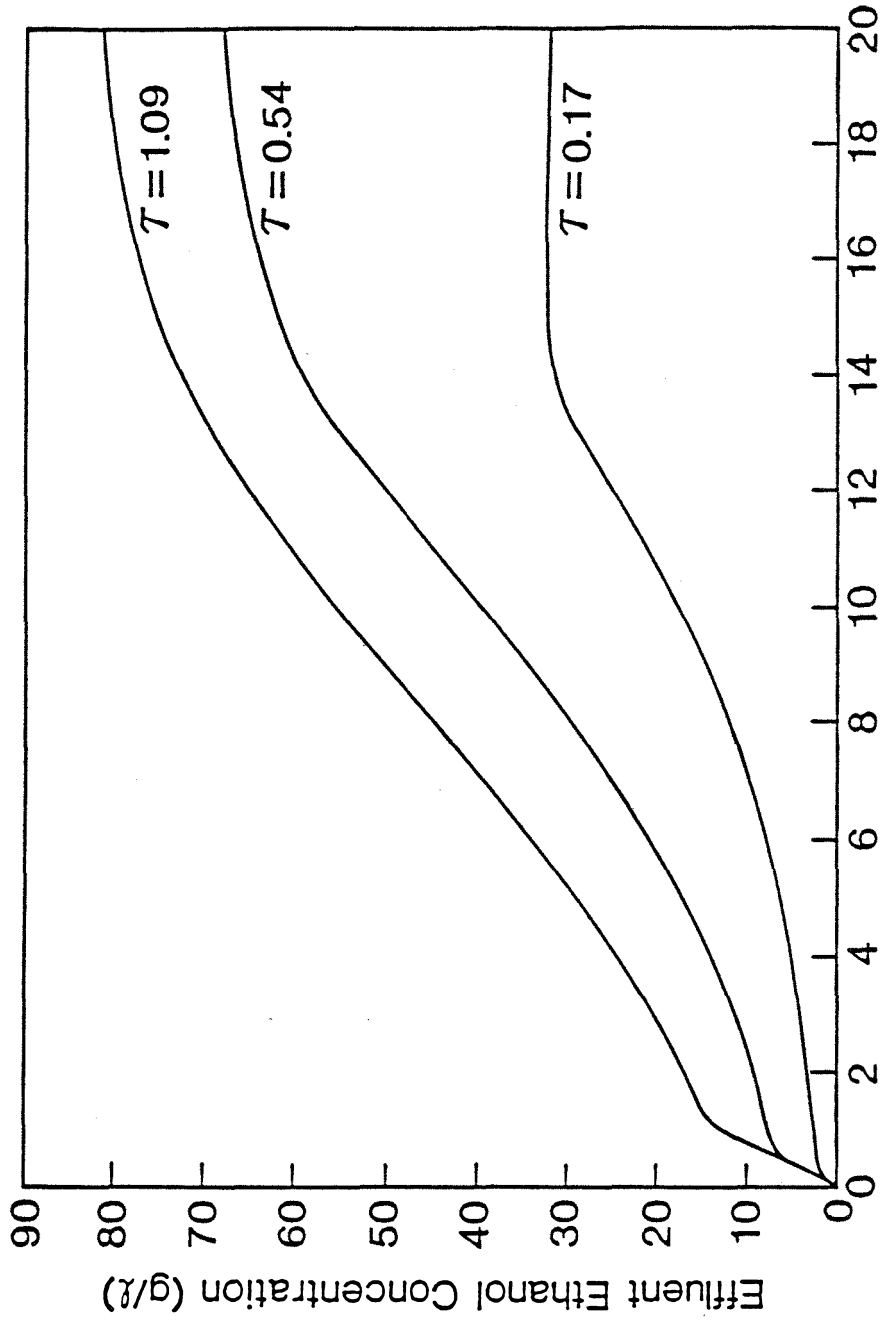

Figure 6.6 **Effect of Residence Time on Effluent Ethanol Concentration of an immobilized cell PFR with a feed glucose concentration of 200 g/l and a bead diameter of 2 mm.**

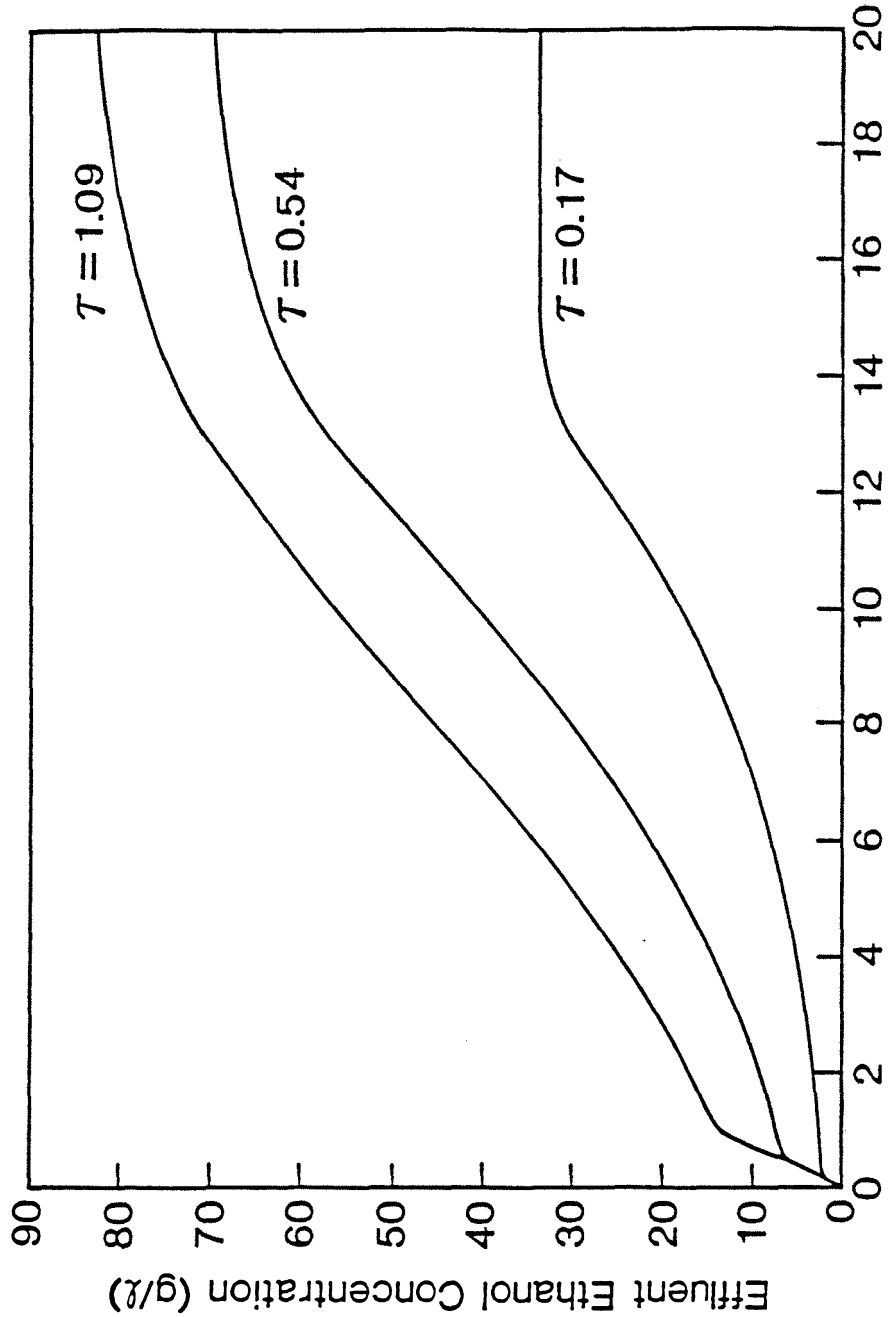

Figure 6.7 **Effect of Residence Time on Effluent Ethanol Concentration of an immobilized cell PFR with a feed glucose concentration of 200 g/l and a bead diameter of 1 mm.**

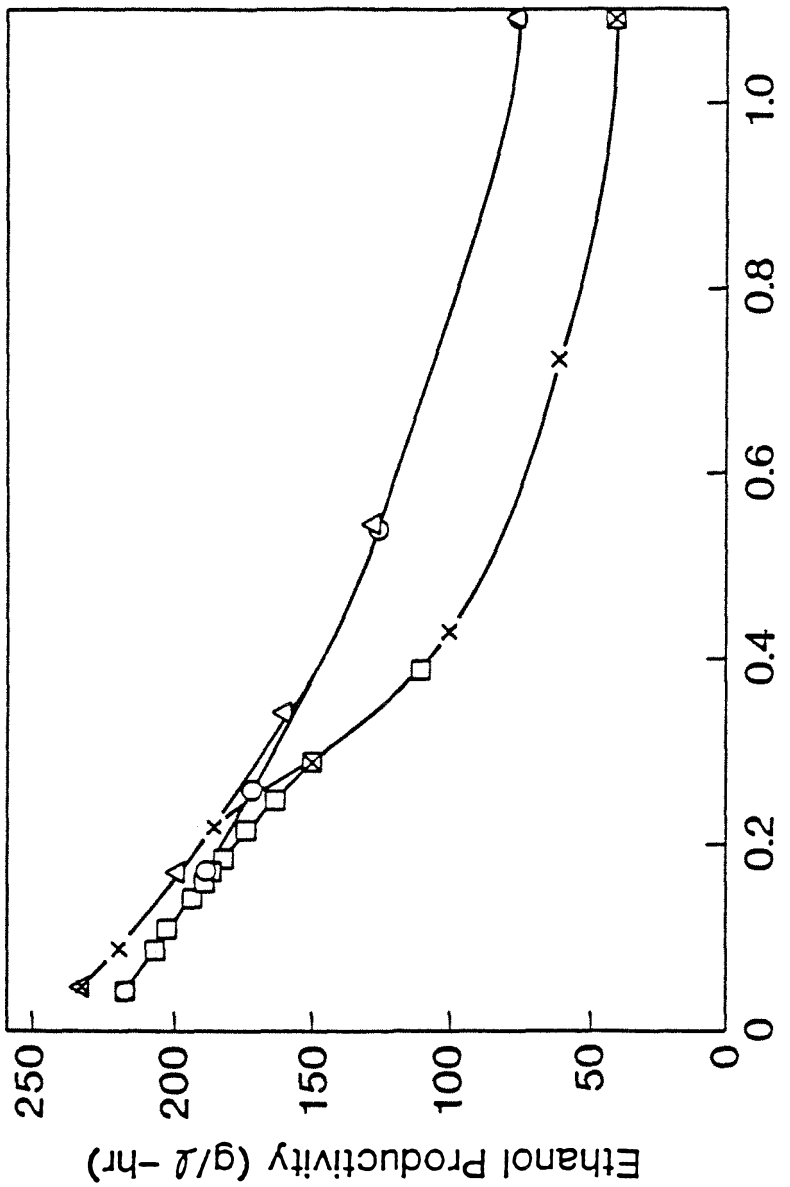

Figure 6.8 **Effect of Residence Time on Ethanol Productivity of an immobilized cell PFR at its maximum biomass loading, $(\square)s_f$ = 100 g/l and D = 2 mm, $(x)s_f$ = 100 g/l and D = 1 mm, $(\bigcirc)s_f$ = 200 g/l and D = 2 mm, $(\Delta)s_f$ = 200 g/l and D = 1 mm.**

diameter improves the ethanol productivity at low residence times but has no effect at high residence times.

The effect of residence time on the steady-state ethanol yield of a PFR is shown in Figure 6.9 for bead diameters of 1 mm and 2 mm and glucose feed concentrations of 100 g/l and 200 g/l. In general, the ethanol yield increases rapidly with residence time at low residence times until the maximum ethanol yield is reached. For 100 g/l glucose feed concentration, the maximum ethanol yield is reached at a residence time of about 0.3 hours, but for a feed glucose concentration of 200 g/l the maximum ethanol yield requires a residence time of more than 1.1 hours. The size of the alginate beads has virtually no effect on the ethanol yield for all residence times less than 1.1 hours.

The steady-state PFR effluent ethanol concentration is shown in Figure 6.10 as a function of residence time for 1 mm and 2 mm diameter beads and 100 g/l and 200 g/l glucose feed concentrations. The effluent ethanol concentration increases rapidly at low residence times, then approaches a maximum concentration at higher residence times. Increasing the glucose feed concentration from 100 g/l to 200 g/l results in a significantly higher effluent ethanol concentration at high residence times, but has no affect at low residence times. As with the ethanol yield, the size of the alginate beads is unimportant for the effluent ethanol concentration at all residence times.

The immobilized cell PFR described previously should be operated at a residence time of about 0.22 hours for a feed glucose concentration of 100 g/l and 2 mm diameter beads. With a residence time of 0.22 hours, the ethanol productivity of the reactor is 175 g/l-hr and the effluent ethanol concentration from the reactor is 38 g/l. The ethanol yield based on glucose feed is 0.38.

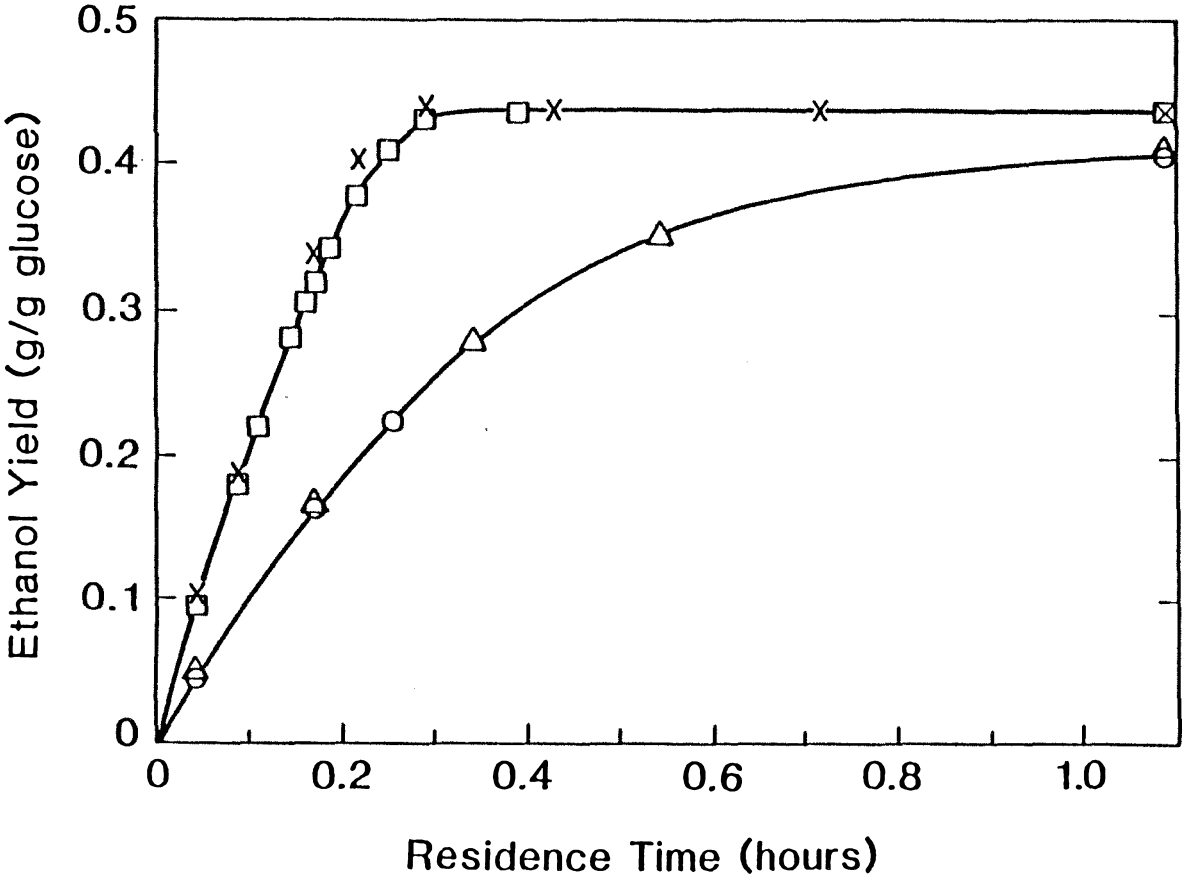

Figure 6.9 **Effect of Residence Time on Ethanol Yield of an immobilized cell PFR at its maximum biomass loading, (□)s_f = 100 g/l and D = 2 mm, (x)s_f = 100 g/l and D = 1 mm, (○)s_f = 200 g/l and D = 2 mm, (Δ)s_f = 200 g/l and D = 1 mm.**

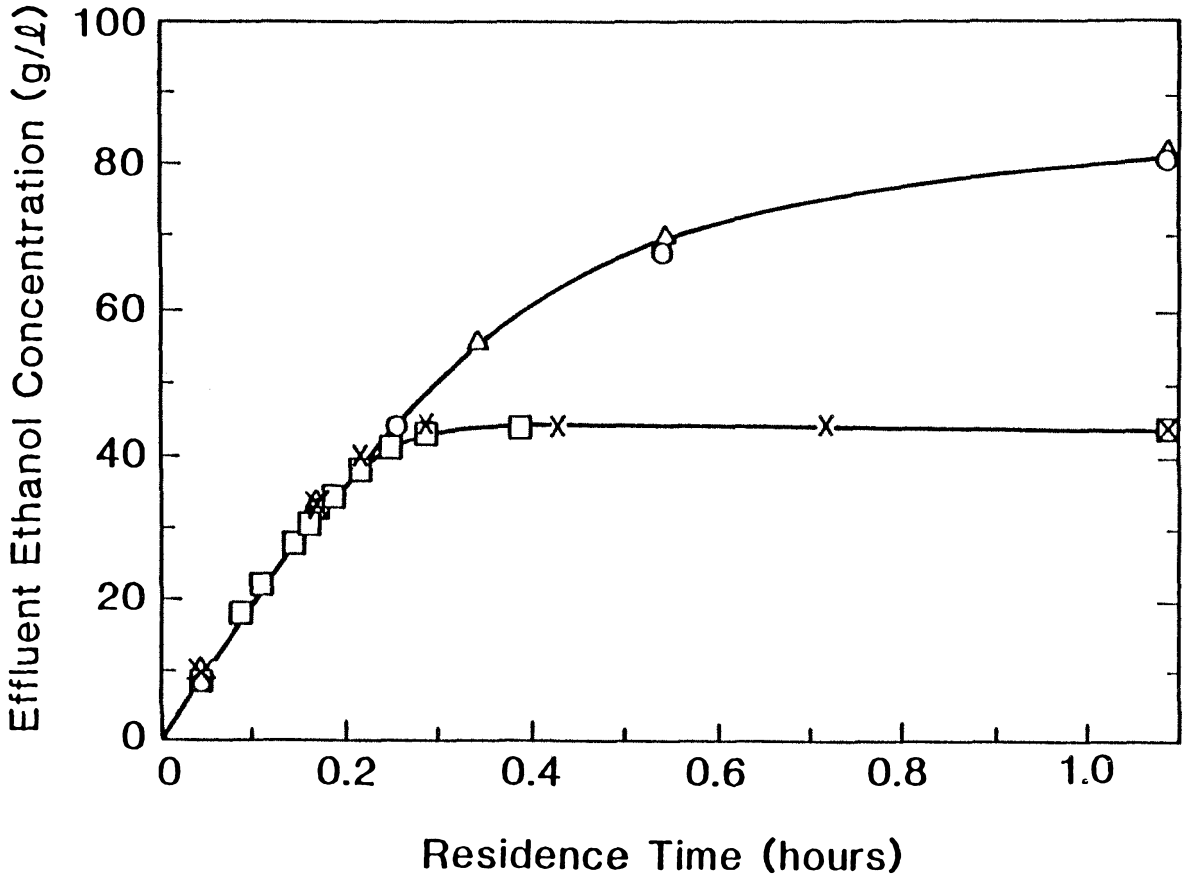

Figure 6.10 **Effect of Residence Time on Effluent Ethanol Concentration of an immobilized cell PFR at its maximum biomass loading, (□)s_f = 100 g/l and D = 2 mm, (x)s_f = 100 g/l and D = 1 mm, (○)s_f = 200 g/l and D = 2 mm, (Δ)s_f = 200 g/l and D = 1 mm.**

Further increases in the residence time above 0.22 hours results in slightly higher effluent ethanol concentrations and ethanol yields, but significantly lower ethanol productivities. Decreasing the residence time below 0.22 hours will produce an unacceptably low effluent ethanol concentration and ethanol yield.

If the reactor is operated with a feed stream containing 200 g/l glucose, higher residence times are required to use the glucose feed stream efficiently. At a residence time of 0.54 hours the ethanol yield has reached only 0.34 when the glucose feed concentration is 200 g/l and 2 mm diameter beads are used. The ethanol productivity of the reactor is 125 g/l-hr, which is 28 % less than the ethanol productivity for a residence time of 0.22 hours and 100 g/l glucose feed. The effluent ethanol concentration, however, is 68 g/l for the reactor with a 200 g/l glucose feed stream. The higher effluent ethanol concentration simplifies downstream processing. By increasing the feed glucose concentration, the effluent ethanol concentration can be increased proportionally, but the residence time must be increased as well, leading to a lower reactor productivity. The choice between a 100 g/l and a 200 g/l feed stream will depend on the cost of the feed streams and the cost of purifying the ethanol downstream. In a commercial process, conservation of the glucose feed stream can be important in determining the reactor operating conditions. Changing from 2 mm diameter beads to 1 mm diameter beads has no significant effect on the reactor performance.

The distributions of biomass in the alginate beads at various times after reactor start-up are shown in Figure 6.11. The biomass profiles in the alginate beads are shown at the reactor inlet and the reactor outlet for time equal to 5,

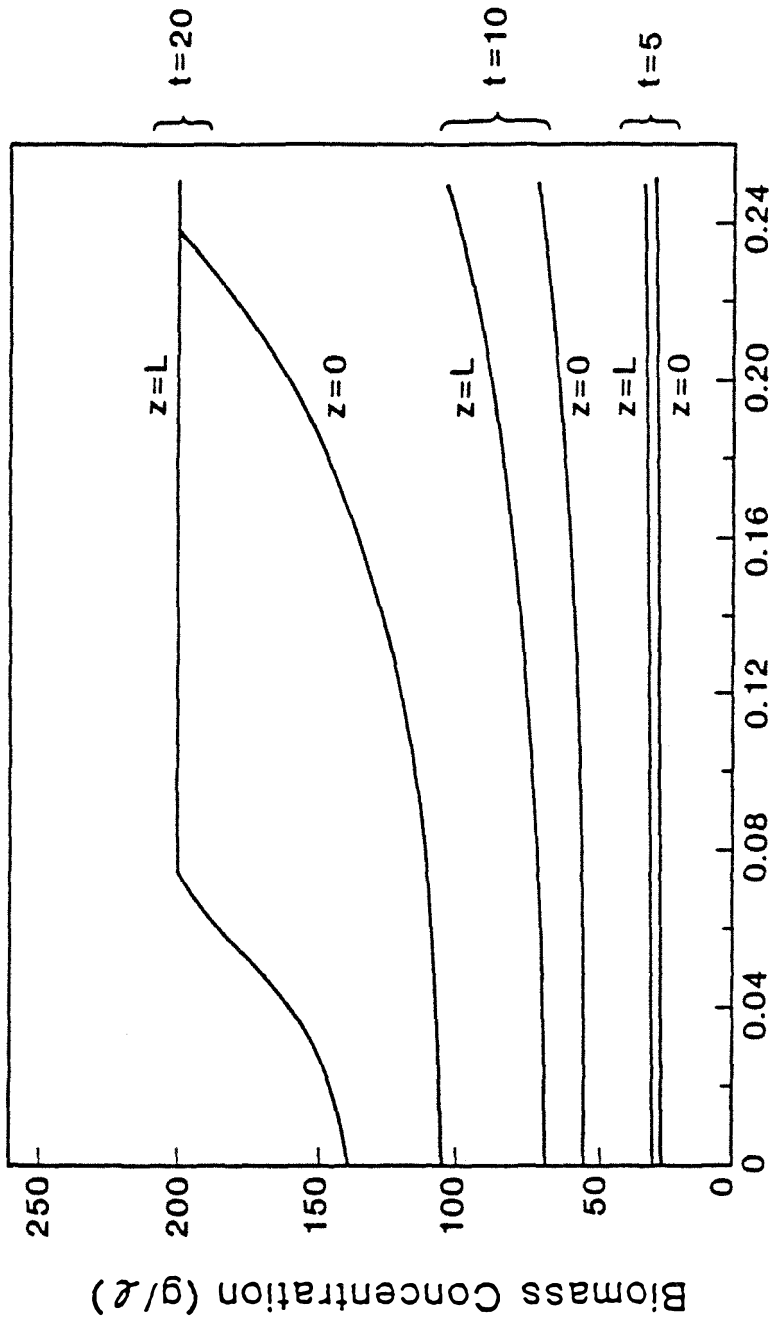

Figure 6.11 **Biomass Concentration Profile in Alginate Bead of an immobilized cell PFR at t = 5, 10, and 20 hours after start-up for 5 mm diameter beads located at the reactor inlet (z = 0) or reactor outlet (z = L) and a residence time of 0.54 hours.**

10, and 20 hours after reactor start-up. The reactor simulations were carried out for 5 mm diameter beads and a feed glucose concentration of 200 g/l with a reactor residence time of 0.54 hours. Five hours after start-up the biomass concentration was uniformly distributed throughout the alginate beads at both the reactor inlet and outlet. Ten hours after start-up, the biomass in the outer region of the alginate beads had begun to increase more rapidly than the biomass towards the center of the beads. Also at ten hours, the beads near the reactor outlet had less biomass than the beads near the reactor inlet. After 20 hours of reactor operation, the biomass concentration was distributed nonuniformly in the alginate beads. For beads close to the reactor inlet, the outer region of the beads contained the maximum biomass concentration, while the inner region contained less biomass. Approximately 97 % of the alginate bead volume contained the maximum biomass concentration. Beads close to the reactor outlet also had a nonuniform distribution of biomass, but the maximum biomass concentration had been reached in only 12 % of the alginate bead volume.

The biomass concentration averaged over the bead volume is shown in Figure 6.12 as a function of distance from the reactor inlet for 5, 10, and 20 hours after reactor start-up. The reactor operation was simulated for a glucose feed concentration of 200 g/l and a 5 mm bead diameter. Five hours after start-up, the biomass concentration is uniform throughout the reactor for residence times of both 0.17 and 0.54 hours. After ten hours of operation, the biomass becomes unevenly distributed with the higher biomass concentration towards the reactor inlet. Also the residence time affects the biomass concentration after ten hours of operation. A lower reactor residence time results in a higher biomass concentration in the reactor. As the reactor operation continues to 20

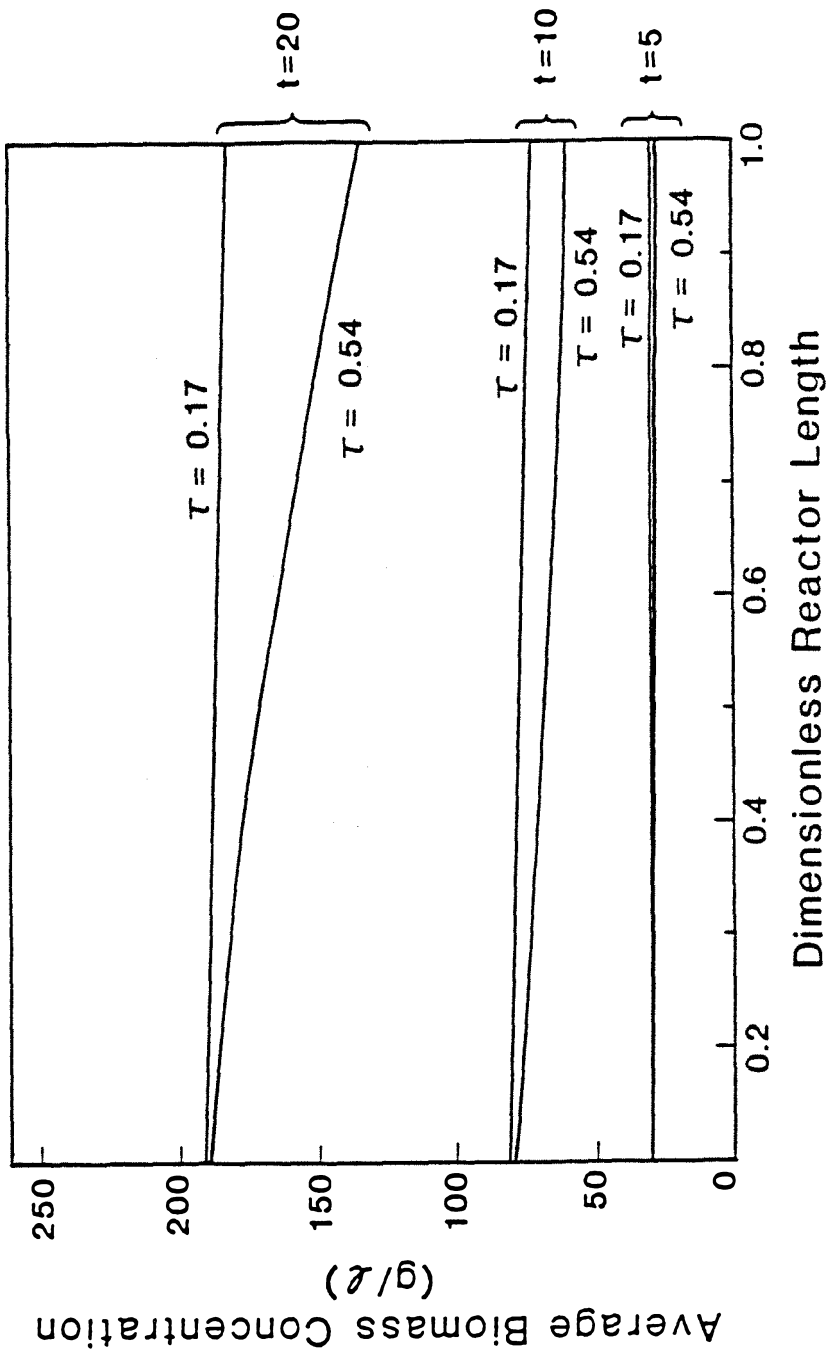

Figure 6.12 **Biomass Concentration in Immobilized Cell PFR as a function of distance from the reactor inlet for 5 mm diameter beads at t = 5, 10, and 20 hours after start-up and residence times of 0.17 and 0.54 hours.**

hours, the biomass distribution becomes more nonuniform.

The concentration of dissolved oxygen in the feed stream can affect the PFR performance. Figure 6.13 shows the effluent ethanol concentration versus time for a PFR with a 100 g/l glucose feed stream and 2 mm diameter beads and a residence time of 0.25 hours. Supplying oxygen in the feed stream at 50 or 100 % of air saturation enhances the reactor performance during the first twelve hours of operation compared to the performance for an anaerobic feed stream. After the first twelve hours, however, the anaerobic feed stream produces the highest ethanol productivity, yield, and effluent concentration. Oxygen increases the growth rate of *S. cerevisiae* but decreases the specific ethanol production rate of the organism. Thus, during the first twelve hours the reactor performs better when oxygen is supplied because the biomass concentration increases more rapidly. As the maximum biomass concentration is approached at later times, oxygen decreases the reactor performance by decreasing the specific ethanol production rate. The effect of supplying oxygen during the first eight hours of operation, then switching to anaerobic feed, is shown in Figure 6.14. The highest ethanol productivity, yield and effluent concentration are reached by using a feed stream with a dissolved oxygen concentration of 100 % air saturation during the initial eight-hour period and then using anaerobic feed at all later times.

The effect of bead size on effluent ethanol concentration is shown in Figure 6.15 when oxygen is supplied to the reactor during the first eight hours of operation. The feed glucose concentration is 100 g/l and the residence time is 0.25 hours. The dissolved oxygen concentration in the feed stream is 100 % air saturation during the first eight hours and 0 % air saturation at later

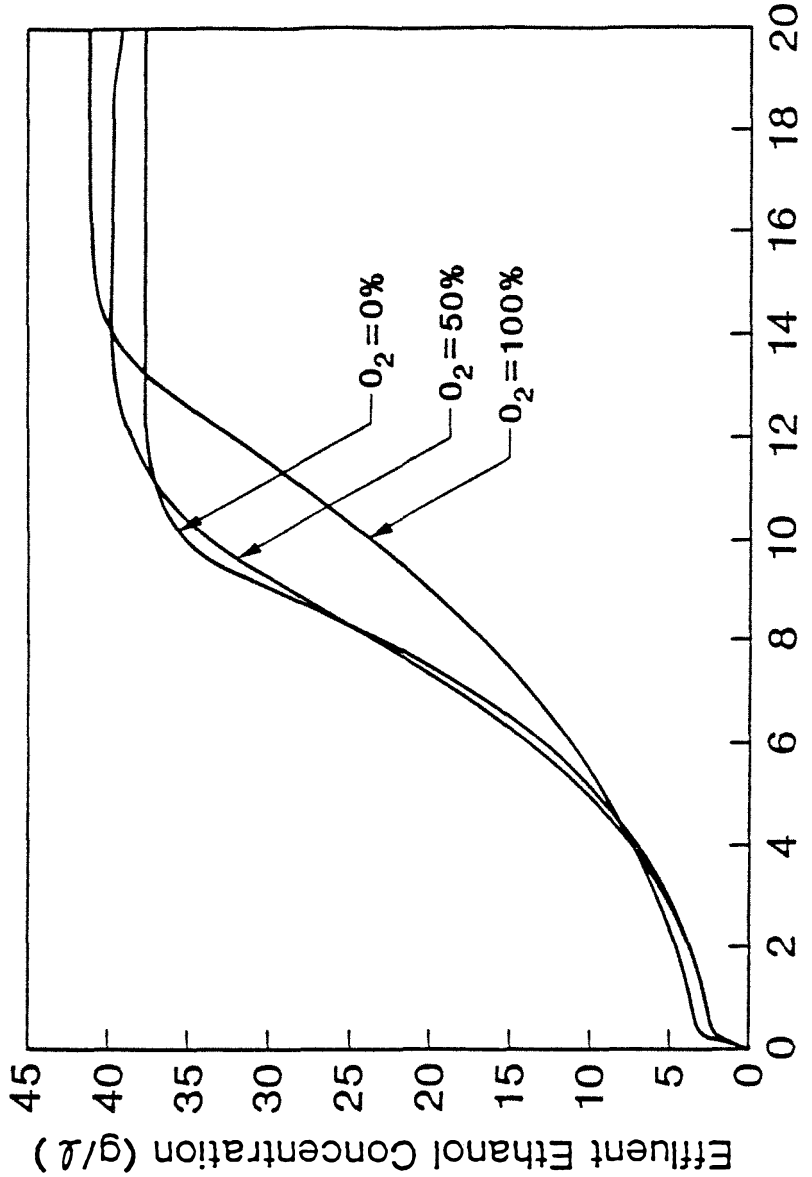

Figure 6.13 **Effect of Dissolved Oxygen Concentration in Feed Stream of immobilized cell PFR on effluent ethanol concentration for feed dissolved oxygen concentrations of 0, 50, and 100 % air saturation.**

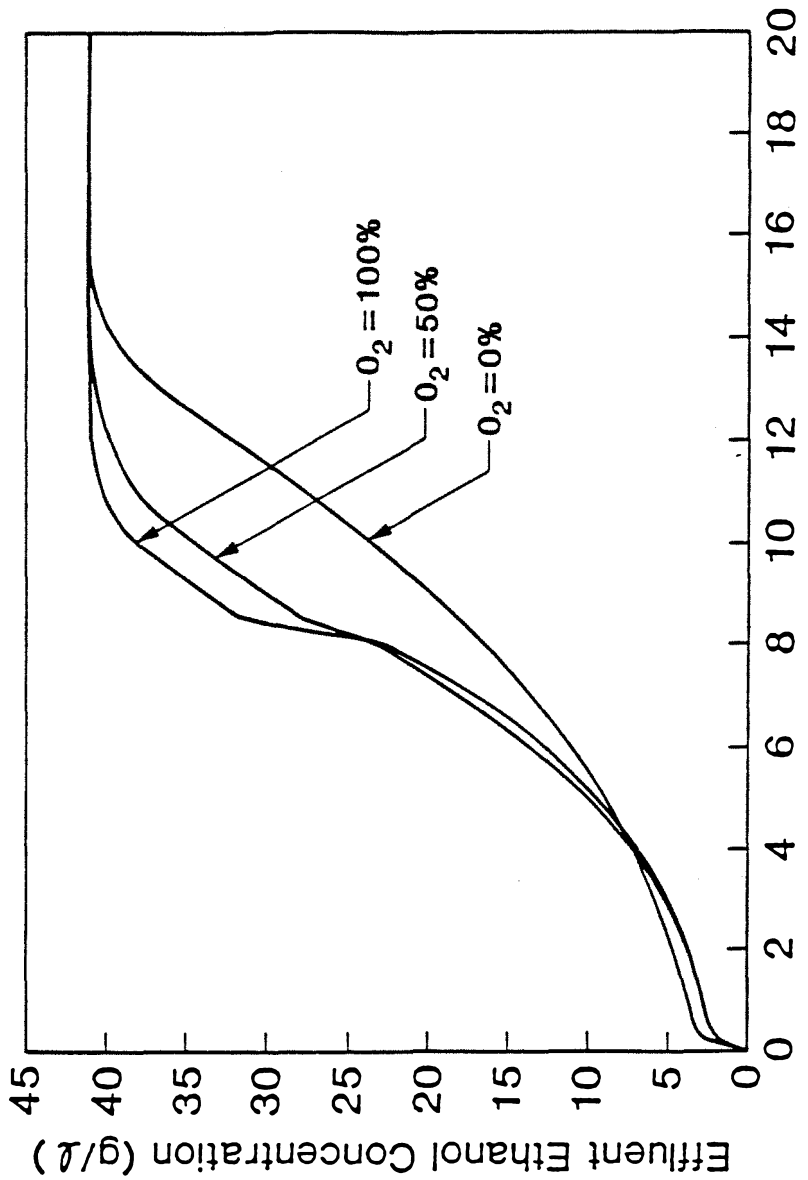

Figure 6.14 **Effect of Supplying Oxygen During First Eight Hours of Reactor Operation on effluent ethanol concentration for feed dissolved oxygen concentrations of 0, 50, and 100 % air saturation.**

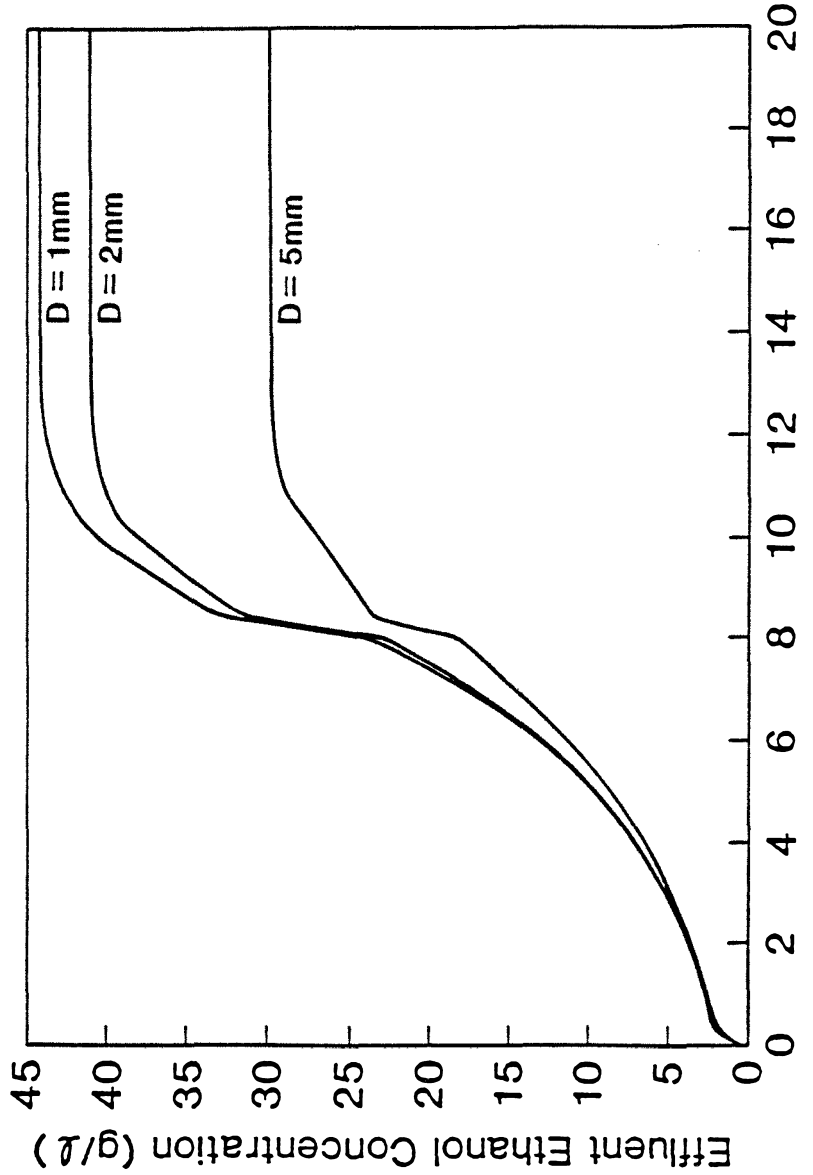

Figure 6.15 **Effect of Bead Diameter on Effluent Ethanol Concentration when dissolved oxygen is supplied in the feed stream of an immobilized cell PFR for the first eight hours of reactor operation.**

times. Figure 6.15 indicates that the alginate bead size in the reactor affects the aerobic reactor performance similarly to the way it affects the anaerobic reactor performance.

The residence time of the PFR was decreased during the start-up period in an attempt to increase the ethanol effluent concentration during start-up. The results are shown in Figure 6.16 for a glucose feed concentration of 100 g/l and 2 mm diameter beads with a final residence time of 0.25 hours. Increasing the reactor residence time from 0.25 to 0.83 hours during the initial eight-hour period causes the ethanol effluent concentration to double at time equals eight-hours without affecting the effluent ethanol concentration at later times.

6.3.2 Continuous Stirred Tank Reactor

An immobilized cell CSTR was modeled in order to investigate the effects of bead size and residence time on the reactor performance. The effect of the alginate bead size is shown in Figure 6.17 for a feed glucose concentration of 100 g/l and a residence time of 1.08 hours. The ethanol productivity is proportional to the area under the curves, since the flow rate is constant in all three simulations. The ethanol yield is proportional to the effluent ethanol concentration because the yield is based on feed glucose. The ethanol productivity, yield, and effluent concentration decrease as the bead diameter increases for all times. At steady state a 5 mm diameter bead results in 67 % of the effluent ethanol concentration of a 1 mm diameter bead. A 2 mm diameter bead has 93 % of the ethanol effluent concentration of a 1 mm diameter bead. The alginate bead size affects the performance of a CSTR the same way it affects the performance of a PFR.

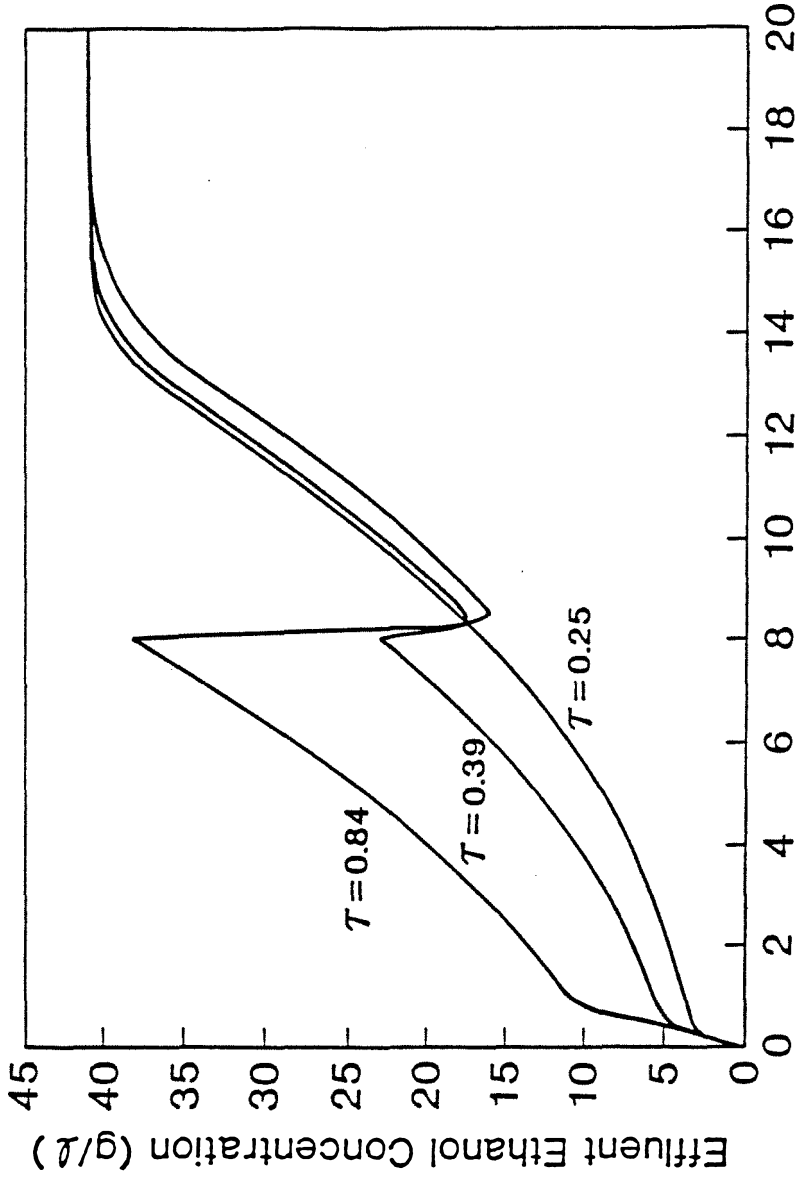

Figure 6.16 **Effect of Increasing Residence Time During Start-Up on effluent ethanol concentration from an immobilized cell PFR.**

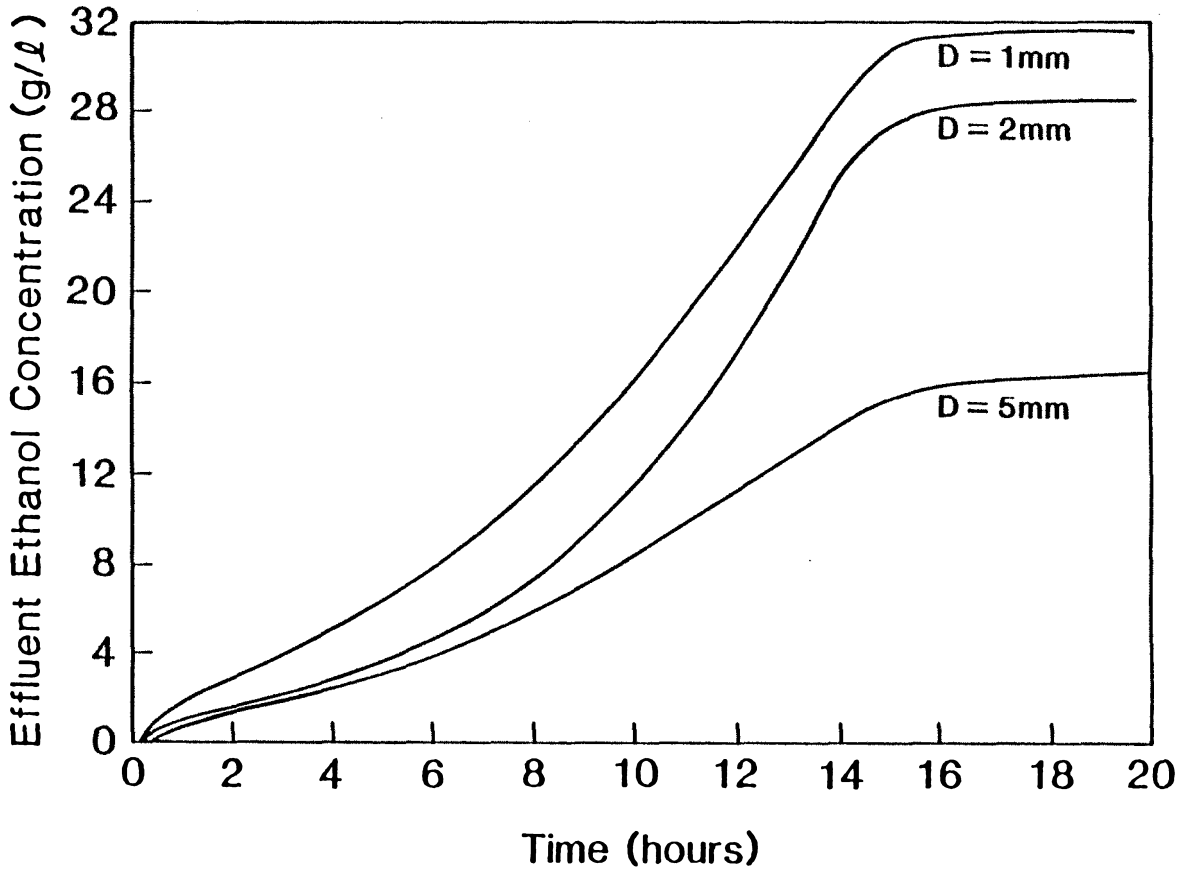

Figure 6.17 **Effect of Bead Diameter on Effluent Ethanol Concentration of an immobilized cell CSTR with a feed glucose concentration of 100 g/l and a residence time of 1.08 hours.**

Figure 6.18 shows the effect of the reactor residence time on the effluent ethanol concentration from a CSTR during the first 20 hours of operation. Increasing the residence time leads to an increase in the effluent ethanol concentration. When the residence time increases by a factor of 2.9 for a feed glucose concentration of 100 g/l and 2 mm diameter beads, the effluent ethanol concentration increases by a factor of 1.4 at steady state.

The steady-state ethanol productivity, ethanol yield, and effluent ethanol concentration are shown in Figures 6.19, 6.20, and 6.21, respectively, as a function of residence time for a CSTR with a feed glucose concentration of 100 g/l and a bead diameter of 2 mm. As for the PFR, the ethanol productivity decreases with residence time, and the ethanol yield and effluent concentration increase with residence time. At a residence time of 2.0 hours the ethanol yield is about 0.4 and the effluent ethanol concentration is close to 40 g/l. The ethanol productivity is about 20 g/l-hr at a residence time of 2.0 hours. The ethanol productivity of the CSTR is less than 12 % of the ethanol productivity of the PFR operating with a similar ethanol yield and effluent concentration. The lower ethanol productivity of the CSTR is due to the lower fraction of alginate beads compared to the PFR and the mixing characteristics of the CSTR. All of the alginate beads in the CSTR have surface concentrations of glucose and ethanol equal to the concentrations in the reactor outlet stream. The PFR contains alginate beads that have much higher glucose surface concentrations and much lower ethanol surface concentrations.

6.4 CONCLUSION

Mathematical models provide a useful tool for designing and optimizing

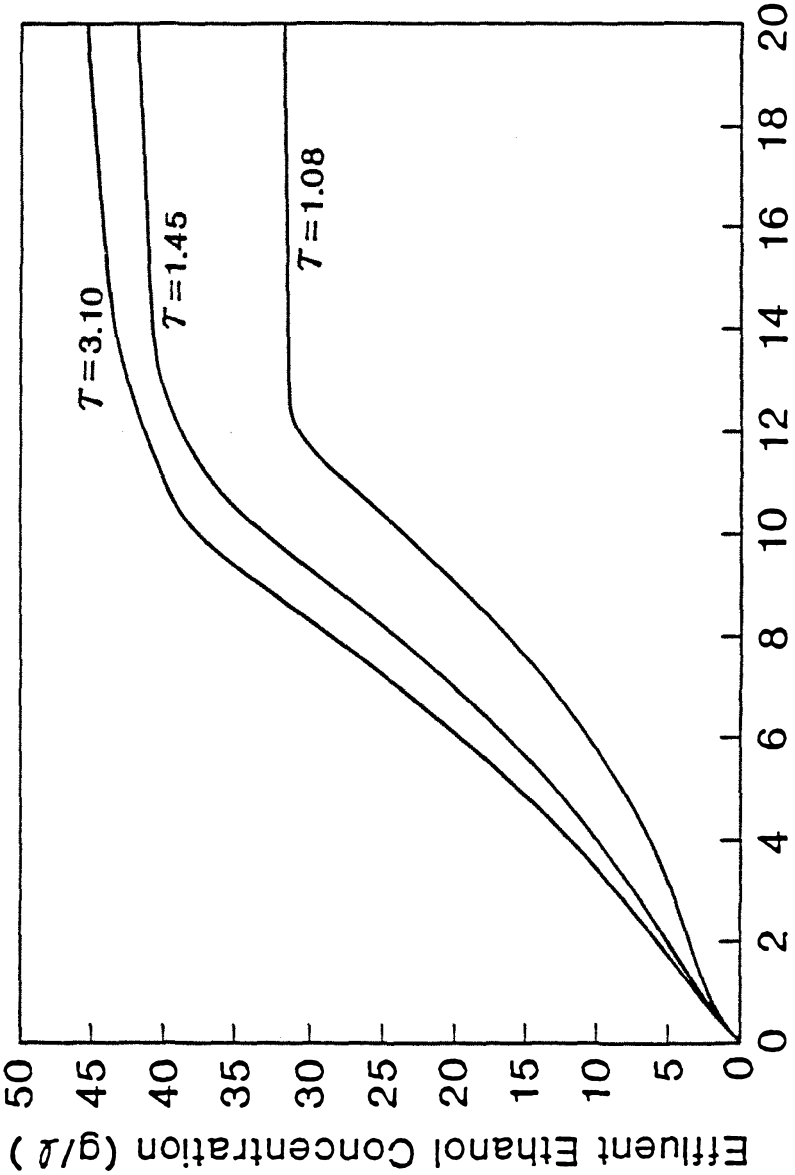

Figure 6.18 **Effect of Residence Time on Effluent Ethanol Concentration of an immobilized cell CSTR with a feed glucose concentration of 100 g/l and a bead diameter of 2 mm.**

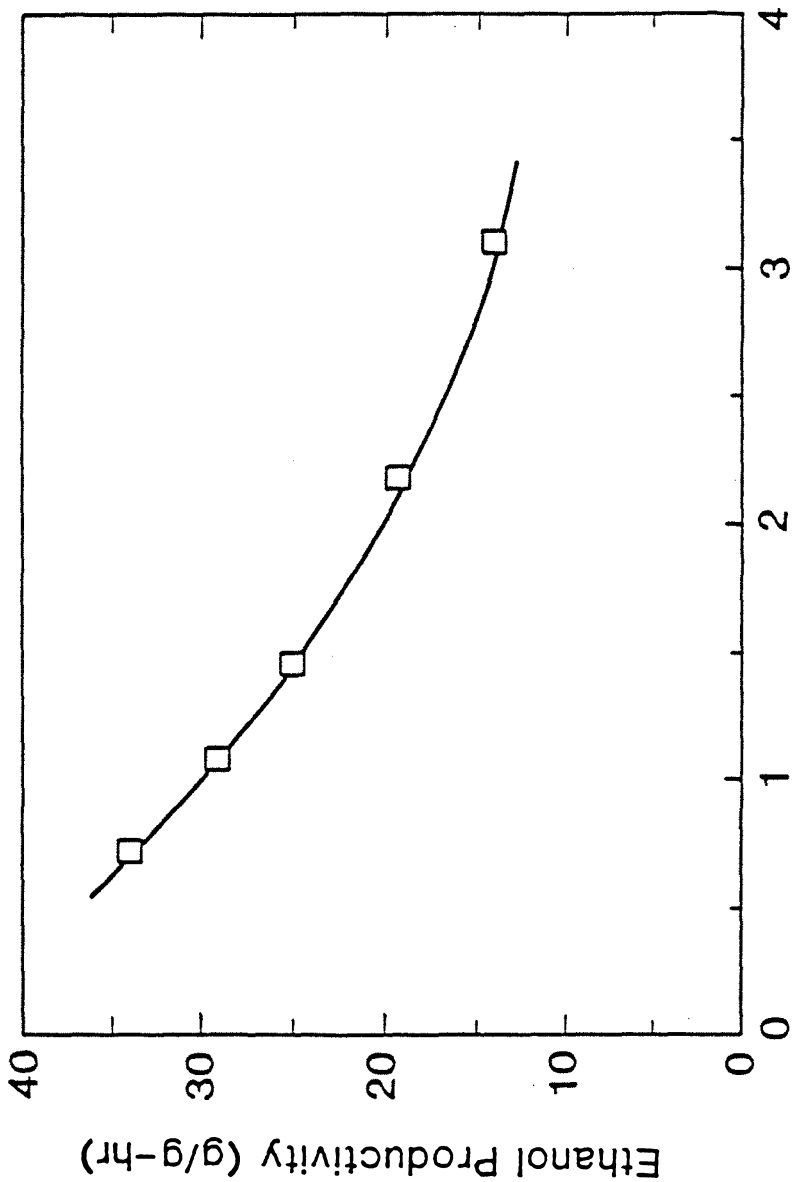

Figure 6.19 **Effect of Residence Time on Ethanol Productivity of an immobilized cell CSTR at its maximum biomass loading for a feed glucose concentration of 100 g/l and 2 mm diameter beads.**

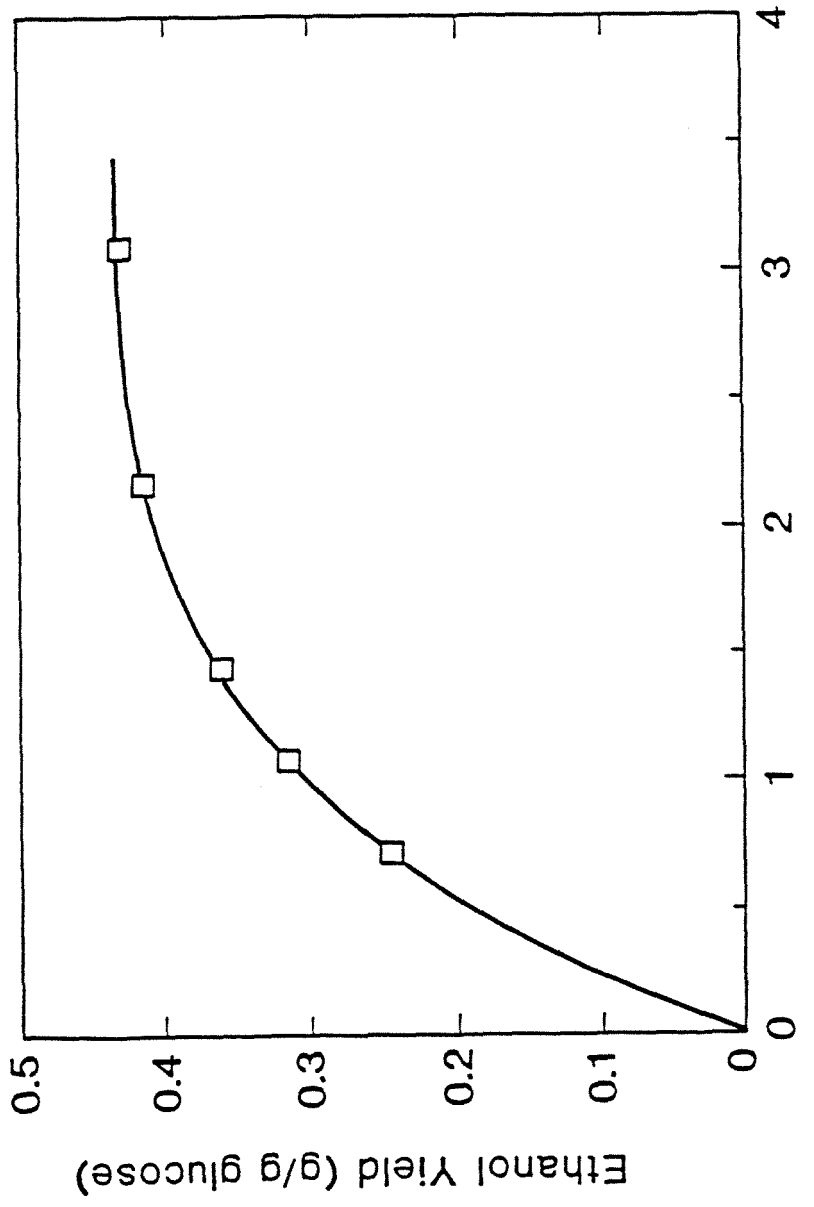

Figure 6.20 **Effect of Residence Time on Ethanol Yield of an immobilized cell CSTR at its maximum biomass loading for a feed glucose concentration of 100 g/l and 2 mm diameter beads.**

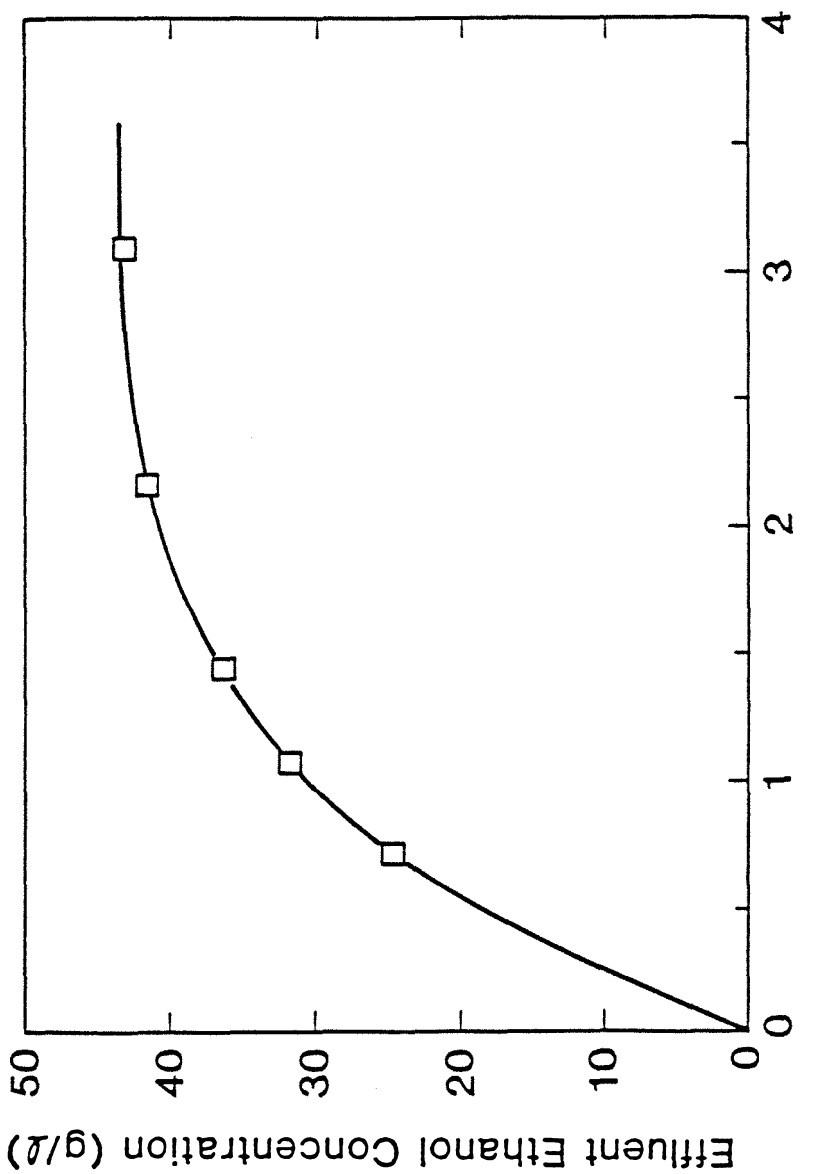

Figure 6.21 **Effect of Residence Time on Effluent Ethanol Concentration of an immobilized cell CSTR at its maximum biomass loading for a feed glucose concentration of 100 g/l and 2 mm diameter beads.**

the performance of immobilized cell reactors. The operating conditions during the reactor start-up can be different from the operating conditions at later times. The ethanol productivity, ethanol yield, and effluent ethanol concentration are all important in evaluating the reactor performance. Increasing the reactor productivity usually requires operating the reactor with a lower ethanol yield and effluent concentration. The optimal operating conditions of an immobilized cell reactor depend on the cost of the feed stream, the amount of product that can be sold, and the cost of concentrating the product downstream.

REFERENCES

(1) Melick, Michael R., M. N. Karim, J. C. Linden, B. F. Dale, and Pal Milhaltz, "Mathematical Modeling of Ethanol Production by Immobilized *Zymomonas mobilis* in a Packed Bed Fermenter," *Biotechnol. Bioeng.*, *29*, 370–382 (1987).

(2) Specchia, V., G. Genon, and A. Gianetto, "Production of Ethanol with *Saccharomyces cerevisiae* in a Continuous Reactor," *Chem. Eng. Commun.*, *23*, 245–258 (1983).

(3) Hamamci, Haluk, and Dewey Y. Ryu, "Performance of Tapered Column Packed-Bed Bioreactor for Ethanol Production," *Biotechnol. Bioeng.*, *29*, 994–1002 (1987).

(4) Doran, Pauline M., and James E. Bailey, "Effects of Immobilization on Growth, Fermentation Properties, and Macromolecular Composition of *Saccharomyces cerevisiae* Attached to Gelatin," *Biotechnol. Bioeng.*, *28*, 73–87 (1986).

(5) Bandyopadhyay, K. K., and T. K. Ghose, "Studies on Immobilized *Saccharomyces cerevisiae*. III. Physiology of Growth and Metabolism on Various Supports," *Biotechnol. Bioeng.*, *24*, 805–815 (1982).

(6) Keller, H. B., "A New Difference Scheme for Parabolic Problems," in *Numerical Solutions of Partial Differential Equations*, vol. 2, J. Bramble, ed., Academic Press, New York, 1970.

APPENDIX

```
C     SOLVE A DIFFUSION-REACTION EQUATION USING THE CRANK
C        NICOLSON METHOD
C     DEFINE PARAMETERS
C       B        BIOMASS CONCENTRATION (G/L)
C       S        SUBSTRATE CONCENTRATION (G/L)
C       S1       CONCENTRATION IN CHAMBER AT X=0
C       S2       CONCENTRATION IN CHAMBER AT X=L
C       CO       OXYGEN CONCENTRATION (PPB)
C       CO1      CONCENTRATION IN CHAMBER AT X=0
C       CO2      CONCENTRATION IN CHAMBER AT X=L
C       P        PRODUCT CONCENTRATION (G/L)
C       P1       CONCENTRATION IN CHAMBER AT X=0
C       P2       CONCENTRATION IN CHAMBER AT X=L
C       MU       SPECIFIC GROWTH RATE (1/HR)
C       RS       SUBSTRATE UPTAKE RATE (G/G-HR)
C       RP       PRODUCTION RATE (G/G-HR)
C       N        NUMBER OF DIVISIONS IN X DIRECTION
C       AREA     AREA AVAILABLE FOR TRANSPORT (CM2)
C       X        POSITION (CM)
C       T        TIME (HR)
C       DX       STEP SIZE IN X DIRECTION (CM)
C       DT       STEP SIZE IN TIME (HR)
C       L        ALGINATE SLAB THICKNESS (CM)
C       TF       FINAL TIME (HR)
C       DS       DIFFUSION COEFFICIENT OF SUBSTRATE (CM2/HR)
C       DO       DIFFUSION COEFFICIENT OF OXYGEN (CM2/HR)
C       DP       DIFFUSION COEFFICIENT OF PRODUCT (CM2/HR)
C       COEF     ELEMENTS OF TRIDIAGONAL MATRIX
C       RHS      RIGHT HAND SIDE VECTOR OF DIF EQN
C       ALPHA    DIMENSIONLESS GROUP FOR SUBSTRATE
C       BETA     DIMENSIONLESS GROUP FOR OXYGEN
C       GAMMA    DIMENSIONLESS GROUP FOR PRODUCT
C       SGRAD    SUBSTRATE GRADIENT AT X=0
C       OGRAD    OXYGEN GRADIENT AT X=0
C       PGRAD    PRODUCT GRADIENT AT X=0
C       QS       TOTAL SUBSTRATE FLUX PER AREA (MG/CM2)
C       QO       TOTAL OXYGEN FLUX PER AREA (MG/CM2)
C       QP       TOTAL PRODUCT FLUX PER AREA (MG/CM2)

      DIMENSION S(550),CO(550),SCOEF(550,3),OCOEF(550,3),SRHS(550),
     1          ORHS(550),P(550),PCOEF(550,3),PRHS(550),
     1          CL(550),RO(550),RS(550),RP(550),
     1          B(550),BAVG(550)
      REAL      L,MU(550)

C     ASSIGN PARAMETER VALUES
      DS=2.8E-2
      DO=8.8E-2
      DP=4.3E-2
      L=0.4
      AREA= 4.714
      N=500
      DT=0.001
      TF=8.0
      S1=1.00
      S2=50.00
      CO1=0.001
      CO2=0.001
```

```
      P1=0.0
      P2=0.0

C     INITIAL CONDITIONS
      DO 10 I=1,N+1
         B(I)=0.400
         S(I)=1.00
         P(I)=0.0
         CO(I)=7500.
   10    CONTINUE

C     COMPUTE SOME PARAMETER VALUES
         DX=L/N
         ALPHA=DS*DT/DX**2
         BETA=DO*DT/DX**2
         GAMMA=DP*DT/DX**2
C     ESTABLISH THE COEFFICIENT MATRIX
C        FIRST AND LAST ROWS
            SCOEF(1,2)=1.0
            SCOEF(1,3)=0.0
            SCOEF(N+1,1)=0.0
            SCOEF(N+1,2)=1.0
            OCOEF(1,2)=1.0
            OCOEF(1,3)=0.0
            OCOEF(N+1,1)=0.0
            OCOEF(N+1,2)=1.0
            PCOEF(1,2)=1.0
            PCOEF(1,3)=0.0
            PCOEF(N+1,1)=0.0
            PCOEF(N+1,2)=1.0
C        REMAINING ROWS
            DO 20 I=2,N
               SCOEF(I,1)=-1.0
               SCOEF(I,2)=2.0/ALPHA + 2.0
               SCOEF(I,3)=-1.0
               OCOEF(I,1)=-1.0
               OCOEF(I,2)=2.0/BETA + 2.0
               OCOEF(I,3)=-1.0
               PCOEF(I,1)=-1.0
               PCOEF(I,2)=2.0/GAMMA + 2.0
               PCOEF(I,3)=-1.0
   20          CONTINUE


C     FIND THE LU DECOMPOSITION OF THE MATRIX
         DO 30 I=2,N+1
            SCOEF(I-1,3)=SCOEF(I-1,3)/SCOEF(I-1,2)
            SCOEF(I,2)=SCOEF(I,2)-SCOEF(I,1)*SCOEF(I-1,3)
            OCOEF(I-1,3)=OCOEF(I-1,3)/OCOEF(I-1,2)
            OCOEF(I,2)=OCOEF(I,2)-OCOEF(I,1)*OCOEF(I-1,3)
            PCOEF(I-1,3)=PCOEF(I-1,3)/PCOEF(I-1,2)
            PCOEF(I,2)=PCOEF(I,2)-PCOEF(I,1)*PCOEF(I-1,3)
   30       CONTINUE

         OPEN(2,FILE='OGR1.DAT',STATUS='NEW')
         OPEN(3,FILE='OPR1.DAT',STATUS='NEW')
         OPEN(4,FILE='OFLS1.DAT',STATUS='NEW')
         OPEN(5,FILE='OFLE1.DAT',STATUS='NEW')
   40 CONTINUE
      T = T + DT
C        CALCULATE THE GROWTH PARAMETERS AT THE PREVIOUS TIME STEP
         DO 50 I=1,N+1
           CALL BJM(S(I),P(I),CO(I),MU(I),RS(I),RP(I),RO(I))
C        FIND THE BIOMASS CONCENTRATION AT THE CURRENT TIME
C           STEP (J+1)
```

```
            A = MU(I)*DT/2.0
            BTEMP=B(I)*(1+A)/(1-A)
C         FIND THE BIOMASS CONCENTRATION AT THE TIME STEP (J+1/2)
            BAVG(I)=(BTEMP+B(I))/2.0
            B(I)=BTEMP
  50        CONTINUE


C       ESTABLISH THE RHS VECTOR
C          FIRST AND LAST ROWS
              SRHS(1)=S1
              SRHS(N+1)=S2
              ORHS(1)=CO1
              ORHS(N+1)=CO2
              PRHS(1)=P1
              PRHS(N+1)=P2
C          REMAINING ROWS
              DO 60 I=2,N
                 SRHS(I)=S(I-1) + (2.0/ALPHA-2.0)*S(I) +
     1                 S(I+1) - 2.0*RS(I)*BAVG(I)*DT/ALPHA
                 ORHS(I)=CO(I-1) + (2.0/BETA-2.0)*CO(I) +
     1                 CO(I+1) - 2.0*RO(I)*BAVG(I)*DT/BETA
                 PRHS(I)=P(I-1) + (2.0/GAMMA-2.0)*P(I) +
     1                 P(I+1) + 2.0*RP(I)*BAVG(I)*DT/GAMMA
  60             CONTINUE


C       SOLVE THE MATRIX FOR THE SUBSTRATE CONCENTRATION AT
C          THE CURRENT TIME STEP (J+1)
           S(1)= SRHS(1)/SCOEF(1,2)
           S(N+1)=SRHS(N+1)/SCOEF(N+1,2)
           CO(1)=ORHS(1)/OCOEF(1,2)
           CO(N+1)=ORHS(N+1)/OCOEF(N+1,2)
           P(1)= PRHS(1)/PCOEF(1,2)
           P(N+1)=PRHS(N+1)/PCOEF(N+1,2)
           DO 70 I=2,N
              S(I)=(SRHS(I)-SCOEF(I,1)*S(I-1))/SCOEF(I,2)
              CO(I)=(ORHS(I)-OCOEF(I,1)*CO(I-1))/OCOEF(I,2)
              P(I)=(PRHS(I)-PCOEF(I,1)*P(I-1))/PCOEF(I,2)
  70          CONTINUE

           DO 80 I=1,N
              K=N+1-I
              S(K)=S(K)-SCOEF(K,3)*S(K+1)
              CO(K)=CO(K)-OCOEF(K,3)*CO(K+1)
              P(K)=P(K)-PCOEF(K,3)*P(K+1)
              IF (S(K) .LT. 0.0) S(K)=0.0
              IF (CO(K) .LT. 0.0) CO(K)=0.0
              IF (P(K) .LT. 0.0) P(K)=0.0
  80          CONTINUE


C       CALCULATE THE FLUX INTO CHAMBER 1
         SGRAD=(S(2)-S(1))/(DX)
         OGRAD=(CO(2)-CO(1))/(DX)
         PGRAD=(P(2)-P(1))/(DX)
         QS=QS + (SGRAD*DS*DT*AREA)
         QP=QP + (PGRAD*DP*DT*AREA)
         QO=QO + (-OGRAD*1.0E-3*DO*DT*AREA)

C     WRITE THE SOLUTION AT THE CURRENT TIME STEP
           M=M+1
           IF (M .EQ. 500) THEN
              DO 100 I=1,N+1,25
                 X=DX*(I-1)
                 WRITE(3,200)T,X,B(I),S(I),P(I),CO(I)
```

```
                WRITE(2,200)T,X,MU(I),RS(I),RP(I),RO(I)
100             CONTINUE
              WRITE(4,300)T,QS
              WRITE(5,300)T,QP
              M=0
              END IF
200  FORMAT(1X,6F10.3)
300  FORMAT(1X,2F10.5)
400  FORMAT(1X,3F10.5,2I5)
     IF (T .LT. TF) GO TO 40
     CLOSE(2)
     CLOSE(3)
     CLOSE(4)
     CLOSE(5)
     STOP
     END



C     A S. CEREVISIAE REACTION MODEL AS A FUNCTION OF DISSOLVED OXYGEN
C        CONCENTRATION FOR GLUCOSE REPRESSED CULTURES

C     A MODEL DEVELOPED BY PERINGER, ET AL FOR MU, RS, RP, AND RO
C        AS A FUNCTION OF SUBSTRATE AND OXYGEN CONCENTRATIONS
      SUBROUTINE BJM(S,E,O,MU,RS,RP,RO)

      REAL MU,KS
      KS = 0.1
      B1 = 5.0E-4
      CL = O/75.0
      MU = S/(KS + S)*(0.24/(1.0 + B1*CL) + 0.12*CL/(14.0 + CL))
     1      *(1.0 - E/93.6)
      RS = S/(KS + S)*(5.8 - (2.2*CL/(7.0 + CL)))
      RP = RS*0.43
      RO = S*1.92*32.0*CL*1000.0/((1.36 + CL)*(KS + S))*
     1      (1.0 - E/93.6)
      RETURN
      END
```

```
C     SOLVE A CSTR MODEL EQUATION

      DIMENSION SB(2),EB(2),OB(2),DSDR(2),DEDR(2),DODR(2),
     +          QS(2),QE(2),QO(2)
      REAL      MU,NU

C     ASSIGN PARAMETER VALUES
      DS=2.8E-2
      DE=4.3E-2
      DO=8.8E-2
      RADIUS=0.168
      DT=0.005
      TF=6.0
      SFEED= 22.0
      EFEED=0.0
      OFEED=1.0E-5
      VR = 0.122
      F = 0.0
      AG = 0.053
      PI = 3.14159

C     INITIAL CONDITIONS
         SB(1) = SFEED
         EB(1) = EFEED
         OB(1) = OFEED

C     INITIALIZE THE CONCENTRATION INSIDE THE ALGINATE BEADS
         INDEX = 0
         CALL BEADCS(INDEX,1,SB(1),EB(1),OB(1),DSDR(1),DEDR(1),DODR(1))
         QS(1) = DS*DSDR(1)*3.0*AG*DT/RADIUS
         QE(1) = DE*DEDR(1)*3.0*AG*DT/RADIUS
         QO(1) = DO*DODR(1)*3.0*AG*DT/RADIUS

      OPEN(3,FILE='BTCHPR.DAT',STATUS='NEW')
      OPEN(2,FILE='BTCHFL.DAT',STATUS='NEW')

   40 T = T + DT
      K = K + 1

C     CALCULATE THE BULK CONC IN CSTR AT T FROM BULK CONC AND GRAD AT
C        PREVIOUS TIME STEP
         SB(2) = SB(1)*(1.0 - F*DT/(VR*(1.0 - AG))) +
     1           F*SFEED*DT/(1.0 - AG) -
     1           QS(1)/(1.0 - AG)
         EB(2) = EB(1)*(1.0 - F*DT/(VR*(1.0 - AG))) -
     1           QE(1)/(1.0 - AG)
         OB(2) = OB(1)*(1.0 - F*DT/(VR*(1.0 - AG))) +
     1           F*OFEED*DT/(VR*(1.0 - AG)) -
     1           QO(1)/(1.0 - AG)
         IF(SB(2) .LT. 0.0) SB(2) = 0.0
         IF(EB(2) .LT. 0.0) EB(2) = 0.0
         IF(OB(2) .LT. 0.0) OB(2) = 0.0
      INDEX = 1
C     DETERMINE THE CONCENTRATION IN THE ALGINATE BEADS AT T
         CALL BEADCS(INDEX,1,SB(2),EB(2),OB(2),DSDR(2),DEDR(2),DODR(2))

C     CALCULATE THE FLUX INTO THE BEADS AT T
         QS(2) = DS*DSDR(2)*3.0*AG*DT/RADIUS
         QE(2) = DE*DEDR(2)*3.0*AG*DT/RADIUS
```

```
          QO(2) = DO*DODR(2)*3.0*AG*DT/RADIUS

          INDEX = 2
C         RECALCULATE THE BULK FLUID CONC AND THE BEAD CONC
          DO 15 M=1,10
             SBNEW = SB(1)*(1.0 - F*DT/(VR*(1.0 - AG))) +
         1           F*SFEED*DT/(VR*(1.0 - AG)) -
         1           (QS(1) + QS(2))/(2.0*(1.0 - AG))
             EBNEW = EB(1)*(1.0 - F*DT/(VR*(1.0 - AG))) -
         1           (QE(1) + QE(2))/(2.0*(1.0 - AG))
             OBNEW = OB(1)*(1.0 - F*DT/(VR*(1.0 - AG))) +
         1           F*OFEED*DT/(VR*(1.0 - AG)) -
         1           (QO(1) + QO(2))/(2.0*(1.0 - AG))
             IF(SBNEW .LT. 0.0) SBNEW = 0.0
             IF(EBNEW .LT. 0.0) EBNEW = 0.0
             IF(OBNEW .LT. 0.0) OBNEW = 0.0
             CALL BEADCS(INDEX,1,SBNEW,EBNEW,OBNEW,DSDRN,DEDRN,DODRN)
             DELTA = ABS(SBNEW-SB(2))
             IF(DELTA .LT. 1.0E-4) GOTO 25
             DSDR(2) = DSDRN
             SB(2) = SBNEW
             DEDR(2) = DEDRN
             EB(2) = EBNEW
             DODR(2) = DODRN
             OB(2) = OBNEW
      15     CONTINUE
      25  CONTINUE
C         WRITE THE SOLUTION AT THE CURRENT TIME STEP
             IF (K .EQ. 200) THEN
                INDEX = 3
                CALL BEADCS(INDEX,1,SBNEW,EBNEW,OBNEW,DSDRN,DEDRN,DODRN)
                ENDIF

C         MOVE THE CURRENT BULK REACTOR CONC INO THE OLD TIME VARIABLE
             IF(K .EQ. 100 .OR. K .EQ. 200)WRITE(2,200) T,SB(2),EB(2),OB(2)
             SB(1) = SB(2)
             DSDR(1) = DSDR(2)
             EB(1) = EB(2)
             DEDR(1) = DEDR(2)
             OB(1) = OB(2)
             DODR(1) = DODR(2)
      30     CONTINUE
          IF (K .EQ. 200) K=0
          IF (T .LT. TF) GOTO 40

      200 FORMAT(1X,4F10.4)

          CLOSE(3)
          CLOSE(2)
          STOP
          END



C         SOLVE A DIFFUSION-REACTION EQUATION USING THE CRANK
C            NICOLSON METHOD
C         DEFINE PARAMETERS
C           B        BIOMASS CONCENTRATION (G/L)
C           S        SUBSTRATE CONCENTRATION (G/L)
C           MU       SPECIFIC GROWTH RATE (1/HR)
C           MUM      MAX SPECIFIC GROWTH RATE (1/HR)
C           KM       CONSTANT FOR GROWTH KINETICS
C           RS       SUBSTRATE UPTAKE RATE (G/G-HR)
C           RSM      MAX SUBSTRATE UPTAKE RATE (G/G-HR)
C           KS       CONSTANT FOR SUBSTATE UPTAKE KINETICS
C           N        NUMBER OF DIVISIONS IN R DIRECTION
```

```
C       PX      INDICATES POSITION IN THE PER
C       R       POSITION IN THE ALGINATE BEAD (CM)
C       T       TIME (HR)
C       DR      STEP SIZE IN R DIRECTION (CM)
C       DT      STEP SIZE IN TIME (HR)
C       RADIUS  RADIUS OF ALGINATE BEAD (CM)
C       TF      FINAL TIME (HR)
C       DS      DIFFUSION COEFFICIENT OF SUBSTRATE (CM2/HR)
C       DE      DIFFUSION COEFFICIENT OF ETHANOL (CM2/HR)
C       DO      DIFFUSION COEFFICIENT OF OXYGEN  (CM2/HR)
C       COEF    ELEMENTS OF TRIDIAGONAL MATRIX
C       RHS     RIGHT HAND SIDE VECTOR OF DIF EQN
C       ALPHA   DIMENSIONLESS GROUP
C       DSDR    SUBSTRATE GRADIENT AT r=R
C       DEDR    ETHANOL GRADIENT AT r=R
C       DODR    OXYGEN GRADIENT AT r=R
C       Q       TOTAL FLUX PER AREA (G/CM2)

      SUBROUTINE BEADCS(INDEX,PX,SBULK,EBULK,OBULK,DSDR,DEDR,DODR)

      DIMENSION B(502),S(502),E(502),O(502),SCOEF(502,3),
     1          ECOEF(502,3),OCOEF(502,3),SRHS(502),ERHS(502),ORHS(502),
     1          MU(502),RS(502),NU(502),RO(502),BAVG(502)
      REAL      MU,MUM,NU
      INTEGER   PX


C     IF THIS IS THE FIRST CALL TO BEAD AT T AND PX
        IF (INDEX .EQ. 1) GOTO 40
C     IF THIS IS THE SECOND CALL TO BEAD AT T AND PX
        IF (INDEX .EQ. 2) GOTO 65
C     IF INDEX EQUALS 3 WRITE THE SOLUTION FROM THE PREVIOUS CALL
        IF (INDEX .EQ. 3) GOTO 83

C     THIS IS THE INITIAL CALL TO BEAD AT T=0

C       ASSIGN PARAMETER VALUES
          DS=2.8E-2
          DE=4.3E-2
          DO=8.8E-2
          PI= 3.14159
          RADIUS=0.168
          N = 50
          DT=0.005
          T = 0.0
C       INITIAL CONDITIONS
          DO 10 I=1,N
            B(I)=11.0
            S(I)= 22.0
            E(I)=0.0
            O(I)=1.0E-5
10        CONTINUE
          B(N+1) = 11.0
          S(N+1) = 22.0
          E(N+1) = 0.0
          O(N+1) = 1.0E-5
C         DSDR = 100.0*FLOAT(N)/RADIUS
          DSDR = 0.0
          DEDR = 0.0
C         DODR = -100.0*FLOAT(N)/RADIUS
          DODR = 0.0
C       COMPUTE SOME PARAMETER VALUES
          DR = RADIUS/N
          ALPHA=DS*DT/DR**2
          BETA=DE*DT/DR**2
```

```
            GAMMA=DO*DT/DR**2
C        ESTABLISH THE COEFFICIENT MATRIX
C           FIRST AND LAST ROWS
            SCOEF(1,2)=2.0/ALPHA + 2.0
            SCOEF(1,3)=-2.0
            ECOEF(1,2)=2.0/BETA + 2.0
            ECOEF(1,3)=-2.0
            OCOEF(1,2)=2.0/GAMMA + 2.0
            OCOEF(1,3)=-2.0
            SCOEF(N+1,1)=0.0
            ECOEF(N+1,1)=0.0
            OCOEF(N+1,1)=0.0
            SCOEF(N+1,2)=1.0
            ECOEF(N+1,2)=1.0
            OCOEF(N+1,2)=1.0
C        REMAINING ROWS
            DO 20 I=2,N
               SCOEF(I,1)=-1.0 + 1.0/(FLOAT(I)-0.5)
               ECOEF(I,1)=-1.0 + 1.0/(FLOAT(I)-0.5)
               OCOEF(I,1)=-1.0 + 1.0/(FLOAT(I)-0.5)
               SCOEF(I,2)=2.0/ALPHA + 2.0
               ECOEF(I,2)=2.0/BETA + 2.0
               OCOEF(I,2)=2.0/GAMMA + 2.0
               SCOEF(I,3)=-1.0 - 1.0/(FLOAT(I)-0.5)
               ECOEF(I,3)=-1.0 - 1.0/(FLOAT(I)-0.5)
               OCOEF(I,3)=-1.0 - 1.0/(FLOAT(I)-0.5)
   20          CONTINUE

C        FIND THE LU DECOMPOSITION OF THE MATRIX
            DO 30 I=2,N+1
               SCOEF(I-1,3)=SCOEF(I-1,3)/SCOEF(I-1,2)
               SCOEF(I,2)=SCOEF(I,2)-SCOEF(I,1)*SCOEF(I-1,3)
               ECOEF(I-1,3)=ECOEF(I-1,3)/ECOEF(I-1,2)
               ECOEF(I,2)=ECOEF(I,2)-ECOEF(I,1)*ECOEF(I-1,3)
               OCOEF(I-1,3)=OCOEF(I-1,3)/OCOEF(I-1,2)
               OCOEF(I,2)=OCOEF(I,2)-OCOEF(I,1)*OCOEF(I-1,3)
   30          CONTINUE
            RETURN

   40       CONTINUE

            IF (PX .EQ. 1) T = T + DT
C        CALCULATE THE CONCENTRATION PROFILE IN THE ALGINATE BEAD AT T AND PX

C        CALCULATE THE GROWTH PARAMETERS AT THE PREVIOUS TIME
C          STEP (J)
            DO 50 I=1,N+1
               CALL BJM(S(I),E(I),O(I),MU(I),RS(I),NU(I),RO(I))
               A=MU(I)*DT/2.0
C           FIND THE BIOMASS CONCENTRATION AT THE CURRENT TIME
C              STEP (J+1)
               BTEMP=B(I)*(1+A)/(1-A)
C           FIND THE BIOMASS CONCENTRATION AT THE TIME STEP (J+1/2)
               BAVG(I)=(BTEMP+B(I))/2.0
               B(I)=BTEMP
               IF(BAVG(I) .GT. 200.) BAVG(I) = 200.0
               IF(B(I) .GT. 200.) B(I) = 200.0
   50          CONTINUE


C        ESTABLISH THE RHS VECTOR
C           FIRST ROWS
               SRHS(1)=(2.0/ALPHA-2.0)*S(1) + 2.0*S(2)
     1                 - 2.0*RS(1)*DT*BAVG(1)/ALPHA
               ERHS(1)=(2.0/BETA-2.0)*E(1) + 2.0*E(2)
     1                 +2.0*NU(1)*DT*BAVG(1)/BETA
```

```
            ORHS(1)=(2.0/GAMMA-2.0)*O(1) + 2.0*O(2)
     1              -2.0*RO(1)*DT*BAVG(1)/GAMMA

C          REMAINING ROWS
              DO 60 I=2,N
                 SRHS(I)=(1.0-1.0/(FLOAT(I)-0.5))*S(I-1)
     +                  + (2.0/ALPHA-2.0)*S(I)
     +                  + (1.0+1.0/(FLOAT(I)-0.5))*S(I+1)
     +                  - 2.0*RS(I)*BAVG(I)*DT/ALPHA
                 ERHS(I)=(1.0-1.0/(FLOAT(I)-0.5))*E(I-1)
     +                  + (2.0/BETA-2.0)*E(I)
     +                  + (1.0+1.0/(FLOAT(I)-0.5))*E(I+1)
     +                  + 2.0*NU(I)*BAVG(I)*DT/BETA
                 ORHS(I)=(1.0-1.0/(FLOAT(I)-0.5))*O(I-1)
     +                  + (2.0/GAMMA-2.0)*O(I)
     +                  + (1.0+1.0/(FLOAT(I)-0.5))*O(I+1)
     +                  - 2.0*RO(I)*BAVG(I)*DT/GAMMA
    60           CONTINUE

C         LAST ROWS
    65           CONTINUE
                 SRHS(N+1)=SBULK
                 ERHS(N+1)=EBULK
                 ORHS(N+1)=OBULK

C       SOLVE THE MATRIX FOR THE SUBSTRATE CONCENTRATION AT
C          THE CURRENT TIME STEP (J+1)
              S(1)=SRHS(1)/SCOEF(1,2)
              E(1)=ERHS(1)/ECOEF(1,2)
              O(1)=ORHS(1)/OCOEF(1,2)
              DO 70 I=2,N+1
                 S(I)=(SRHS(I)-SCOEF(I,1)*S(I-1))/SCOEF(I,2)
                 E(I)=(ERHS(I)-ECOEF(I,1)*E(I-1))/ECOEF(I,2)
                 O(I)=(ORHS(I)-OCOEF(I,1)*O(I-1))/OCOEF(I,2)
    70           CONTINUE

              DO 80 I=0,N
                 K=N+1-I
                 S(K)=S(K)-SCOEF(K,3)*S(K+1)
                 E(K)=E(K)-ECOEF(K,3)*E(K+1)
                 O(K)=O(K)-OCOEF(K,3)*O(K+1)
                 IF (S(K) .LT. 0.0) S(K)=0.0
                 IF (E(K) .LT. 0.0) E(K)=0.0
                 IF (O(K) .LT. 0.0) O(K)=0.0
    80           CONTINUE

    83        IF (INDEX .EQ. 3) THEN
                 WRITE(3,90)'TIME =',T,'  PX=',PX
                 DO 85 I=1,N+1,5
                    R = DR*(I-1)
                    WRITE(3,95)R,B(I),S(I),E(I),O(I)
    85              CONTINUE
              ENDIF
C        DETERMINE THE DERIVATIVE AT THE BOUNDARY r=R
              DSDR = (S(N+1) - S(N))/DR
              DEDR = (E(N+1) - E(N))/DR
              DODR = (O(N+1) - O(N))/DR

    90 FORMAT(1X,A,F10.3,A,I2)
    95 FORMAT(1X,5F10.4)

              RETURN
              CALL EXIT
              END
```

```
C     A S. CEREVISIAE REACTION MODEL AS A FUNCTION OF DISSOLVED OXYGEN
C        CONCENTRATION FOR GLUCOSE REPRESSED CULTURES

C     A MODEL DEVELOPED BY PERINGER, ET AL FOR MU, RS, RP, AND RO
C        AS A FUNCTION OF SUBSTRATE AND OXYGEN CONCENTRATIONS
      SUBROUTINE BJM(S,E,O,MU,RS,RP,RO)

      REAL MU,KS
      KS = 0.1
      B1 = 5.0E-4
      MU = S/(KS + S)*(0.24/(1.0 + B1*O) + 0.12*O/(14.00 + O))
     1      *(1.0 - E/93.6)
      RS = S/(KS + S)*(5.8 - (2.2*O/(14.00 + O)))
      RP = RS*0.43
      RO = S*8.19*O/((1.36 + CL)*(KS + S))*
     1      (1.0 - E/93.6)
      RETURN
      END
```

```
C     SOLVE A PFR MODEL EQUATION USING THE BOX SCHEME

      PROGRAM CRPFRE

C     INDEX   0 FOR CALLS AT T=0
C             1 FOR FIRST CALLS AT ALL OTHER T
C             2 FOR SECOND CALLS AT ALL OTHER T

      DIMENSION SB(11,2),EB(11,2),DSDR(11,2),DEDR(11,2),
     +          OB(11,2),DODR(11,2)
      REAL L,DZ,DT,Z,T,Q
      INTEGER NZ,I,J

      CALL LINK('//')

      NZ = 11
      L = 35.7
      F = 12716.0
      FSS = 12716.0
      A = 60.8
      AG = 0.50
      DZ = L/(NZ - 1)
      DT = 0.005
      T = 0.0
      Z = 0.0
      DFS = 2.8E-2
      DFE = 4.3E-2
      DFO = 8.8E-2
      RADIUS = 0.05
      BETA = F*DT/(A*DZ*(1.0-AG))

C     INITIALIZE THE REACTOR CONDITIONS
      INDEX = 0
      DO 5 I=1,NZ
         SB(I,1) = 100.0
         EB(I,1) = 0.0
         OB(I,1) = 1.0E-5
         DSDR(I,1) = 0.0
         DEDR(I,1) = 0.0
         DODR(I,1) = 0.0
    5    CONTINUE
      SB(1,2) = 100.0
      EB(1,2) = 0.0
      OB(1,2) = 1.0E-5

C     INITIALIZE THE CONCENTRATION INSIDE THE ALGINATE BEADS
         CALL BEAD(INDEX,NZ,SB(1,1),EB(1,1),OB(1,1),DSDR(1,1),
     +             DEDR(1,1),DODR(1,1))

      OPEN(UNIT=2,FILE='run66',STATUS='NEW')
      OPEN(UNIT=3,FILE='py66',STATUS='NEW')
      OPEN(UNIT=4,FILE='prf66',STATUS='NEW')

   10 CONTINUE
      T = T + DT
      K = K + 1
      INDEX = 1
C     DETERMINE THE CONC IN THE ALGINATE AT THE REACTOR INLET
         CALL BEAD(INDEX,1,SB(1,2),EB(1,2),OB(1,2),DSDR(1,2),
     +             DEDR(1,2),DODR(1,2))
C     DETERMINE THE CONC IN THE ALGINATE THROUGHOUT REACTOR
```

```
      DO 20 I=2,NZ
         SB(I,2) = ((1.0-BETA)/(1.0 + BETA))*(SB(I,1) - SB(I-1,2))
     +          + SB(I-1,1) - (DT*3.0*DFS*(DSDR(I,1) + DSDR(I-1,1))
     +            *AG/(RADIUS*(1.0-AG)*(1.0 + BETA)))
         EB(I,2) = ((1.0-BETA)/(1.0 + BETA))*(EB(I,1) - EB(I-1,2))
     +          + EB(I-1,1) - (DT*3.0*DFE*(DEDR(I,1) + DEDR(I-1,1))
     +            *AG/(RADIUS*(1.0-AG)*(1.0 + BETA)))
         OB(I,2) = ((1.0-BETA)/(1.0 + BETA))*(OB(I,1) - OB(I-1,2))
     +          + OB(I-1,1) - (DT*3.0*DFO*(DODR(I,1) + DODR(I-1,1))
     +            *AG/(RADIUS*(1.0-AG)*(1.0 + BETA)))
         IF (SB(I,2) .LT. 0.0) SB(I,2) = 0.0
         IF (EB(I,2) .LT. 0.0) EB(I,2) = 0.0
         IF (OB(I,2) .LT. 0.0) OB(I,2) = 0.0
         INDEX = 1
         CALL BEAD(INDEX,I,SB(I,2),EB(I,2),OB(I,2),DSDR(I,2),
     +            DEDR(I,2),DODR(I,2))
C        WRITE(4,400)T,I,DSDR(I,2)
         INDEX = 2
C        RECALCULATE THE BULK CONC AND ALGINATE CONC
            DO 15 M=1,10
            SBNEW = ((1.0-BETA)/(1.0 + BETA))*(SB(I,1) - SB(I-1,2))
     +           + SB(I-1,1) - (DT*3.0*DFS*(DSDR(I,1) + DSDR(I-1,1)
     +           + DSDR(I,2) + DSDR(I-1,2))*AG/(RADIUS*(1.0-AG)*2.0
     +           *(1.0 + BETA)))
            EBNEW = ((1.0-BETA)/(1.0 + BETA))*(EB(I,1) - EB(I-1,2))
     +           + EB(I-1,1) - (DT*3.0*DFE*(DEDR(I,1) + DEDR(I-1,1)
     +           + DEDR(I,2) + DEDR(I-1,2))*AG/(RADIUS*(1.0-AG)*2.0
     +           *(1.0 + BETA)))
            OBNEW = ((1.0-BETA)/(1.0 + BETA))*(OB(I,1) - OB(I-1,2))
     +           + OB(I-1,1) - (DT*3.0*DFO*(DODR(I,1) + DODR(I-1,1)
     +           + DODR(I,2) + DODR(I-1,2))*AG/(RADIUS*(1.0-AG)*2.0
     +           *(1.0 + BETA)))
            IF (SBNEW .LT. 0.0) SBNEW = 0.0
            IF (EBNEW .LT. 0.0) EBNEW = 0.0
            IF (OBNEW .LT. 0.0) OBNEW = 0.0
            CALL BEAD(INDEX,I,SBNEW,EBNEW,OBNEW,DSDRN,DEDRN,DODRN)
            DELTA = ABS(SBNEW-SB(I,2))
            IF (DELTA .LT. 1.0E-4) GOTO 25
            DSDR(I,2) = DSDRN
            SB(I,2) = SBNEW
            DEDR(I,2) = DEDRN
            EB(I,2) = EBNEW
            DODR(I,2) = DODRN
            OB(I,2) = OBNEW
   15       CONTINUE
   25    CONTINUE
         IF(K .EQ. 200 .AND. I .EQ. 2) JKL = JKL + 1
         IF(JKL .EQ. 5 .OR. JKL .EQ. 10 .OR. JKL .EQ. 20) THEN
            IF (K .EQ. 200) THEN
            INDEX = 3
            CALL BEAD(INDEX,I,SBNEW,EBNEW,OBNEW,DSDRN,DEDRN,DODRN)
            ENDIF
            ENDIF
   20    CONTINUE

C     MOVE THE CURRENT BULK REACTOR CONC INTO THE OLD TIME VARIABLE
      DO 30 I=1,NZ
C        Z = (I-1)*L/(NZ-1)
         SB(I,1) = SB(I,2)
         DSDR(I,1) = DSDR(I,2)
         EB(I,1) = EB(I,2)
         DEDR(I,1) = DEDR(I,2)
         OB(I,1) = OB(I,2)
         DODR(I,1) = DODR(I,2)
   30    CONTINUE
```

```
      JK = JK + 1
      SUM = SUM + F*EB(NZ,1)/(A*L)
      SUM2 = SUM2 + EB(NZ,1)/SB(1,1)
      PROD = SUM/(FLOAT(JK))
      YIELD = SUM2/(FLOAT(JK))


      IF (K .EQ. 100 .OR. K .EQ. 200 .OR. K .EQ. 50
     +    .OR. K .EQ. 150) THEN
          WRITE(2,40)T,SB(NZ,2),EB(NZ,2),OB(NZ,2)
          WRITE(3,50)T,PROD,YIELD
          END IF

      Z = 0.0
      IF (K .EQ. 200) K = 0
      IF (T .GE. 8.0) THEN
            BETA = FSS*DT/(A*DZ*(1.0-AG))
            F = FSS
            END IF
      IF (T .LE. 20.) GOTO 10
   40 FORMAT(1X,5F10.3)
   50 FORMAT(1X,3F10.3)

      CLOSE(UNIT=2)
      CLOSE(UNIT=3)
      CLOSE(UNIT=4)

      STOP
      CALL EXIT
      END



C     SOLVE A DIFFUSION-REACTION EQUATION USING THE CRANK
C        NICOLSON METHOD
C     DEFINE PARAMETERS
C       B        BIOMASS CONCENTRATION (G/L)
C       S        SUBSTRATE CONCENTRATION (G/L)
C       MU       SPECIFIC GROWTH RATE (1/HR)
C       MUM      MAX SPECIFIC GROWTH RATE (1/HR)
C       KM       CONSTANT FOR GROWTH KINETICS
C       RS       SUBSTRATE UPTAKE RATE (G/G-HR)
C       RSM      MAX SUBSTRATE UPTAKE RATE (G/G-HR)
C       KS       CONSTANT FOR SUBSTATE UPTAKE KINETICS
C       N        NUMBER OF DIVISIONS IN R DIRECTION
C       PX       INDICATES POSITION IN THE PFR
C       R        POSITION IN THE ALGINATE BEAD (CM)
C       T        TIME (HR)
C       DR       STEP SIZE IN R DIRECTION (CM)
C       DT       STEP SIZE IN TIME (HR)
C       RADIUS   RADIUS OF ALGINATE BEAD (CM)
C       TF       FINAL TIME (HR)
C       DS       DIFFUSION COEFFICIENT OF SUBSTRATE (CM2/HR)
C       DE       DIFFUSION COEFFICIENT OF ETHANOL (CM2/HR)
C       DO       DIFFUSION COEFFICIENT OF OXYGEN  (CM2/HR)
C       COEF     ELEMENTS OF TRIDIAGONAL MATRIX
C       RHS      RIGHT HAND SIDE VECTOR OF DIF EQN
C       ALPHA    DIMENSIONLESS GROUP
C       DSDR     SUBSTRATE GRADIENT AT r=R
C       DEDR     ETHANOL GRADIENT AT r=R
C       DODR     OXYGEN GRADIENT AT r=R
C       Q        TOTAL FLUX PER AREA (G/CM2)

      SUBROUTINE BEAD(INDEX,PX,SBULK,EBULK,OBULK,DSDR,DEDR,DODR)

      DIMENSION B(11,502),S(11,502),E(11,502),O(11,502),SCOEF(502,3),
```

```
     1          ECOEF(502,3),OCOEF(502,3),SRHS(502),ERHS(502),ORHS(502),
     1          MU(502),RS(502),NU(502),RO(502),BAVG(502)
      REAL      MU,MUM,NU
      INTEGER   PX


C     IF THIS IS THE FIRST CALL TO BEAD AT T AND PX
         IF (INDEX .EQ. 1) GOTO 40
C     IF THIS IS THE SECOND CALL TO BEAD AT T AND PX
         IF (INDEX .EQ. 2) GOTO 65
C     IF INDEX EQUALS 3 WRITE THE SOLUTION FROM THE PREVIOUS CALL
         IF (INDEX .EQ. 3) GOTO 83

C     THIS IS THE INITIAL CALL TO BEAD AT T=0

C        ASSIGN PARAMETER VALUES
            DS=2.8E-2
            DE=4.3E-2
            DO=8.8E-2
            PI= 3.14159
            RADIUS=0.05
            N = 500
            DT=0.005
            T = 0.0
C        INITIAL CONDITIONS
            DO 15 K=1,PX
               DO 10 I=1,N+1
                  B(K,I)=10.0
                  S(K,I)=100.0
                  E(K,I)=0.0
                  O(K,I)=1.0E-5
   10             CONTINUE
   15          CONTINUE
               DSDR = 0.0
               DEDR = 0.0
               DODR = 0.0
C        COMPUTE SOME PARAMETER VALUES
            DR = RADIUS/N
            ALPHA=DS*DT/DR**2
            BETA=DE*DT/DR**2
            GAMMA=DO*DT/DR**2
C        ESTABLISH THE COEFFICIENT MATRIX
C           FIRST AND LAST ROWS
            SCOEF(1,2)=2.0/ALPHA + 2.0
            SCOEF(1,3)=-2.0
            ECOEF(1,2)=2.0/BETA + 2.0
            ECOEF(1,3)=-2.0
            OCOEF(1,2)=2.0/GAMMA + 2.0
            OCOEF(1,3)=-2.0
            SCOEF(N+1,1)=0.0
            ECOEF(N+1,1)=0.0
            OCOEF(N+1,1)=0.0
            SCOEF(N+1,2)=1.0
            ECOEF(N+1,2)=1.0
            OCOEF(N+1,2)=1.0
C        REMAINING ROWS
            DO 20 I=2,N
               SCOEF(I,1)=-1.0 + 1.0/(FLOAT(I)-0.5)
               ECOEF(I,1)=-1.0 + 1.0/(FLOAT(I)-0.5)
               OCOEF(I,1)=-1.0 + 1.0/(FLOAT(I)-0.5)
               SCOEF(I,2)=2.0/ALPHA + 2.0
               ECOEF(I,2)=2.0/BETA + 2.0
               OCOEF(I,2)=2.0/GAMMA + 2.0
               SCOEF(I,3)=-1.0 - 1.0/(FLOAT(I)-0.5)
               ECOEF(I,3)=-1.0 - 1.0/(FLOAT(I)-0.5)
```

```
                OCOEF(I,3)=-1.0 - 1.0/(FLOAT(I)-0.5)
   20           CONTINUE

C          FIND THE LU DECOMPOSITION OF THE MATRIX
              DO 30 I=2,N+1
                 SCOEF(I-1,3)=SCOEF(I-1,3)/SCOEF(I-1,2)
                 SCOEF(I,2)=SCOEF(I,2)-SCOEF(I,1)*SCOEF(I-1,3)
                 ECOEF(I-1,3)=ECOEF(I-1,3)/ECOEF(I-1,2)
                 ECOEF(I,2)=ECOEF(I,2)-ECOEF(I,1)*ECOEF(I-1,3)
                 OCOEF(I-1,3)=OCOEF(I-1,3)/OCOEF(I-1,2)
                 OCOEF(I,2)=OCOEF(I,2)-OCOEF(I,1)*OCOEF(I-1,3)
   30            CONTINUE
          RETURN

   40     CONTINUE

          IF (PX .EQ. 1) T = T + DT
C       CALCULATE THE CONCENTRATION PROFILE IN THE ALGINATE BEAD AT T AND PX

C       CALCULATE THE GROWTH PARAMETERS AT THE PREVIOUS TIME
C         STEP (J)
          DO 50 I=1,N+1
             CALL BJM(S(PX,I),E(PX,I),O(PX,I),MU(I),RS(I),NU(I),RO(I))
             A=MU(I)*DT/2.0
C            FIND THE BIOMASS CONCENTRATION AT THE CURRENT TIME
C               STEP (J+1)
                BTEMP=B(PX,I)*(1+A)/(1-A)
C            FIND THE BIOMASS CONCENTRATION AT THE TIME STEP (J+1/2)
                BAVG(I)=(BTEMP+B(PX,I))/2.0
                B(PX,I)=BTEMP
                IF(BAVG(I) .GT. 200.) BAVG(I) = 200.0
                IF(B(PX,I) .GT. 200.) B(PX,I) = 200.0
   50           CONTINUE


C         ESTABLISH THE RHS VECTOR
C            FIRST ROWS
                SRHS(1)=(2.0/ALPHA-2.0)*S(PX,1) + 2.0*S(PX,2)
     1                 - 2.0*RS(1)*DT*BAVG(1)/ALPHA
                ERHS(1)=(2.0/BETA-2.0)*E(PX,1) + 2.0*E(PX,2)
     1                 +2.0*NU(1)*DT*BAVG(1)/BETA
                ORHS(1)=(2.0/GAMMA-2.0)*O(PX,1) + 2.0*O(PX,2)
     1                 -2.0*RO(1)*DT*BAVG(1)/GAMMA

C            REMAINING ROWS
                DO 60 I=2,N
                   SRHS(I)=(1.0-1.0/(FLOAT(I)-0.5))*S(PX,I-1)
     +                    + (2.0/ALPHA-2.0)*S(PX,I)
     +                    + (1.0+1.0/(FLOAT(I)-0.5))*S(PX,I+1)
     +                    - 2.0*RS(I)*BAVG(I)*DT/ALPHA
                   ERHS(I)=(1.0-1.0/(FLOAT(I)-0.5))*E(PX,I-1)
     +                    + (2.0/BETA-2.0)*E(PX,I)
     +                    + (1.0+1.0/(FLOAT(I)-0.5))*E(PX,I+1)
     +                    + 2.0*NU(I)*BAVG(I)*DT/BETA
                   ORHS(I)=(1.0-1.0/(FLOAT(I)-0.5))*O(PX,I-1)
     +                    + (2.0/GAMMA-2.0)*O(PX,I)
     +                    + (1.0+1.0/(FLOAT(I)-0.5))*O(PX,I+1)
     +                    - 2.0*RO(I)*BAVG(I)*DT/GAMMA
   60              CONTINUE

C          LAST ROWS
   65           CONTINUE
                SRHS(N+1)=SBULK
                ERHS(N+1)=EBULK
                ORHS(N+1)=OBULK
```

```
C       SOLVE THE MATRIX FOR THE SUBSTRATE CONCENTRATION AT
C          THE CURRENT TIME STEP (J+1)
           S(PX,1)=SRHS(1)/SCOEF(1,2)
           E(PX,1)=ERHS(1)/ECOEF(1,2)
           O(PX,1)=ORHS(1)/OCOEF(1,2)
           DO 70 I=2,N+1
              S(PX,I)=(SRHS(I)-SCOEF(I,1)*S(PX,I-1))/SCOEF(I,2)
              E(PX,I)=(ERHS(I)-ECOEF(I,1)*E(PX,I-1))/ECOEF(I,2)
              O(PX,I)=(ORHS(I)-OCOEF(I,1)*O(PX,I-1))/OCOEF(I,2)
   70         CONTINUE

           DO 80 I=0,N
              K=N+1-I
              S(PX,K)=S(PX,K)-SCOEF(K,3)*S(PX,K+1)
              E(PX,K)=E(PX,K)-ECOEF(K,3)*E(PX,K+1)
              O(PX,K)=O(PX,K)-OCOEF(K,3)*O(PX,K+1)
              IF (S(PX,K) .LT. 0.0) S(PX,K)=0.0
              IF (E(PX,K) .LT. 0.0) E(PX,K)=0.0
              IF (O(PX,K) .LT. 0.0) O(PX,K)=0.0
   80         CONTINUE

   83      IF (INDEX .EQ. 3) THEN
              BSUM = 0.0
              DO 87 I=1,N+1
                 BSUM = BSUM + B(PX,I)
   87            CONTINUE
              BMED = BSUM/(FLOAT(N+1))
              WRITE(4,90)'TIME=',T,'  PX=',PX,'  BMED=',BMED
              IF (PX .EQ. 2 .OR. PX .EQ. 6 .OR. PX .EQ. 11) THEN
                 DO 85 I=1,N+1,25
                    R = DR*(I-1)
                    WRITE(4,95)R,B(PX,I),S(PX,I),E(PX,I),O(PX,I)
   85               CONTINUE
                 ENDIF
              ENDIF
C       DETERMINE THE DERIVATIVE AT THE BOUNDARY r=R
           DSDR = (S(PX,N+1) - S(PX,N))/DR
           DEDR = (E(PX,N+1) - E(PX,N))/DR
           DODR = (O(PX,N+1) - O(PX,N))/DR

   90 FORMAT(1X,A,F10.3,A,I2,A,F10.3)
   95 FORMAT(1X,5F10.4)

           RETURN
           CALL EXIT
           END


C       A S. CEREVISIAE REACTION MODEL AS A FUNCTION OF DISSOLVED OXYGEN
C          CONCENTRATION FOR GLUCOSE REPRESSED CULTURES

C       A MODEL DEVELOPED BY PERINGER, ET AL FOR MU, RS, RP, AND RO
C          AS A FUNCTION OF SUBSTRATE AND OXYGEN CONCENTRATIONS
         SUBROUTINE BJM(S,E,O,MU,RS,RP,RO)

         REAL MU,KS
         KS = 0.1
         B1 = 5.0E-4
         MU = S/(KS + S)*(0.24/(1.0 + B1*O) + 0.12*O/(14.00 + O))
        1       *(1.0 - E/93.6)
         RS = S/(KS + S)*(5.8 - (2.2*O/(14.00 + O)))
        1       *(1.0 - E/93.6)
         RP = RS*0.43
         RO = S*8.19*O/((1.36 + O)*(KS + S))*
        1       (1.0 - E/93.6)
         RETURN
```